Regulation of postnatal hypothalamic neurogenesis by fibroblast growth factor (FGF) signalling

Benediktas Kaminskas

Thesis submitted for the degree of Doctor of Philosophy

School of Biological Science

University of East Anglia

Norwich Research Park

Norwich, Norfolk NR4 7TJ

September 2018

Abstract

The hypothalamus is crucial for maintaining homeostasis. It regulates energy balance, circadian rhythms and other processes through the activity of neuronal nuclei and specialised cells lining the third ventricle wall called tanycytes. Hypothalamic tanycytes are candidate neural stem/progenitor cells that give rise to neurons in appetite-regulating nuclei in adult hypothalamus. The fibroblast growth factor (FGF) system is emerging as an important regulator of hypothalamic neurogenesis and metabolism. However, the endogenous FGF/FGFR signalling partners in tanycytes and their exact functions remain unknown. In this study, three approaches were taken to address this. First, the expression of FGF ligands, receptors and signalling modulators in the hypothalamus were examined by using RT-PCR, in situ hybridization, immunohistochemistry and reporter mice. FGF receptors were found to be restricted to the β-tanycyte domain and multiple cognate FGF ligands were also expressed by tanycytes. Second, the in vivo function of FGF receptors in postnatal hypothalamic neurogenesis was assessed by conditionally deleting *Fgfr1* and *Fgfr2* in *Fgf10*+ β-tanycytes and subsequent lineage tracing of these cells. This resulted in amplification of lineage traced cells, revealing a role for FGFR signalling in regulating the number of tanycytes and neurons generated in postnatal hypothalamus, likely by inhibiting proliferation. Recent reports showed that modulation of FGFR signalling in mediobasal hypothalamus, including tanycytes, results in hypophagia and greatly improved glucose homeostasis. Here, the metabolic functions of *Fgfr1* and *Fgfr2* were assessed by conditional deletion in β-tanycytes of lean and diet-induced-obese mice. Subtle effects on weight and glucose metabolism were observed, suggesting that endogenous FGFR signalling in tanycytes may not play a major role in regulating metabolism. Third, RNA-seq identified a downregulation of the orexigenic neuropeptide *Agrp* in FGF10 KO embryonic hypothalamus. Here, the importance of FGFR-independent FGF10 signalling for regulating *Agrp* expression and the potential molecular mechanisms were confirmed by in situ hybridization.

Acknowledgements

First and foremost, I would like to thank my supervisor Dr Mohammad K. Hajihosseini for providing support, guidance and inspiration to strive for excellence during these four years. My secondary supervisor Dr Mette Mogensen has also provided valuable support and suggestions towards the success of my project.

I am very grateful to Dr Timothy Goodman, as he provided mentorship, scientific expertise, friendship and a calming presence that helped me find my feet on the ground when I started out in the lab. I couldn't have asked for better lab mates than Dr Marta Mikolajczak, Stuart Nayar, Hannah Felstead, Shaun Clare and Estela Perez Santamarina who were always full of brilliant ideas and solutions. Their comradery inside and outside of the lab made my days brighter.

I would like to thank Prof. Ulrike Mayer for allowing me to use her cryostat and Dr Tom Wileman for the use of his microscope. On the topic of microscopes, Dr Paul Thomas has provided invaluable technical guidance and support.

Our collaborators Prof. Saverio Bellusci, Prof. David Ornitz, Prof. Sabine Werner and their respective lab members have my gratitude for providing transgenic mice and tissue required for this project.

Of course, without the BBSRC none of this would have been possible, I am very grateful for the funding that has provided me with this opportunity.

Special thanks go to Irene Pla Navarro, Dr Tope Amodu, Dr Camille Viaut, Anna Saukkonen, James Barron and James O'Mullane for the good times we've had and their friendship.

I thank my family for all the support and care given even while being separated by a thousand miles and more.

Finally, I am eternally grateful to Kadri Oras for always being there for me, sharing the highs and the lows, and being my sunshine.

List of Figures

List of Tables

Chapter 1

Introduction

1.1 – Adult Neurogenesis

Adult neurogenesis is the process whereby new neurons are generated in the adult brain and incorporated into existing networks. This process consists of many steps starting with the proliferation of neural stem/progenitor cells (NSPCs), migration and differentiation of intermediate progenitors and neuroblasts, apoptosis or survival of immature neurons and finally their maturation and functional integration. For long it was thought that such a phenomenon could not exist. Ramon y Cajal performed his seminal studies on the nervous system in the late nineteenth and early twentieth century and one of his conclusions was that no new neurons are born after embryonic development, pronouncing: 'Everything may die, nothing may be regenerated' (Colucci-D'Amato et al., 2006). Over the following century, this has been the dogma and the earliest findings contrary to it, such as the discovery of birth of new cells in the dentate gyrus of the hippocampus in the 1960s, were not received warmly and quickly forgotten (Altman and Das, 1965). Studies describing adult neurogenesis in songbirds had a more favourable reception (Goldman and Nottebohm, 1983), while the final coup de grâce to the dogma were the isolation of multipotent, neurosphere forming stem cells from the adult brain (Reynolds and Weiss, 1992) as well as experiments showing that some cells in the adult CNS are labelled by 5'-bromo-2'-deoxyuridine (BrdU), a radioactive thymidine analogue that is incorporated into DNA during the S phase of mitosis and can be easily detected by immunolabeling (Taupin, 2007). Since the 1990s, research on adult neurogenesis has grown rapidly, many advancements and discoveries have been made as well promises of clinical applications for brain injury, psychiatric disorders and neurodegenerative diseases.

1.1.1 - Canonical Adult Neurogenic Niches in the Mammalian Brain

Adult neurogenesis does not occur throughout the whole brain and is thought to be limited to anatomically circumscribed zones, called neurogenic niches. These niches possess the cellular types and architecture, extracellular molecules and matrix that create a microenvironment permissive for sustained adult neurogenesis (Riquelme et al., 2008). The universally accepted neurogenic niches in the adult rodent brain are found in the subgranular zone (SGZ) of the hippocampus and the subventricular zone (SVZ) of the lateral ventricles.

1.1.1.1 – Subgranular Zone

The subgranular zone niche is positioned between the granule cell layer and the hilus in hippocampus dentate gyrus. The neural stem/progenitor cells (NSPCs) that reside here generate granule cell neurons throughout rodent life (Kempermann et al., 2015). Type I radial-glia like neural stem cells have the signatures of $GFAP^{+}/Nestin^{+}/BLBP^{+}/Sox2^{+}$ and are largely quiescent and can give rise to neurons and astrocytes (Bonaguidi et al., 2011). They first give rise to transient amplifying progenitors called Type II cells of which there are two subtypes – Type IIa ($GFAP^{+/-}/Nestin^{+}/BLBP^{+}/Sox2^{+}$) and committed Type IIb cells which express markers of neural fate markers ($Nestin^{+}/DCX^{+}/PSA\text{-}NCAM^{+}/NeuroD^{+}/Prox1^{+}$) (Steiner et al., 2006). Type IIb cells divide rapidly and give rise to Type III neurally committed neuroblasts ($DCX^{+}/PSA\text{-}NCAM^{+}/NeuroD^{+}/Prox1^{+}$). Neuroblasts may still proliferate, albeit at a low rate under normal conditions (Jessberger et al., 2005). The majority of immature, postmitotic neurons ($Calretinin^{+}/NeuN^{+}/DCX^{+}/PSA\text{-}NCAM^{+}/NeuroD^{+}/Prox1^{+}$) in the granular zone undergo apoptosis (Cameron and McKay, 2001; Dayer et al., 2003). Surviving neurons extend dendrites and axons, making functional connections with the CA3 and entorhinal cortex. Further maturation steps are the development of dendritic spines and the establishment of mature membrane properties (Piatti et al., 2011).

Glial, immune, endothelial and neural cells, as well as the extracellular matrix, are also integral parts of the niche. Astrocytes provide signals that promote proliferation and neural fate commitment (Song et al., 2002), for example, IL-1β, IL-6, IGFBP6, decorin, Wnt and Ephrin-B2 (Lie et al., 2005; Barkho et al., 2006; Ashton et al., 2012). In addition, niche astrocytes, including Type I cells, are coupled via gap junctions, which seems to have an important role in regulating neurogenesis, as knockout of connexin 30 and connexin 43 in GFAP expressing cells strongly inhibits proliferation in the subgranular zone (Kunze et al., 2009). Microglia are important for phagocytising newborn cells that are undergoing apoptosis (Sierra et al., 2010). In addition, they may have a supportive role in subgranular zone neurogenesis during injury (McPherson et al., 2011). The Type I stem cells are in direct contact with endothelial cells through their end-feet and receive signals such as Vascular endothelial growth factor (VEGF) and Vascular endothelial growth factor-B (VEGFB) which stimulate neurogenesis (Filippov et al., 2003; Schanzer et al., 2004; Sun et al., 2006).

Throughout this process, the stem cells, progenitors, and neuroblasts neurons receive GABAergic innervation which affects cell proliferation and differentiation (Tozuka et

al., 2005; Renzel et al., 2013; Giachino et al., 2014). Immature newborn neurons receive GABAergic inputs, important for their maturation (Ge et al., 2007). Additionally, cholinergic inputs may have a role in promoting survival (Cooper-Kuhn et al., 2004).

The majority of newborn cells in the dentate gyrus die within 1 month of being generated (Cameron and McKay, 2001; Dayer et al., 2003). It has been shown that proliferation-related genes have a much lower influence than survival related genes in determining the total number of new neurons generated (Kempermann et al., 2006). Finally, there is a myriad of reported factors that influence progenitor cell proliferation. This has prompted the hypothesis that the main determining factors that control adult hippocampal neurogenesis are ones that modulate survival, while proliferation modulating factors are not as specific and may have a lesser influence on the final number of neurons generated (Kempermann et al., 2015). These survival-controlling influences come in the form of neurotrophic and growth factors such as BDNF and FGF2, neurotransmitters like GABA, glutamate, acetylcholine and serotonin and hormones such as glucocorticoids (Sairanen et al., 2005; Mirescu and Gould, 2006; Tashiro et al., 2006; Shih-Jen et al., 2007; Jagasia et al., 2009; Campbell et al., 2010; Werner et al., 2011).

The newly generated, mature granule neurons are integrated into existing networks that are important for cognitive functions, among which are memory consolidation and behavioural pattern separation (Kitamura and Inokuchi, 2014; Lacar et al., 2014). In addition, disturbed hippocampal neurogenesis has been linked to psychiatric disorders such as depression and schizophrenia (Lee et al., 2013b) and neurodegenerative diseases like Alzheimer's (Winner and Winkler, 2015), which underscores the importance of studying this process.

There have been a number of studies that support the existence of hippocampal neurogenesis in the adult human brain. These include the analysis of post-mortem human tissue, including of cancer patients that received BrdU infusions (Eriksson, 1998), immunohistochemical detection of proliferation, progenitors and mature neurons (Knoth et al., 2010). High levels of radioactive ^{14}Carbon were released into the environment during cold war nuclear tests, which gets incorporated into DNA as it is synthesised replicating cells. This can be used to birthmark cells, as ones born during the peak of ^{14}C in the environment will have also a signature of increased radioactive carbon in genomic DNA. Such measurements have provided more evidence that adult hippocampal neurogenesis occurs in humans and roughly 700

new neurons are added per day (Spalding et al., 2013). However, some recent high-quality histological studies have called into question whether this process occurs in humans after adolescence and if the subgranular zone in the anatomical form found in rodent brain even exists in the human brain at all (Spalding et al., 2013; Dennis et al., 2016). These studies reveal the methodological difficulties and limitations of studying adult neurogenesis in the human brain and a lack of consensus as to its existence in the human hippocampus.

1.1.1.2 – Subventricular Zone

The neural stem cells of the subventricular zone neurogenic niche are present along the walls of the cerebrospinal fluid (CSF)-filled lateral ventricles (Fig. 1.1). These astrocytic, GFAP+/Nestin+/BLBP+/Sox2+ cells are referred to as Type B1 cells and are located adjacent to ependymal cells that form the ventricle walls (Lim and Alvarez-Buylla, 2016). They can either be in a quiescent or activated state, and expression of Nestin and EGFR is a signature of the active state (Codega et al., 2014; Mich et al., 2014). Activated Type B1 cells divide symmetrically to self-renew or asymmetrically to also produce Mash1+/Dlx2+ transit amplifying cells termed Type C cells (Aguirre et al., 2004). Type C cells expand and give rise to Dlx2+/DCX+/PSA-NCAM+ neuroblasts named Type A cells (Doetsch et al., 1997). These cells may also proliferate while migrating to the olfactory bulbs (Smith and Luskin, 1998). Therein they mature and differentiate into various neuronal types, which can be categorised into granule cells found within the granule cell layer, and periglomerular interneurons within the glomerular layer.

Radial-glia cells (RGCs) are embryonic NSCs that are in contact with the ventricles and give rise to glial and neural cells in the embryonic brain (Kriegstein and Alvarez-Buylla, 2009). They also give rise to Type B1 cells in the adult subventricular zone (Merkle et al., 2004). Type B1 cells share qualities with radial glial cells: both are glial cell types that possess a primary cilium on the apical surface that is in contact with the CSF (Doetsch et al., 1999) and both are capable of self-renewal and generation of glial and neural lineages (Menn et al., 2006). The primary cilium of Type B cells is surrounded by multiciliated ependymal cells in a pinwheel fashion (Mirzadeh et al., 2008). The primary cilium may be important for sensing and transducing signals in the CSF, such as IGF-2 (Lehtinen et al., 2011).

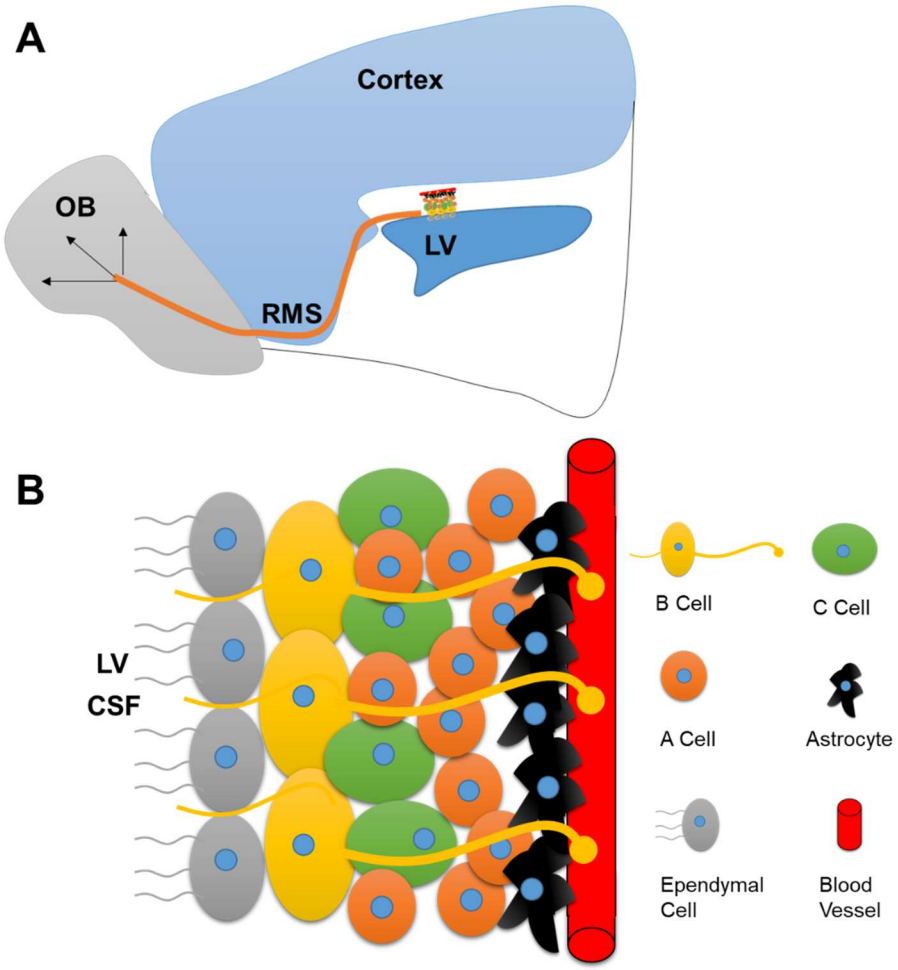

Figure 1.1 – Organization of the subventricular zone neurogenic niche. (A) Schematic shows anatomical location of the SVZ neurogenic niche, the rostral migratory stream (RMS) and olfactory bulb (OB). Neuroblasts born in the SVZ niche migrate rostrally through the RMS in glial tubes formed by astrocytes. Once the neuroblasts reach the olfactory bulbs they migrate tangentially into the granule and glomerular layers, where they mature into granule or periglomerular neurons respectively. (B) Schematic representation of the subventricular zone adult neurogenic niche. Multiciliated ependymal cells line the lateral ventricle, while multipotent NSPCs (B cells) reside in the next cell layer. Each B cell contains a single apical primary cilium that reaches the lateral ventricle CSF and extends a basal process that forms a contact with the niche vasculature through its endfeet. B cells can divide symmetrically and asymmetrically to self-renew and give rise to transit-amplifying cells (C cells). C cells divide rapidly to produce neuroblasts (A cells) or cells of glial lineage. Glial cells such as astrocytes modulate the niche by secreting factors that regulate proliferation and differentiation. CSF – cerebrospinal fluid; LV – lateral ventricle; OB – olfactory bulb; RMS – rostral migratory stream. Adapted from Song et al., (2011).

Ependymal cells are important for regulating SVZ neurogenesis. They release Noggin, blocking BMP signalling in Type B cells, therefore promoting neurogenesis and suppressing gliogenesis (Lim et al., 2000). Their beating cilia are also important for regulating the flow of CSF signals and neuroblast migration (Sawamoto et al., 2006).

Type B cells also extend a basal process which terminates on blood vessels (Mirzadeh et al., 2008). This gives access not just to the many signals that endothelial cells secrete (Goldman and Chen, 2011), but also contact-dependent cues such as ephrinB2 and Jagged1, which maintain stem cell quiescence (Ottone et al., 2014). In addition, the SVZ blood-brain-barrier (BBB) is modified and more permissive, increasing NSPC access to circulating signals (Tavazoie et al., 2008).

As in the SGZ, astrocytes are involved in the regulation of neurogenesis by secreting various factors that influence cell proliferation and differentiation (Morrens et al., 2011). For example, NSC and microglia co-culturing experiments indicate that microglia can secrete factors important for neurogenesis (Walton et al., 2006).

The proliferation of progenitors and neuroblasts is controlled by neurotransmitters such as serotonin and GABA (Brezun and Daszuta, 1999; Banasr et al., 2004; Liu et al., 2005; Fernando et al., 2011). Proliferation stimulating neurotrophic and growth factors include CNTF, BDNF and FGF2 (Kuhn et al., 1997; Zigova et al., 1998; Emsley and Hagg, 2003a). Ephrins and their ligands are negative regulators of proliferation (Holmberg et al., 2005). Interestingly, acetylcholine also increases proliferation and may do so in part by synergising with FGFR signalling (Paez-Gonzalez et al., 2014). Additionally, ATP was shown to promote the proliferation of rapidly dividing type C cells by binding to their P2Y1 receptors, a mechanism that may have similarities to ATP-mediated regulation of radial-glial cell proliferation (Weissman, Riquelme et al. 2004, Suyama, Sunabori et al. 2012).

Among factors that influence the decision between glial and neuronal fates of newborn cells are PDGF, Olig2, Pax6, BMP, LIF, Wnt-3a and Wnt-5a, Notch, histone deacetylases, chromatin modifying factor Mll1, long non-coding RNA Dlx1as, microRNAs miR-124 and miR-137 (Gaiano and Fishell, 2002; Bonaguidi et al., 2005; Hack et al., 2005; Marshall et al., 2005; Menn et al., 2006; Yu et al., 2006; Siebzehnrubl et al., 2007; Colak et al., 2008; Silber et al., 2008; Lim et al., 2009; Ramos et al., 2013).

From their site of birth, over 30,000 Type A neuroblasts per day start their journey migrating rostrally into the rodent olfactory bulb (Lois and Alvarez-Buylla, 1994). One

of the ways that neuroblasts interact with each other is through gap junctions, formed by hemichannels, each composed of six connexin43 or connexin45 proteins (Yamamoto, Ochalski et al. 1990, Miragall, Albiez et al. 1997)(Marins et al., 2009). These gap junctions are involved in the long-distance migration of neuroblasts along the rostral migratory stream (RMS) (Marins, Xavier et al. 2009) (Fig. 1.1 A). Astrocytes form a glial tube, surrounding chains of migrating neuroblasts (Lois et al., 1996) and the disruption of its formation leads to severely impaired migration and therefore arrival of new neurons in the OB (Kim et al., 2007). However, the glial tube is absent in neonatal brain (Law et al., 1999). Extracellular matrix molecules such as laminin are important for the directionality of neuroblast migration (Murase and Horwitz, 2002; Emsley and Hagg, 2003b). Other molecular determinants of migration include PSA-NCAM (Chazal et al., 2000) and chemorepulsive Slit-ROBO signalling (Hu, 1999; Kaneko et al., 2010). Once Type A cells reach the olfactory bulb, they migrate radially to reach their distinct destinations in granule and glomerular layers guided by olfactory activity-dependent signals such as Tenascin-R (Saghatelyan et al., 2004).

Newborn granule and periglomerular cells are GABAergic interneurons (Lledo et al., 2006). However, new evidence suggests that some glutamatergic juxtaglomerular interneurons are also generated during adult SVZ neurogenesis (Brill et al., 2009). Newborn cells start expressing NeuN 10 days after birth (Winner et al., 2002), granule cells in the olfactory bulb elaborate their dendrites and assume mature morphology within two weeks (Petreanu and Alvarez-Buylla, 2002) whilst periglomerular cells assume mature properties in around 4 weeks (Belluzzi et al., 2003). Around half of the newborn neurons undergo apoptosis, while neurons that have survived the first 3 months remain for at least 19 months (Winner et al., 2002). The critical period for the survival of newborn cells is between day 14 and 28 after birth and their survival depends on sensory inputs (Yamaguchi and Mori, 2005). Though not fully understood, the function of the SVZ neurogenesis may be to improve the plasticity of networks involved in olfaction and to facilitate learning (Lledo and Valley, 2016).

SVZ neurogenesis takes place in foetal and infant human brain, the RMS with migrating DCX+ neurons leads to the olfactory bulbs and in addition, to the prefrontal cortex (Sanai et al., 2011). However, this process is highly reduced in specimens older than 18 months. In the human adult brain, there is a ribbon of GFAP+ astrocytes associated with the lateral ventricles, but no RMS (Sanai, 2004). Radioactive carbon analysis showed that there are no, or a very minimal number of new neurons generated in the adult olfactory bulb (Bergmann et al., 2012). This apparent lack of olfactory bulb neurogenesis may be due to the relatively diminished importance of

olfaction in humans compared to rodents, although recently the notion that the human sense of smell is inferior has been called into question (McGann, 2017).

1.1.2 – Non–Canonical Neurogenic Niches

There have been many reports of adult neurogenesis occurring in other regions of the brain (Fig. 1.2), such as the, substantia nigra, and the amygdala neocortex (Gould et al., 2001; Bernier et al., 2002; Zhao, 2003; Dayer et al., 2005; Shapiro et al., 2009; Zhao and Janson Lang, 2009). These niches are controversial and in some adult neurogenesis might only occur in the postnatal brain or post-injury as a repair mechanism (Feliciano and Bordey, 2013). Some of the difficulties in studying these niches are the low rates of cell proliferation, the lack of knowledge of what the precursor cells may be and the stimuli that may impact it. For example, the presence of PSA-NCAM+/DCX+ cells in the piriform cortex has been interpreted as a sign of adult neurogenesis in this region, but more recent studies have shown that these are not newborn neurons, but ones that retain immature characteristics throughout life (Gomez-Climent et al., 2008; Klempin et al., 2011), highlighting the need for careful interpretation of marker expression. Despite these limitations, non-canonical neurogenic niches remain a promising area of research.

Of particular interest is striatal neurogenesis. This process may occur in the rat, mice, rabbit and monkey brain (Bedard et al., 2002; Dayer et al., 2005; Bedard et al., 2006; Luzzati et al., 2006; Shapiro et al., 2009). Through a combination of iododeoxyuridine (IdU, a thymidine analogue) supplied to cancer patients, neuronal markers and radioactive carbon dating, it was recently shown that new calretinin and NPY-expressing neurons are generated in the adult human brain (Ernst et al., 2014). The location of progenitors and origin of DCX+ neuroblasts that were found in the striatum is unknown. It is possible that this source is the SVZ, due to its close proximity to the striatum. However, in mice, downregulation of Notch1 in striatal astrocytes by stroke or by deletion of its transcription factor RBP-Jκ stimulates these astrocytes to produce new neurons (Magnusson et al., 2014). Adult human striatal neurogenesis was also found to be reduced in Huntington's disease and therefore this might be a promising new area of investigation with potential clinical applications for neurological disease (Ernst et al., 2014).

The most comprehensively studied and most widely accepted non-canonical neurogenic niche resides in the adult hypothalamus (Feliciano et al., 2015). Increasing evidence suggests that this neurogenic niche consists of putative NSPCs

called tanycytes that line the 3rd ventricle and constitutively give rise to neurons in the abutting parenchyma. Neurogenesis in the hypothalamus will be discussed in greater detail in the following sections.

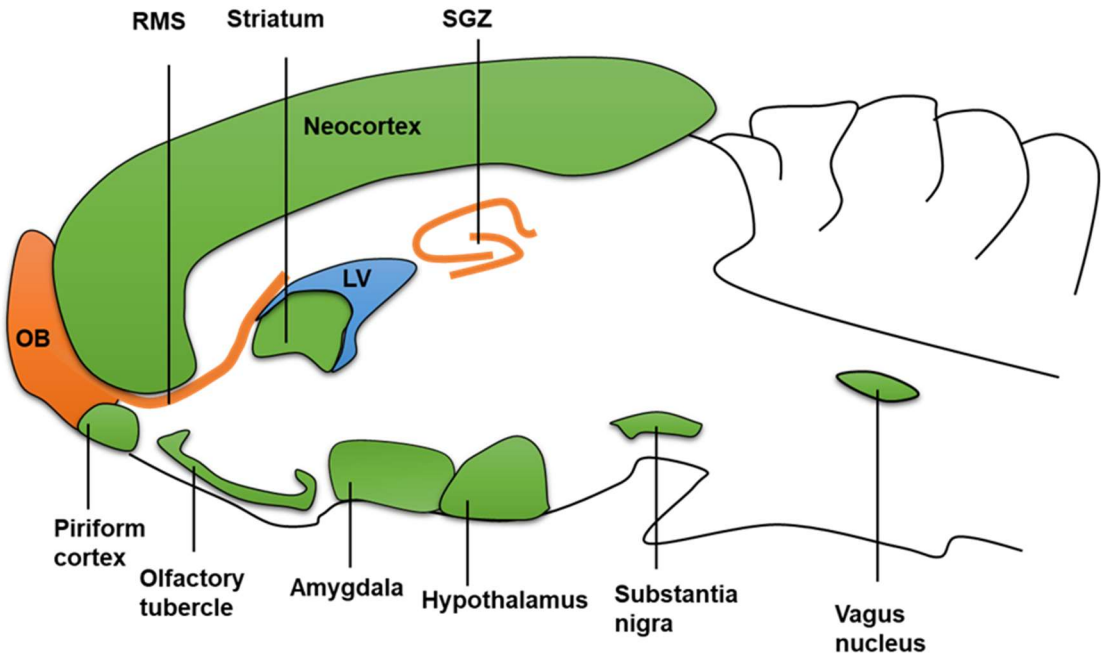

Figure 1.2 – Non–canonical niches in the rodent brain. Schematic shows the anatomical location of canonical (orange) and non-canonical (green) neurogenic niches in adult rodent brain. LV – lateral ventricle; OB – olfactory bulb; RMS – rostral migratory stream; SGZ – subgranular zone. Adapted from (Gould, 2007).

1.2– Hypothalamus Structure and Function

1.2.1 – Anatomy and Homeostatic Functions of the Hypothalamus

The hypothalamus is a small brain structure that constitutes less than 1% of the adult human brain weight (Saper and Lowell, 2014). It is positioned just above the pituitary and below the thalamus. Its rostral boundary is defined by the optic chiasm, lamina terminalis and anterior commissure and it continues caudally up to the vertebral peduncle and interpeduncular fossa (Lechan and Toni, 2000). Various hypothalamic neuronal nuclei and fiber tracts are symmetrically distributed along and on either side of the third ventricle, which runs along the midline. The median eminence is located at the base of the hypothalamus and forms a connection with the pituitary gland through the hypophysial portal system (Yin and Gore, 2010).

The hypothalamus is often categorised into three areas along the rostrocaudal axis: preoptic, tuberal and posterior (Saper and Lowell, 2014)(Fig. 1.3).

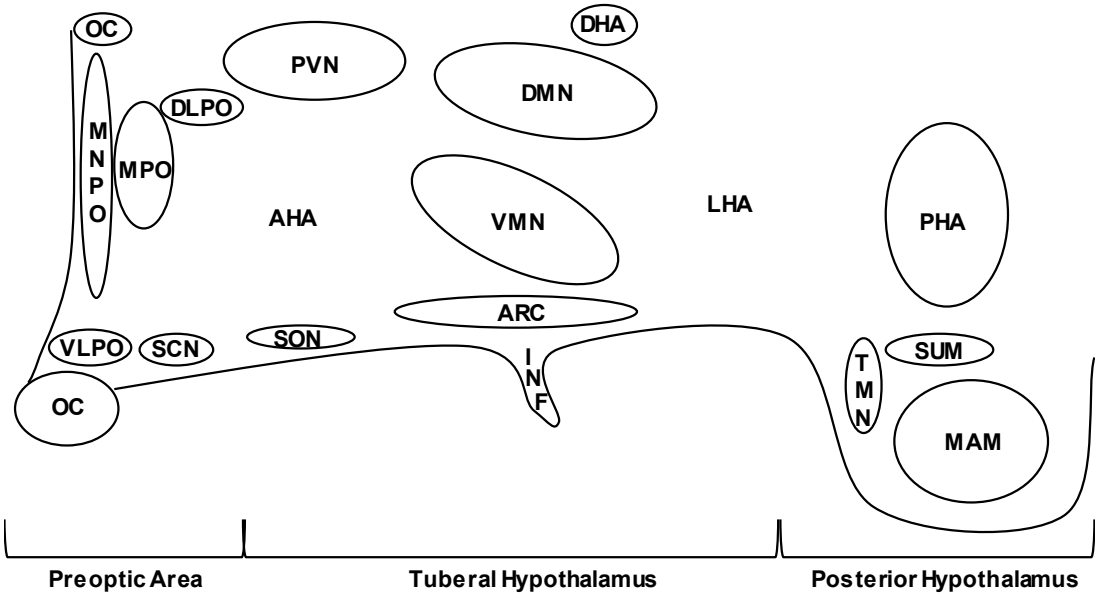

Figure 1.3 – Neuronal nuclei located in the hypothalamus. A schematic displaying hypothalamus anatomy, neuronal nuclei and their relative locations in rat brain in a sagittal section. Adapted from (Saper and Lowell, 2014). AC - anterior commissure; AHA - anterior hypothalamic area; ARC - arcuate nucleus; DHA - dorsal hypothalamic area; DLPO - dorsolateral preoptic area; DMN - dorsomedial nucleus; Infundibulum – INF; LHA - lateral hypothalamic area; MAM - mammillary nuclei; MNPO - median preoptic nucleus; MPO - medial preoptic area; OC - optic chiasm; PHA - posterior hypothalamic area; PVN - paraventricular hypothalamic nucleus; SCN - suprachiasmatic nucleus; SON - supraoptic nucleus; SUM - supramammillary nucleus; TMN - tuberomammillary nucleus; VLPO - ventrolateral preoptic nucleus; VMN - ventromedial nucleus.

Preoptic, paraventricular, suprachiasmatic and supraoptic nuclei are located in the preoptic area. The preoptic nuclei are involved in sexual motivation (Balthazart et al., 2013) and thermoregulation (Boulant, 2000). The paraventricular nucleus is important for the regulation of stress-related glucocorticoid hormone release (Herman et al., 2016) as well as the release of the multifunctional neuropeptide oxytocin (Jezova et al., 1993). The suprachiasmatic nucleus is vital for circadian rhythms (Musiek and Holtzman, 2016). Cells in the supraoptic nucleus release oxytocin and vasopressin, a neuropeptide that regulates water homeostasis (Armstrong and Stern, 1998).

The tuberal hypothalamus is composed of arcuate, ventromedial and dorsomedial nuclei. These nuclei are important for maintaining energy balance, and this role will be further discussed in the next section. In addition to this role, neurons in the arcuate also regulate cardiovascular function (Sapru, 2013), while the ventromedial nucleus is involved in sexual function and behaviour (Matsumoto and Yamanouchi, 2000). The dorsomedial nucleus has an additional role in modulating emotional stress response (Ebner et al., 2013).

In terms of the posterior hypothalamus, the posterior nucleus regulates aggressive behaviour (Sano et al., 1970), the tuberomammillary nucleus is important for wakefulness (Parmentier et al., 2009) and appetitive behaviours (Contreras et al., 2016), while the mammillary bodies are crucial for encoding episodic memories (Vann, 2010).

The lateral hypothalamic area is important for feeding behaviour (Stuber and Wise, 2016).

It is evident that the hypothalamus is a complex structure involved in a wide range of homeostatic functions.

1.2.2 – Energy Balance Regulating Centres

The hypothalamus contains neural circuits that are essential for maintaining energy homeostasis. Many of the neurons that regulate this are present in the arcuate (ARC), ventromedial (VMN), dorsomedial (DMN), paraventricular (PVA) nuclei and the lateral hypothalamic area (LHA).

The arcuate nucleus contains two main populations of neurons that are crucial for regulating appetite – anorexigenic (appetite-suppressing) POMC expressing and orexigenic (appetite-stimulating) NPY/Agrp expressing neurons. POMC (pro-opiomelanocortin) is a precursor peptide, which produces α-melanocyte-stimulating hormone (α-MSH). α-MSH released by POMC neurons can bind to melanocortin receptors 3 and 4 in the hypothalamus, reducing food intake, and PVN neurons are one of the main targets (Krashes et al., 2016). Agrp (agouti-related peptide) is an antagonist of melanocortin receptors (Ollmann et al., 1997), although recent studies show it is a biased agonist of these receptors as it causes a decrease in cAMP activity while increasing phosphorylation of ERK1/2 (Yang and Tao, 2016). NPY (neuropeptide Y) is an orexigenic neuropeptide that stimulates appetitive behaviours (Seeley et al., 1995). NPY is an agonist for Y receptors, of which Y1 and Y5 are

implicated in the control of food intake (Nguyen et al., 2012). Germline knockout of *Npy* and *Agrp* in mice does not cause overt changes in energy balance, suggesting that the roles of these neuropeptides are subtle (Qian et al., 2002). Instead, the main mechanism by which these neurons affect appetite seems to be the inhibition of POMC and PVA neurons through their release of GABA (Tong et al., 2008; Atasoy et al., 2012).

Due to the proximity of the arcuate nucleus to fenestrated capillaries (Ciofi, 2011), neurons in the arcuate nucleus may receive hormonal and metabolic cues from the circulation. Among these are the satiety signal leptin, which stimulates POMC neurons and inhibits NPY/Agrp neurons (Cowley et al., 2001), and ghrelin, a stomach peptide hormone, which is produced during hunger and has the opposite effect (Cowley et al., 2003).

The PVN receives inputs from the arcuate nucleus in the form of NPY, AGRP and GABA. These cues then influence the release of thyrotropin-releasing hormone (TRH) (Fekete et al., 2000; Fekete et al., 2004) and corticotropin-releasing hormone (CRH) (Lu et al., 2003) from PVN neurons.

The dorsomedial nucleus contains NPY-expressing neurons, whose role has been researched in OLETF (Otsuka Long-Evans Tokushima Fatty) rats (Bi, Ladenheim et al. 2001). Hailing from an outbred colony of Long Evans rats, the strain develops spontaneous obesity and hyperglycaemia, thus serving as a rodent model for these disorders (Kawano, Hirashima et al. 1992). These rats lack functional receptors for the satiety hormone CCK (cholecystokinin) and exhibit elevated expression of NPY in the DMN, leading to increased food intake (Moran, Katz et al. 1998, Bi, Ladenheim et al. 2001). Intriguingly, knockdown of NPY specifically in the dorsomedial nucleus of OLETF rats by AAV-mediated RNAi abolishes the hyperphagia, obesity and diabetes phenotypes, suggesting the importance of this neurotransmitter in DMN neurons (Yang et al., 2009). Further studies showed that NPY expressed in the DMN influences food intake, physical activity, thermogenesis and the development of brown fat in a rat strain (Sprague Dawley) that is metabolically normal (Chao et al., 2011).

The VMN is home to neurons that express steroidogenic factor 1 (SF1) and BDNF. SF1 expressing neuron activity is regulated in part by leptin signalling, and the conditional deletion of leptin receptor (Lepr) in these neurons causes increased body weight and adiposity (Dhillon et al., 2006; Bingham et al., 2008). The conditional inactivation of SF1 itself exacerbates diet-induced obesity by increasing body weight and adiposity and reduced thermogenesis (Kim et al., 2011). BDNF is also important

for controlling feeding behaviour and body weight. A *de novo* mutation of the gene encoding the BDNF receptor Tropomyosin receptor kinase B (TrkB) caused hyperphagia and obesity in the case of an 8-year-old male child (Yeo et al., 2004), while intraventricular injection of BDNF prevents hyperphagia in MC4R mutant mice fed a high-fat diet (Xu et al., 2003).

The lateral hypothalamus contains Orexin A and Orexin B expressing neurons. Intracerebroventricular administration of these peptides leads to increased feeding behaviour (Sakurai et al., 1998). Melanin-concentrating hormone (MCH) neurons are also orexigenic, as the overexpression of *Mch* in the lateral hypothalamus increases food intake and leads to obesity, while mice deficient in melanocortin-concentrating hormone 1 (MCH1R) are hyperphagic, but at the same time exhibit increased activity, leading to a lean phenotype with reduced adiposity, even when fed high fat diet (Marsh et al., 2002).

Thus, the hypothalamic neurons in these nuclei form complex energy balance regulating networks within and outside of the hypothalamus (Timper and Brüning, 2017).

1.2.3 – Hypothalamus-Pituitary Axis

The hypothalamus and pituitary gland are intimately connected and serve as master regulators of the endocrine system. The hypothalamus integrates central and peripheral information and then releases hormones that reach the pituitary and from there to the bloodstream. To understand the function of the hypothalamus-pituitary axis, its anatomy must be discussed.

The pituitary is composed of the anterior and posterior lobes and an intermediate zone. The posterior lobe receives axons from the PVN neurons expressing oxytocin and vasopressin through the hypothalamohypophyseal tract. The stimulation of these PVN neurons (Veenema and Neumann, 2008) results in the release of oxytocin and vasopressin into the capillary plexus to then be distributed throughout the body.

The anterior lobe does not directly receive inputs from hypothalamic neurons. Instead, the axons of hypothalamic neurons release hormones into portal capillaries that are present in the median eminence. These hormones then travel through the hypophyseal portal veins into the anterior pituitary. Here, these hormones trigger or inhibit the production of hormones in the pituitary. The hormones produced in the anterior pituitary are released into the secondary capillary plexus and enter the

bloodstream, either acting directly on the target tissues (growth hormone and prolactin) or triggering the production and release of hormones in other glands in the body (thyroid-stimulating, adrenocorticotropic, luteinizing and follicle-stimulating hormones).

Based on the hormones involved, there are a few neuroendocrine axes that act through the anterior pituitary. These include the hypothalamic-pituitary-adrenal (HPA) (Smith and Vale, 2006), hypothalamic-pituitary-gonadal (HPG) (Plant, 2015) and hypothalamo-pituitary-thyroid (HPT) axes. A short description of the hypothalamo-pituitary-thyroid axis follows as an example of how these systems function.

Thyrotropin-releasing hormone (TRH) is synthesised by TRH neurons in the PVN and released in the median eminence, entering the anterior pituitary through the hypophyseal portal system (Lechan and Fekete, 2006). Here, TRH stimulates the production and release of thyroid-stimulating hormone (TSH) into the circulation (Geras and Gershengorn, 1982). In turn, TSH stimulates the production and secretion of thyroid hormones triiodothyronine (T3) and thyroxine (T4) in the thyroid gland, which increase metabolism (Mullur et al., 2014). The heightened concentration of these hormones then acts as a negative feedback loop by inhibiting the release of TRH and TSH (Dietrich et al., 2012).

This is a very simplified account of the HPT. The regulation of the HPT depends on other factors including circadian rhythms and feeding (Costa-e-Sousa and Hollenberg, 2012) as well as a crucial component of the neuroendocrine system – tanycytes.

1.2.4 – Tanycytes

Tanycytes are a modified ependymal cell type found in the circumventricular organs – structures of the brain associated with the ventricular system and fenestrated capillaries (Kaur and Ling, 2017). In the hypothalamus, they line the ventral parts of the third ventricle (3V) wall. Befitting their name (“tanos” means elongated or stretched in Greek), each tanycyte possesses a long basal process often in contact with blood vessels, while on the apical surface they are in contact with the CSF. During embryonic development of the hypothalamus, radial glial cells also reside in the 3V wall and due to their morphological similarities, their shared markers, such as GFAP, vimentin, nestin and GLAST as well as their neurogenic potential, tanycytes are thought to be either residual radial glial cells or their descendants with distinct features

(Rodriguez, Blazquez et al. 2005, Goodman and Hajihosseini 2015, Rizzoti and Lovell-Badge 2017). Additional cell markers that distinguish tanycytes from other cells lining the hypothalamic third ventricle wall include Rax, DARPP-32 and GPR50 (Meister, Hokfelt et al. 1988, Batailler, Mullier et al. 2012, Miranda-Angulo, Byerly et al. 2014).

Hypothalamic tanycytes are not a homogeneous population and they are usually classified into 4 subpopulations, arranged along the dorsoventral axis (Prevot et al., 2018). β2-tanycytes constitute the floor of the 3V wall and their basal processes make contact with their endfeet on the portal capillaries of the median eminence. β1-tanycytes are located in the ventrolateral walls of the 3V and extend their basal process that contact the lateral portal capillaries or nearby ventromedial-arcuate nucleus (vmARC) capillaries that exhibit variable permeability (Langlet et al., 2013). α2-tanycytes are more dorsal and project into the arcuate nucleus, while the most dorsal, α1-tanycytes, project into the ventromedial and dorsomedial nuclei (Rodriguez et al., 2005). These tanycytes populations also display differential gene expression and this is the basis of useful domain-specific immunohistochemical markers such as GFAP and S100β, which are expressed in the α-tanycyte domain and absent from the β-tanycyte domain, while FGF10 is only present in the β-tanycyte domain (Goodman and Hajihosseini, 2015). Finally, α-tanycytes are biciliated, while β-tanycytes each possess only a primary cilium (Mirzadeh et al., 2017). While this is a useful and broad way to classify tanycytes, it has been recently suggested that it may not fully reflect the full diversity of tanycytes, calling for a more refined classification system (Prevot et al., 2018).

β-tanycytes form a barrier that separates the median eminence with its fenestrated capillaries from the CSF, preventing the free flow of substances between these compartments. β2-tanycytes express tight junction proteins zonula occludens 1 (ZO1) and occludin, claudin 1 and 5 as a continuous belt around their cell bodies, thus forming an impermeable barrier between the CSF and the median eminence, while α-tanycytes do not form such a barrier between the CSF and hypothalamus parenchyma (Mullier et al., 2010). The barrier is plastic at the level of β1 tanycytes. Intriguingly, in fasted mice lowered blood glucose levels cause tanycytes to upregulate and release VEGF-A, which binds to VEGF receptors on capillaries in the vmARC, inducing fenestrations (Langlet et al., 2013). β1-tanycytes that contact these newly fenestrated leaky capillaries increase their tight junction protein expression to match that of β2-tanycytes. This allows for peripheral signals such as ghrelin to reach metabolically important POMC and NPY neurons in the vmARC while preventing their leakage into

the CSF (Schaeffer et al., 2013). Upon refeeding, this process is reversed and both the fenestrations in the vmARC capillaries and the barrier properties of tanycytes contacting them return to their previous state (Langlet et al., 2013). This may present a new plastic layer of metabolic regulation dependent on tanycytes (Prevot et al., 2013).

The barrier formed by β2-tanycytes prevents diffusion of blood leptin that enters the median eminence into the rest of the brain (Balland et al., 2014). Furthermore, circulating leptin is taken up by tanycytes and shuttled into the CSF in an ERK and leptin receptor-dependent manner, from where it may reach hypothalamic parenchyma as there is no barrier formed at the level of the arcuate, ventromedial and dorsomedial nuclei (Balland et al., 2014). Ghrelin is also internalised by tanycytes, suggesting their potential role in shuttling this hormone from the blood into the CSF (Collden et al., 2015).

Tanycytes have important roles in regulating the hypothalamus-pituitary-gonadal and hypothalamus-pituitary-thyroid axes. Their processes surround the axon terminals of gonadotropin-releasing hormone (GnRH) neurons, preventing GnRH release into the portal capillaries (Prevot et al., 1998; Baroncini et al., 2007). Tanycytes retract their processes, allowing GnRH to reach the anterior pituitary, in an estrous cycle dependent manner (Prevot et al., 1999) based on signalling cues such as estradiol, nitric oxide, and TGFβ1 Semaphorin7A (Prevot et al., 2003; De Seranno et al., 2004; de Seranno et al., 2010; Parkash et al., 2015). Recently, tanycytes were also shown to block access to pituitary vessels by increasing their endfeet size in response to activation of thyrotropin-releasing hormone receptor 1 (TRH receptor 1) and therefore reducing the access of TRH into the hypophyseal portal system (Müller-Fielitz et al., 2017).

Another way tanycytes control the hypothalamus-pituitary-thyroid axis is through the activity of deiodinases 2 (DIO2) and 3 (DIO3). DIO2 converts T4 into the more biologically active T3, while DIO3 converts T4 and T3 into inactive reverse triiodothyronine (rT3) or 3,3'-Diiodothyronine (3,3'-T_2) molecules. Tanycytes express these enzymes in a photoperiod and FGF signalling dependent fashion (Barrett et al., 2007; Samms et al., 2015). In addition, they express thyroid hormone transporters OTP1c1 (Nakao et al., 2006) and MCT8 (Herwig et al., 2009), indicating a role for shuttling thyroid hormones across the blood-CSF barrier. Finally, they express PPII which inactivates TRH at the site of TRH neuron axon and tanycyte interactions near the portal capillaries (Sanchez et al., 2009).

Tanycytes express glucose transporter 2 (GLUT2) (Garcia et al., 2003), glucokinase (GK) (Millan et al., 2010) and K-ATP channels (Thomzig et al., 2005), therefore sharing the molecular machinery required for glucose sensing with pancreatic β-cells (Schuit et al., 2001). Indeed, application of glucose to tanycytes in live slice cultures causes an increase in intracellular Ca^{2+} and ATP release (Frayling et al., 2011; Orellana et al., 2012). Tanycytes can also sense non-nutritive sweeteners such as sucralose through sweet-taste receptor Tas1r2/Tas1r3 (Benford et al., 2017) and amino acids through the receptors Tas1r1/Tas1r3 and mGluR4 which are important for umami taste perception (Lazutkaite et al., 2017), in both cases resulting in increased intracellular Ca^{2+} and release of ATP. The exact significance of tanycytes' ability to sense these nutrients remains unknown.

Due to their similarities and potential descendancy from radial glia (Rodriguez et al., 2005), tanycytes are a likely candidate as NSPCs of the adult hypothalamic niche and a growing body of evidence is in support of this notion. The following section discusses neurogenesis in the hypothalamus in greater detail.

1.3 – Postnatal and Adult Neurogenesis in the Hypothalamus

Many studies have reported cell proliferation and birth of new cells of neuronal and glial lineage in the postnatal and adult hypothalamus. However, the characterization of this niche is still in its early stages compared to the canonical subgranular and subventricular zone niches. As such, there is still a lack of information and consensus regarding the niche organisation, the identity of the NSPCs, intermediate steps and function of newborn cells.

Proliferation and birth of new neurons in the hypothalamus has been assessed by detecting synthetic thymidine analogues like bromodeoxyuridine which are incorporated into DNA during the S-phase (Taupin, 2007), lineage tracing using inducible the transgenic inducible Cre-LoxP system or viral infection (Kretzschmar and Watt, 2012) and cell cycle markers like PCNA and Ki67 (von Bohlen und Halbach, 2011). A few potential neurogenic sites were reported in the hypothalamus, which can be very broadly categorised into tanycytes and hypothalamus parenchyma. While tanycytes are now widely accepted to have NSPC qualities, the presence of NSPCs in the parenchyma is much more controversial (Yoo and Blackshaw, 2018).

Tanycytes express many cell markers that are also present in NSPCs in the subgranular and subventricular zone, namely Nestin, BLBP, Musashi1, Sox2, GFAP,

GLAST, Vimentin, UGS148 and Prss56 (Haan et al., 2013; Ma et al., 2015; Jourdon et al., 2016). They also share the radial glia-like morphology of stem cells in the canonical niches (Kriegstein and Alvarez-Buylla, 2009). Self-renewing neurospheres that contain neurons, astrocytes and oligodendrocytes are formed from tanycytes cultures (Weiss et al., 1996; Bennett et al., 2009; Robins et al., 2013). Tanycytes give rise to both NeuN+ neurons and GFAP+ glial cells and may self-renew by generating other tanycytes (Haan et al., 2013; Robins et al., 2013). Parenchymal newborn cells are found in the arcuate, ventromedial, dorsomedial nuclei (Haan et al., 2013; Robins et al., 2013). Some studies also report their presence in the median eminence, posterior hypothalamus, preoptic area of the hypothalamus and lateral hypothalamus (Matsuzaki et al., 2009; Lee et al., 2012; Haan et al., 2013; Chaker et al., 2016) (Fig. 1.4). This suggests a role for adult hypothalamic neurogenesis in regulating energy balance.

As mentioned previously, tanycytes can be classified into α1, α2, β1 and β2 subtypes (Fig. 1.4). There is no agreement as to the which of these domains contains NSPCs of the hypothalamic niche. One study reported high proliferative activity of β2-tanycytes in postnatal mice which generated new neurons mostly in the median eminence, but also much smaller numbers in the arcuate, ventromedial and dorsomedial nuclei (Lee et al., 2012). Some of these neurons respond to leptin injections as shown by their expression of pSTAT3, indicating that they are functionally integrated. In young adults, neurogenesis was dramatically increased when mice were fed high-fat diet for a month, compared to chow-fed animals, and irradiation of ventrobasal hypothalamus and therefore abrogation of neurogenesis led to reduced weight and fat gain, as well as increased energy expenditure in adult mice fed a high fat diet, indicating an energy homeostasis role for the newborn neurons. *Fgf10* expression in the hypothalamus is restricted to β1 and β2 tanycytes and a study used $Fgf10^{LacZ}$ mice, which allows for transient lineage tracing, and $Fgf10^{CreERT2}$::$Rosa26^{tdTomato}$ for inducible lineage tracing of these β-tanycytes (Haan et al., 2013). It was found that *Fgf10*+ β-tanycytes give rise to neurons and astrocytes mostly in the arcuate, but also ventromedial, dorsomedial and lateral nuclei and some of these express NPY and, upon fasting and injection of leptin, c-Fos and pSTAT3. In both studies, the proliferation of β-tanycytes was higher in postnatal ages compared to young adult, but significant numbers of proliferating cells were seen even in animals that were BrdU pulsed at P60, and only in the β-tanycyte domain (Lee et al., 2012; Haan et al., 2013).

The neurogenic potential of α-tanycytes has been assessed through lineage tracing of GLAST^{CreERT2}::Rosa26R^{GFP} or GLAST^{CreERT2}::Rosa26R^{LacZ} mice (Robins et al., 2013). Lineage tracing of adult mice GLAST+ α-tanycytes revealed their potential to constitutively generate neurons and astrocytes at a low rate, as well as tanycytes, including β-tanycytes. In addition, intracerebroventricular injection of FGF2 caused a large increase in proliferation of α2-tanycytes, especially of GFAP- ventral α2-tanycytes, but not of β2-tanycytes or α1-tanycytes. By isolating regions containing α1-tanycytes, dorsal α2-tanycytes, ventral α2-tanycytes or β-tanycytes, they were able to demonstrate that only the GFAP+ population can form self-renewing neurospheres, although ventral α2-tanycytes show high proliferative potential. Collectively, this suggested that α2 tanycytes are FGF responsive NSPCs that can self-renew, give rise to neurons, astrocytes and other tanycytes subtypes.

One important issue that needs to be mentioned here is the disparate ways the tanycyte domains are named. In the Robins et al., (2013) paper, tanycytes were classified into GFAP expressing α1-, dorsal α2-tanycytes, and GFAP- ventral α2- and β- tanycytes, instead of the widely used GFAP+ α1, α2 and GFAP- β1 and β2 tanycytes classification (Goodman and Hajihosseini, 2015). Indeed, there is probably significant or complete overlap between the ventral α2 and β1 domains based on GFAP expression. It is possible therefore that by both using GLAST (Robins et al., 2013) and FGF10 (Haan et al., 2013) Cre drivers, the same neurogenic ventral α2/β1 population of tanycytes was detected.

In one study, lineage tracing of Nestin expressing tanycytes showed that neurogenesis occurs even in mice as old as 9 months and that deletion of IGF-1 receptors in Nestin expressing cells and their progeny enhances neurogenesis (Chaker et al., 2016). The authors conclude that in their study, α-tanycytes are the neurogenic cell population and that they are affected by IGF-1 receptor deletion, yet their criteria for distinguishing domains is based on anatomical location and morphology, following that of Robins et al., (2013), but not marker expression. As Nestin is expressed in both α- and β-tanycytes, it is difficult to distinguish the domains without markers and in this study, the α-domain seems to be restricted to the level of the arcuate nucleus and the β domain confined to the floor of the third ventricle. It is, therefore, possible that the neurogenic region identified here was overlapping with dorsal or ventral α2-tanycytes (Robins et al., 2013) and β1-tanycytes (Haan et al., 2013).

While hypothalamic neurogenesis has been implicated in thermoregulation (Shido and Matsuzaki, 2015) and regulation of reproduction (Lévy et al., 2017), its most investigated potential role is in energy balance. An early study suggested that ICV infusion of CNTF into the lateral ventricles of high-fat diet fed animals causes long-term reductions in body weight and increases the generation of new neurons, many of which were leptin-responsive and some of which expressed NPY and POMC (Kokoeva et al., 2005). When CNTF wa s infused with Ara-C, a mitosis blocking drug, the weight loss effect was short-lived and mice rapidly regained weight through increased food intake. Many studies that explored the link between hypothalamic neurogenesis and energy homeostasis followed. In some, high-fat diet was reported to reduce neurogenesis (Li et al., 2012; McNay et al., 2012), while in some high-fat diet increases neurogenesis (Lee et al., 2012; Gouazé et al., 2013). There are many factors that may lead to such discrepancies, for example, analysis after acute versus long-term high fat diet, or the sex of the animals analysed, as it has been shown that neurogenesis in the ME is affected by high-fat diet and has a role in weight gain only in female mice (Lee et al., 2014). Part of these sex-related differences may be due to the effects of oestradiol (Bless et al., 2014; Bless et al., 2016), underscoring the importance of analysing animals of the same sex.

The occurrence of adult hypothalamic neurogenesis in humans using BrdU or analysis of radioactive carbon has not been directly assessed, unlike for the canonical niches (Eriksson, 1998; Bergmann et al., 2012; Spalding et al., 2013). However, Vimentin expressing tanycytes are found in the adult human hypothalamus and exhibit similar distribution and morphology as in other mammals (Koopman et al., 2017). Furthermore, doublecortin (DCX), a marker expressed in neuroblast and immature neuron marker during adult subgranular and ventricular zone neurogenesis, is present in adult human median eminence, arcuate and ventromedial nuclei (Batailler et al., 2013). Human tanycytes also express NSPC markers Sox2 and Nestin, as well as GFAP and GLAST, and other cells in the adult human hypothalamus were found to express NSPC markers, namely tanycytes, ependymal cells, stellate cells in the suprachiasmatic nucleus and a ribbon of stellate cells near the third ventricle (Pellegrino et al., 2017). While this suggests the potential presence of NSPCs in the adult human hypothalamus, further studies are needed that more directly assess if neurogenesis does take place in the adult human hypothalamus.

In summary, adult hypothalamic neurogenesis is a process with many unknowns in aspects such as age-related dynamics, anatomical destinations of new neurons and the molecular and physiological determinants, among others. However, there is much

interest in potential clinical interventions for metabolic disorders that would target hypothalamic neurogenesis and cause long-term modulation of homeostatic processes (Rojczyk-Golebiewska, Palasz et al. 2014, Recabal, Caprile et al. 2017). The work described in this thesis was performed to provide a better understanding of how the FGF signalling system, described in the following section, is involved in regulating the dynamics of adult hypothalamic neurogenesis and what role it may have in energy balance.

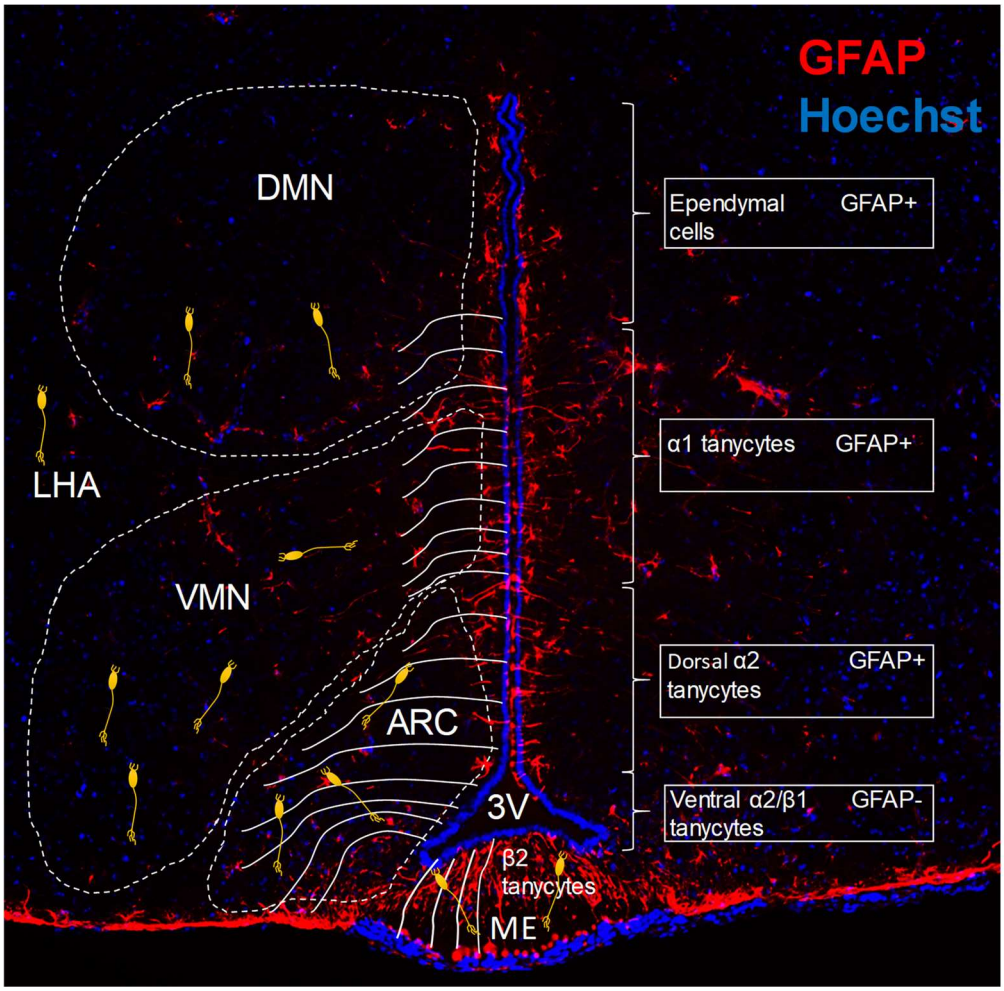

Figure 1.4 – Organisation of adult hypothalamus neurogenic niche. Representation of the hypothalamus neurogenic niche. Tanycytes line the 3V wall and are putative NSPCs in the postnatal and adult mammalian hypothalamus. The precise identity and lineage hierarchy have not been established in terms of tanycytes subtype, but likely NSPC candidates are β2-tanycytes, ventral α2/β1-tanycytes and dorsal α2-tanycytes. New neurons (represented as yellow cells) have been detected in the nearby parenchyma, including the median eminence, lateral hypothalamic area, arcuate, ventromedial and dorsomedial nuclei. White broken lines demarcate the neural nuclei. White solid lines represent tanycytic projections: β2-tanycytes projections terminate on portal blood capillaries in the median eminence; ventral α2/β1 tanycytes project onto laterally positioned portal capillaries or in the ventromedial part of the arcuate nucleus; dorsal α2-tanycytes extend their processes into the dorsal part of the arcuate nucleus, while α1-tanycyte projections terminate in the ventromedial and dorsomedial nuclei. 3V – third ventricle; ARC- arcuate nucleus; DMN – dorsomedial nucleus; GFAP – glial fibrillary acidic protein; LHA – lateral hypothalamic nucleus; ME – median eminence; VMN – ventromedial nucleus. Adapted from Goodman and Hajihosseini, (2015).

1.4 – Fibroblast Growth Factor (FGF) Signalling System

1.4.1 – FGFs and FGF receptors

The FGF signalling system is comprised of 22 FGFs, and 5 FGF receptors (Ornitz and Itoh, 2015). FGFs can be classified into 7 subfamilies based on their phylogeny (Itoh and Ornitz, 2004; Itoh and Ornitz, 2008) (Fig. 1.5 A). Fifteen FGFs (FGFs 1-10, 15-18, 20, 22) act in a paracrine/autocrine mode of action and bind to FGF receptor and heparin sulphate proteoglycan (HSPG) complexes. Endocrine FGFs 15 (mouse) / 19 (human), 21 and 23 act as hormones that bind to FGF receptor and α-Klotho / β-Klotho complexes. FGFs 11-14 lack a signal peptide and act intracellularly in a receptor-independent fashion.

FGF receptors 1-4 typically have two intracellular tyrosine kinase domains, a transmembrane domain and three extracellular immunoglobulin-like domains (Fig. 1.5 B, C), while FGF receptor 5, also known as Fibroblast growth factor-like 1 (FGFRL1), lacks the tyrosine kinase domains (Sleeman et al., 2001) (Fig. 1.5 D). Upon ligand binding, FGF receptors dimerise, forming a 2:2:2 FGF:FGFR:HSPG (Schlessinger et al., 2000) or 1:2:1 FGF:FGFR:α/β-Klotho complexes (Ming et al., 2012). This brings their tyrosine kinase domains to close proximity, allowing transphosphorylation and activation of intracellular signalling pathways (Furdui et al., 2006). The major intracellular pathways activated by FGFR signalling are RAS-MAPK, PI3K-AKT, STAT and PLCγ (Goetz and Mohammadi, 2013) (Fig. 1.6).

FGFR5 has important roles in the development of the diaphragm, kidney and skull (Baertschi et al., 2007; Catela et al., 2009; Gerber et al., 2009; Rieckmann et al., 2009). Its functions are likely mediated by the extracellular domains, as the global deletion of conserved intracellular motifs results in no obvious phenotype, apart from a small reduction in glomeruli number (Bluteau et al., 2014). Instead, FGFR5 and its extracellular domains may act as a cell adhesion molecule based on embryonic kidney cell culture experiments (Yang et al., 2016).

Further complexity is added due to FGF receptor 1, 2 and 3 alternative splicing which generates the major IIIb and IIIc splice isoforms of these receptors (Fig. 1.5 B, C) with different ligand-receptor binding affinities (Zhang et al., 2006a) (Fig. 1.5 A). Multiple mechanisms exist to control FGF ligand and receptor activities and FGF signalling levels, making it an exceedingly complex signalling system with little or no functional redundancy among each of its members (Goetz and Mohammadi, 2013).

Autocrine/paracrine FGF signalling is essential for embryogenesis and fetal development, where it controls multiple processes such as epithelial-mesenchymal signalling in organogenesis and neural development (De Moerlooze et al., 2000; Dorey and Amaya, 2010; Guillemot and Zimmer, 2011). In adult tissues, it has multiple roles, notably paracrine FGFs control tissue homeostasis: angiogenesis, tissue repair, stem cell self-renewal and proliferation (Murakami and Simons, 2008; Coutu and Galipeau, 2011; Maddaluno et al., 2017).

Intracellular FGFs do not interact with FGF receptors (Olsen et al., 2003), but instead associate with voltage-gated sodium channels in neurons (Goldfarb et al., 2007) and cardiomyocytes (Wang et al., 2011), influencing their excitability. FGF13 is also a microtubulin stabilizing protein, with a role in the migration and polarization of newborn neurons (Wu et al., 2012). Recently, FGF11 has been shown to be induced by hypoxia and interact with HIF-1α, stabilising it and in this way further regulating the expression of hypoxia-related genes in a line of human liver cancer cells (Lee et al., 2016).

Figure 1.5 – Members of the FGF signalling system. (A) Table summarises the FGF subfamilies, their members and receptor binding affinities. Subfamily names coloured in blue denote paracrine FGFs, in green – endocrine FGFs and in red – intracellular FGFs. Note that members of the FGF4 and FGF19 subfamilies can only bind FGFR4 and IIIc splice isoforms of FGFR1-3, while FGFs in the FGF7 subfamily can only bind IIIb splice isoforms of FGFR1 and FGFR2. Table adapted from Zhang et al., 2006. (B, C, D) Schematic representations of FGF receptor structure, adapted from Ornitz and Itoh, (2015). FGF receptors typically contain a signal peptide, three immunoglobulin (IgG) -like domains and a transmembrane domain and a linker region between the second and first IgG-like domains (grey box). FGFR1-4 also have two intracellular tyrosine kinase domains (C, D), while FGFR5 lacks these domains (D). The third IgG-like domain of FGFR1-3 has 2 major splice isoforms: IIIb (B) and IIIc (C). I, II, III – IgG-like domains; TK1 – tyrosine kinase domain 1; TK2 – tyrosine kinase domain 2; TM – transmembrane domain; SP – signal peptide. S—S – disulfide bonds.

A

FGF Subfamily	FGF	Cognate Receptor
FGF1 Subfamily	FGF1 →	All FGFRs
	FGF2 →	FGFR 1c, 3c > 2c, 1b, 4
FGF4 Subfamily	FGF4 FGF5 FGF6	FGFR 1c, 2c > 3c, 4
FGF7 Subfamily	FGF3 FGF7 FGF10 FGF22	FGFR 2b > 1b
FGF8 Subfamily	FGF8 FGF17 FGF18	FGFR 3c > 4 > 2c > 1c >> 3b
FGF9 Subfamily	FGF9 FGF16 FGF20	FGFR 3c > 2c > 1c, 3b >> 4
FGF19 Subfamily	FGF19 FGF21 FGF23	FGFR 1c, 2c, 3c, 4 (Requires α/β-Klotho)
FGF 11 Subfamily	FGF11 FGF12 FGF13 FGF24	No Receptor Binding

B

C

D

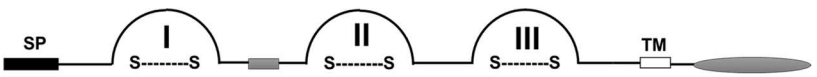

Endocrine FGFs have very low HSPG binding affinities and can diffuse into the bloodstream when released, and bind FGFR-Klotho α/β coreceptor complexes (Itoh et al., 2015). FGF15/19 is synthesised in the ileum and regulate bile acid homeostasis (Inagaki et al., 2005), and glucose metabolism through its effects in the liver (Kir et al., 2011). FGF23 is expressed by osteoblasts and osteocytes, binds to FGFR and β-Klotho complexes in the kidney and regulates phosphate and vitamin D metabolism (Quarles, 2012). FGF21 is an endocrine ligand highly expressed in the liver (Nishimura et al., 2000), pancreas and adipose tissue (Fon Tacer et al., 2010). It has a wide range of metabolic functions, including regulatory roles in fatty acid and glucose metabolism (Fisher and Maratos-Flier, 2016). In addition, FGF21 can readily cross the BBB (Hsuchou et al., 2007) and the effects of FGF21 in the CNS have become an exciting area of research. FGF21 increases glucocorticoid levels, reduces physical activity and changes circadian behaviour: features of adaptive starvation response (Bookout et al., 2013). Moreover, the suprachiasmatic nucleus, where β-Klotho is expressed, is involved in mediating these effects of FGF21. Infusion of FGF21 into the lateral ventricles of diet-induced obese mice for 2 weeks causes increased food intake, energy expenditure and insulin sensitivity (Sarruf et al., 2010). Conditional knockout of β-Klotho under the Camk2a Cre driver specifically in the brain of diet-induced obese mice showed that FGF21 in the CNS regulates energy expenditure through the modulation of sympathetic activity on brown adipose tissue and consequently thermogenesis (Owen et al., 2014).

1.4.2 – Regulation of FGFR signalling levels

FGF signalling levels determine its outcome. For example, development of the midbrain is specified by lower levels of FGFR signalling elicited by FGF8a, FGF17 and FGF18, while higher levels of signalling induce cerebellar fate, evoked by FGFR8b and its higher affinity for FGFR3 IIIc isoform (Guillemot and Zimmer, 2011). Similarly, during coronal suture development, osteoprogenitor cells proliferate when low levels of FGF2 signals through FGFR2 and FGFR3, but differentiate to osteoblasts due to higher levels of FGF2 signalling through upregulated FGFR1 (Teven et al., 2014). In vitro studies of human cortical NSPCs as well as adult rat hippocampal progenitors suggest that low levels of FGF signalling might induce neural differentiation, while high levels suppress this, and promote proliferation and self-renewal (Nelson and Svendsen, 2006; Chen et al., 2007; Keenan et al., 2012). Likewise, inhibition of MEK/ERK1/2 or PI3K/Akt pathways suppresses proliferation

while ERK1/2 inhibition prevents neural differentiation of adult rat spinal cord NSPCs (Chan et al., 2013). These FGF2 effects have been shown to be modulated by the presence of other growth factors which are likely to influence FGF signalling outcomes (Chen et al., 2007).

Due to the importance of regulating FGF signalling levels, it is of no surprise that a complex, multi-layered regulatory system has evolved.

Important elements of that system are extracellular molecules, particularly heparan sulphate proteoglycans (HSPGs). They are part of the FGF ligand-receptor complex as they stabilise their interaction (Yayon et al., 1991). They regulate FGF signalling by sequestering the ligand near the site of action and by create ligand gradients, which are important in embryonic development for processess such as collective cell migration (Venero Galanternik et al., 2015) (Yan and Lin, 2009). Due to these qualities, HSPGs play a vital role in the adult brain neurogenic niches by controlling growth factor activity (Mercier 2016).

FGF receptor signalling itself induces expression of downstream intracellular regulators (Hajihosseini, 2008) (Fig. 1.6). These are mostly negative regulators of FGF receptor signalling and therefore act as part of negative feedback loop, preventing excessive FGF receptor activation. These regulators include dual-specificity MAP kinase phosphatase 6 (DUSP6/MKP3); similar expression to fibroblast growth factor (Sef); Ets variant 4 (ETV4) and the Sprouty family.

- MKP3 acts by binding to and dephosphorylating ERK1/2 (Muda et al., 1996).
- ETV4 is a transcription factor. Although its target genes are not fully defined, it might act on MKP3, mediating the induction of its expression by FGFR (Znosko et al., 2010).
- Sef can inhibit FGFR induced activation of ERK/MAPK as well as pkB/Akt, but also increases phosphorylation of p38 MAPK, depending on Sef isoform and cell type (Kovalenko et al., 2003).
- The Sprouty family of RTK signalling modulators includes 4 members (Sprouty 1, Sprouty 2, Sprouty 3 and Sprouty 4). They are inhibitors of ERK but interact with many other molecules in a complex way to influence cell proliferation, differentiation and survival (Masoumi-Moghaddam et al., 2014).

Their involvement in the regulation of cellular processes during development has been demonstrated (Mao et al., 2009; Newitt et al., 2010; Felfly and Klein, 2013) and

it can be hypothesised that they might continue to modulate stem/progenitor cell responses to FGF signalling in the adult CNS.

Figure 1.6 – FGF receptor signalling pathways. Schematic representation of FGFR intracellular signalling pathways. Upon binding of FGF ligand to the receptor, the receptors dimerise forming a 2:2:2 FGFR:FGF:HSPG complex. Transphosphorylation of tyrosine kinase domains leads to activation of intracellular signalling pathways. The docking protein FRS2α is phosphorylated, leading to further recruitment of GRB2 and SOS and activation of the MAPK and PI3K-Akt pathways which affect gene expression. This includes the induction of genes such as Etv4, MKP3, SPRY and SEF, which then act to inhibit FGFR signalling. Activation of STAT1, STAT3 and STAT5 by FGF receptors also leads to changes in gene expression. PLCγ is recruited and activated by phosphorylated FGFR tyrosine kinases, leading to hydrolysis of PIP2, resulting in the formation of IP3 and DAG. IP3 causes the release of Ca^{2+} from intracellular stores, while DAG activates PKC which stimulates the MAPK pathway and phosphorylates other downstream targets. Adapted from (Yashiro and Matsuoka, 2016) and (Ornitz and Itoh, 2015). Akt – protein kinase B; DAG - diacylglycerol; ERK - extracellular signal-regulated kinase; Ets - E26 transformation-specific; Etv4/5 - ETS translocation variant 4/5; FOXO1 - Forkhead box protein O1; FRS2α -FGFR substrate 2α; GAB1 - GRB2-associated binding protein 1; GRB2 - growth factor receptor-bound 2; HSPG – heparan sulphate proteoglycan; IP3 - inositol triphosphate; MEK - mitogen-activated protein kinase kinase; MKP3 - mitogen-activated protein kinase phosphatase 3; PI3K - phosphoinositide 3-kinase; PIP2 - 2-phosphatidylinositol-4,5-biphosphate; PKC - protein kinase C; PLCγ - phospholipase Cγ; RAF - rapidly accelerated fibrosarcoma; RAS – rat sarcoma; Sef - similar expression to FGF; SOS - son of sevenless; Spry – sprout; STAT1/3/5 - signal transducer and activator of transcription 1/3/5.

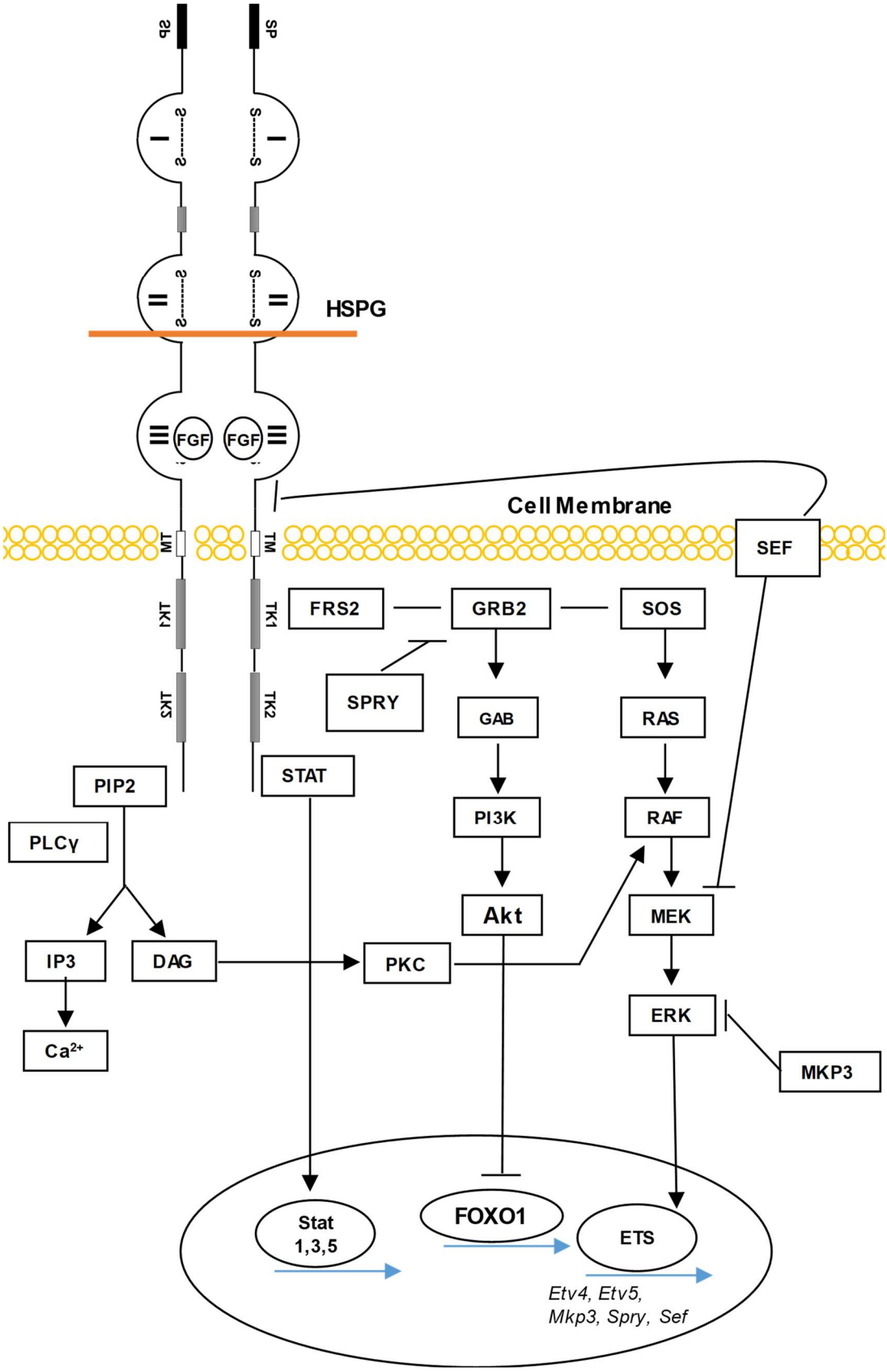
SP
SP
HSPG
FGF
FGF
Cell Membrane
MT
TM
TK1
TK2
TK1
TK2
SEF
FRS2
GRB2
SOS
SPRY
GAB
RAS
STAT
PIP2
PI3K
RAF
PLCγ
Akt
MEK
IP3
DAG
PKC
ERK
Ca2+
MKP3
Stat
1,3,5
FOXO1
ETS
Etv4, Etv5,
Mkp3, Spry, Sef

1.5 – The Roles of FGF Signalling in Adult Neurogenesis

Multiple members of the FGF signalling family are present in the adult CNS in wide distribution. Studies investigating the localisation of certain FGFs and FGFRs found that different members of the FGF signalling family are present within neurogenic niches and that FGF2, FGFR1 and FGFR2 are present within the hippocampus, SVZ and hypothalamus.

In the hippocampus, FGF2 is expressed by astrocytes within the DG, CA1, CA2 and CA3, although in CA2 it is also expressed by neurons. In the SGZ, doublecortin positive immature neurons do not express FGF2 but are surrounded by cells that do (Shetty et al., 2005). FGFR1, FGFR2 and FGFR3 are also expressed in the dentate gyrus (Mudò et al., 2009).

FGF2 is expressed by ependymal cells as well as choroid plexus of the 3rd ventricle and lateral part of the lateral ventricles. These cells might release it to the CSF, thereby possibly having effects on hypothalamic and SVZ adult neurogenesis (Hayamizu et al., 2001). Cells lining the third ventricle also express FGF10, FGF18, FGFR1-IIIc and FGFR2-IIIc (Gonzalez et al., 1994a; Hajihosseini et al., 2008; Robins et al., 2013).

1.5.1 – Subgranular Zone

Genetic studies utilising transgenic mouse have been very informative in elucidating the role of endogenous FGF signalling. The effects on adult hippocampal neurogenesis of *Fgfr1* conditional knockout under the Nestin Cre driver have been described (Zhao et al., 2007). The proliferation of *Fgfr1* deficient SGZ NSPCs is greatly reduced compared to control mice, while cell death is unchanged (TUNEL assay). New neuron generation is also impaired as seen by the 73.9% reduction in new neuron numbers, while astrocyte numbers are also decreased, although to a lower degree. Moreover, LTP in the hippocampus and memory consolidation are greatly impaired. This, therefore, suggests that FGFR1 signalling in Nestin+ NSPCs and their progeny is important for proliferation and neuron generation.

FGFR2 conditional knockout mice under the GFAP CreERT2 driver also show impaired proliferation and generation of new immature neurons in the adult hippocampus, correlated with short-term memory deficiency (Stevens et al., 2012).

Interestingly, FGF2$^{-/-}$ mice show no deficits in proliferation within the DG as pH3 positive cell numbers are unchanged in these animals (Werner et al., 2011). However, newly-formed neurons expressing NeuroD were 65%, DCX ~50% and calretinin 38% less numerous in FGF2 knockout mice. Caspase-3 staining showed that there was no difference in cell death and double labelling with BrdU also suggested that proliferation was not affected, but neural differentiation was reduced. Therefore, it seems that endogenous FGF2 is required for neural differentiation but seemingly not for cell proliferation. It is possible that other FGF ligands signalling through FGFR1 influence proliferation and that is why proliferation is disturbed in FGFR1 conditional knockout, but not FGF2$^{-/-}$ mice (Zhao et al., 2007).

FGF2 levels in the DG and whole hippocampus decrease by middle age due to reduced numbers of astrocytes that express FGF2 (Shetty et al., 2005) and FGFR1 expression is also reduced in aged DG (Bernal and Peterson, 2011). In line with this, following the same BrdU infusion paradigm, 20-month-old mice have BrdU/DCX positive cell numbers in the DG that are only 10% of that seen in 3-month-old mice, and a similar 50% reduction seen in the SVZ. Intracerebroventricular injection of FGF2 returns neurogenesis levels in aged mice to young adult mice levels, indicating that exogenous application of FGFs is effective at increasing neurogenesis in the aged brain (Jin et al., 2003b).

Conditional deletion of *Fgfr1, Fgfr2* and *Fgfr3* (loss of function, LOF) in NSPCs under the Nestin CreER driver causes reduced numbers of DCX or PSA-NCAM expressing immature neurons and NeuN+ mature neurons, while FGFR3 gain-of-function (GOF) in Nestin+ cells causes an increase in the numbers of these cells (Kang and Hébert, 2015). GOF also stimulates proliferation and reverses the reduction of neurogenesis seen in older animals, bringing it to levels on par with ones seen in young adult mice.

1.5.2 – Subventricular Zone

Exogenous FGF2, chronically infused for two weeks into the lateral ventricle of adult rats, results in increased numbers of BrdU labelled cells in the SVZ (Kuhn et al., 1997). No BrdU positive cells were observed in the RMS just after cessation of infusion. However, 4 weeks later, their increased numbers were detected in the granule cell layer in OBs, 96% of which were neurons. This might be due to FGF increasing cell proliferation at a high rate within the SVZ, disrupting migration, which can only occur after supplementation ceases. No changes were observed in the DG, however, possibly due to inefficient FGF2 transport from the ventricles into the

hippocampus (Gonzalez et al., 1994b). Similar results are seen after single subcutaneous FGF2 injection. Mitotic cell numbers triple in the SVZ and olfactory tract, but again, no effects observed in the DG (Wagner et al., 1999). Mitotic effects are similar in neonates (P1, P7-21) and adults (P60) in SVZ.

Another strategy to deliver FGF2 is intranasal administration. In healthy mice, this results in 70% increased BrdU labelling in the SVZ, while also increasing DCX positive neuroblast numbers, and a 40% increase in BrdU labelled OB cells (Jin et al., 2003a). However, no effects were seen in the DG, possibly due to lower availability of FGF2 to the DG through intranasal administration.

Intracerebroventricular (ICV) FGF2 injection has also been found to induce PDGFαR negative neural progenitors to differentiate into PDGFαR positive oligodendrocyte progenitor cells in the SVZ as well as increasing proliferation of both cell types and their migration from the SVZ (Azim et al., 2012).

1.5.3 – Hypothalamus

It is apparent that FGF signalling has important roles in regulating adult neurogenesis in the canonical niches. However, few studies have investigated the role of FGF signalling in adult hypothalamic neurogenesis, owing to the relatively recent emergence of the field.

Injections of FGF2 into the third ventricle have been performed, dramatically increasing the usually low BrdU labelling in the ependymal lining, more so than EGF or BDNF injections (Xu et al., 2005). These injections induce numerous cells with astrocytic morphology and expressing BLBP, a radial glial cell marker. A month after injection, BrdU labelled astrocytes and neurons were also present, some expressing Orexin A, a peptide involved in appetite regulation.

Intracerebroventricular injections of FGF2 for a week increase proliferation of ventral α2/β1 -tanycytes immediately after the treatment (Robins et al., 2013). Another study confirmed that intracerebroventricular FGF2 infusion causes proliferation of tanycytes in 3-month old mice, and lineage-traced Prss56 expressing GFAP- tanycytes were also co-labelled with BrdU (Jourdon et al., 2016). In a similar vein, a recent paper showed that adult hypothalamic neurogenesis is enhanced in stroke-prone spontaneously hypertensive rats that performed wheel running (Niwa et al., 2015). This enhancement was associated with increased FGF2 in subependymal $GFAP^+$ cells and cerebrospinal fluid.

The expression of FGF10 in β-tanycytes and their neurogenic potential has been reported (Hajihosseini et al., 2008; Haan et al., 2013). However, while these tanycytes express FGF10, it is not clear what its function or mode of action is, considering the fact that only IIIc splice isoforms of FGF were detected in the hypothalamus by RT-PCR, while FGF10 can only bind to IIIc splice isoforms (Hajihosseini et al., 2008). This suggests that FGF10 might have an intracellular, receptor-independent mode of action as postulated by (Mikolajczak et al., 2016).

FGF18 is also expressed in GFAP- ventral α2/β1-tanycytes, although its role has not been described yet (Robins et al., 2013).

FGF1 is released from rat ependymal cells lining the third ventricle after a meal or glucose injection into the third ventricle and acts on parenchymal neurons to reduce food intake (Oomura et al., 1992). Intriguingly, a single injection of FGF1 into the lateral ventricles of diabetic mice causes sustained remission of hyperglycaemia lasting at least 17 weeks (Scarlett et al., 2016). In this study, FGF1 activated tanycytes as evidenced by induction of c-Fos and HSP25, suggesting that tanycytes may have a role in mediating the long-term effects, potentially through stimulation of neurogenesis.

1.6 – Aims

It is evident that some tanycytes form a population of neural stem/progenitor cells in the postnatal and adult hypothalamus that proliferate in response to exogenous application of FGF2. Furthermore, tanycytic FGF signalling may have roles in metabolism. However, the lack of knowledge of which endogenous FGFs and FGF receptors are expressed in tanycytes and the nearby parenchyma and their exact location in these compartments are a hurdle to a fuller understanding of these processes and their regulation by FGF signalling. In addition, cellular and physiological responses to exogenous FGFs suggest important roles of tanycytic receptors, yet their endogenous signalling has scarcely been explored.

The aims of this project and the approaches taken are detailed below:

1. Current knowledge of FGF signalling system expression in the hypothalamic neurogenic niche is fragmented and incomplete. To discover previously undescribed expression patterns of endogenous FGF signalling components in the adult hypothalamus neurogenic niche and to determine the precise

tanycyte compartment of their expression, a gene expression survey was conducted.

2. While exogenous application of FGF ligands has been shown to increase tanycyte proliferation, studies of other growth factors have reported differing tanycyte responses to exogenous and endogenous signalling modulation (Perez-Martin, Cifuentes et al. 2010, Chaker, George et al. 2016). This project aimed to determine if endogenous FGF receptor signalling in tanycytes has roles in regulating their proliferation, differentiation and other cellular processes, in this way impacting postnatal and adult hypothalamic neurogenesis. This was assessed by lineage tracing *Fgf10* expressing tanycytes deficient in these receptors.
3. Metabolic effects of modulating FGF signalling in the hypothalamus have been reported, but the interventions vary in their type, have widespread sites of action and the findings of different studies can be difficult to reconcile. To ascertain if β-tanycytes are mediators of the metabolic effects of hypothalamic FGF signalling found in these studies, FGF receptors were deleted specifically in *Fgf10* expressing tanycytes and the impact on physiology measured in metabolically challenged animals.
4. Initial investigations into receptor-independent FGF10 signalling in the embryonic hypothalamus have suggested that it is involved in regulating the expression of several genes, including the orexigenic molecule Agouti-related neuropeptide (*Agrp*). To confirm these preliminary findings and explore the molecular mechanisms involved, the downregulation of *Agrp* in FGF10 KO embryonic hypothalamus was validated along with other genes that may be involved.

Chapter 2

Materials and Methods

2.1 - Transgenic mouse lines

Mice were bred on a mixed C57BL6/129Ola background, under a 12-hour light/dark cycle. The studies were conducted in line with local regulations concerning work with transgenic animals.

Brains of $Fgf18^{CreERT2}$::$Rosa26^{tdTomato}$ and $Fgf9^{LacZ}$ animals were received from David Ornitz group (Washington University School of Medicine, St. Louis, Missouri, USA), and $Etv4^{GFP}$ animals from Saverio Bellusci group (Justus Liebig University, Giessen, Germany), therefore these mice were not bred in our animal facility.

2.1.1 – $Fgf10^{LacZ}$

The $Fgf10^{LacZ}$ transgenic mouse line has the *Mlc1v-nlacZ-24* transgene inserted into *Fgf10* regulatory regions 114 kb upstream of the *Fgf10* coding sequence (Fig 2.1 A) (Kelly et al., 2001). In these mice, expression of *LacZ* closely matches expression patterns of *Fgf10* and can be used for transient lineage tracing of *Fgf10* expressing cells due to the bacterial origin of the protein product β-galactosidase. Detection of β-galactosidase in tissues collected from $Fgf10^{LacZ}$ mice was performed using 5-bromo-4-chloro-3-indolyl-β-d-galactoside (X-gal).

2.1.2 - $Fgf10^{CreERT2}$

To generate this mouse line, tamoxifen-inducible Cre recombinase (Cre-ERT2-IRES-YFP) was inserted into the first exon of the Fgf10 locus (Fig 2.1 B) (El Agha et al., 2012). This disrupts Fgf10 function, as $Fgf10^{CreERT2}$ homozygous mice show near absent expression levels of *Fgf10*, have lung and limb defects. They are useful for studying the function of *Fgf10* in embryonic development but do not survive after birth. However, heterozygous $Fgf10^{CreERT2}$ mice are fertile and viable. When bred with mice carrying floxed alleles, tamoxifen administration causes recombination specifically in Fgf10 expressing cells. Therefore, these animals can be used for examining *Fgf10* expression, lineage tracing of *Fgf10* expressing cells and deletion of genes in *Fgf10* expressing cells.

2.1.3 – Rosa26^{tdTomato}

The Rosa26 locus is a common target for insertion of transgenes for constitutive expression (Soriano, 1999). In the Rosa26^{tdTomato} strain, tdTomato is inserted into the Rosa26 locus, downstream of a STOP cassette which is flanked by *flox* sites (Fig 2.1 C) (Madisen et al., 2009). Crossing mice carrying these alleles with Fgf10^{CreERT2} mice allows to conditionally induce expression of tdTomato in *Fgf10* expressing cells.

2.1.4 – Fgfr1^{Flox}

In this mouse line, LoxP sites were incorporated into intron 7 and 15 of the *Fgfr1* locus (Fig 2.1 D) (Hébert et al., 2003). Therefore, Cre mediated recombination results in excision of exons 8-15, essential for *Fgfr1* function.

2.1.5 – Fgfr2^{Flox}

Insertion of LoxP sites into intron 7 and 10 of the *Fgfr2* locus results in the Fgfr2^{Flox} allele (Fig 2.1 E) (Yu et al., 2003). Cre mediated recombination causes the excision of exons 8-10, disrupting *Fgfr2* function.

2.1.6 – Fgfr2-IIIb^{null}

Deletion of exon 8 of *Fgfr2* (Fig 2.1 F) results in transgenic mice that can express Fgfr2-IIIc, but not Fgfr2-IIIb splice isoforms (De Moerlooze et al., 2000). Mice homozygous for this allele do not survive after birth as they exhibit major developmental defects, including that of the limbs, lungs and skull.

2.1.7 - Fgf18^{CreERT2}::Rosa26^{tdTomato}

This mouse line was generated by insertion of SA-eGFP:CreERT2 into the first intron of *Fgf18* (Fig 2.1 G) (Zhang et al., 2016). Fgf18^{CreERT2}::Rosa26^{tdTom} mice can, therefore, be used for detecting expression of *Fgf18* and lineage tracing of *Fgf18* expressing cells.

2.1.8 – Fgf9^{LacZ}

A SA-LacZ gene, inserted into the first intron of *Fgf9* (Fig 2.1 H) allows for the detection of β-galactosidase in *Fgf9* expressing cells (Huh et al., 2015).

2.1.9 – Etv4^{GFP}

The Etv4-GFP BAC line was generated by fusing exon 9 of *Etv4* with EGFP and replacing *Etv4* exons 10-13 (Fig 2.1 I), resulting in EGFP expression that matches the endogenous *Etv4* expression pattern, but no functional exogenous *Etv4* protein (Lamballe et al., 2011).

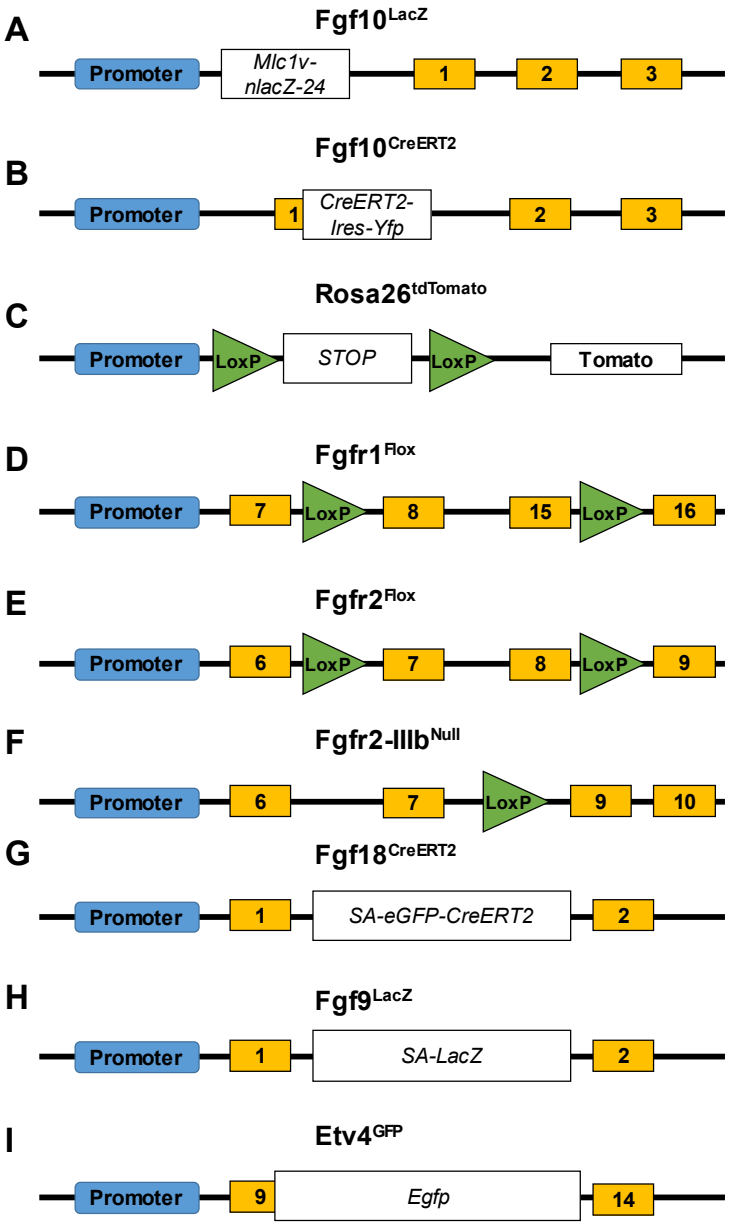

Figure 2.1 – Transgenic mouse alleles. Simplified representations of the transgenic mouse alleles used. Orange boxes represent exons, green triangles - LoxP sites, blue boxes - promoter regions, white boxes – gene cassettes.

2.2 – Genotyping

Genomic DNA for genotyping was isolated from these tissues:

1. Tail (~ 5 mm snip).
2. Ear (~ 2 mm disk).

The tissue was digested overnight in microcentrifuge tubes containing 100-200 µl digestion buffer (0.1 M Tris Base, 5 mM EDTA, 0.2 M NaCl, 0.2 % w/v SDS, diluted in double distilled H_2O, pH 8.0) supplemented with 7 µg/ml Proteinase K (Sigma), placed in a 55 °C hybridization oven. The DNA was isolated by applying an equal volume of Isopropanol and vigorously shaking the microcentrifuge tubes for 5 minutes. The DNA was then spooled out using sterile pipette tips and dissolved in 30% TBE overnight in a 37 °C water bath.

The PCR reactions were carried out in a thermocycler (MJ Research) using the *Expand Long Template System* (Roche). Cycles and primers are described in Table 2.1 and Table 2.2 respectively.

2.3 – Reverse Transcriptase PCR

RT-PCR was carried out in a thermocycler (MJ Research) using isolated hypothalamic mRNA and *illustra Ready-To-Go*™ RT-PCR beads (GE Healthcare Life Sciences). Primers used are detailed in Annex Tables 1-4. Cycles used were as follows. First strand synthesis with Oligo $(dT)_{12\text{-}18}$ primers (Invitrogen): 15 minutes at 42 °C, 5 minutes at 95 °C and 6 °C. After adding 1.5 pmol of forward and reverse gene-specific primers, PCR was carried out with these cycles: 30 seconds at 95 °C, then 34 cycles of 30 s at 60 °C, 1min at 68 °C, followed by one cycle at 6 °C. The product was resolved on 1% w/v agarose gel, stained and visualised with ethidium bromide. An RT-PCR reaction with β-Actin primers was used as a positive control.

2.4 – Tamoxifen administration

Pups were administered 100µg tamoxifen (Sigma), diluted in 10% ethanol/corn oil (Mazola), by manual suckling at P4 and P5.

Young adult mice received intraperitoneal (IP) injections of tamoxifen (100 mg/kg) once daily at P44 and P45 for lineage tracing, or IP injections P44-P50, followed by

14 days of *ad libitum* chow supplemented with supplied with 0.4g tamoxifen citrate salt for physiological experiments described in Chapter 6.

Andrew Hagan (David Ornitz Group, Washington University School of Medicine, St. Louis, Missouri, USA) performed tamoxifen IP injections (300 mg/kg) on $Fgf18^{CreERT2}$::$Rosa26^{tdTomato}$ mice at P50, P51 and P52, brain dissection at P53.

2.5 – Isolation and Sectioning of Tissue

Mice were sacrificed by CO_2 asphyxiation. For tissue to be used for in situ hybridization or immunohistochemistry, this was followed by transcardial perfusion with pre-cooled 4% paraformaldehyde (PFA, pH 7.0). This was done in order to better preserve the anatomical structures studied, while preventing imunohistological artefacts and the degradation of mRNA (ISH) and protein (IHC) (Adickes, Folkerth et al. 1997, Lavenex, Lavenex et al. 2009). Brains were then dissected out and fixed overnight by immersion in 4% PFA at 4 °C. Alternatively, after asphyxiation and cervical dislocation, the hypothalami were dissected out for RNA isolation, flash frozen in centrifuge tubes on dry ice and stored at -80 C°; if required, the fat pads were also dissected and weighed. In this case, cervical dislocation and flash freezing of tissue sufficed for preservation of mRNA, as the anatomical architecture need not be completely intact for mRNA isolation and subsequent RT-PCR, whereas PFA fixation would interfere with mRNA extraction and therefore transcardial perfusion was not appropriate (Auer, Mobley et al. 2014). For dissecting embryonic brains, mothers were sacrificed via cervical dislocation, the embryos taken out of the placenta and brains dissected out, fixed overnight in 4% PFA at 4 °C, then processed either for in situ hybridization on cryostat sections or whole mount in situ hybridization. Immersion fixation of the dissected embryonic brain tissue is adequate due to the much smaller size of embryonic brains, allowing for sufficient penetration of the fixative and similar fixation procedures have been described elsewhere (Muñoz-Elias, Marcus et al. 2004).

For in situ hybridization on cryostat sections, the brains were washed with DEPC treated PBS (DEPC-PBS), transferred into tubes containing 30% w/v sucrose diluted in DEPC-PBS for 48 hours at 4 °C. Afterwards, they were put into foil cryomoulds filled with optimal cutting temperature compound (OCT), frozen on dry ice and stored at -80 °C.

A mouse brain atlas was used to determine the anatomical location of sections, as defined by Bregma coordinates (Franklin and Paxinos 2008). These coordinates refer to the rostro-caudal position in relation to the intersection point of the midline and anterior sutures, in millimetres (McIntyre 2006). Positive values denote anterior positions, while negative values refer to caudal positions and are referred to in figures, where appropriate.

Brains were sectioned using a freezing microtome (MicroM HM560) to yield 20 µm thick coronal sections containing central median eminence (Bregmas -1.58 to -1.94). These were collected on previously baked (180°C, overnight) superfrost (ThermoFisher Scientific) slides and stored at -80 °C until use.

For immunohistochemistry on vibratome sections, fixed brains were washed with PBS before undergoing serial dehydration in solution with increasing alcohol concentration (30%, 50%, 70%, 90%; 1 hour per dilution) before being stored at 4 °C in absolute ethanol. Brains kept at absolute ethanol were rehydrated and embedded in 3% w/v agar overnight, before being sectioned by a vibrating microtome (Leica) to obtain 60 µm thick coronal sections containing median eminence (Bregmas -1.46 to -2.18).

For whole mount in situ hybridization, embryos or adult hypothalami were dehydrated in ascending series of Methanol diluted in DEPC-PBST (30%, 50%, 70%. 90%, 100%; 5-10 minutes for each step), stored at -20 °C until required.

Programme Name	Temperature (C°)	Length (s)	Cycle Repeats
FGF10-CreERT2	94	120	1
	94	30	9
	61	30	
	68	160	
	94	30	17
	61	30	
	68	160 (+40s each cycle)	
	68	420	1
	6	600	1
Rosa26-Tomato	94	120	1
	94	30	15
	60	30	
	68	70	
	94	30	17
	60	30	
	68	70 (+20s each cycle)	
	68	420	1
	6	600	1
Fgfr1-flox	94	120	1
	94	30	10
	55	50	
	68	180	
	94	30	15
	55	50	
	68	240 (+30s each cycle)	
	68	420	1
	6	600	1
Fgfr2-flox	94	120	1
	94	30	15
	58	30	
	68	190	
	94	30	17
	58	30	
	68	190 (+20s each cycle)	
	68	420	1
	6	600	1
Fgfr2-IIIb	94	120	1
	94	30	10
	61	30	
	68	190	
	94	30	16
	61	30	
	68	190 (+20s each cycle)	
	6	900	1
	68	60	3

Table 2.1 – Genotyping PCR Cycles.

Allele	Primer Sequence (5'-3')	Product size (kb)	Cycle
Fgf10^{CreERT2}	AGC AGG TCT TAC CCT TCC AGT ATG TTC C	CreERT2: 0.5	FGF10-CreERT2
	TCC ATG AGT GAA CGA ACC TGG TCG		
	AGC AGG TCT TAC CCT TCC AGT ATG TTC C	WT: 0.3	
	CTC CTT GGA GGT GAT TGT AGC TCC G		
Rosa26-Tomato	CTG TTC CTG TAC GGC ATG G	Tomato: 0.2	Rosa26-Tomato
	GGC ATT AAA GCA GCG TAT CC		
	AAG GGA GCT GCA GTG GAG TA	WT: 0.3	
	CCG AAA ATC TGT GGG AAG TC		
Fgfr1^{flox}	GTT ATT AGG TCC CTC GAC GGT ATC	Flox: 0.5	Fgfr1-flox
	GCT CTT GGC CAG CTT GTG CAC AG		
	CCC CAT CCC ATT TCC TTA CCT	WT: 1.0	
	GCT CTT GGC CAG CTT GTG CAC AG		
	GTT ATT AGG TCC CTC GAC GGT ATC	Null: 0.5	
	TCT TCC ACC AAC TGC TTG AAC G		
Fgfr2^{flox}	ATA GGA GCA ACA GGC GG	WT: 0.2 Flox: 0.15	Fgfr2-flox
	TGC AAG AGG CGA CCA GTC AG		
	ATA GGA GCA ACA GGC GG	Null: 0.5	
	CAT AGC ACA GGC CAG GTT G		
Fgfr2-IIIb^{null}	CCC ATC CTC CAA GCT GGA CTG CCT	Null: 1.7 WT: 2.8	Fgfr2-IIIb
	CAG AAC TGT CAA CAA TGC AGA GTG		

Table 2.2 - Primers used for Genotyping.

2.6 – RNA isolation

Following dissection, hypothalami were homogenised by triturating in 1 ml of TRIzol (Invitrogen) using a pipette. After adding 200 µl of chloroform, the samples were centrifuged (15 minutes at 12,000 x*g)*. The aqueous layer was removed and RNA precipitated with 500 µl of Isopropanol by briefly vortexing the sample and a 10-minute

incubation at RT. The samples were centrifuged (15 minutes at 12,000 xg). The supernatant was removed carefully, 1 ml of 75% ethanol diluted in molecular grade water (Sigma) was added and the samples centrifuged (12 minutes at 5,200 xg). The RNA pellet was then briefly air dried, resuspended in molecular grade water (Sigma) at 55 C° for 10 minutes, and the concentration and quality measured with a spectrophotometer (Nanodrop ND-1000, Thermo Scientific). RNA stored at -80 C° until use.

2.7 – Immunohistochemistry

Primary antibodies and conditions are described in Table 2.3.

Antibody	Host	Dilution	Sectioning method	Antigen Retrieval	TSA	Manufacturer
Anti-GFAP	Mouse	1:1000	Cryostat/ Vibratome	No	No	Merck Millipore
Anti-S100β	Mouse	1:200	Cryostat/ Vibratome	Citrate Buffer	No	Abcam
Anti-DsRed	Rabbit	1:1000	Vibratome	No	No	Clontech
Anti-Phospho-pERK	Rabbit	1:200	Vibratome	No	No	Cell Signalling Technology
Anti-GFP	Rabbit	1:1000	Vibratome	No	No	Abcam
Anti-PCNA	Mouse	1:500000	Vibratome	Acid/Alcohol	Yes	Chemicon
Anti-AGRP	Rabbit	1:200	Cryostat	No	No	Phoenix Pharmaceuticals
Anti-Digoxigenin-AP	Sheep	1:5000	Cryostat	No	No	Roche
Anti-Digoxigenin-POD	Sheep	1:1000	Cryostat	No	Yes	Roche

Table 2.3 - Primary antibodies and conditions. Anti-Digoxigenin-AP and Anti-Digoxigenin-POD antibodies were used for in situ hybridization experiments, the rest were used for immunohistochemistry.

Pre-treatments were performed when required and in this order:

For acid/alcohol treatment, floating sections were incubated in 5% glacial acetic acid/95% ethanol solution (pre-chilled at -20°C) for 20 minutes, followed by three 10-minute washes in PBS.

Sodium citrate buffer antigen retrieval was performed by incubating floating sections in sodium citrate buffer (10mM Tri-sodium citrate, 0.05% Tween-20, pH 6.0) for 10

minutes at room temperature and subsequently for 15 minutes at 70°C, followed by two 10-minute washes with PBS.

Tyramide signal amplification requires horseradish-peroxidase to catalyse the deposition of label (Warford et al., 2014). Therefore, endogenous peroxidases needed to be inactivated before the TSA reaction, to prevent background. To do this, floating sections were bleached with 6% hydrogen peroxide, diluted in PBS, for 90 minutes at room temperature, followed by a 10-minute wash with PBS.

Floating sections were incubated for 2 hours in blocking solution (20% heat-inactivated normal goat serum (hiNGS), 1% Triton X-100 (TX), diluted in PBS) and then incubated overnight at 4 °C in primary antibody solution (0.2% hiNGS and 0.1% TX, diluted in PBS) containing primary antibodies (Table 2.3). After overnight incubation, sections were washed five times for 1 hour at room temperature in a solution containing 0.2% hiNGS and 0.1% TX diluted in PBS. This was followed by an overnight incubation with relevant secondary fluorophore-conjugated antibodies (Table 2.4) diluted in secondary antibody solution (0.2% hiNGS and 0.5% NP-40, diluted in PBS) at 4°C.

Antibody	Conjugate	Host	Dilution	Manufacturer
Anti-Mouse IgG	HRP	Goat	1:1000	Sigma-Aldrich
Anti-Rabbit IgG	Chromeo 488	Goat	1:1000	Active Motif
Anti-Mouse IgG	Chromeo 488	Goat	1:1000	Active Motif
Anti-Rabbit IgG	Alexa Fluor 568	Goat	1:1000	Abcam
Anti-Mouse IgG	Alexa Fluor 568	Goat	1:1000	Invitrogen
Anti-Mouse IgG2a	Biotin-SP	Goat	1:300	Jackson ImmunoResearch
Streptavidin	Cy2	N/A	1:800	Jackson ImmunoResearch

Table 2.4 - Secondary antibodies.

Six 30-minute washes with PBS were followed by Hoechst counterstaining, after which the sections were mounted on slides and cover-slipped in Vectashield (Vector Labs).

For TSA based detection, following the primary antibody incubation and washes, sections were treated with second blocking solution (1% bovine serum albumin, 0.3% TX, 0.2% powdered skim milk, diluted in PBS) for one hour before overnight incubation at 4 C with relevant secondary antibodies (Table 2.4) diluted in second blocking solution. After six 30-minute washes with PBS/0.05% Tween-20, sections

were mounted on slides. This was followed by tyramide signal amplification and subsequent washes, performed using the TSA Plus Fluorescein kit as per manufacturer instructions (Perkin Elmer). After counterstaining, the slides were cover-slipped in Vectashield (Vector Labs).

2.7.1 – PCNA/DsRed immunohistochemistry

Simultaneous PCNA and DsRed immunohistochemical detection required a slightly modified protocol, potentially due to the extremely low concentration of the anti-PCNA antibody used (1:500,000).

First, acid/alcohol and peroxidase quenching were performed, followed by blocking of unspecific binding sites with first blocking solution and overnight incubation with only the anti-PCNA antibodies diluted in primary antibody solution. This was followed by five 1-hour washes with 0.2% hiNGS and 0.1% Triton X-100 diluted in PBS, blocking of unspecific binding sites with first blocking solution and overnight incubation at 4 C° with anti-DsRed antibodies diluted in primary antibody solution. After five 1-hour washes with 0.2% hiNGS and 0.1% Triton X-100 diluted in PBS, sections were incubated for 1 hour in second blocking solution and then overnight at 4 C° in second blocking solution with secondary antibodies. After these steps, the washes and TSA steps were carried out as described previously.

2.7.2 – Immunohistochemistry on cryostat sections

Immunohistochemistry using anti-AGRP antibodies (Table 2.3) was carried out on 20 µm thick cryostat sections mounted on glass slides. All steps were performed in a humidified chamber.

Non-specific binding sites were blocked by incubating the sections for an hour in a solution containing 10% hiNGS and 1% Triton X-100, diluted in PBS. Sections were then incubated overnight at 4 C° in a solution containing anti-AGRP antibodies, 0.2% hiNGS and 0.1% Triton X-100, diluted in PBS. Afterwards, the unbound primary antibody was washed off with a solution of 0.2% hiNGS and 0.1% diluted in PBS for three times, 5 minutes each. After a 2-hour incubation at RT with the secondary antibody, diluted in 0.2% hiNGS, 0.5% NP-40 and PBS, sections were washed 3 times with PBS, counterstained with Hoechst and cover-slipped.

2.8 – X-gal staining

Detection of β-galactosidase in Fgf10$^{LacZ/+}$ and Fgf9$^{LacZ/+}$ tissue was performed slightly differently, as the former was performed by our lab and the latter by members of the David Ornitz group (Washington University School of Medicine, St. Louis, Missouri, USA).

2.8.1 – X-gal staining for Fgf10$^{LacZ/+}$ mice

Brains dissected from Fgf10$^{LacZ/+}$ mice were collected and stained by Dr Niels Haan as follows:

Freshly dissected tissue was incubated in X-gal solution (0.12 mM Crystalline Potassium Ferricyanide, 0.12 mM Potassium Ferricyanide Trihydrate, 0.05 millimolar MgCl2, 1.22 mM X-gal, 2.5% v/v N,N Dimethylformamide; diluted in PBS) overnight at 37 °C in a hybridization oven while rotating. The tissue was then post-fixed in 4% PFA solution for 1 hour and then rehydrated to be processed for vibratome sectioning.

2.8.2 - X-gal staining for *Fgf9*$^{LacZ/+}$ mice

Brains from *Fgf9*$^{LacZ/+}$ mice were collected and X-gal stained by Dr Kannan Karuppaiah (David Ornitz Group, Washington University School of Medicine, St. Louis, Missouri, USA). The staining was performed as follows:

The tissue was fixed in Mirsky's fixative (National Diagnostics) overnight at 4 ºC. It was then washed three times with PBT (PBS with 0.1% Tween-20) before being incubated with the LacZ staining solution (2 mM MgCl2, 5 mM K3, 5 mM K4, 0.02% v/v NP-40, 0.1% v/v X-Gal; diluted in PBS) at 37 ºC for 30 minutes. The solution was then washed off with PBS and tissue post fixed with 4% PFA, then rehydrated to be processed for vibratome sectioning.

2.9 – cRNA probe design and synthesis

Primers were designed to amplify target gene sequences and generate cDNA template for riboprobe synthesis (Appendix Tables 1, 2, 3 and 4). This was done by using NCBI primer-BLAST to ensure primer specificity. T7 polymerase promoter sequence (TAATACGACTCACTATAGGG) was added to the 5' end of the reverse

primers to allow in vitro transcription of antisense cRNA probes. (Hajihosseini and Heath, 2002)

NCBI BLAST was used to ensure that riboprobe sequences were specific to the target mRNA.

Digoxigenin labelled antisense RNA probes were generated by using T7 RNA polymerase (ThermoFisher Scientific) and DNA templates either from plasmids or RT-PCR products (Appendix Tables 1, 2, 3 and 4) tagged with T7 polymerase promoter sequence.

The purified riboprobes were kept at -20 °C until use.

2.10 – Whole Mount In Situ Hybridization (WMISH)

Tissues were rehydrated in descending series of Methanol diluted in DEPC-PBST (90%, 70%. 50%, 30%, DEPC-PBTS; 5-10 minutes for each step). They were then digested with 10 µg/ml Proteinase K in DEPC-PBST for 50 minutes at room temperature, then washed with DEPC-PBST for 5 minutes. Afterwards, tissues were fixed in a 4% PFA, 0.1% glutaraldehyde solution for 20 minutes and washed twice with DEPC-PBST for 5 minutes. Prehybridization was carried out at 55 °C in hybridization buffer (50% formamide, 5mM EDTA, 1.3X SSC, 0.5% CHAPS, 0.1% Tween-20, 1% blocking powder (BBR, Merk), 100µg/ml yeast tRNA, 50 µg/ml heparin; diluted in DEPC d.d. H_2O) for 5 hours. Afterwards, cRNA probes were added at 2000 – 2500 ng/ml concentration and hybridized overnight at 55 °C.

After hybridization, post-hybridization washes at 55 °C were as follows: once for 30 minutes in hybridization buffer, twice for 30 minutes in a solution of 50% formamide, 2x SSC, once for 20 minutes in a solution of 25% formamide, 1x SSC, diluted in Tris-buffered saline with 0.1% Tween-20 (TBST). Tissues were then washed at room temperature twice for 30 minutes in TBST, twice for 10 minutes in maleic acid buffer with Tween-20 (0.1 M maleic acid, 0.15 M NaCl, 0.1% Tween-20, diluted in water; MABT) and then once in MABT with 10% heat-inactivated goat serum (hiNGS). Blocking of non-specific binding sites was carried out by incubating tissues for 2 hours in MABT with 20% hiNGS, then alkaline phosphatase conjugated antibodies were added to the blocking solution at 1:2000 dilution and incubated overnight at 4 °C.

After the overnight incubation with antibodies, six washes were carried out for one hour with MABT at room temperature and then a wash with MABT overnight at 4 °C.

Tissues were then washed twice for 15 minutes in alkaline phosphatase buffer (0.1 M Tris buffer pH 9.5, 0.1 M NaCl, 20 mM $MgCl_2$, 0.1 % Tween-20, 2 mM Levamisole, diluted in water; NTMT). The chromogenic reaction was then carried out in the dark in a solution of NTMT supplemented with 375 µg/ml NBT and 187.5 µg/ml BCIP. The reaction was stopped when sufficient colouration has occurred, by washing twice with PBST for 5 minutes and fixing tissues in 4 % PFA for 30 minutes. After a wash in PBST, tissues were kept in PBS at 4 ºC and before being imaged.

2.11 – In Situ Hybridization on Cryosections (ISH)

Slides containing cryosections were removed from -80 °C storage, placed in a slide box and equilibrated at room temperature for 1 hour. This was followed by fixation in 4% PFA at room temperature and three 5-minute washes with DEPC-PBS. Digestion with proteinase K buffer (50 mM pH 8.0 Tris-HCl, 5 mM EDTA, 1µg/ml Proteinase K) was performed for 50 minutes with slow rocking. Sections were then post-fixed with 4% PFA at room temperature for 5 minutes, followed by three 5-minute washes with DEPC-PBS. Sections were then incubated in acetylation solution (1.355% triethanolamine, 0.175% HCl, 0.25% acetic anhydride) while shaking vigorously for 10 minutes, followed by three 5-minute washes in DEPC-PBS. Prehybridization was performed by covering the sections with hybridization buffer (50% formamide, 5x salt sodium citrate buffer (SSC), pH 7.0, 5x Denhardt's solution, 0.25 mg/ml salmon sperm DNA, 0.5 mg/ml yeast tRNA) for 4 hours. Afterwards, sections were hybridized at 68 °C or 72 °C (Table 2.5) in a hybridization oven for 16-18 hours with 500 ng/ml riboprobe, diluted in hybridization buffer.

After hybridization with riboprobes, sections were washed with 5x SSC for 5 minutes at the temperature used for hybridization, followed by three 30-minute washes with 0.2x SSC at hybridization temperature and a wash with 0.2x SSC at room temperature. Sections were then washed with Tris-HCl/saline buffer (100 mM Tris-HCl, pH 7.5, 150 mM NaCl) at room temperature and then blocked in Tris-HCl/saline buffer with 10% hiNGS. Incubation with an anti-digoxigenin antibody conjugated with alkaline phosphatase (Table 2.3) diluted in Tris-HCl/saline buffer with 3% hiNGS was carried out at 4 °C overnight.

After incubation with antibody, sections were washed six times for 15 minutes in Tris-HCl/saline buffer, then equilibrated for 5 minutes with NTM buffer (0.1 M Tris-HCl, pH 9.5, 0.1 M NaCl, 50 mM $MgCl_2$) and then incubated at room temperature in NTM buffer

containing 2 mM Levamisole, 375 µg/ml NBT and 187.5 µg/ml BCIP. Sections were incubated in this solution until specific staining is observed, with overnight incubation performed at 4 °C if needed. The reaction is stopped by three 5-minute washes with PBS, followed by a wash with 95% ethanol, diluted in d.d. H_2O, for 1 hour, shaking lightly. Sections are then rehydrated in d.d. H_2O for 15 minutes before being coverslipped in 50% glycerol, diluted in PBS.

cRNA Probe	Hybridization Temperature (°C)
Fgfr1	68
Fgfr2	68
Fgfr3	68 and 72
Fgf1	68 and 72
Fgf2	68 and 72
Fgf12	72
Fgf13	72
Fgf14	72
Spry1	68 and 72
Spry2	68 and 72
Mkp3	68 and 72
Agrp	68
Foxo1	68
Bsx	68 and 72
Yap1	68 and 72
Npy	68 and 72
Bdnf	68 and 72

Table 2.5 - Temperatures used for ISH experiments

2.12 – In situ hybridization combined with immunohistochemistry

After completion of the in situ hybridization protocol, sections were incubated for 1 hour in blocking solution (10% heat-inactivated normal goat serum (hiNGS), 0.3% Triton X-100 (TX), diluted in PBS) followed by overnight incubation at 4 °C with mouse anti-GFAP or mouse anti-S100β antibodies (Table 2.3) in a solution containing 0.2% hiNGS and 0.1% TX diluted in PBS. After three 5-minute PBS washes, the DAB staining reaction was performed using a DAB peroxidase substrate kit (Vector Labs, USA) according to the manufacturer's instructions. After five 1-minute washes with double distilled water, the slides were coverslipped in 50% glycerol/PBS solution.

2.13 – Microscopy

Images were captured using a Zeiss Axioplan 2 microscope, using Axiovision 4.8 software. For quantification and co-expression analysis, images were captured as optical sections using an Apotome attachment, allowing for 3D reconstruction.

Tomato positive cells were counted either by directly looking through the eyepiece and changing the plane of focus if the density of cells was low, or by counting them in the imaged stacks if the density was high.

Whole-mount embryos processed through in situ hybridization were imaged using a Zeiss SV11 stereo microscope and Axiovision 4.8 software.

Images were post-processed (adjustment of brightness/contrast/levels and unsharp mask, scale bars) with FIJI, Axiovision, GIMP and Photoshop.

2.14 – Glucose and Insulin tolerance tests

Mice were deprived of food by being put into clean cages with no food pellets supplied. After 16 hours of food deprivation, the tip of the tail for each mouse was snipped to take blood samples. Baseline fasted blood glucose measurements were taken using an AlphaTRAK 2 glucose meter and blood glucose strips. Mice were then IP injected with either glucose (2.5 g per kg body mass) or insulin (0.375 units per kg body weight) and their blood glucose was measured 15, 30, 60 and 120 minutes post-injection. The

mice were then housed in their usual cages with food. Mice were given 2 weeks to recover in-between glucose and insulin tolerance tests.

Rarely, some mice did not respond to glucose or insulin injection with an increase or reduction in blood glucose levels respectively. This may have been due to technical issues with the intraperitoneal injection (Steward et al., 1968) or due to a spike in blood glucose due to a heightened stress response in the case of ITT (Nonogaki, 2000). Therefore, for GTT, if blood glucose levels for a given animal did not at least double at any time-point compared to fasted baseline, the injection was not taken as successful (3 out of 50 cases). For ITT, the injections were not considered valid if glucose levels increased compared to fasted baseline after insulin injection (3 out of 50 cases).

2.15 – Statistical Analysis

Statistical analysis was performed and graphs were made using GraphPad Prism 7.00. When comparing two means, unpaired t-test was used. To control for type II errors when comparing means of more than two groups, ANOVA was used. The significance level was set at 0.05.

One-way ANOVA (analysis of variance) is a statistical significance test designed to compare the means (one continuous, dependent variable, for example weight) of two or more groups (one nominal, independent variable, for example genotype) (McDonald 2009). Two-way ANOVA meanwhile compares means (one continuous, dependent variable, for example weight) of two or more groups of two nominal, independent variables (for example, genotype and time) (McDonald 2009). For experiments described in chapter 6, one-way ANOVA was used for statistical comparisons of one dependant variable between three genotype groups (multiple comparisons: each genotype compared to the two others). Other experiments described in chapter 6 also had multiple measurements taken of the same animal over time, therefore time-points were considered a second independent variable. For these experiments, a multiple comparisons repeated measures two-way ANOVA was performed as recommended by published guidelines on metabolic studies (Bowe, Franklin et al. 2014).

Most of the data was plotted as line or bar charts. These types of charts are very prevalent in the literature and provide easily identifiable information on the means and standard errors. However, it has been argued that box plots are provide more

information on the underlying data, as they can simultaneously show the median, the quartiles and minimum/maximum values (other variations exist), while not being too complex, and can therefore be considered as an alternative to bar charts where appropriate (Streit and Gehlenborg 2014).

The experiments described in chapter 6 were performed as a pilot study, as there is not enough information in the literature to inform the potential metabolic impact that a downregulation of FGF signalling specifically in tanycytes may have, or the associated effect sizes. A pilot study can help in the design of further studies and can be especially helpful in determining the needed sample size through statistical power calculations. This is because statistical power depends on three factors: the alpha level, effect size and sample size (McHugh 2008). Once an estimation of the effect size is obtained in a pilot study, a sample size calculation can be derived for the desired statistical power and alpha level. The formulae vary depending on the statistical test to be used and there are helpful statistical software packages available for calculating the needed sample size for a specific study design (Zodpey 2004, Rodriguez Del Aguila and Gonzalez-Ramirez 2014).

Chapter 3

Optimisation of situ hybridization protocols for detecting FGF signalling pathway genes

3.1 – Introduction

The FGF signalling system plays crucial roles in controlling adult neurogenesis in the dentate gyrus and subventricular zone (Zhao et al., 2007; Stevens et al., 2012; Kang and Hébert, 2015). In the hypothalamus, exogenous FGF2 induces proliferation of tanycytes and there is an increasing interest in the functions of endogenous FGF signalling in the hypothalamic niche (Xu et al., 2005; Robins et al., 2013). To understand endogenous FGF signalling, the expression patterns of FGF ligands and receptors must be determined. This information is crucial for determining which cells in the niche are capable of releasing FGF ligands, and which express the receptors for receiving these signals from within or outside of the niche. Therefore, any method used for this purpose must have single cell resolution while maintaining the cellular architecture of the niche. Immunohistochemistry (IHC) and mRNA in situ hybridization (ISH) on tissue sections meet these requirements.

Apart from the main distinction that they detect protein or mRNA respectively, IHC and ISH both have their advantages and disadvantages. The primary deciding factor of which method to use in the expression screen was the availability of antibodies or cRNA probes specific to the gene product of interest since FGFs show a high degree of similarity of nucleotide and amino acid sequences (Ornitz and Itoh, 2001). This puts ISH in favour as cRNA probes can be designed and produced relatively rapidly and at little expense. Specific signal can be attained even when ~75% of the probe sequence is shared with other genes, as long as the ISH conditions are sufficiently stringent (Yaylaoglu et al., 2005). In addition, primers used for the initial reverse-transcriptase PCR (RT-PCR) screen can be tagged with a T7 promoter sequence and used for making templates for in vitro transcription of cRNA probes. In contrast, specific commercial antibodies that are suitable for IHC are only available for some FGF signalling system members. For example, numerous antibodies for detecting FGF10 were tested in our lab, but as of yet none have produced specific staining when used in immunohistochemistry, therefore causing a need to rely on transgenic mouse models to detect expression of *Fgf10* (Kelly et al., 2001; El Agha et al., 2012). Moreover, creating or ordering custom antibodies and validating them is a costly and time-consuming process. In light of these factors, ISH was the primary method of choice.

While in situ hybridization for the detection of mRNA in wholemount mouse embryo preparations has been previously used in our lab (Hajihosseini and Heath, 2002), ISH on adult brain tissue had not been attempted.

3.1.1 - Aims

An in situ hybridization protocol suitable for use with adult brain tissue was established and optimised to ascertain the expression patterns of FGF signalling system members in the adult hypothalamus neurogenic niche.

3.2 – Results

3.2.1 – Whole-mount in situ hybridization of whole adult hypothalamus

A whole-mount mRNA in situ hybridization (WMISH) protocol for detecting gene expression in whole mouse embryos had been established and routinely used in our lab (Hajihosseini and Heath, 2002). It was plausible that this WMISH protocol could be successfully used with whole-mount adult mouse hypothalamus. Therefore, this was the first approach attempted.

RNA probes complementary to *Fgfr1*, *Fgfr2* and *Fgf10* mRNA were used. These target genes were chosen because expression of *Fgf10*, *Fgfr1* and *Fgfr2* in adult mouse hypothalamus has been described in the literature and should, therefore, be easily detectable, serving as good positive controls for this protocol (Lein et al., 2006; Hajihosseini et al., 2008). However, no staining was observed at the end of this experiment.

One of the possible reasons was that the protocol might not be suitable for wholemount adult tissue, as it might potentially need much harsher permeabilisation conditions, among other optimisations. Therefore, ISH was performed using the same cRNA probes on 20µm cryosections with a modified protocol. Thin sections were chosen to address the permeabilisation issues and allow for the detection of multiple genes expressed in serial sections. The brains were fixed and processed for cryosectioning, as this is a common method found in the literature. The same conditions and solutions were used as in WMISH, but wash times were shortened in line with published protocols for mRNA in situ hybridization on cryosections. After an unsuccessful first attempt, carbethoxylation by an active diethylpyrocarbonate (DEPC) pretreatment before hybridization was added to the protocol as it has been reported to increase specificity and strength of in situ hybridization signal (Braissant and Wahli, 1998). This too did not produce any staining.

Ribonucleases are abundant, very stable and active enzymes. They can effectively degrade target and probe RNA. Therefore, work involving RNA requires care to

prevent contamination by ribonucleases. Examples of precautionary measures are the pretreatment of most solutions with DEPC, baking of glass- and metalware, and the cleaning of work surfaces with RNAseZAP (Ambion). To make sure these cautionary measures were effective, and the protocol works in my hands, WMISH was carried out on E10.5 embryos with FGF8 cRNA probes. FGF8 is a gene that is abundantly expressed at the apical ectodermal ridge (AER) of the developing limb buds at E10.5 (Crossley and Martin, 1995). Furthermore, the probe had been successfully used in our lab and the WMISH protocol was originally designed for E10.5-E11.5 embryos.

Indeed, the AER showed strong and specific staining with the FGF8 riboprobe after 1 hour of colour development (Fig. 3.1 A, A'), while the negative control embryo (no probe) showed little staining even after overnight colour development (Fig. 3.1 B, B'). This suggests that the protocols for cRNA probe synthesis and WMISH are suitable. However, it also suggested that the protocol may not be appropriate for adult brain tissue sections.

3.2.2 - Establishing a protocol for in situ hybridization on sections and optimizations to achieve signal specificity

After the attempts described above, a published protocol for in situ hybridization on adult mouse brain cryosections was tested (Palop et al., 2011). The most notable modification was the reduced hybridization and post-hybridization wash temperatures, more in-line with the majority of protocols found in the literature and previously used in our lab. This protocol immediately produced strong staining as evidenced by in situ hybridization with *Neuropeptide Y* (*Npy*) cRNA probes. *Npy* is an orexigenic peptide expressed in a population of neurons in the arcuate nucleus (Hahn et al., 1998) and ISH using these probes resulted in specific detection of *Npy* in this population (Fig. 3.2 A). ISH experiments were performed using these conditions with several different probes, producing staining in the majority of cases. (*Npy*) detection was used as a positive control for these experiments. However, after some time it became apparent that the *Npy* riboprobe can produce diffuse and moderately strong staining in the hippocampus (Fig. 3.2 B''), cortex (Fig. 3.2 B''') and hypothalamus, especially the arcuate nucleus and the floor of the 3rd ventricle (Fig. 3.2 B, B').

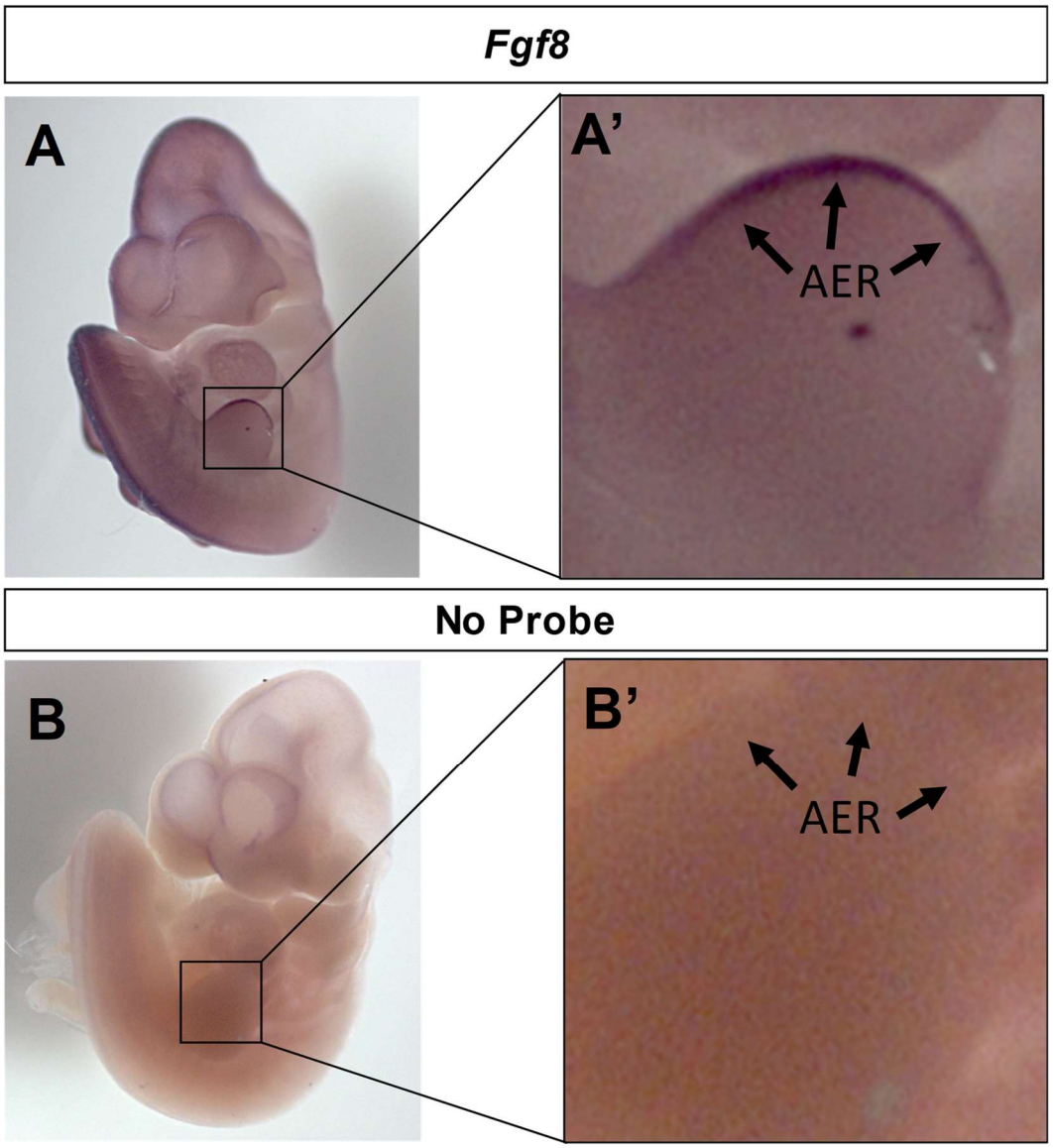

Figure 3.1 – Successful *Fgf8* ISH on whole-mount mouse embryo. *Fgf8* WMISH was performed on E10.5 mouse embryos to test the reagents and protocol. The *Fgf8* cRNA probe produced strong, specific staining in the apical ectodermal ridge (AER) (A, A'), while the no probe negative control was devoid of staining in the AER (B, B').

Worryingly, a similar pattern was observed when most other riboprobes were used for in situ hybridization, mostly only with variations of how intense and widespread the staining is, but always staining the floor of the 3V, arcuate nucleus, hippocampus and cortex. Moreover, most probes showed much wider expression patterns than those described in the literature. This suggested that the staining observed was not always specific and the protocol needed refinement.

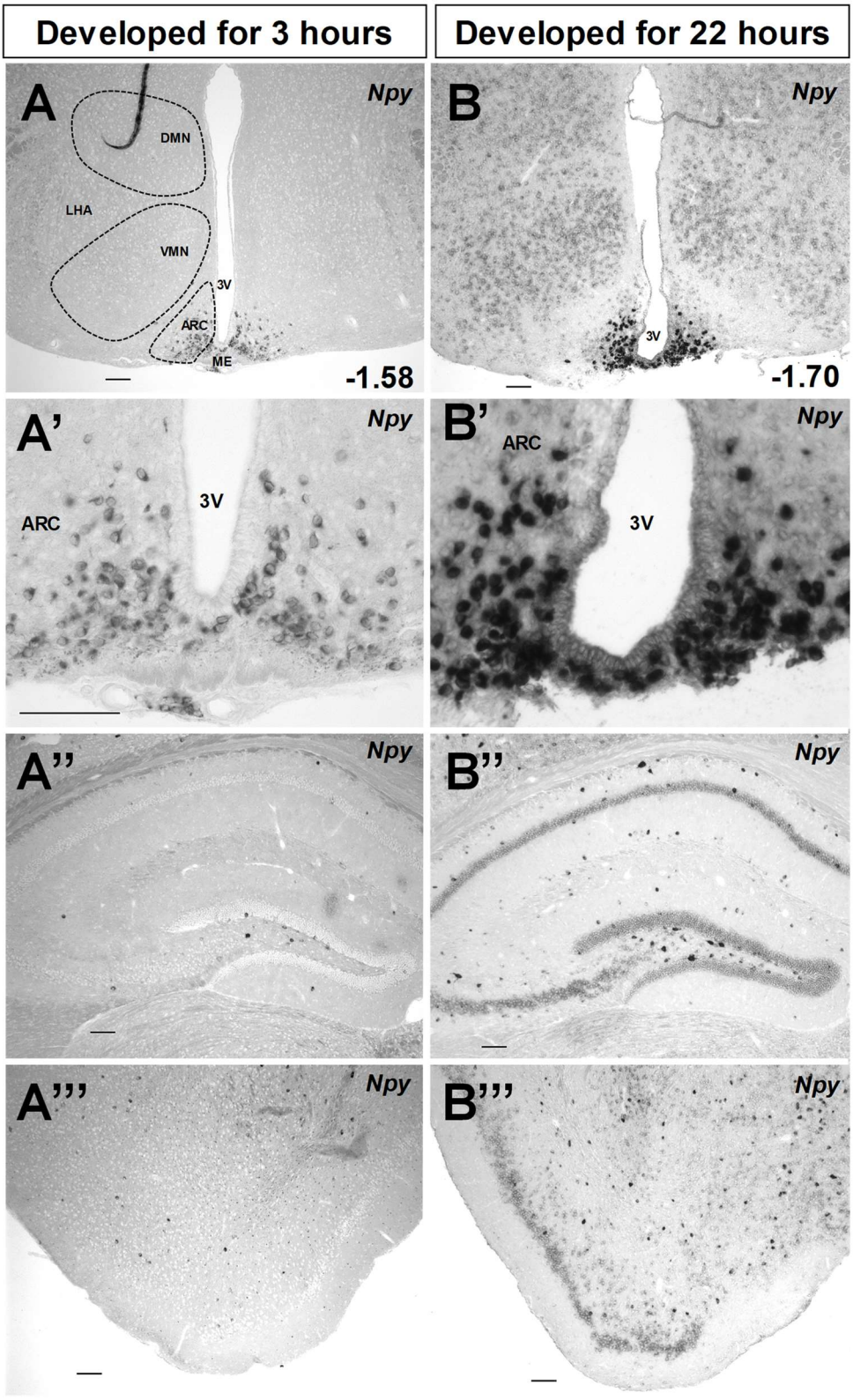

Figure 3.2 – Development reaction time determines the specificity of the signal. (A, A', A'', A''') The *Npy* probe produces strong and specific staining when developed for 3 hours, however, if developed overnight, a fainter background staining appears in the hypothalamus (B, B'), hippocampus (B'') and cortex (B'''). Numbers in the bottom right corners refer to Bregma coordinates. Scale bar - 100 µm.

The main determinants of the specificity of in situ hybridization stringency are:

1. The concentration of formamide in the hybridization buffer.
2. The concentration of salts (effectively, the concentration of SSC) in the hybridization buffer.
3. The temperature of cRNA hybridization.
4. The temperature and solution used for the post-hybridization washes.
5. The length of the riboprobe used.
6. The concentration of riboprobe in the hybridization buffer.

The first step to make the conditions more stringent was to reduce the concentration of riboprobe present in the hybridization buffer. This was reduced from 2000 to 500 ng/ml, as measured using a spectrophotometer (NanoDrop ND-1000, ThermoFisher). The next step was to determine the optimal hybridization temperatures that would produce specific staining. This was done using an empirical formula that takes into account the contents of the hybridization buffer (the concentration of formamide and salts) and the length of the riboprobe, yielding a range of temperatures to be used for hybridization (Casey and Davidson, 1977). Most of the temperatures calculated using this formula were higher than the 58-60 °C used in the previous experiments. These two improvements led to considerably improved specificity of signal, and it also revealed that many patterns observed previously were due to nonspecific background staining (Fig. 3.3).

This experience highlighted the importance of specificity controls and additional measures to reduce background. One approach to tackle this is to perform a wash with a solution containing 20 µg/ml RNase A (Sigma) for 30 minutes after hybridization with the probe, before the post-hybridization washes. This digests the unbound or weakly bound cRNA probe that may get trapped in tissue sections and produce background staining, while the specific cRNA-mRNA hybrids are much more resistant to RNase A. This treatment did reduce background staining in experiments using *Npy* cRNA probe. However, for other probes, it also greatly reduced the signal intensity and increased development time. Due to these undesirable qualities, alternative approaches were explored.

A very common alternative approach is to use sense cRNA probes obtained from the same cDNA template as the anti-sense riboprobes. They are not complementary to tissue mRNA but have the same biochemical properties as the anti-sense probe used to detect mRNA. Using sense probes, it was observed that some probes that had relatively restricted expression patterns with the anti-sense probe also exhibited the

same pattern with sense probes. However, in all of these cases, the previously described characteristic staining in the cortex, hippocampus and hypothalamus was also observed. For some genes, the staining produced by the sense probe is eliminated when hybridization and post-hybridization washes are performed at 68-72 °C, while the signal is preserved using the anti-sense probe. Therefore, the rest of the experiments were performed in the 68-72 °C hybridization and post-hybridization temperature range. Where the distinctive widespread staining pattern in the hippocampus, cortex and hypothalamus was found, sense probes were used as additional specificity controls. Where possible, the patterns were compared with ones found in the literature as additional confirmation. Finally, multiple probes were used in each hybridization experiment, revealing different, restricted expression patterns. The use of these controls and guidelines provides confidence in the specificity of the staining observed.

3.2.3 - Developing a protocol for in situ hybridization combined with immunohistochemistry

In some cases, the simultaneous detection of protein and mRNA in the same tissue section provides valuable information. This is needed, for example, to determine tanycyte domain specific expression of various genes. This would be made possible by performing mRNA in situ hybridization for the gene of interest, followed by immunohistochemistry against α-tanycyte markers such as GFAP or S100β. Ideally, both ISH and IHC would be fluorescent, as this would allow for easier analysis of co-localisation compared to chromogenic detection methods.

For these reasons, a fluorescent in situ hybridization protocol was optimized. A few different options were considered:

1. Probes made with an RNA labelling mix that contains Fluorescein-12-UTP instead of the DIG-11-UTP previously used.
2. Probes made with an RNA labelling mix that contains DIG-11-UTP and the use of an Anti-Digoxigenin-Fluorescein antibody.
3. Probes made with an RNA labelling mix that contains DIG-11-UTP and the use of an Anti-Digoxigenin-HRP antibody, followed by detection with tyramide signal (TSA) amplification methods.

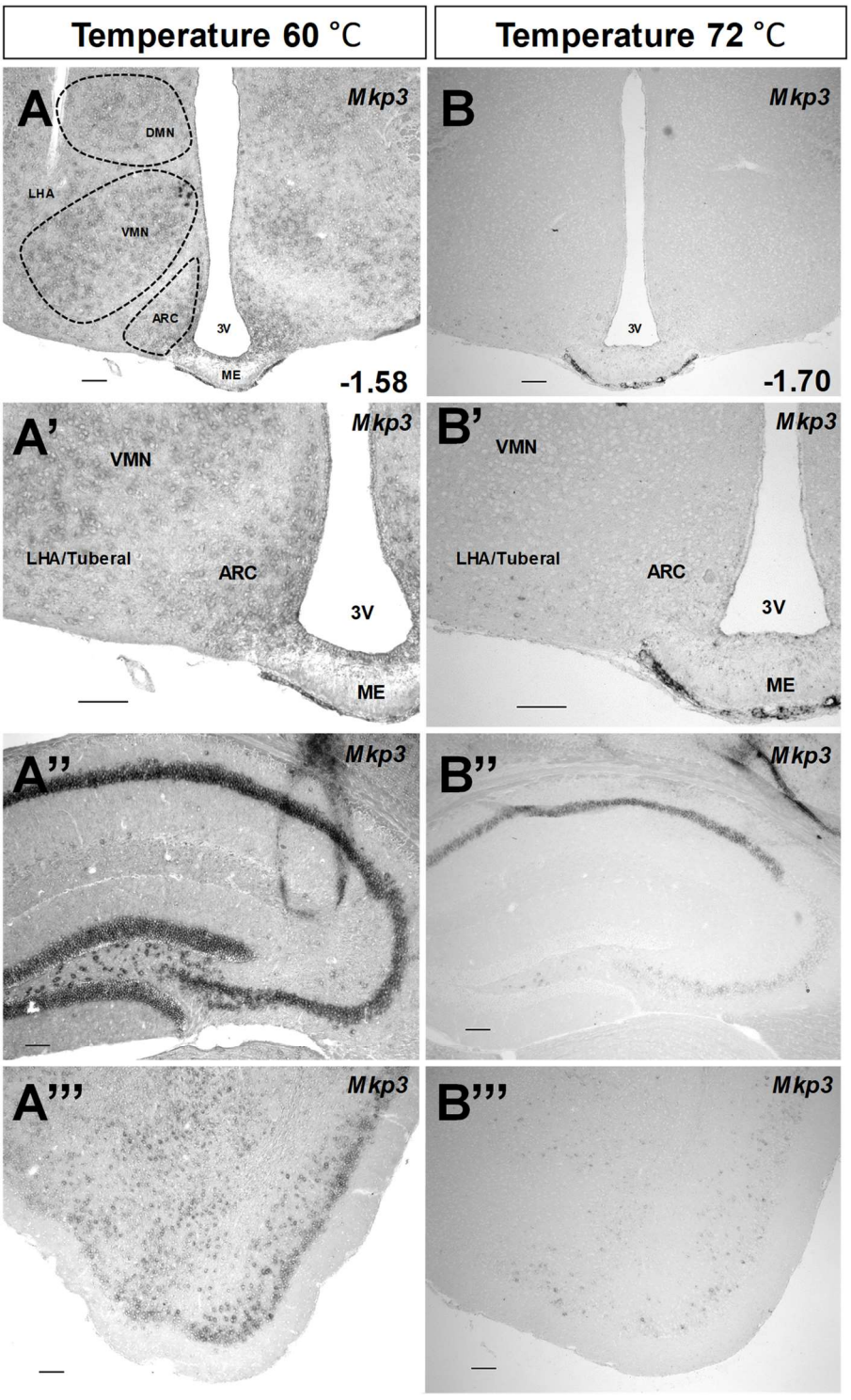

Figure 3.3 – Increased hybridization temperature and reduced cRNA probe concentration improve the specificity of ISH reactions. (A, A', A'', A''') *Mkp3* probe produced very wide staining, akin to that seen in overdeveloped reactions with the *Npy* probe. After reducing the probe concentration (2000 ng/µl to 500 ng/µl) and increasing hybridization and post-hybridization wash temperatures (60 ºC to 72 ºC), the staining becomes specific (B, B', B'', B'''). Numbers in the bottom right corners refer to Bregma coordinates. Scale bar - 100 µm.

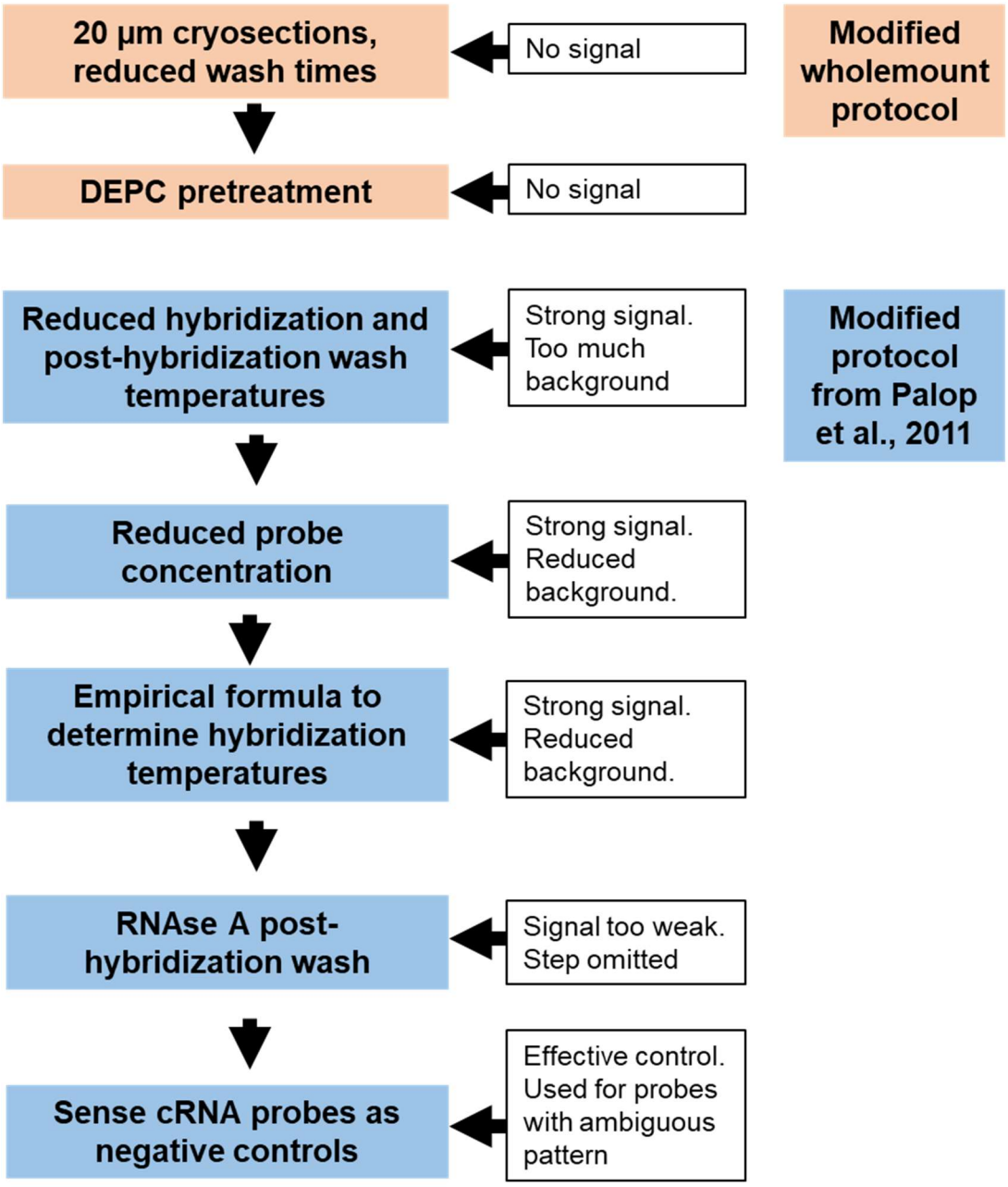

Figure 3.4 – The optimisation of a protocol for ISH on adult brain sections. Flowchart describes ISH protocols and the major modifications for optimising them.

The benefit of using Fluorescein-12-UTP is that it requires no detection with antibody and therefore the sections can be imaged after the post-hybridization washes. However, this method is the least sensitive. Fluorescent in situ hybridization with TSA (PerkinElmer) adds some additional steps to the protocol, but it is the most sensitive method. Meanwhile, the use of an Anti-Digoxigenin-Fluorescein antibody is somewhere in-between both in terms of sensitivity and protocol complexity. Eventually, tyramide signal amplification was chosen as it offered the best sensitivity, while the additional steps are not so time-consuming to make it prohibitive.

At first, the chromogenic in situ hybridization protocol was tried. All the ISH steps were kept the same with the exception of substituting Tris-HCl/saline to PBS for washes, blocking and antibody solutions (1% bovine serum albumin, 0.2% skim milk powder and 0.3% Triton X-100, diluted in PBS), and incubation with an Anti-Digoxigenin-POD antibody (1:1000 dilution; 30-minute incubation on a shaker set at 100 rpm). TSA amplification steps were then carried out according to the manufacturer's instructions.

The first results were encouraging. The *Npy* cRNA probe produced very strong and specific staining and could be combined with IHC to detect GFAP (Fig. 3.5 A). However, some nonspecific background staining was encountered. In addition, apart from *Npy* (Fig. 3.5 A), only *Agrp* (Fig. 3.5 B) and *Fgfr1* (Fig. 3.5 C) exhibited specific staining, while other probes produced either no staining or only background (Fig. 3.5 D). Therefore, although the combination of fluorescent in situ hybridization and immunohistochemistry worked in principle, it was not adequate for most of the cRNA probes tested.

Next, a combination of chromogenic in situ hybridization and immunohistochemistry was attempted. The immunohistochemistry step was carried out directly after the standard in situ hybridization protocol, using HRP conjugated secondary antibodies. A detection kit using DAB (Vector Labs) as a substrate was then used, producing a brown colour stain, which is easy to distinguish from the purple in situ hybridization stain. The protocol resulted in good staining for both mRNA and protein (Fig. 3.6 A, A', B, B') on the very first try and was therefore used for all subsequent experiments requiring simultaneous detection of both.

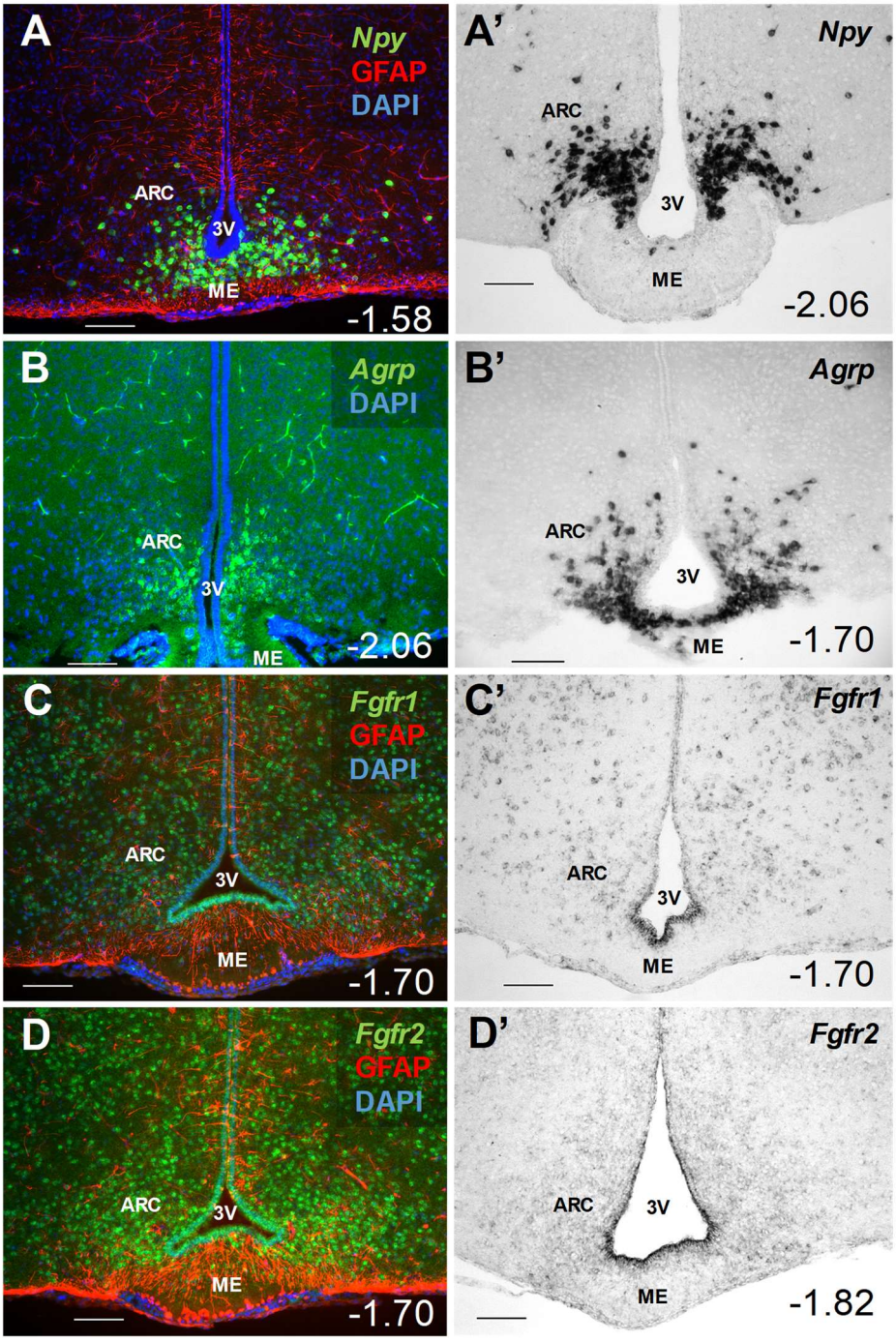

Figure 3.5 – Fluorescent in situ hybridization combined with immunohistochemistry is inadequate for the majority of cRNA probes tested. Fluorescent ISH (A - D) recapitulated the patterns seen in chromogenic reactions (A' – D') for *Npy* (A, A') and *Agrp* (B, B'). The pattern seen in *Fgfr1* fluorescent ISH experiments (C) matches the chromogenic reaction (C') but presents much more background. The *Fgfr2* fluorescent ISH (D) is more representative of the rest of the probes tested, producing either only no fluorescence or only strong background, compared to the chromogenic reaction (D'). Numbers in the bottom right corners refer to Bregma coordinates. Scale bar - 100µm.

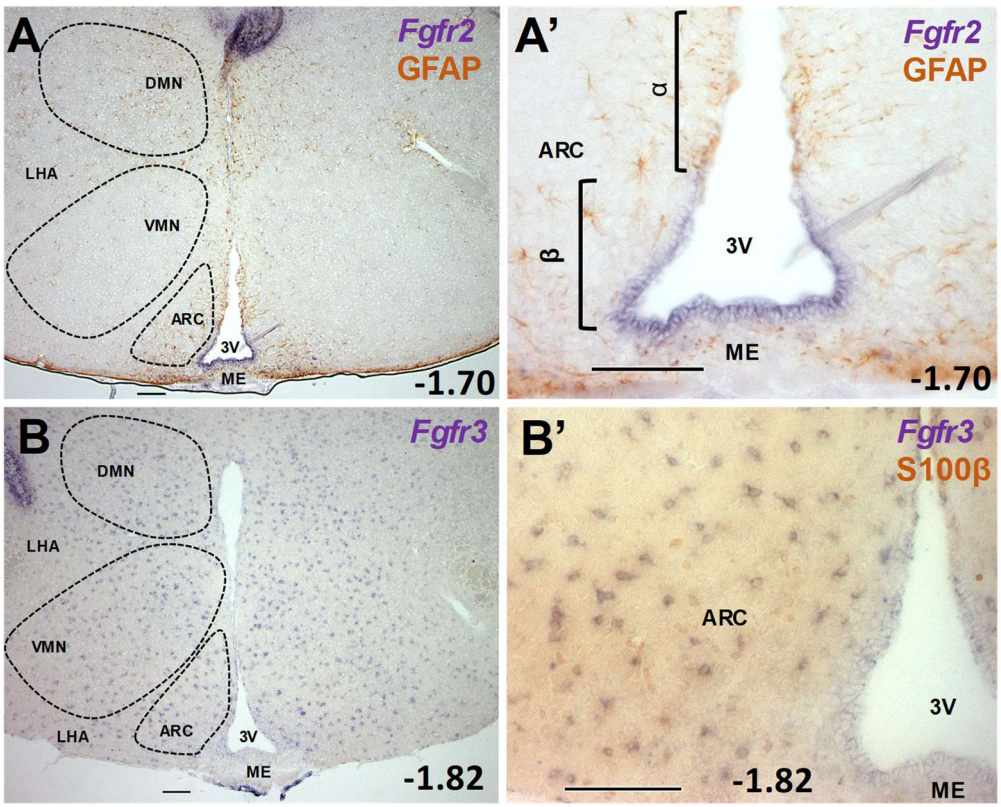

Figure 3.6 – Chromogenic in situ hybridization combined with immunohistochemistry allows for simultaneous detection of mRNA and protein. *Fgfr2* expression is mutually exclusive from GFAP expression (A, A'), an α-tanycyte marker (Goodman and Hajihosseini, 2015). *Fgfr3* is co-expressed in the parenchymal with S100β (B'), a predominantly glial marker (Steiner et al., 2007). Numbers in the bottom right corners refer to Bregma coordinates. Scale bar – 100 µm.

3.3 – Discussion

Gathering information on the expression of FGF signalling components is an essential step to improving our understanding of its endogenous functions in the hypothalamus. It was therefore imperative to establish a method that would allow for this mapping.

Antibodies that can discriminate different FGF family members are not available due to homology, as exemplified by an FGF10 antibody that produces western blot bands when used on proteins extracted from FGF10 KO tissue (Niels Haan PhD Thesis, UEA, 2012). A protocol for detecting messenger RNA in thin cryostat brain tissue sections was therefore optimised. The protocol results in stained sections and maintains the integrity of the cellular architecture. This is paramount when studying the hypothalamus neurogenic niche, as it is organised in a specific manner, whereby tanycytes, the putative neural stem progenitor cells, line the third ventricle wall and generate neurons that contribute to the abutting neuronal nuclei (Haan et al., 2013; Robins et al., 2013). It is also relatively quick and simple to create custom cRNA probes for any gene of interest using our approach. In addition, many cRNA probes produced strong, clean staining with minimal background, allowing for mRNA detection at single cell resolution. Finally, with the combined ISH and IHC protocol, it was possible and straightforward to visualise both mRNA and a protein marker in the same tissue section, in this way supplying information on which cell types (e.g. glial cells using S100β as a marker) or tanycyte domains (GFAP/S100β as a marker for the α-tanycyte domain) express the genes of interest.

The protocol is not without its drawbacks. Some cRNA probes did not produce any staining, or only staining that was later confirmed to be background, even after testing a wide range of hybridization and post-hybridization temperatures. This is a problem faced by many in situ hybridization protocols. Probe sequences were chosen according to the same standards as used by the Allen brain institute (Allen-Mouse-Brain-Atlas, 2011). However, it can be noted that some of their in situ hybridization experiments also yield no staining or only weak background, even if convincing expression patterns for the same gene are reported elsewhere. An example of this is Allen Brain Atlas ISH for *Fgfr3*, experiment #448, compared to ISH reported here (Fig. 3.6 B, B'). It is possible that by generating and testing a few different cRNA probes from different parts of the sequence for the same gene, at least one probe would be produced that works for most of the genes of interest. Therefore, for future experiments, it may be sensible to make a workflow that incorporates this if cost considerations do not preclude it.

In addition, while performing inadequately in my hands, fluorescence detection methods can be an easier and more definitive option when looking for co-localisation between different mRNA and/or protein markers. This is because it is possible to perform 3D reconstructions of images and the different markers do not mask each other. Indeed, multiplex protocols have been developed to identify mRNA of multiple genes at once with different fluorochromes (Tholouli et al., 2006).

Finally, mRNA in situ hybridization does not inform of the protein product and its subcellular localization. However, this can be very important information to understand the mode of action of some proteins. For example, FGF2 can act as both a paracrine signalling molecule as well as a nuclear protein with an intracellular mode of action (Dunham-Ems et al., 2009). Immunohistochemistry and Western Blotting can both provide information on the likely mode of action, due to different molecular weights of the paracrine and intracellular isoforms of FGF2, but in situ hybridization is not suited for this.

To counteract some of the cases where this protocol was inadequate, reporter mouse lines can be used (*Fgf9*^{LacZ}, *Fgf18*^{CreERT2}::Rosa26^{tdTomato}, *Etv4*^{GFP}, and previously *Fgf10*^{LacZ} and *Fgf10*^{CreERT2}::Rosa26^{tdTomato}, as described in Chapter 2 and Chapter 4). Additionally, antibodies can be used for certain cell type markers (e.g. GFAP and S100β as mentioned previously) or to detect phosphorylated proteins (phosphorylated-ERK), which is impossible with ISH.

Conclusion

The process of finding the right protocol and modifying it for specific needs was in itself a useful learning experience. As for most methods, the method described here has its drawbacks, but it has also served its purposes well, allowing our lab to create valuable and detailed gene expression maps in the adult hypothalamic neurogenic niche and elsewhere in the embryonic, postnatal and adult brain.

Chapter 4

A genetic survey of FGF signalling family members and modulators in adult mouse hypothalamus

4.1 – Introduction

The hypothalamus is part of the diencephalon, positioned ventral to the thalamus and dorsal to the pituitary. The ventral part and floor of the third ventricle runs medially across the hypothalamus. The parenchyma is situated on either side of the third ventricle and is composed of a multitude of neuronal nuclei that are involved in the central control of homeostatic functions, such as thermoregulation, sexual behaviour, circadian rhythms and energy balance (Saper and Lowell, 2014).

Tanycytes are emerging as an important component of the neuroendocrine system. They are residual radial glial cells that line the ventral third ventricle (3V) wall and are categorised into α1, α2, β1 and β2 subtypes based on their position along the dorsal-ventral axis, morphology and termination of their processes, expression of domain markers, and cilia arrangement (Goodman and Hajihosseini, 2015). Their apical surface is in contact with the cerebrospinal fluid and they each possess a long single basal process that contacts portal capillaries of the central and median eminence, or terminate within arcuate, ventromedial and dorsomedial nuclei (Rodriguez et al., 2005). These hypothalamic nuclei contain neurons that are crucial for maintaining energy homeostasis (Schneeberger et al., 2014). Tanycytes have recently attracted much interest for the multitude of roles they play. They are sensors of nutrients such as glucose and amino acids in the cerebrospinal fluid (CSF) (Benford et al., 2017; Lazutkaite et al., 2017). They also control the flow of peripheral signals reaching the hypothalamus such as leptin, and central signals like GnRH entering the periphery, by modulating access to portal capillaries (Goodman and Hajihosseini, 2015). In addition, they have been established as bona fide neural stem/progenitor cells (NSPCs) of the postnatal and adult rodent hypothalamus, generating new neurons that regulate energy balance (Lee et al., 2012; Haan et al., 2013; Robins et al., 2013). However, the molecular mechanisms that control these processes are poorly understood.

Fibroblast growth factor signalling is emerging as an important regulator of hypothalamic tanycyte and neuron function. The fibroblast growth factor (FGF) signalling family is composed of 22 FGFs, 4 tyrosine kinase receptors (FGFR1-4) and a receptor lacking the tyrosine kinase domains (FGFR5) (Ornitz and Itoh, 2015). Tyrosine kinase FGF receptors act through activation of intracellular RAS-MAPK, PI3K-AKT, PLCγ, and STAT signalling pathways. Their activation induces the expression of intracellular regulators such as *Sprouty1-4* and *Mkp3* via a negative feedback loop, inhibiting or modulating FGF receptor signalling levels. Based on their

mode of action, FGFs can be categorised into paracrine and endocrine subfamilies whose members bind to receptors, as well as the receptor-independent intracellular subfamily. Paracrine FGFs interact with heparan sulphate, which stabilises FGF binding to FGF receptors and limits their diffusion. Endocrine FGFs lack heparin sulphate binding sites and can, therefore, freely diffuse from their site of release into the bloodstream and act as hormones, with α- and β-Klotho proteins substituting heparan sulphate as cofactors for receptor binding (Goetz and Mohammadi, 2013). To date, paracrine FGF1 and endocrine FGFs -19 and -21 have been implicated in the central control of energy homeostasis with potential use as clinical agents in the management of type 2 diabetes (Degirolamo et al., 2016; Gasser et al., 2017).

Hypothalamic tanycytes express *Fgfr1,* and exogenously applied FGF ligands or FGFR antagonists can cause changes in neurogenesis and metabolism (Lein et al., 2007). For example, intracerebroventricular (ICV) injection of FGF2 increases tanycyte proliferation (Xu et al., 2005; Robins et al., 2013). Furthermore, a single ICV injection of FGF1 induces c-Fos and HSP25 expression in tanycytes and causes sustained remission of diabetes symptoms in a diabetic mouse model, while FGFR1-blocking antibodies bind to tanycytes and other mediobasal hypothalamus targets, causing hypophagia and weight loss (Sun et al., 2007; Lelliott et al., 2014; Scarlett et al., 2016).

It is clear that exogenous FGF signalling can influence tanycytes and the processes they are involved in. However, our knowledge of the FGFs and FGF receptors expressed in tanycytes and the surrounding hypothalamic nuclei is fragmented and incomplete, which is a major limiting factor to understanding endogenous FGF signalling and its effects.

4.1.1 – Aims

To find out which FGF signalling system components and modulators are expressed in the hypothalamus, an RT-PCR screen was performed. Detailed spatial information of their expression in the 3V wall and abutting parenchyma was then obtained through mRNA in situ hybridization combined with immunohistochemistry and the use of transgenic reporter mice.

4.2 – Results

4.2.1 – RT–PCR reveals expression of a wide range of FGF signalling pathway components in the mouse hypothalamus

To determine which members of the FGF signalling system and their modulators are present in the hypothalamus, a reverse transcriptase polymerase chain reaction (RT-PCR) screen was performed on mRNA isolated from post-weaned mice (P30-P45), as at this age most brain development processes are finished and brain volume is stable in 3 week old mice (Semple et al., 2013; Hammelrath et al., 2016).

Alternative splicing affecting the immunoglobulin-like domain III can produce two major isoforms of FGF receptors 1, 2 and 3. These isoforms are called IIIb and IIIc and they are important for determining ligand binding specificity (Gong, 2014). Primer sets used to detect FGF receptors 1, 2 and 3 were designed to detect either IIIb or IIIc splice isoforms of these receptors (Hajihosseini and Dickson, 1999). RT-PCR detected only the IIIc isoform of receptors in the adult hypothalamus (Fig. 4.1 A). Additionally, *Fgfr4* (Fig. 4.1 A) and *Klb* (Fig. 4.1 D), a coreceptor required for FGF15/19 and FGF21 signalling, were also found.

RT-PCR with primer pairs for all 22 mouse FGFs detected products of expected sizes for the majority of the genes (Fig. 4.1 B, C). Products corresponding to *Fgf- 1, 2, 5, 8, 9, 10, 11, 12, 13, 14, 16, 17, 18, 20* and *21* were found. Bands indicating the presence of different *Fgf5* and *Fgf8* isoforms were also detected (Hattori et al., 1996; Sunmonu et al., 2011). Based on the band sizes detected, transcript variant 1 (NCBI Ref: NM_010203.5; band size: 652) and 2 (NCBI Ref: NM_001277268.1; band size: 548) of *Fgf5* and transcript variants 3 (NCBI Ref: NM_001166362.1; band size: 568) and 4 (NCBI Ref: NM_001166363.1; band size: 535) of *Fgf8* are expressed in the hypothalamus (Fig. 4.1 B) Therefore, a variety of FGFs are present in the hypothalamus, with ligands representing each FGF subfamily.

Modulators of the FGF signalling pathway were also screened for and products of *Spry1*, *Spry2*, *Spry3*, *Sef*, *Etv4* and *Mkp3* were found (Fig. 4.1 D).

Reactions with β-Actin primers (Fig. 4.1 A, D), or primers of other genes known to be expressed in the median eminence, such as *Fgf10* (Fig. 4.1 B) and *Fgf18* (Fig. 4.1 C) were performed as positive controls (Hajihosseini, De Langhe et al. 2008, Robins, Stewart et al. 2013). Negative controls were not used, and sequencing of RT-PCR products was not performed due to the additional costs and labour involved, in addition to the fact that cRNA probes for in situ hybridization were generated from

cDNA templates created with the same primers and RT-PCR parameters. Therefore, the in situ hybridization experiments that exhibit diverse and specific staining patterns, described further, serve as an additional confirmation of the specificity of RT-PCR and the cRNA probes derived from it.

4.2.2 – Expression of FGF receptors in the 3V wall is restricted to the β–tanycyte domain

The RT-PCR screen was performed using mRNA isolated from the whole hypothalamus, a brain structure composed of various neuronal nuclei. To examine which genes are expressed in tanycytes and nearby parenchyma containing the arcuate (ARC), ventromedial (VMN), dorsomedial (DMN) and lateral hypothalamus area (LHA), mRNA in situ hybridization experiments were performed on coronal sections containing the central part of the median eminence (Bregmas -1.58 to -1.94) from P60-P80 mice.

Glial fibrillary acidic protein (GFAP) expression in the hypothalamus 3rd ventricle wall marks the α-tanycyte domain and dorsal ependymal cells, but it is absent in the β-tanycyte domain (Haan et al., 2013). The localisation of GFAP, therefore, serves as a useful method to determine compartment specificity of gene expression.

By combining in situ hybridization and antibodies against GFAP, it was possible to determine that *Fgfr1* and *Fgfr2* are expressed in the β-tanycyte, but not α-tanycyte domain (Fig. 4.2 A, A', B, B').

More specifically, strongest staining with the *Fgfr1* cRNA probe was observed in the floor of the 3rd ventricle, the β2-tanycyte domain (Fig. 4.2 A'). In addition to tanycytes, *Fgfr1* expression was also detected in cells within the ARC, DMN and LHA regions, especially strong in the VMN (Fig. 4.2 A).

Strong staining with *Fgfr2* cRNA probe was detected in both β2- and the more dorsal β1-tanycyte domains (Fig. 4.2 B'). Scarce, weakly stained cells were also detected in the ARC, VMN, DMN and LHA as well as subependymal ME.

Expression of *Fgfr3* was restricted to the hypothalamic parenchyma, including the ARC, VMN, DMN and LHA, as well as in some sporadic cells in subependymal ME (Fig. 4.2 C, C'). A combined protocol of in situ hybridization with *Fgfr3* probes and immunohistochemistry with anti-S100β antibodies, a predominantly glial cell marker, suggest that most Fgfr3 expressing cells in the parenchyma are glial cells (Fig. 4.3 C') (Steiner et al., 2007).

In situ hybridization experiments with the *Fgfr4* cRNA probe did not produce any staining. The *Klb* probe produced variable results: either no signal or low intensity, diffuse staining. This was confirmed to be background staining by performing parallel ISH reactions with *Klb* antisense probe and sense negative control.

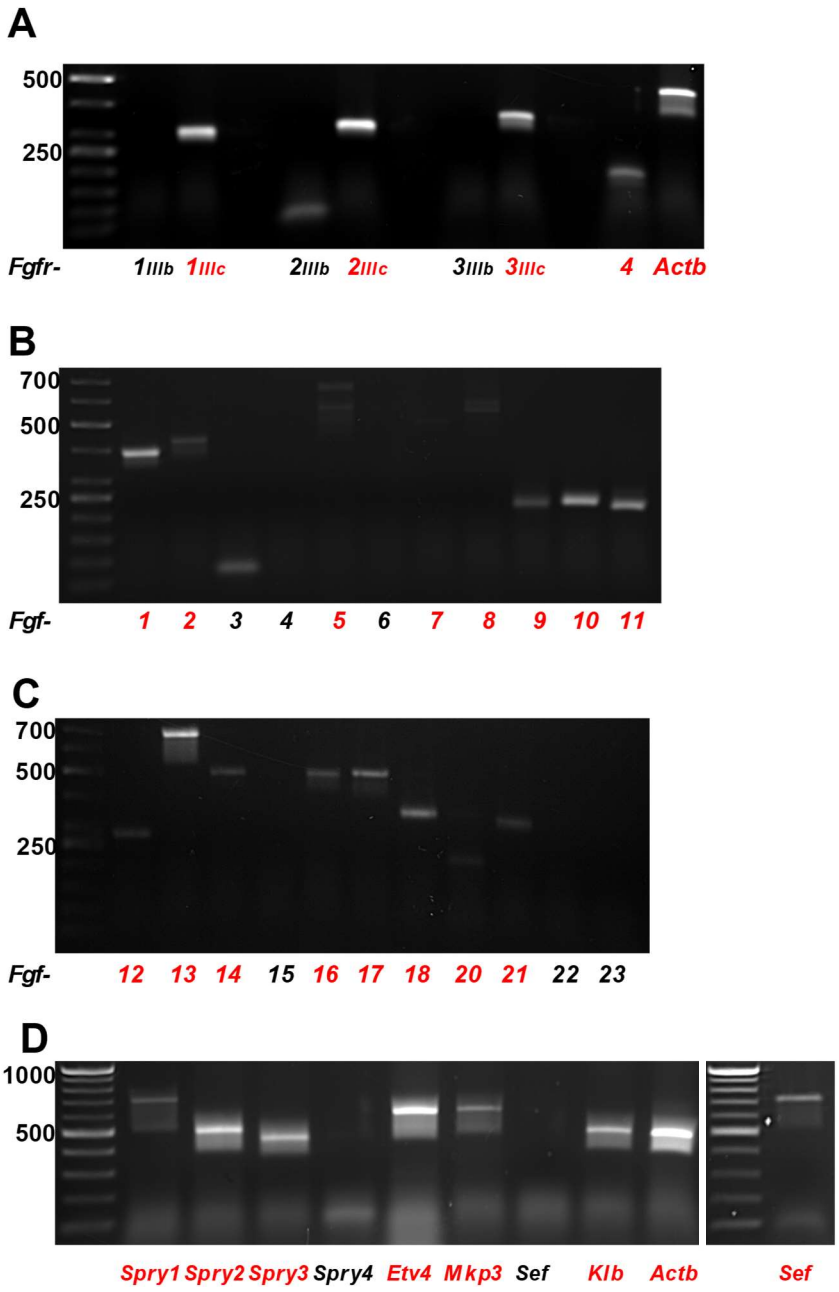

Figure 4.1 - A wide array of FGF signalling components are present in the mouse hypothalamus. Numbers denote size (bp) of DNA ladder reference bands of defined sizes (bp). Specific bands were observed for genes highlighted in red. The small bands for *Fgfr2 IIIB* and *Fgf3* are unspecific products (A)**.** The rest of the RT-PCR products match their expected sizes. Both *Fgf8* and *Fgf5* appear as two bands, indicating expression of different isoforms of those genes (B). *Sef* was detected in all experiments except for one (D).

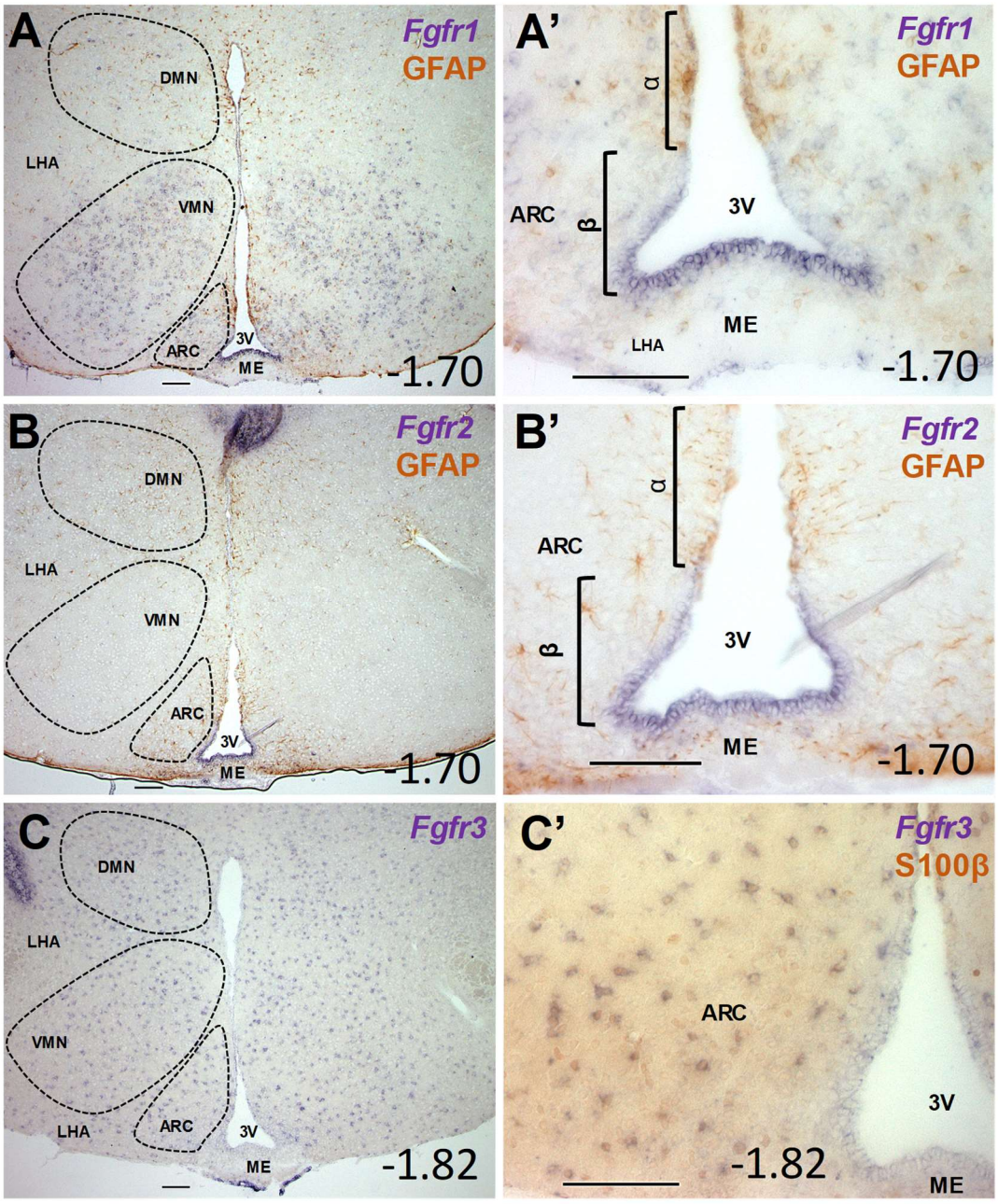

Figure 4.2 - *Fgfr1* and *Fgfr2* are expressed in β–tanycytes while *Fgfr3* is present in S100β+ parenchymal glial cells. Representative images of in situ hybridization experiments using *Fgfr1* (A, A'), *Fgfr2* (B, B') and *Fgfr3* (C, C') cRNA probes, combined with GFAP (A, A') or S100β (C') immunohistochemistry. *Fgfr1* and *Fgfr2* staining in the 3rd ventricle wall is restricted to β-tanycytes (A, A', B). *Fgfr1* is also expressed in hypothalamus parenchyma (A). *Fgfr3* expressed in S100β positive glial cells in hypothalamus parenchyma (C'), but absent from 3V wall. Numbers in the bottom right corners refer to Bregma coordinates. Scale bar – 100 μm.

4.2.3 – FGF receptor modulator and effector expression overlaps that of FGF receptors

To obtain clues about the localisation of activity of FGF receptors and its regulators, in situ hybridization of FGFR modulator genes was performed.

In situ hybridization with *Spry1* riboprobe (Fig. 4.3 A, A') exhibited a wide staining pattern. Its strongest staining was detected in β-tanycytes and the arcuate nucleus. High levels of *Spry1* were also detected in the VMN, DMN and LHA. Co-labelling with GFAP antibodies revealed that it is also expressed in the α-tanycyte domain, albeit the staining intensity was comparatively weaker (Fig. 4.3 A').

In contrast, in situ hybridization with *Spry2* (Fig. 4.3 B, B') riboprobe showed very restricted patterns exhibiting weak staining only in β-tanycytes, predominantly in the β2 domain, diminishing dorsally in the β1 domain. Rare, sporadic expression of *Spry2* in the ARC, LHA and subependymal median eminence was also observed.

Mkp3 signal was restricted to few, but strongly stained cells in the LHA/Tuberal nucleus, lateral in respect to the arcuate nucleus and ventral to the VMN (Fig. 4.3 C, C'). *Etv4* is a transcription factor and a transcriptional target of FGF signalling (O'Hagan and Hassell, 1998; Roehl and Nusslein-Volhard, 2001; Klein et al., 2008; Yaguchi et al., 2009). Using the *Etv4*-GFP reporter mouse we observed *Etv4* expression in the caudal LHA only, starting at around bregma –1.94 (fig. 4.3 D, D').

MAPK/ERK is one of the major intracellular signalling pathways downstream of growth factor receptor activation and it is also a target of inhibition by Sprouty proteins (Ozaki et al., 2001). To detect the activation of this pathway, an antibody specific to phosphorylated ERK (pERK) was used.

Figure 4.3 – FGFR signalling modulators are expressed in β–tanycytes and parenchyma. Representative images of *Spry1* (A, A'), *Spry2* (B, B'), *Mkp3* (C, C') in situ hybridization experiments, GFP (D, D') and GFAP (A, A', B, B', D, D') immunohistochemistry. *Spry1* staining was found in β- and α-tanycyte domains as well as hypothalamic parenchyma (A, A'). *Spry2* expression was observed in β-tanycytes, chiefly in the β2 subdomain, and sporadic cells in the hypothalamic parenchyma (B). *Mkp3* (C, C') and *Etv4* (D, D') were both found in the lateral hypothalamic area, but *Etv4* was also found in caudal DMN (D). Numbers in the bottom right corners refer to Bregma coordinates. Scale bar – 100 μm.

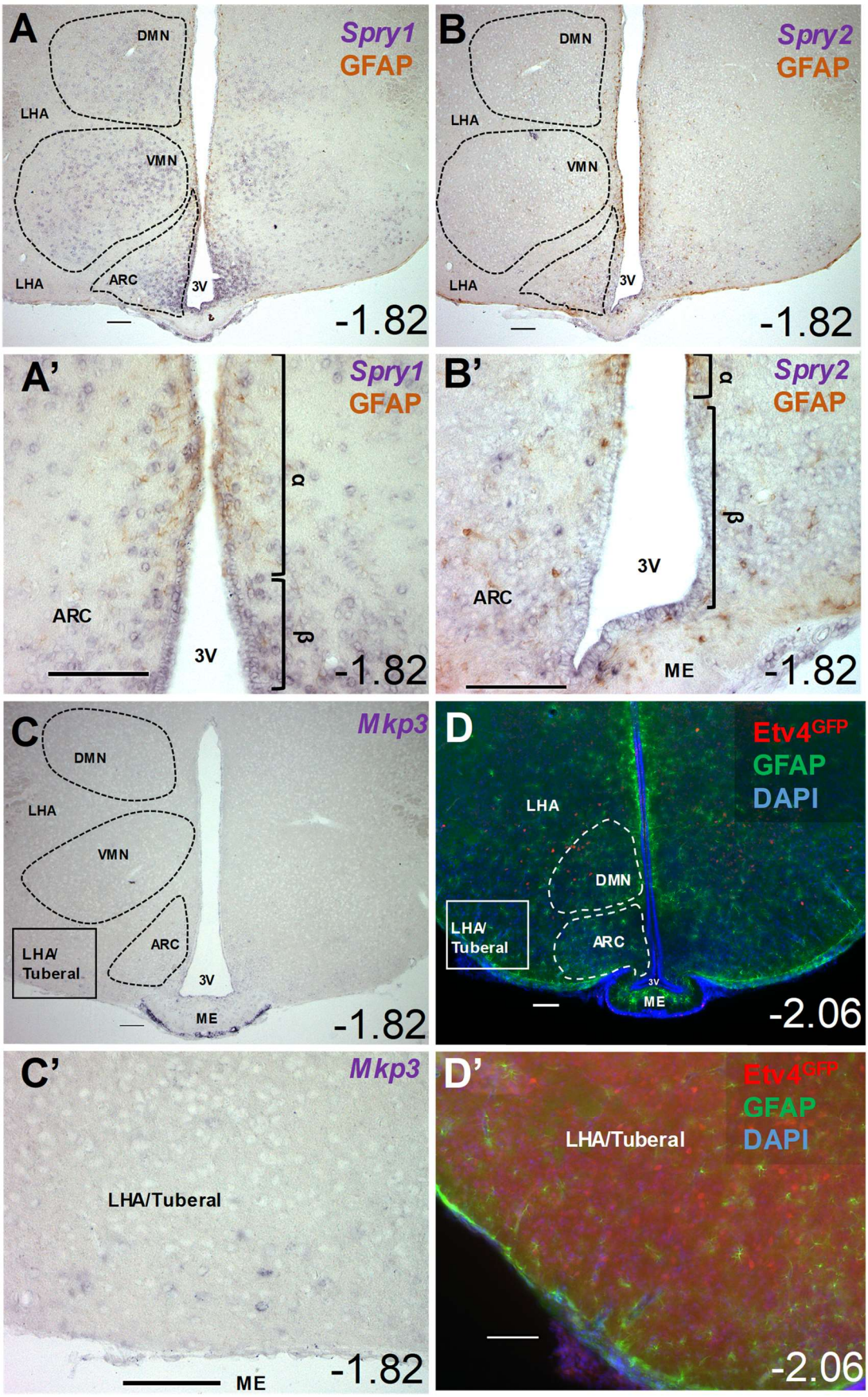
A
DMN
LHA
VMN
LHA
ARC
3V
Spry1
GFAP
-1.82
B
DMN
LHA
VMN
LHA
3V
Spry2
GFAP
-1.82
A'
ARC
3V
α
β
Spry1
GFAP
-1.82
B'
α
β
3V
ARC
ME
Spry2
GFAP
-1.82
C
DMN
LHA
VMN
LHA/
Tuberal
ARC
3V
ME
Mkp3
-1.82
D
LHA
DMN
LHA/
Tuberal
ARC
3V
ME
Etv4GFP
GFAP
DAPI
-2.06
C'
LHA/Tuberal
ME
Mkp3
-1.82
D'
LHA/Tuberal
Etv4GFP
GFAP
DAPI
-2.06

Phosphorylated ERK was found in many cells of the adult hypothalamic parenchyma (Fig. 4.4 A, B) including the ARC, DMN and LHA, but largely absent from the VMN. It was also rarely present in alpha tanycytes and even scarcer in β-tanycytes (Fig. 4.4 A', B'). However, dense groups of pERK-positive alpha and β-tanycytes were present caudally, beyond Bregma -2.06 and until the third ventricle recedes (Fig. 4.4 B').

Spry3 ISH reactions produced only weak background staining. Reactions with the *Sef* probe were confirmed to be unspecific background by using a *Sef* sense probe negative control.

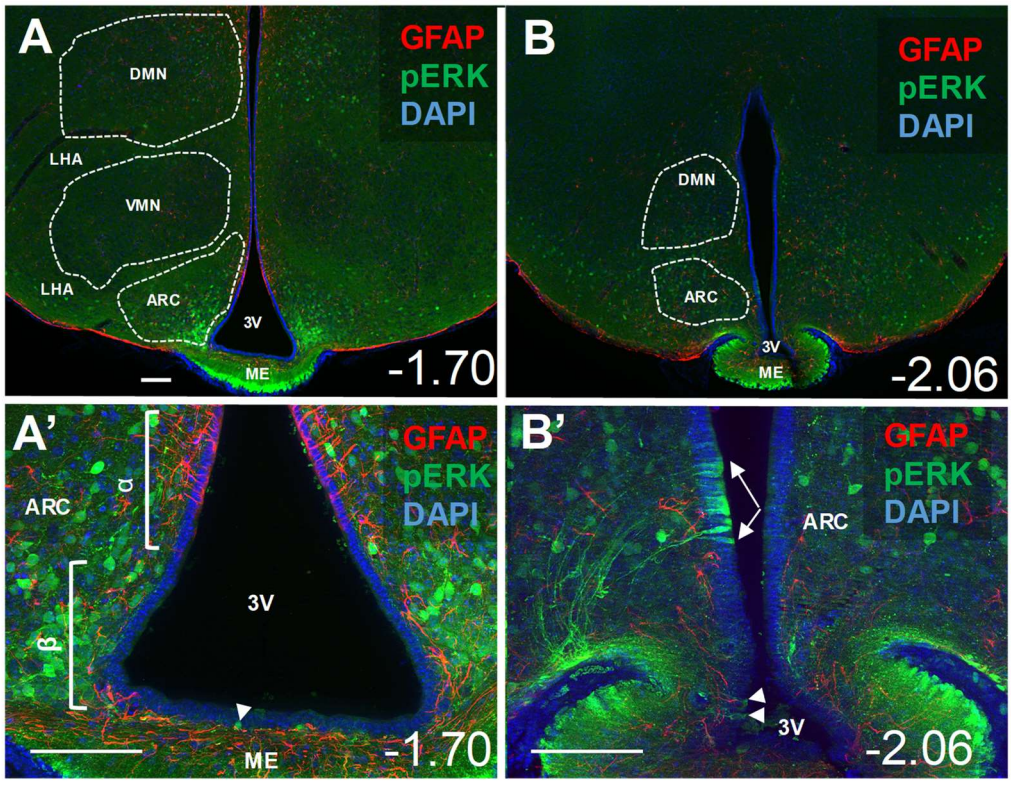

Figure 4.4 – Phosphorylation of ERK is widespread in the arcuate and dorsomedial nuclei, but rare in tanycytes. Representative images of pERK (green) and GFAP (red) immunohistochemistry in central (A, A') and caudal (B, B') median eminence sections. pERK was detected with rabbit anti-Phospho-pERK primary and goat anti-Rabbit IgG Chromeo 488 secondary antibodies. GFAP was detected with mouse anti-GFAP primary and goat anti-Mouse IgG Alexa Fluor 568 secondary antibodies. Numbers in the bottom right corners refer to Bregma coordinates. White arrows indicate pERK containing cells in the third ventricle ependyma. Scale bar – 100 μm.

4.2.4 – FGF ligands are expressed in 3V wall and abutting parenchyma

The expression of FGF receptors, modulators and signalling pathway components in the 3V wall suggests a source of cognate ligands. To determine which FGF ligands might act on FGF receptors in tanycytes in situ hybridization was performed using FGF specific cRNA probes. Moreover, transgenic reporter mice were also analysed. Two largely overlapping patterns of FGF expression were found.

Expression of *Fgf1* and *Fgf9* in the 3V wall was restricted to α-tanycytes (Fig. 4.5 A', A'', B', B''). Their parenchymal staining (Fig. 4.5 A, B) was found to be most intense in the VMN, while weaker and more sporadic staining was found in the ARC, DMN and LHA. It should be noted that *Fgf9* expression in the 3V wall was restricted to rostral sections and absent in more caudal ones (bregma -1.82 onwards).

In contrast, expression of *Fgf2* and *Fgf18* was restricted to β1- and ventral α-tanycytes (Fig. 4.6 A', B). *Fgf2* expression in the α-tanycyte domain tapers off sharply dorsally, so is likely confined to the α2-tanycyte subtype, while sporadic *Fgf18-tdTomato* cells were found throughout the 3V wall. However, it must be noted that $Fgf18^{creERT2}$::$Rosa26^{tdTomato}$ mice and tamoxifen administration paradigm used to determine *Fgf18* expression allows for lineage tracing. In essence, the *Fgf18-tdTomato* α-tanycytes might not express the *Fgf18* gene themselves but may have been generated by *Fgf18* expressing β1 tanycytes. This interpretation is consistent with reported *Fgf18* in situ hybridization data where its expression is restricted to β1 tanycytes (Robins et al., 2013). In other regions of the brain, expression of *Fgf18* was also found along the lateral ventricle walls, in neurons of the olfactory bulb and choroid plexus cells in the third, fourth and lateral ventricles (data not shown).

Using the *Fgf5* and *Fgf17* cRNA probes, weak signal was found only in the hippocampus, CA2 and dentate gyrus, but not in the hypothalamus. The *Fgf7* probe produced some staining in the dorsal part of the 3V wall, most likely ependymal cells. However, the staining was very weak and diffuse, therefore likely only background. *Fgf8* and *Fgf20* probes produced staining typical of broad, diffuse background, which was identical to that produced by *Fgf20* sense probe. Probes for *Fgf16* and *Fgf21* did not produce any staining.

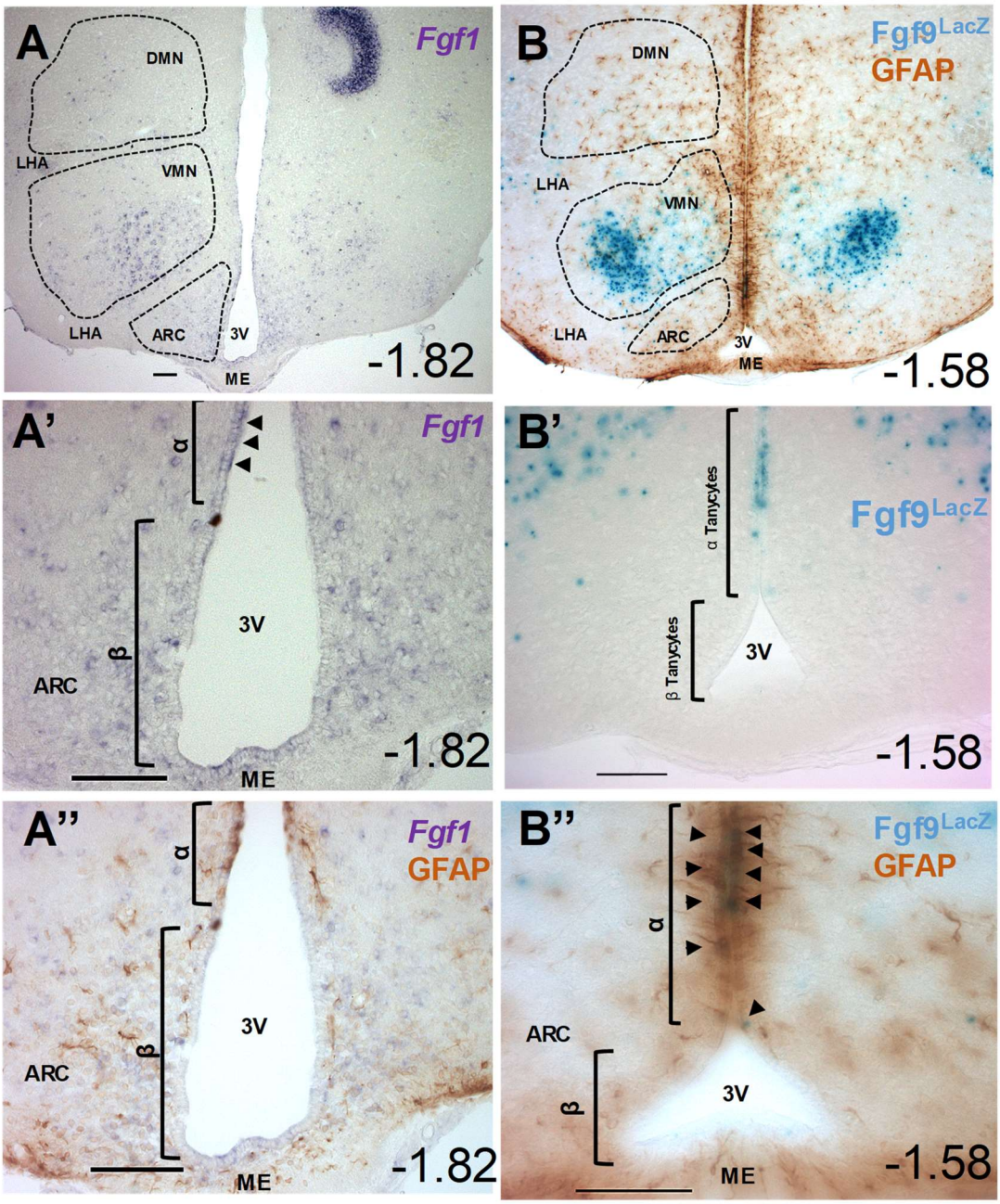

Figure 4.5 - *Fgf1* and *Fgf9* are expressed in overlapping patterns in α–tanycytes and parenchyma. Representative images of in situ hybridization experiments using *Fgf1* (A, A', A'') cRNA probe and *Fgf9*-LacZ X-gal staining (B, B', B'') combined with GFAP immunohistochemistry (A'', B, B''). Expression of *Fgf1* and *Fgf9* was broadly overlapping, observed strongest in the VMN and in addition in the α-tanycyte domain, sporadically in rest of hypothalamus parenchyma (A, A', A''). Black arrows point to α-tanycytes expressing *Fgf1* (A') or *Fgf9* (B''). Numbers in the bottom right corners refer to Bregma coordinates. Scale bar – 100 μm.

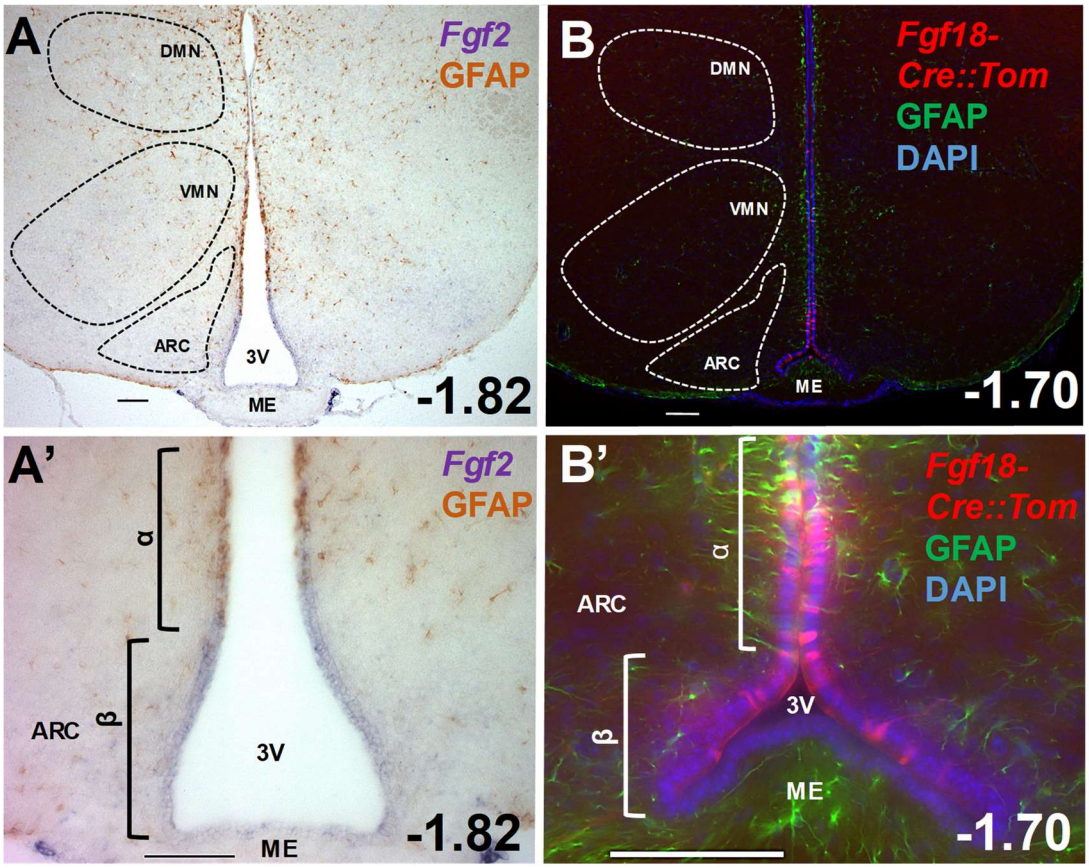

Figure 4.6 – *Fgf2* and *Fgf18* expression is restricted to β1– and ventral α–tanycytes. Representative images of in situ hybridization experiments using *Fgf2* (C) cRNA probes and GFAP (A, A', B, B'), Fgf18-tdTomato (B, B') immunohistochemistry. Both *Fgf2* and *Fgf18* were absent from the parenchyma, but detected in ventral α- and β1-tanycyte domains, the *Fgf18* domain of expression extending further dorsally (B). Numbers in the bottom right corners refer to Bregma coordinates. Scale bar – 100 μm.

4.2.5 – Intracellular FGF mRNA is present in energy regulating centres of the hypothalamus

In situ hybridization with cRNA probes for intracellular FGFs revealed their expression in the hypothalamus parenchyma, but not in tanycytes. *Fgf12* expression had the widest pattern, it is present in the DMN, ARC and LHA, with the strongest staining in the VMN (Fig. 4.7 A). *Fgf13* is restricted to DMN, ARC and very few cells in the LHA, ventrolateral VMN, and subependymal ME (Fig. 4.7 B). Only some cells in the most dorsal part of the ARC express *Fgf14* (Fig. 4.7 C).

No staining was observed using the *Fgf11* probe.

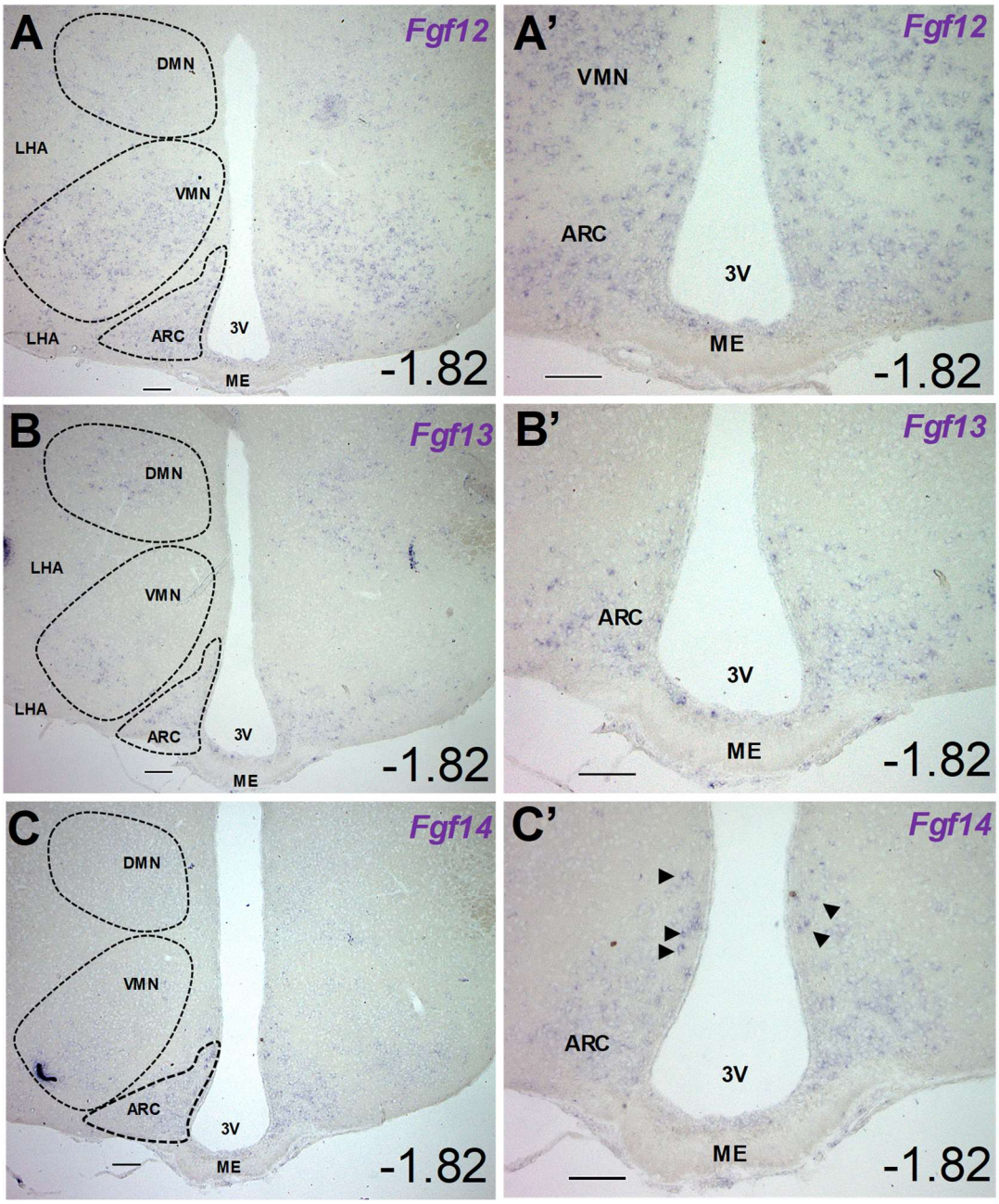

Figure 4.7 - Intracellular FGFs are expressed in hypothalamus parenchyma. Representative images of in situ hybridization experiments with *Fgf12* (A), *Fgf13* (B) and *Fgf14* (C) cRNA probes. *Fgf12* (A) expression is widespread in the hypothalamus parenchyma, *Fgf13* (B) is more restricted and *Fgf14* (C) is only present in some dorsal arcuate nucleus cells. Notably, no intracellular FGFs were detected in the 3rd ventricle wall. Numbers in the bottom right corners refer to Bregma coordinates. Scale bar – 100 µm.

4.3 – Discussion

Although it has been shown that tanycytes are responsive to FGF signalling and stimulation and inhibition of FGF signalling induces effects on neurogenesis and metabolism, our knowledge of the endogenous FGF signalling pathway components at play has been limited. Through the use of RT-PCR, mRNA ISH and gene reporter mice this study reports novel restricted and varied expression patterns of a variety of endogenous FGF receptors, cognate ligands and signalling components in tanycytes and the surrounding parenchyma (Table 4.1).

		3rd Ventricle Wall						
	Median Eminence				Parenchymal Nuclei			
Gene	Subependymal	β2 tanycytes	β1 tanycytes	α tanycytes	ARC	VMN	DMN	LHA
Fgfr1					*		**	**
Fgfr2	*				*	*	*	*
Fgfr3	*				**	**	**	**
Spry1								*
Spry2	*				*			*
Mkp3								*
Etv4								*
pERK	*	*	*	*		*		*
Fgf1					*		**	*
Fgf2								
Fgf9					*		*	*
Fgf18								
Fgf12							**	**
Fgf13	*				**	*	**	*
Fgf14					*			

Table 4.1. Expression pattern summary of FGF signalling family members and modulators in adult hypothalamus. Darker colour indicates higher intensity of observed staining. * - only sporadic cells stained in nucleus/compartment; ** - salt-and-pepper staining pattern.

4.3.1 – Expression of FGF receptors in 3V ependyma is restricted to the β-tanycyte domain

Previous reports have established that *Fgfr1* and *Fgfr2* are expressed in tanycytes, but the precise domain of their expression was not assessed (Lein et al., 2007). In situ hybridization experiments in conjunction with GFAP as a marker of α-tanycyte domain and dorsal ependymal cells, reported here, showed that these receptors are restricted to the β-tanycyte domain, in line with findings of a recent study that used Drop-seq to profile gene expression in the median eminence and arcuate nucleus (Campbell et al., 2017). Tanycytic expression of any other FGF receptors was not found, suggesting that in the hypothalamus 3V wall ependyma, only β-tanycytes are responsive to FGF ligands. One of the implications of this is that experiments utilising

exogenous injection of FGF ligands or FGF receptor blockers into the third ventricle are likely exerting their effects on β-tanycyte FGF receptors. Specifically, increased proliferation of β-tanycytes after ICV injection of FGF2 is likely caused directly by their binding to FGFR1 and/or FGFR2 expressed by β-tanycytes (Xu et al., 2005; Robins et al., 2013). Similarly, the effects of FGFR1 agonist and antagonist antibodies have been shown to accumulate in the mediobasal hypothalamus, median eminence and tanycytes and cause changes in food intake and glucose control (Sun et al., 2007; Lelliott et al., 2014). Any direct effects they have on tanycytes would be restricted to the β-tanycyte domain, which may then influence other signalling systems such as leptin and CNTF, or cells involved in the aforementioned processes (Severi et al., 2012; Balland et al., 2014).

Expression of *Spry1* and *Spry2* in β-tanycytes suggests that growth factor signalling takes place in these cells and that their intracellular signalling cascades are being modulated. However, the expression of *Spry1* is more widespread than both of FGF receptors and ligands – while the strongest staining was observed in β-tanycytes, it does continue into the α-tanycyte domain and it is also particularly strong and widespread in the arcuate nucleus. This may be due to the fact that Sprouty expression can be elicited by the activity of a variety of growth factor receptors that are expressed in the hypothalamus and third ventricle wall, including Ntrk2, VEGFR-3, CNTFRα, ErbB1 and ErbB2 (Prevot et al., 2003; Lein et al., 2007; Hou et al., 2011; Severi et al., 2012).

Activation of the MAPK/ERK intracellular signalling pathway is one of the main ways FGF receptors exert their effects (Brewer et al., 2016). Here, it was found that there are very few cells containing phosphorylated ERK in the 3V wall and in the VMN, areas where FGF receptor expression is highest. In contrast, intense pERK staining was observed in the DMN and especially the ARC, where ERK phosphorylation has been shown to be caused by leptin signalling (Rahmouni et al., 2009). The fact that very few β- and α-tanycytes contain high amounts of pERK may be explained by non-constitutive FGF ligand release and binding to receptors and/or by strong Sprouty expression setting a threshold and preventing phosphorylation of ERK. As mentioned previously, other growth factor receptors are also expressed in tanycytes and pERK has been shown to be required for Leptin shuttling between the periphery and hypothalamic neurons, making it difficult to determine the contribution of FGF signalling (Balland et al., 2014). It is possible that individual cells are receiving multiple and distinct molecular signals due to heterogeneous receptor expression profiles and

the different functions these cells have. There may also be rostrocaudal differences in the expression of receptors, which may explain the occurrence of pERK containing clusters of β-tanycytes in caudal sections, which are absent in rostral sections. In addition to the MAPK/ERK pathway, FGF receptors signal through the PI3K-AKT, PLCγ, and STAT signalling pathways. Staining with antibodies against phosphorylated components of these pathways after ICV injection of FGFs would help better understand which downstream signalling pathways are recruited by FGF receptors *in vivo*.

Caveolin-1 is a scaffolding protein involved in the control of many cellular processes and is important for regulating stem cell activity (Baker and Tuan, 2013). It can affect cell signalling through its involvement in endocytosis and recycling of growth factor receptors and other signalling molecules or by bringing signalling component molecules closer to each other. Interestingly, just like *Fgfr1* and *Fgfr2*, caveolin-1 expression in tanycytes is restricted to the β-tanycyte domain (Peruzzo et al., 2004). Previous reports indicate that FGF2/FGFR1 signalling is controlled by caveolin-1 in endothelial cells *in vitro* (Feng et al., 2012). The required components for such control are present in β-tanycytes, therefore caveolin-1 may play an important role in regulating FGF signalling in these cells.

4.3.2 – FGF1, FGF9, FGF2 and FGF18 are likely autocrine/paracrine ligands for tanycytic FGF receptors

It has been reported previously that FGF10 is expressed in β-tanycytes (Hajihosseini et al., 2008; Haan et al., 2013). However, FGF10 can only bind IIIc splice isoforms of FGFR2 and FGFR1, but these are not present in the adult hypothalamus (Fig. 4.1 A)(Zhang et al., 2006b; Hajihosseini et al., 2008). A novel intracellular mode of action has recently been reported for FGF10 and it is plausible that it may act this way in the hypothalamus (Mikolajczak et al., 2016).

Here, *Fgf2* and *Fgf18* were found to be expressed in the β1-tanycyte domain, and both have high affinity to FGFR1, FGFR2 and FGFR3 IIIc splice isoforms, therefore these endogenous ligands may act in an autocrine/paracrine fashion to regulate the neurogenic behaviour of β1-tanycyte NSPCs or their metabolic functions (Zhang et al., 2006b).

Intense staining was observed in the β2-tanycyte domain using *Fgfr1* and *Fgfr2 cRNA* probes, but no expression of cognate FGF ligands. In the rat brain, *Fgf5* expression

in β2-tanycytes has been observed in fasting and re-fed rats (Li et al., 1999). The concentration of FGF1 in rat CSF is increased after a glucose injection into the 3V, indicating that FGF1 is released into the 3V as well as the parenchyma (Oomura et al., 1992). It is possible that other FGFs (FGF-2,9,18) that are expressed in the 3V wall may be released into the CSF as well and is provided to β2-tanycytes and/or other areas of the hypothalamus through diffusion or currents created by beating cilia (Faubel et al., 2016).

Integrated nuclear FGFR1 signalling (INFS) refers to the ability of FGFR1 to accumulate in the nucleus and affect gene regulation (Stachowiak et al., 2015). This is facilitated by the binding of high-molecular-weight FGF2 (23 kDa) which has a nuclear localisation sequence and is not released extracellularly but is transported into the nucleus (Gu and Kay, 1998; Dunham-Ems et al., 2009). In tanycytes, *Fgf2* is expressed in the more dorsal part of the β1-tanycyte domain and tapers off ventrally, meanwhile, the opposite is true for *Fgfr1*: its expression is strongest in the β2-tanycyte domain and tapers off in the ventral part of the β1-tanycyte domain. This suggests that FGF2 and FGFR1 domains of expression may be mutually exclusive, precluding INFS. This is consistent with the role of β-tanycytes as NSPCs, since in the subventricular zone neurogenic niche FGFR1 acts as a cell surface receptor in NSPCs, while INFS occurs in differentiating cells (Fang et al., 2005; Stachowiak et al., 2009). Less is known about FGFR2 localisation to the nucleus, but it occurs in breast development and cancer of breast tissue (Lu et al., 2008; Martin et al., 2011). The localisation of FGFR2 to the nucleus has been shown to be dependant on FGF9 signalling in male gonads (Schmahl et al., 2004). In addition, nucleolar FGFR2 was shown to interact with FGF2 and promote ribosomal DNA transcription, promoting osteoprogenitor proliferation while suppressing differentiation (Neben et al., 2014). β1-tanycytes express *Fgfr2*, *Fgf2* and are in close proximity to *Fgf9* expressing α-tanycytes. It would, therefore, be interesting to investigate if FGFR2 nuclear localisation and its regulation by FGF2 and FGF9 occur in these cells and if so, what are the functions of this poorly understood process.

The expression of *Fgf18* messenger RNA has been previously reported in ventral α2-tanycytes by mRNA in situ hybridization (Robins et al., 2013). In this paper, tanycytes were divided into GFAP expressing α1, dorsal α2, ventral α2 tanycytes and GFAP negative β tanycytes. It is important to note that the classification of tanycytes and the domain boundaries used in this paper differed slightly to ones used in this thesis. Here, GFAP expression is used as a boundary marker between the α and β domains

(Goodman and Hajihosseini, 2015). In the Robins et al. paper (2013), tanycytes were also defined according to their location in relation to parenchymal nuclei: α1 are adjacent to ventromedial and dorsomedial nuclei, α2 are at the level of the arcuate nucleus and β tanycytes form the floor of the third ventricle. This classification neglects the β1 tanycyte subtype which is also found at the level of the arcuate nucleus but is GFAP negative (Prevot et al., 2018). Indeed, Robins et al., (2013) distinguish dorsal and ventral α2 tanycytes based on the presence or absence of GFAP expression respectively. Therefore it seems clear that ventral α2 tanycytes are equivalent to β1 tanycytes as defined in this thesis and other reports and may also encompass a transitional zone between α- and β-tanycyte domains (Goodman and Hajihosseini, 2015; Campbell et al., 2017; Prevot et al., 2018). These differing definitions can explain how ventral α2 tanycytes reportedly respond to FGF2 by proliferating (Robins et al., 2013), although in this thesis and other reports (Campbell et al., 2017) it was shown that FGF receptors were absent from the α-tanycyte domain. Differing classification systems and criteria have caused some confusion in the field and standardisation would help avoid further misunderstandings. There are suggestions for refinements of the classification system (Prevot et al., 2018). In this thesis, perhaps an imperfect, but widely used and simple classification method is used by distinguishing α and β tanycytes through GFAP and S100β expression.

Here, the expression of *Fgf18* in β1-tanycytes was confirmed by using a $Fgf18^{CreERT2}$::$Rosa26^{tdTomato}$ transgenic reporter mouse model which allows for lineage tracing (Zhang et al., 2016). Interestingly, in addition to the β1-tanycyte domain, tdTomato expressing cells were located throughout the third ventricle wall, including α-tanycytes and ependymal cells. Since the mRNA is restricted to β1-tanycytes (Robins et al., 2013), a possible explanation is that *Fgf18* expressing β1-tanycytes divide and their lineage traced progeny migrate dorsally to give rise to α-tanycytes and ependymal cells. This is also supported by the fact that β1-tanycytes show very high BrdU staining after ICV FGF2 injections (Robins et al., 2013). Taken together, it is possible that *Fgf18* expressing β1-tanycytes form a population of progenitors responsive to FGF signalling. However, further experiments would be needed to determine if *Fgf18* expressing cells coexpress FGF receptors and whether they respond to the application of *Fgf18* or *Fgf2* and longer-term lineage tracing to see if they generate neural or glial cells in the parenchyma or replenish the 3V ependyma.

Tanycytes of the median eminence have privileged access to systemic metabolic signals due to their projections contacting fenestrated capillaries. The expression of

FGF receptors in β-tanycytes raises the exciting possibility that they are receptive to endocrine FGF19 and FGF21 which are being investigated as therapeutic agents (Degirolamo et al., 2016). β-Klotho (Klb), is a co-receptor required for the binding of these endocrine FGFs. It has been established that significant *Klb* expression in the hypothalamus is restricted to the suprachiasmatic nucleus. However, its expression in the third ventricle ependyma had not been assessed (Bookout et al., 2013). Here, in situ hybridisation was performed using a *Klb* cRNA probe, but the staining was weak and likely unspecific. In addition, ICV injection of FGF1, but not FGF19, causes induction of c-Fos (Scarlett et al., 2016). FGF19 and FGF21 have similar binding affinities to FGFR-Klb complexes, so it is likely that tanycytes are also not responsive to FGF21 (Zhang et al., 2006b). Additionally, both FGF19 and FGF21 have been shown to bypass the blood-brain barrier. It is, therefore, possible that the suprachiasmatic nucleus may indeed be the exclusive target of endocrine FGFs in the hypothalamus (Hsuchou et al., 2007, 2013). Some recent reports show that *Fgf21* is expressed in the brain at low levels, but provide no information as to the region or regions of the brain where it is expressed (Petryszak et al., 2016). *Fgf21* was also detected in the current RT-PCR screen, confirming that it is expressed in the hypothalamus (Fig. 4.1 D) and it would be useful to know the precise pattern of its expression within the hypothalamus. One hypothetical option is close to the suprachiasmatic nucleus cells that express *Klb*.

4.3.3 – FGF signalling components are expressed in the hypothalamus parenchyma

Expression of *Fgfr1* in the parenchyma is quite widespread and the strongest staining was observed in the ventromedial nucleus. Interestingly, no or very little coexpression of *Fgfr1* with GFAP, an astrocyte marker, was observed indicating that *Fgfr1* is most likely expressed by neurons within the appetite-regulating centres of VMN, ARC, LHA and DMN. Interestingly, both *Fgf1* and *Fgf9* expression in the parenchyma is similar and matches that of *Fgfr1*. FGF9 has an atypical signal sequence and is secreted efficiently, therefore the source of FGF ligands for parenchymal FGF receptors may come from both tanycytes and parenchyma (Revest et al., 2000). FGF1 has been previously shown to be expressed in the rat third ventricle wall and released into the parenchyma after feeding or glucose infusion, potently inhibiting food intake (Oomura et al., 1992). It is possible that FGF9 may have a similar function.

Fgfr3 was present in S100β expressing glial cells, punctate but widespread in the hypothalamus parenchyma. This is consistent with earlier studies which show that

Fgfr3 is expressed in astrocytes and their precursors in the developing CNS (Pringle et al., 2003). Interestingly, these *Fgfr3*/S100β cells are also located periventricularly. ICV injections of FGF1 cause induction of Fos and HSP27 in periventricular hypothalamus astrocytes, but not in neurons of the parenchyma (Suzuki et al., 2001a; Suzuki et al., 2001b; Scarlett et al., 2016). Importantly, this effect occurs shortly after injection and coincides with feeding suppression effects. It is, therefore, possible that *Fgf1*, expressed in α-tanycytes is released postprandially and acts on periventricular *Fgfr3*/S100β glial cells through FGFR3 activation, leading to food intake suppression and other energy balance regulating effects. *Fgf9* is expressed in a similar expression pattern and binds to FGFR3, suggesting it may have a similar role and act as a redundant molecule or a distinct component of feeding control.

Expression of *Etv4*, a transcription factor induced by FGFR signalling, has previously been used as an FGF signalling readout (Roehl and Nusslein-Volhard, 2001; Klein et al., 2008; Yaguchi et al., 2009). In this study, expression of *Etv4*-GFP was restricted to the caudal LHA. The LHA contains important feeding regulating circuitry and radioactive ^{125}I-FGF1 and ^{125}I-FGF2 injected into the third ventricle are transported and internalised in LHA neurons, potentially conferring the later onset metabolic effects of ICV FGF1 injections. ((Ferguson and Johnson, 1991; Stuber and Wise, 2016) via Review (Gasser et al., 2017)) Therefore *Etv4* may correspond to FGF and FGFR expression and signalling in the LHA. Even more restricted expression of *Mkp3* was observed, with very few *Mkp3*+ cells located in the LHA, positioned laterally to the ARC and ventrally to the VMN, akin to the strong pERK staining that was observed in this region.

Intracellular FGFs form a family of four signalling peptide lacking FGFs: FGF11-14. FGF12-14 can associate with voltage-gated sodium channels in the CNS and consequently modulate the electrical properties of neurons (Zhang et al., 2012). In addition, FGF13 has been shown to be a microtubulin stabilizing protein, required for migration and polarization of newborn neurons in developing mouse neocortex and hippocampus (Wu et al., 2012). To my knowledge, the expression and functions of intracellular FGFs in the adult hypothalamus have not previously been reported. Through ISH it was found that *Fgf12*, *Fgf13* and *Fgf14* are expressed in the hypothalamic centres important for regulating energy balance, but absent in tanycytes. This may suggest their involvement in modulating the electrical activity of energy balance controlling neurons or, in the case of *Fgf13,* involvement in the

migration and maturation of newborn neurons during adult hypothalamic neurogenesis as it is found in their destinations (ARC, VMN, DMN).

As mentioned previously, the mRNA for RT-PCR was isolated from a much larger region of the hypothalamus than the restricted region where ISH was performed (Bregmas -1.58 to -1.94). This can explain why some genes found by the RT-PCR screen were not detected by in situ hybridization. This is exemplified by *Etv4*, which was not detected by ISH, but its expression was found using the $Etv4^{GFP}$ mouse line starting at Bregma -1.94, more caudally than the tissue sections used for ISH experiments. Of course, it is possible that ISH conditions for some probes were not suitable. Therefore, the experiments detailed in this chapter form a valuable contribution, but cannot be considered as completely comprehensive.

Conclusion

These experiments revealed novel expression patterns and established that β-tanycytes and the surrounding parenchyma are enriched with expression of FGF receptors, their cognate ligands and signalling modulators, making them targets of both endogenous FGF signalling and mediators of pharmacological interventions that target FGF signalling components. The detailed spatial gene expression information allows for the modelling of likely endogenous signalling interactions and events (Fig. 4.8). This should prove to be a useful resource for understanding FGF signalling in hypothalamic neurogenesis and regulation of metabolism as well as design and interpretation of studies that investigate these processes.

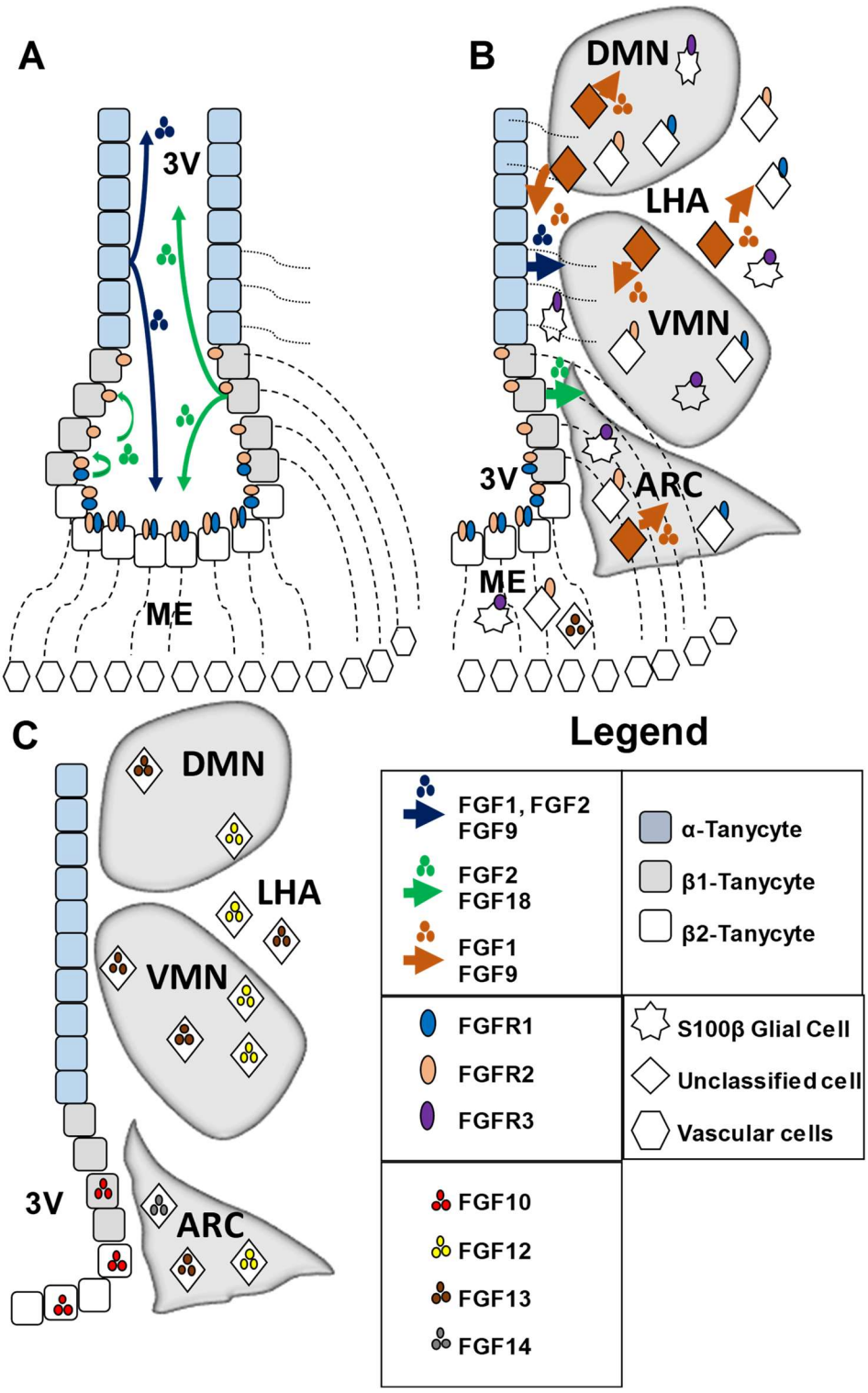

Figure 4.8 - Expression of FGFs, FGF receptors and their likely interactions in tanycytes and hypothalamic energy balance regulating nuclei. Schematics display FGF receptors, their likely ligands and mode of action in the hypothalamus. Autocrine/paracrine FGF signalling in tanycytes (A) and neighbouring parenchyma (B). Note that the cellular location of FGFR proteins in tanycytes, for example, if they are expressed on the apical side facing the CSF, is not known. Expression of intracellular FGFs (C).

Chapter 5

Fgfr1 and Fgfr2 signalling regulates tanycytes and neuron amplification in postnatal mice

5.1 – Introduction

Research in adult hypothalamic neurogenesis has been growing since the initial report of multipotent neurospheres derived from adult mammalian hypothalamus (Weiss et al., 1996), due to its potential roles in regulating energy balance (Sousa-Ferreira et al., 2014). These efforts have started elucidating neurogenesis in the hypothalamus, however, many questions about the precise location and identity of the neural stem/progenitor cells (NSPCs) in this niche, its functional significance and molecular regulation remain to be answered (Yoo and Blackshaw, 2018).

Growth factors play crucial roles in the regulation of adult neurogenesis in the classical subgranular and subventricular zone niches (Liu and Song, 2016). The FGF signalling system has been shown to play a pivotal role in neurogenesis in these niches (Zhao et al., 2007; Stevens et al., 2012; Kang and Hébert, 2015). In hypothalamic neurogenesis, FGF signalling has been shown to be important for promoting the proliferation of tanycytes in vivo through intracerebroventricular administration (Xu et al., 2005; Robins et al., 2013; Yulyaningsih et al., 2017) and in cell culture (Weiss et al., 1996; Xu et al., 2005; Robins et al., 2013). However, caution should be exercised, as studies of endogenous and exogenous growth factor signalling may not always yield congruous findings (Perez-Martin, Cifuentes et al. 2010, Chaker, George et al. 2016). Unlike the classical niches where endogenous FGF signalling function has been investigated and important insights into its function were gained, in the hypothalamus niche, endogenous FGF signalling in vivo has been scarcely studied.

The expression pattern survey of endogenous FGF signalling components, detailed in chapter 4, was a first step to addressing this gap in knowledge. Among the most important findings was that *Fgfr1* and *Fgfr2* were the only FGF receptors expressed in tanycytes, indicating their potential importance in regulating NSPCs. Their expression was restricted to β-tanycytes which do not express GFAP (Goodman and Hajihosseini, 2015). Expression patterns of endogenous FGFs and FGF receptor modulators were also mapped, giving further clues on FGF signalling in this niche. However, the function of endogenous signalling still needs to be investigated.

One of the most informative ways to explore endogenous functions of a gene of interest is through the use of gene knockout mice. Global knockout of either *Fgfr1* or *Fgfr2* results in embryonic lethality and is therefore not a feasible option (Yamaguchi et al., 1994; Xu et al., 1998). A different and viable option is to use conditional gene knockout strategies. This can be achieved by crossing Cre driver mice, where Cre is driven by the promoter of a cell-type specific gene, with transgenic lines that have

functionally important regions of the gene of interest flanked by LoxP sites (Friedel et al., 2011). In the resulting cross, Cre mediated recombination causes excision of the floxed regions and loss of gene function. This will occur in all cells that express the gene that drives Cre expression, as well as their progeny. To achieve temporal specificity of recombination, a Cre and human estrogen ligand binding domain mutant fusion protein (CreERT2) can be used (Feil et al., 1997) instead of Cre, as its activation requires exposure to tamoxifen and its metabolites.

Our lab has successfully used $Fgf10^{CreERT2}$::$Rosa26^{tdTomato}$ mice (Cre/Tomato, referred to as CT) to lineage trace *Fgf10* expressing β-tanycytes and in doing so showed that they are capable of producing neurons in the post-weaned hypothalamus (Haan et al., 2013). Since expression of *Fgf10*, *Fgfr1* and *Fgfr2* in the 3V wall is restricted to β-tanycytes, administering tamoxifen to $Fgf10^{CreERT2}$::$Rosa26^{tdTomato}$::$Fgfr1^{Flox/Flox}$::$Fgfr2^{Flox/Flox}$ (conditional knockout, referred to as CKO) animals would cause *Fgfr1*/*Fgfr2* deficiency specifically in β-tanycytes and their progeny. The deletion of both FGF receptors should abrogate all FGF receptor signalling in the affected cells and prevent potential compensation by either receptor. Lineage tracing of these cells would allow investigations into the roles that these endogenous receptors may have in regulating NSPCs and neurogenic processes such as proliferation, migration and survival.

5.1.1 – Aims

Recent studies of endogenous growth factor signalling in tanycytes have revealed differing effects compared to exogenous growth factor application (Perez-Martin, Cifuentes et al. 2010, Chaker, George et al. 2016). To fill the gap in the literature and explore the roles of endogenous FGF signalling in the hypothalamus neurogenic niche, *Fgfr1/Fgfr2* conditional knockout animals were used to assess any changes in lineage traced cell morphology, distribution and numbers, along with PCNA, an S phase marker (Celis and Celis, 1985), to detect changes in proliferation.

5.2 – Results

5.2.1 – Tamoxifen administration to *Fgfr1/Fgfr2* CKO animals allows for temporal lineage tracing of β-tanycytes deficient in FGF receptors

Excision of floxed regions in the *Fgfr1* and *Fgfr2* locus of CKO animals (Fig. 5.1 A) only occurs in *Fgf10* expressing cells upon tamoxifen administration. One way to determine if a tamoxifen administration regime results in effective recombination in the hypothalamus is to detect tdTomato positive cells. tdTomato is only expressed when the LoxP flanked STOP cassette is excised due to Cre mediated recombination. Therefore, any cell expressing tdTomato likely had deletion of *Fgfr1* and *Fgfr2* exons. Our lab has already established methods of administrating tamoxifen, suitable for lineage tracing of tdTomato positive tanycytes. However, the observation of tdTomato cells is not definitive proof that recombination of all floxed alleles occurred. For further confirmation that deletion of *Fgfr1* and *Fgfr2* sites took place, CKO animals were tamoxifen pulsed, DNA was isolated from the hypothalamus and PCR performed using primers that detect a band of defined size only if FGFR excision had occurred.

The primers for detecting *Fgfr2* null alleles have been described previously (Yu et al., 2003) (Fig. 5.1 C). Without excision, these primers would produce a band of around 5.2 kb. However, due to the excision LoxP flanked exons, the PCR product is truncated to 471 bp. The primers for *Fgfr1* deletion band were designed with the help of Shaun Clare. Before recombination, they would detect a band of around 7.5 kb. After excision of floxed exons, the detected product size reduced to around 400-500 bp.

In CKO mice, the number of hypothalamus cells where recombination takes place is relatively low, as it would only happen in a subset of *Fgf10* expressing cells. Therefore, it can be difficult to detect low numbers of null copies. To determine the optimal conditions for the PCR cycles and if the primers are suitable, DNA extracted from PGK^{Cre}::$Fgfr1^{Flox/+}$::$Fgfr2^{Flox/+}$ mouse tissue was used as a positive control. PGK^{Cre} causes LoxP recombination in most cells due to its early activation in the diploid phase of oogenesis, greatly increasing null copy numbers and making detection of the deletion bands easier (Lallemand et al., 1998). Therefore, DNA from these animals was very useful for testing whether the deletion PCR conditions and primers were suitable to detect deletion bands and to optimise the reaction parameters. Later, it was useful to run these positive control reactions to confirm that the PCR reactions were run correctly and for easier confirmation of whether PCR reactions using CKO animal DNA produced correct deletion band sizes.

CKO pups were manually suckled tamoxifen at P5 and P6, the hypothalamus was then dissected at P8. The *Fgfr1* deletion PCR worked well with DNA extracted from the hypothalamus of these mice and produced a PCR product in the expected range (Fig. 5.2 B). The PCR reaction using PGK^{Cre}::$Fgfr1^{Flox/+}$::$Fgfr2^{Flox/+}$ positive control hypothalamus DNA produced a band of the same size. These mice were heterozygous for *Fgfr1* and *Fgfr2* floxed alleles, therefore only one copy of *Fgfr1* and *Fgfr2* was deleted. Meanwhile PCR on negative control DNA from an untreated $Fgf10^{CreERT2}$::$Fgfr1^{Flox/+}$::$Fgfr2^{Flox/Flox}$ mouse did not produce a deletion band.

More difficulties were encountered with *Fgfr2* deletion band PCR. Although PCR reactions with PGK^{Cre}::$Fgfr1^{Flox/+}$::$Fgfr2^{Flox/+}$ positive control hypothalamus DNA produced a deletion band of the expected size, DNA from pulsed CKO animals, as used in *Fgfr1* deletion PCR, did not produce the deletion band. It is likely that the *Fgfr1* deletion PCR conditions and primers were more optimal to detect low copy numbers than ones for *Fgfr2* deletion. The DNA was extracted from the whole hypothalamus, therefore null allele copies are dilute, as recombination would happen only in tanycytes. To increase the chances of detection, vibratome sections from a CKO mouse brain IP pulsed at P44/P45 and dissected at P55 were used. A fluorescent microscope was used to look for the hypothalamus region containing the highest density of tdTomato positive cells (median eminence, tanycytes, arcuate and ventromedial nuclei). This region was crudely dissected from the sections using a scalpel and used for DNA extraction. Using this DNA, *Fgfr2* deletion reactions were performed that yielded a weak but clearly discernible deletion band, the same size as the one seen with PGK^{Cre}::$Fgfr1^{Flox/+}$::$Fgfr2^{Flox/+}$ mouse positive control DNA (Fig. 5.2 C). Reactions with non-injected $Fgf10^{CreERT2}$::$Fgfr1^{Flox/+}$::$Fgfr2^{Flox/Flox}$ mouse negative control DNA did not produce a deletion band.

These experiments provided confidence that excision of *Fgfr1* and *Fgfr2* floxed alleles does occur in the hypothalamus of CKO mice in at least some of the lineage traced cells. Therefore, the function of FGF receptors in *Fgf10* expressing tanycytes and their progeny can be assessed using these mice.

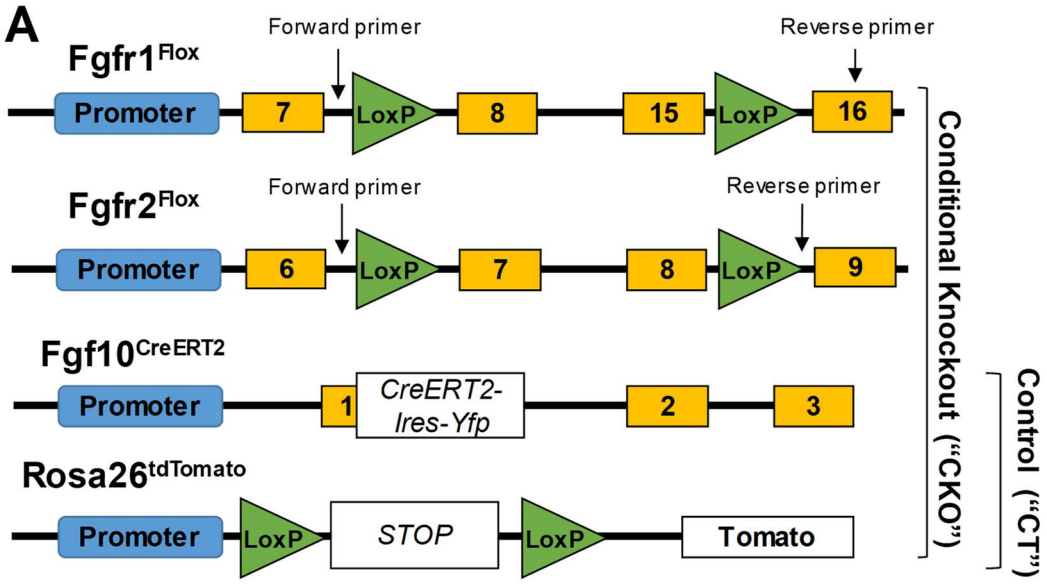

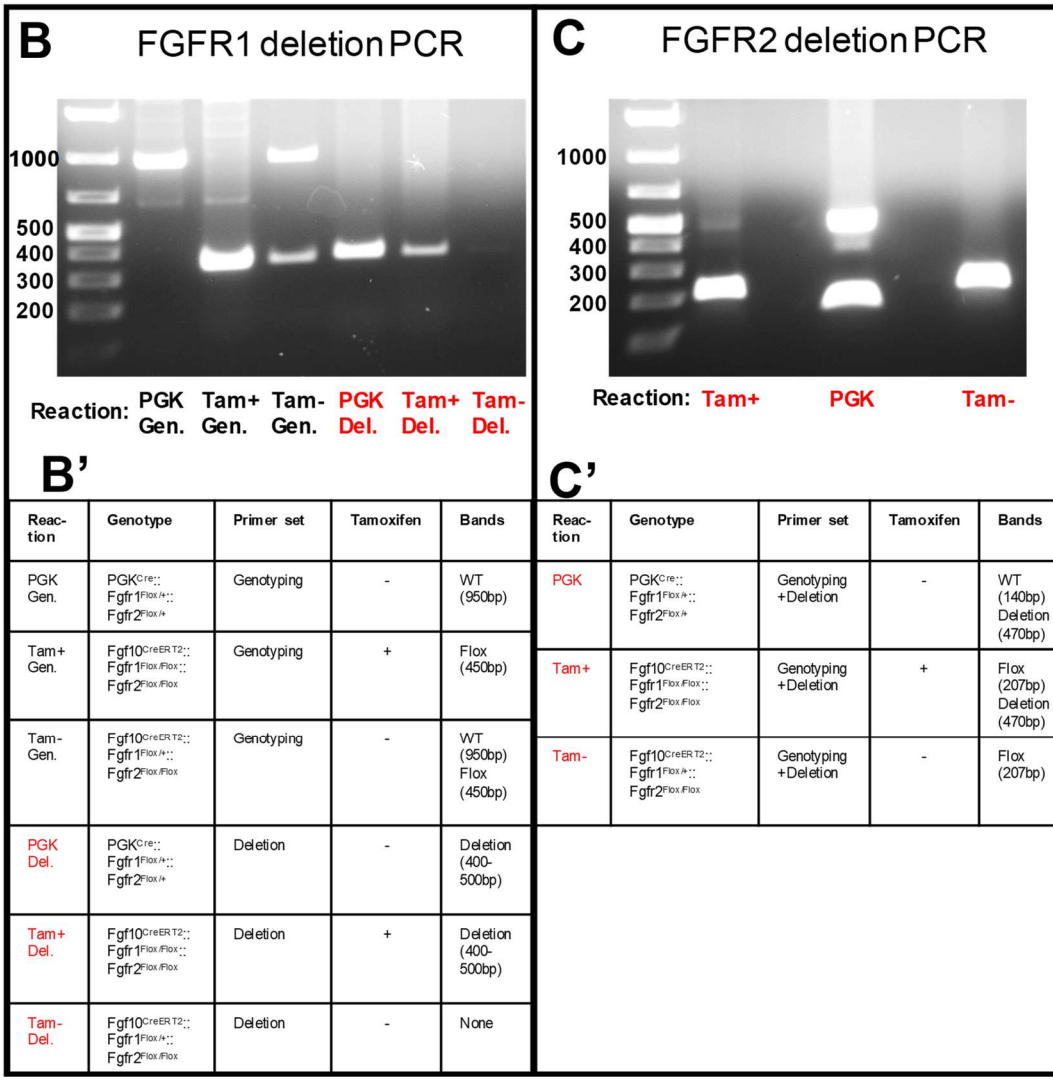

B'

Reac-tion	Genotype	Primer set	Tamoxifen	Bands
PGK Gen.	PGK^{Cre}::Fgfr1$^{Flox/+}$::Fgfr2$^{Flox/+}$	Genotyping	-	WT (950bp)
Tam+ Gen.	Fgf10^{CreERT2}::Fgfr1$^{Flox/Flox}$::Fgfr2$^{Flox/Flox}$	Genotyping	+	Flox (450bp)
Tam- Gen.	Fgf10^{CreERT2}::Fgfr1$^{Flox/+}$::Fgfr2$^{Flox/Flox}$	Genotyping	-	WT (950bp) Flox (450bp)
PGK Del.	PGK^{Cre}::Fgfr1$^{Flox/+}$::Fgfr2$^{Flox/+}$	Deletion	-	Deletion (400-500bp)
Tam+ Del.	Fgf10^{CreERT2}::Fgfr1$^{Flox/Flox}$::Fgfr2$^{Flox/Flox}$	Deletion	+	Deletion (400-500bp)
Tam- Del.	Fgf10^{CreERT2}::Fgfr1$^{Flox/+}$::Fgfr2$^{Flox/Flox}$	Deletion	-	None

C'

Reac-tion	Genotype	Primer set	Tamoxifen	Bands
PGK	PGK^{Cre}::Fgfr1$^{Flox/+}$::Fgfr2$^{Flox/+}$	Genotyping +Deletion	-	WT (140bp) Deletion (470bp)
Tam+	Fgf10^{CreERT2}::Fgfr1$^{Flox/Flox}$::Fgfr2$^{Flox/Flox}$	Genotyping +Deletion	+	Flox (207bp) Deletion (470bp)
Tam-	Fgf10^{CreERT2}::Fgfr1$^{Flox/+}$::Fgfr2$^{Flox/Flox}$	Genotyping +Deletion	-	Flox (207bp)

Figure 5.1 – PCRs confirming excision of *Fgfr1* and *Fgfr2* floxed alleles. Schematic representation of the $Fgfr1^{Flox}$, $Fgfr2^{Flox}$, $Fgf10^{CreERT2}$, $Rosa26^{tdTomato}$ alleles and the combinations that were bred (CKO and CT), black arrows indicating the binding sites of primers used for detecting deletion bands (A). PCR reactions were used to genotype (PGK Gen., Tam+ Gen., Tam- Gen.; reaction name in black) or confirm excision of *Fgfr1* and *Fgfr2* floxed regions (PGK Del., Tam+ Del., Tam- Del.; reaction name in red) (B, C). Tables B' and C' provide detail on each of the reactions shown in images B and C. The PGK deletion reactions (PGK Del.) served as a positive control and produced bands of the same size as in the reactions using DNA of CKO animals treated with tamoxifen (Tam+ Del.) (B, C). Negative control reactions using DNA of CKO tamoxifen untreated animals (Tam- Del.) did not produce such bands (B, C). Note that *Fgfr1* genotyping and deletion bands are of similar size, so separate reactions were performed only with primers that detect the deletion band (B).

5.2.2 – Deletion of *Fgfr1/Fgfr2* in *Fgf10*+ β–tanycytes does not elicit a discernible phenotype in young adult mouse hypothalamus

To explore the function of *Fgfr1* and *Fgfr2* in postnatal hypothalamic neurogenesis, CKO and CT mice received IP injections of tamoxifen at P44 and P45 and were dissected at P55 (Fig. 5.2 A). This lineage tracing paradigm was previously tested using CT mice and was found to be suitable for studying hypothalamic neurogenesis (Haan et al., 2013). Additionally, the expression pattern information on FGF signalling system components in the hypothalamus, as detailed in the previous chapter, was gathered at a similar age (P60-P80). S100β was used as an α- tanycyte domain marker (Goodman and Hajihosseini, 2015) and Hoechst staining was used to distinguish the parenchymal nuclei.

At P55, lineage traced cells were found in the β- and α-tanycyte domains (Fig. 5.2 B, B', C, C') and some in the VMN, ARC and DMN nuclei (Fig. 5.2 B'', B''', C'', C'''), in both CKO and CT animals. *Fgfr1*/*Fgfr2* deficient cells exhibited tanycyte and parenchymal cell morphology indistinguishable from cells traced in CT animals. In both CT and CKO animals, lineage traced parenchymal cells predominantly exhibited neuronal cell morphology (B''', C''') with long processes, although very few cells were found that exhibited glial/immature morphology (similar examples shown in Fig. 5.12 D, E). However, they did not co-express S100β.

Quantifications were performed by counting lineage traced cells contained in these compartments: α-tanycytes, β-tanycytes, the arcuate, ventromedial and dorsomedial nuclei. Cells were counted noting which compartment they are positioned in, and in

sections of bregma -1,46 to -2,18, which cover most of the extent of these compartments (Franklin and Paxinos 2008, Haan, Goodman et al. 2013). Cell count normalisation to volume was not performed due to categorising the cell counts to their location in the compartments and due to the α-tanycyte and β-tanycyte domains being comprised of just one cell-layer surrounding the third ventricle with varying extent along the rostro-caudal axis.

Quantification of lineage traced cells did not reveal any significant cell number differences in the 3V wall (**CT**: 161.3 ± 71.32, n=4; **CKO**: 249.5 ± 74.01, n=4; p=0.4235, 95% confidence interval on the difference between means = -163.3 to 339.8) (Fig. 5.3 A) or parenchyma (**CT**: 24.25 ± 16.01, n=4; **CKO**: 29 ± 8.436, n=4; p=0.8017, 95% confidence interval on the difference between means = -43,19 to 52,69) (Fig. 5.3 B). The majority of lineage traced cells were found in the β-tanycyte domain (Fig. 5.3 A') and the VMN (Fig. 5.3 B') in the 3V wall and parenchyma respectively. Subgroup analysis was performed to compare tdTomato+ cell numbers and distribution between CKO and CT mice in α- and β-tanycyte domains (Fig. 5.3 A, A') or VMN, DMN and ARC (Fig. 5.3 B, B'). No significant differences were found.

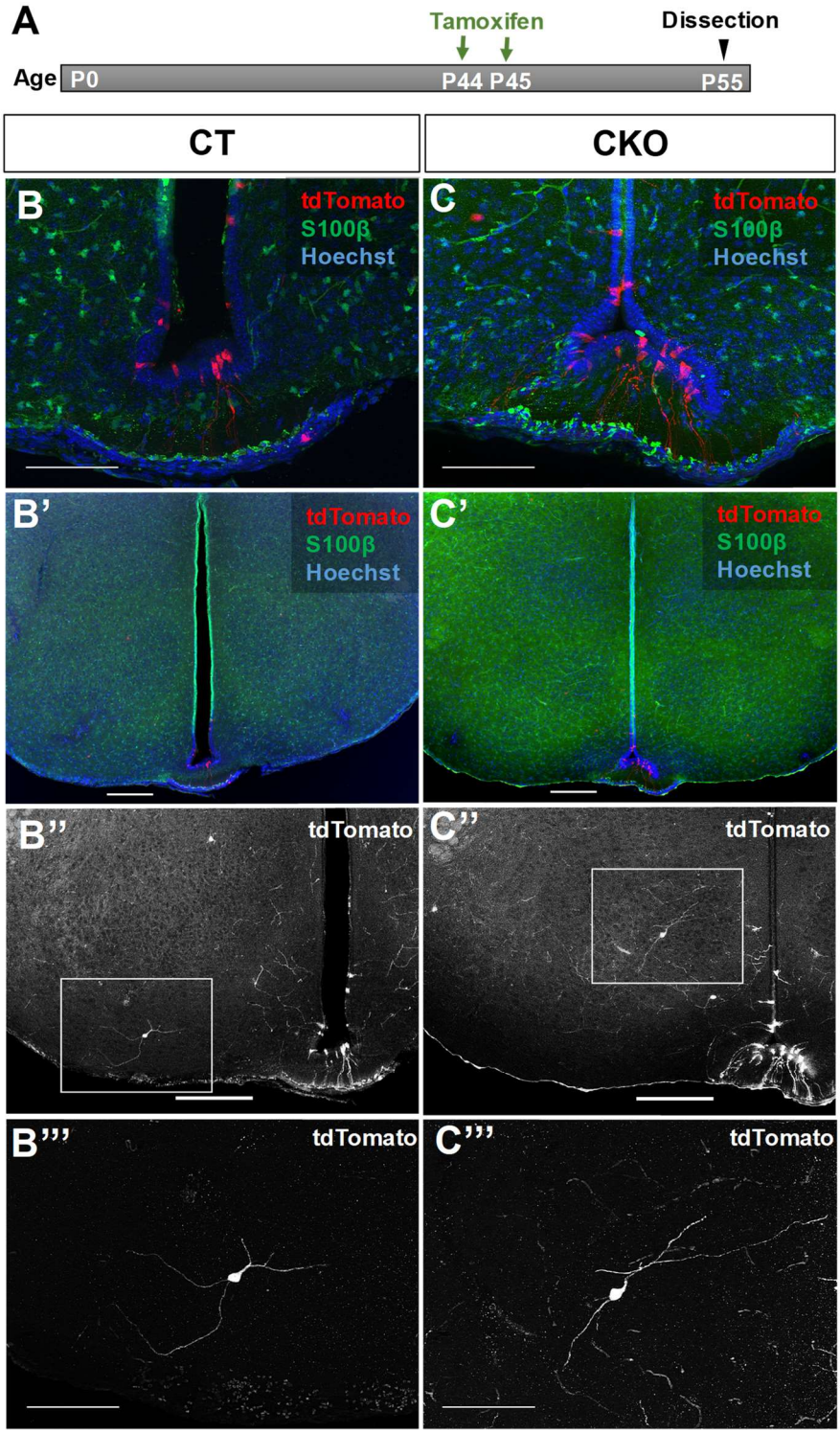

Figure 5.2 – Morphology of lineage traced FGF receptor-deficient cells is unaltered in the young adult hypothalamus. Schematic displaying the tamoxifen administration and dissection paradigm (A). Immunohistochemistry revealed no visible differences in the morphology of lineage traced tanycytes (B, C), and parenchymal cells (B'', B''', C'', C''') in young adult CT and CKO hypothalamus. Cells in the parenchyma had mainly neuronal morphology with long processes (B''', C'''). Scale bar – 100 µm.

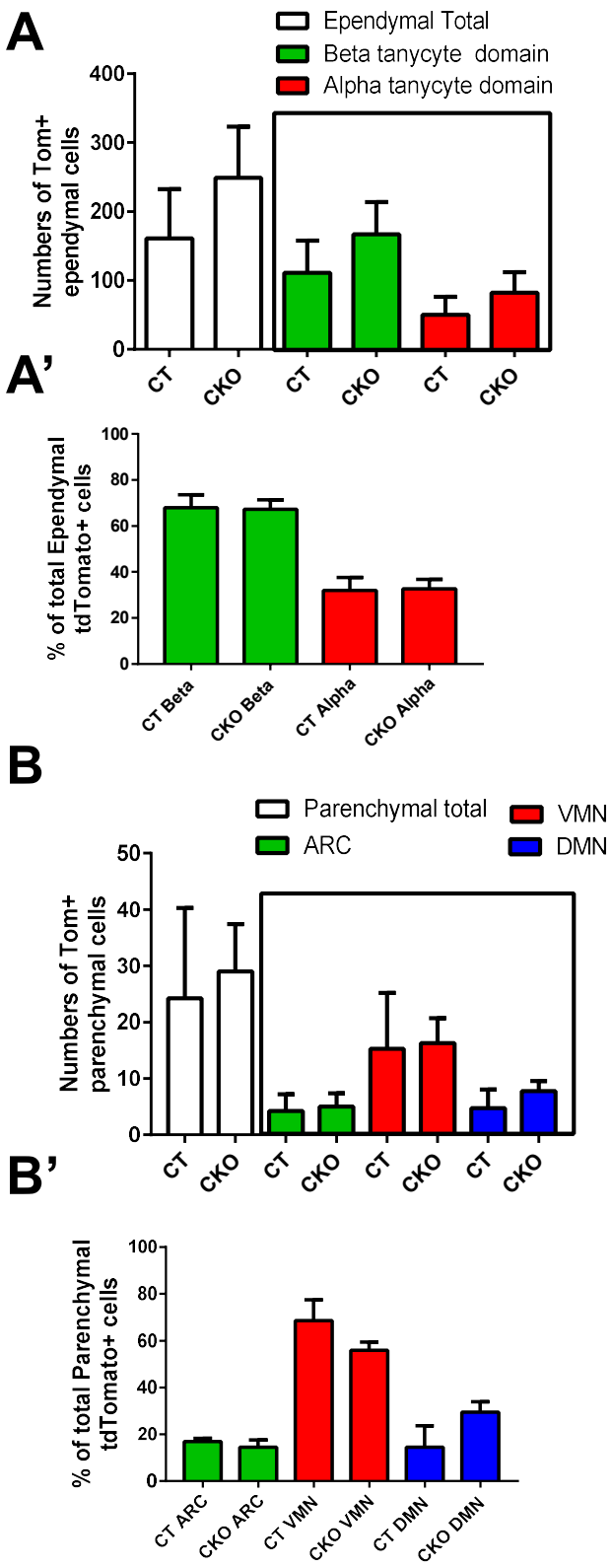

Figure 5.3 – FGF receptor deficiency does not lead to changes in lineage traced cell numbers and distribution in the young adult hypothalamus. Graphs display numbers and distribution of lineage traced cells in the 3V wall (A, A') and parenchyma (B, B') of CT (n=4) and CKO (n=4) young adult hypothalamus. No significant changes were detected.

5.2.3 – *Fgfr1* and *Fgfr2* are expressed in postnatal hypothalamus neurogenic niche

It has been shown that FGF10 expressing tanycyte proliferation and neurogenesis is most active perinatally and declines with age (Haan et al., 2013). In addition, previous work in our lab has shown that *Fgf10* expressing tanycytes lineage traced starting at P4 can robustly generate neurons and glial cells (Goodman et al., in preparation). Multiple time-points (P6, P8, P10, P12 and P28) and proliferation, cell type, cell-death markers were used for analysis in this study, allowing for a description of a lineage hierarchy, whereby β-tanycytes give rise to parenchymal neurons and glial cells through a transient, proliferating α-tanycyte population.

To determine if *Fgfr1* and *Fgfr2* are expressed in the postnatal hypothalamus and may, therefore, have potential roles in regulating postnatal neurogenesis, in situ hybridization was performed on P8 mouse brain sections. This revealed patterns of expression similar to ones seen at P60-P80 (Chapter 4). *Fgfr1* was expressed in β tanycytes and VMN, but absent from the α-tanycyte domain (Fig. 5.4 A, A'). Unlike in P60-P80 animals, *Fgfr2* was expressed not only in β-tanycytes but also in α-tanycytes (Fig. 5.4 B, B'). *Fgfr3* was absent from the 3V ependymal but expressed in parenchymal S100β positive cells (Fig. 5.4 C, C'). Expression of *Fgf10* in β-tanycytes at P4 has been previously demonstrated using $Fgf10^{LacZ}$ mice (Haan et al., 2013). Therefore, CKO mice can be used to explore the potential roles of FGF signalling in postnatal hypothalamic neurogenesis.

5.2.4 – Deletion of *Fgfr1/Fgfr2* from β–tanycytes causes amplification of lineage traced β–tanycytes and VMN cells in postnatal mice

To investigate the potential roles of FGFR signalling in the postnatal hypothalamus, CKO and CT pups were manually suckled tamoxifen at P4 and P5, then dissected at P6 for acute chase (Fig 5.5 A) and at P28 for long chase analysis (5.7 A). In the acute chase animals, the majority of tdTomato+ cells were found in the 3V wall (Fig. 5.5 B, B'', C, C''). Few, faint tdTomato+ parenchymal cells were found and they had short projections (Fig. 5.5 B'', B''', C'', C'''). There were no visible morphological differences between the groups. In both groups, very faint cells were also found that likely did not express adequate levels of tdTomato and could not be counted.

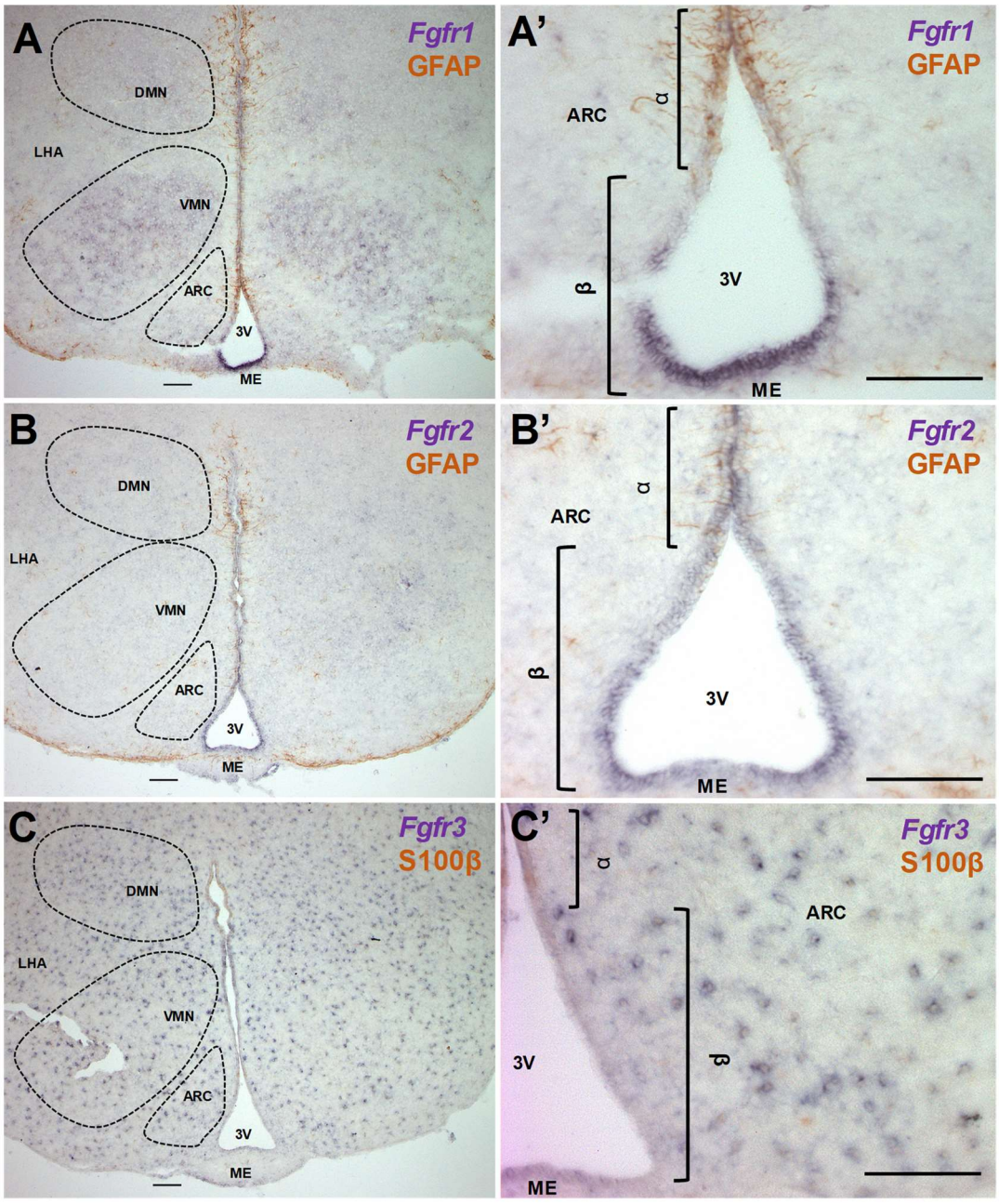

Figure 5.4 – Fgfr1 and Fgfr2 are expressed in postnatal mouse β–tanycytes. In situ hybridization on P8 hypothalamus tissue detected expression of *Fgfr1* in the hypothalamus parenchyma, strongest in the VMN (A), and restricted to β-tanycytes in the 3V wall (A'). *Fgfr2* expression was restricted to the 3V wall (B), but not confined to the β-tanycyte domain (B'). *Fgfr3* was only expressed in S100β+ parenchymal cells (C, C'). Scale bar – 100 µm.

Quantifications showed that at P6, the majority of tdTomato+ cells were in the β-tanycyte domain (Fig. 5.6 A, A'), with much fewer α tanycytes and very few parenchymal cells (Fig. 5.6 B, B'). Furthermore, CT animals had significantly more tdTomato cells in the β-tanycyte domain than CKO animals (CT: 132.5±12.5, n=2; CKO: 104.7±5.4; multiple comparisons one-way ANOVA P ≤ 0.05, CI=0,16 to 55,51), although the number of brains analysed, and the effect size was small.

No gross morphological changes in *Fgfr1*/*Fgfr2* deficient lineage traced cells compared to CT were observed at P28 (Fig. 5.7 B, B'', B''', C, C'', C''). However, there was a striking increase in the density of lineage traced FGFR deficient β-tanycytes compared to CT (Fig. 5.7 B, C). Quantification of lineage traced cells indicated that there were about twice as many tdTomato+ cells in both the 3V wall (**CT**: 229.3 ± 32.43, n=7; **CKO**: 541 ± 89.46, n=7; p=0,0066, 95% confidence interval on the difference between means = 89.98 to 533.4) and parenchyma (**CT**: 32.29 ± 4.33, n=7; **CKO**: 77.71 ± 10.89, n=7; p = 0,0022, 95% confidence interval on the difference between means : 18.32 to 72.53) of CKO animals compared to CT animals. Domain analysis showed that in the 3V wall ependymal, β-tanycyte numbers were increased significantly (**CT**: 133.5±23.25, n=4; **CKO**: 372±87.16, n=4; ANOVA: P ≤ 0.05, 95% confidence interval on the difference between means = 59.06 to 417.9), while α-tanycyte numbers only showed a trend of increase (Fig 5.8 A). In the parenchyma, VMN tdTomato+ cells were significantly more numerous in CKO (**CT**: 21.86±2.899, n=7; **CKO**: 53.57±8.109 n=7; ANOVA: P ≤ 0.0001, 95% confidence interval on the difference between means = 18.02 to 45.41), while numbers of DMN and ARC cells also showed only trends of increased numbers (Fig. 5.8 B). However, the relative distribution of lineage traced cells in the ARC, VMN and DMN was unchanged (Fig. 5.8 B').

Parenchymal cells in both groups mostly exhibited neuronal morphology, with the rare exceptions of cells that display glial/immature morphology (Fig. 5.11 D, E), however, none of them co-localised with S100β.

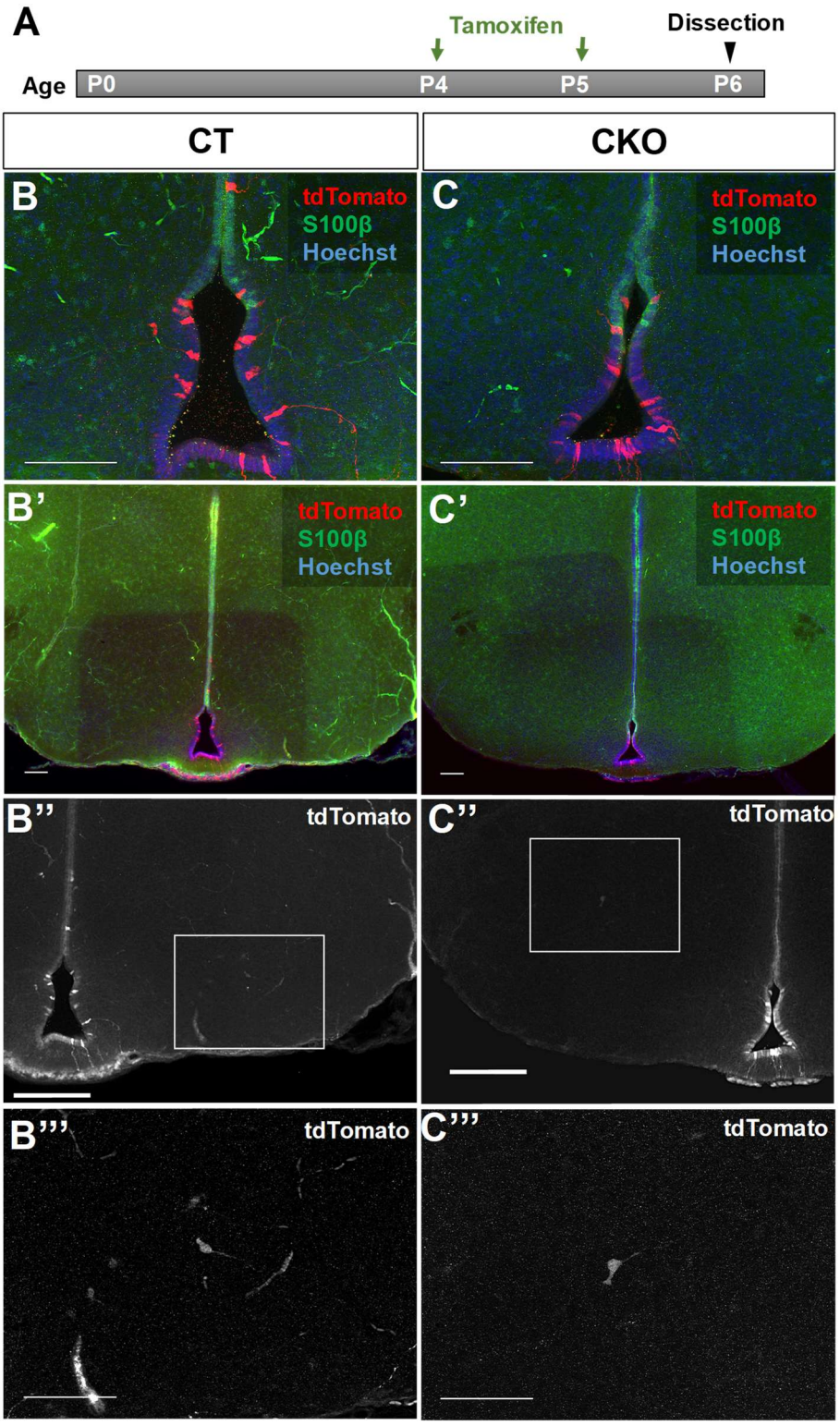

Figure 5.5 – Acute lineage tracing reveals no cell morphology changes in the *Fgfr1/Fgfr2* deficient hypothalamus. Schematic displays the timing of tamoxifen administration and brain dissection (A). Immunohistochemistry revealed no visible differences in the morphology of lineage traced tanycytes (B, C), and parenchymal cells (B'', B''', C'', C''') in young adult CT and CKO hypothalamus. Cells in the parenchyma were faint and had very short processes (B''', C'''). Scale bar – 100 µm.

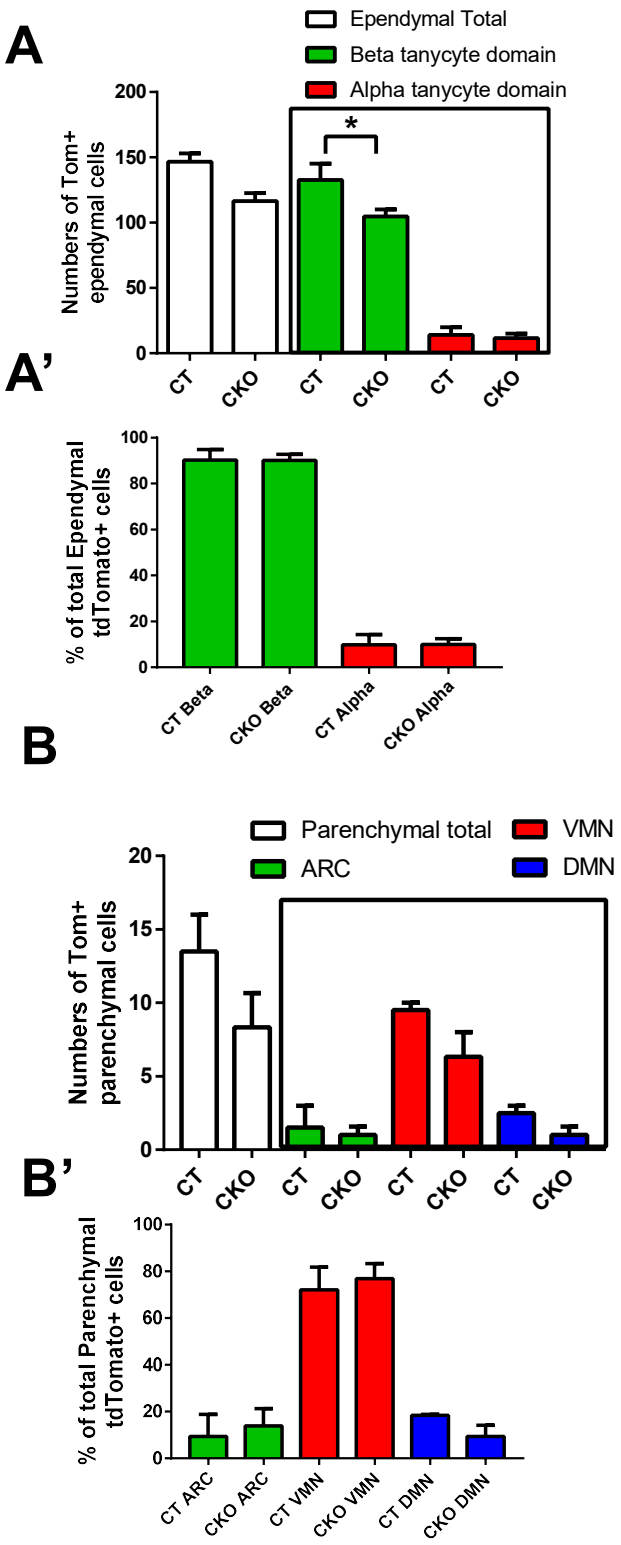

Figure 5.6 – Acute lineage tracing reveals no cell number and distribution alterations in the *Fgfr1/Fgfr2* deficient hypothalamus at P6. Graphs display numbers and distribution of lineage traced cells in the 3V wall (A, A') and parenchyma (B, B') of CT (n=2) and CKO (n=3) postnatal hypothalamus. There were significantly fewer tdTomato+ β-tanycytes in CKO animals compared to CT (multiple comparisons one-way ANOVA, $P \leq 0.05$) (A).

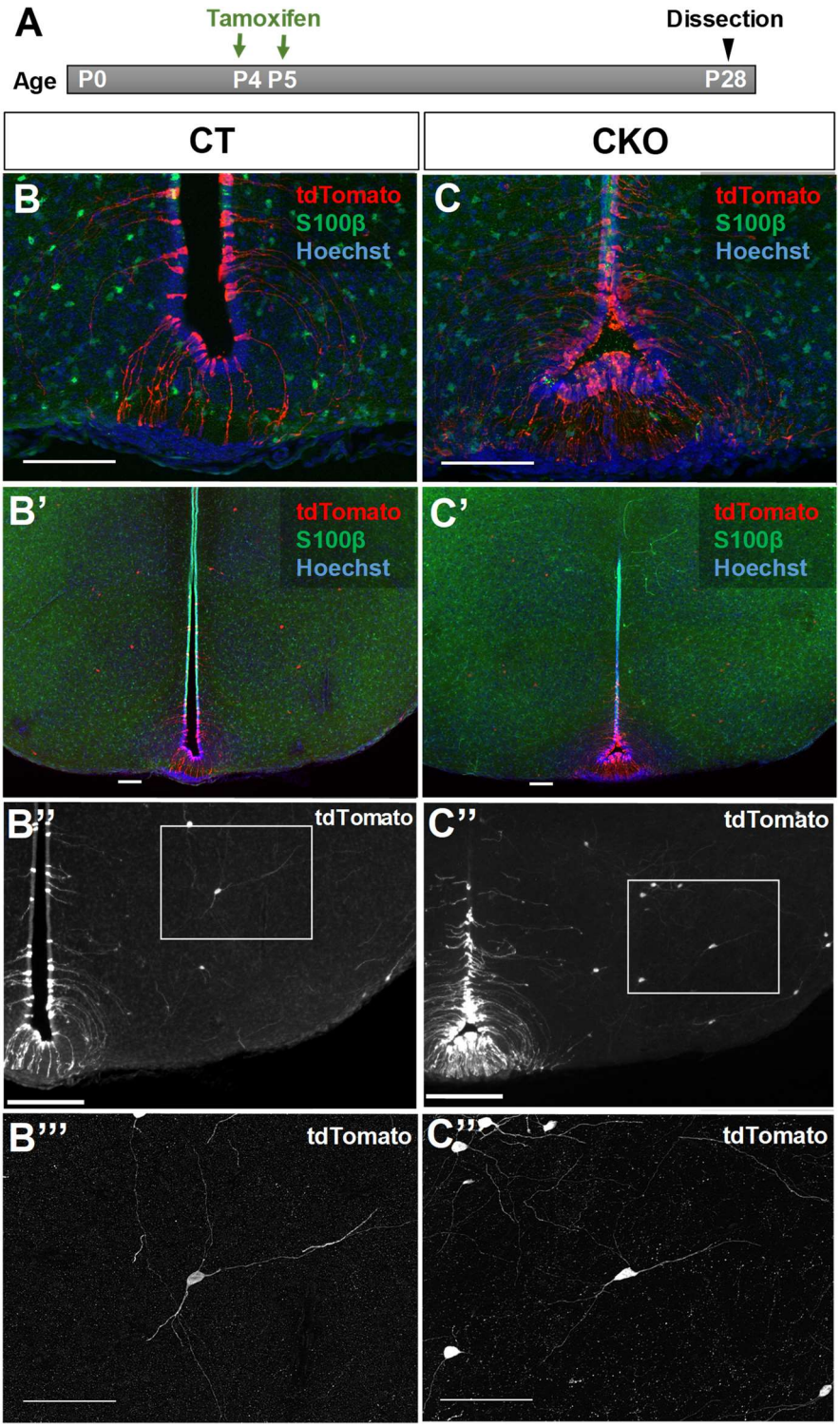

Figure 5.7 – Morphology of lineage traced FGF receptor-deficient cells is unaltered in the long-chase post-weaned hypothalamus. Schematic displays the timing of tamoxifen administration and brain dissection (A). Immunohistochemistry revealed no apparent differences in the morphology of lineage traced tanycytes (B, B'', C, C''), and parenchymal cells (B'', B''', C'', C''') in long-chase post-weaned CT and CKO hypothalamus. Most cells in the parenchyma had neuronal morphology with long processes (B''', C'''). Scale bar – 100 μm.

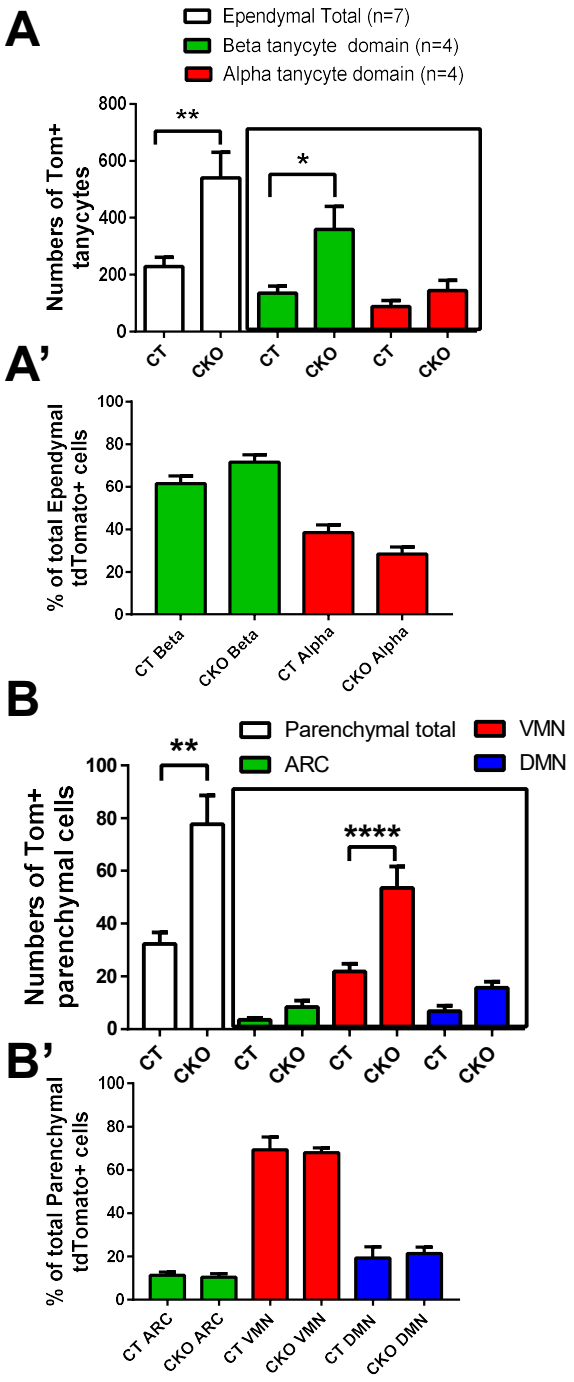

Figure 5.8 – FGF receptor deficiency amplifies the number of lineage traced cells in the 3V wall and parenchyma in the postnatal hypothalamus. Graphs display numbers and distribution of lineage traced cells in the 3V wall (A, A') and parenchyma (A, A') of CT (n=7) and CKO (n=7) postnatal hypothalamus. There were significantly more tdTomato+ cells in the 3V ependyma ($p \leq 0.01$) and specifically β-tanycytes (multiple comparisons one-way ANOVA, $P \leq 0.05$) in CKO animals compared to CT (A). Lineage traced cells were also more numerous in the parenchyma of CKO animals ($p \leq 0.01$) and specifically in the VMN (multiple comparisons one-way ANOVA, $P \leq 0.0001$) (B).

5.2.5 – *Fgfr1/Fgfr2* expressed in *Fgf10*+ β–tanycytes may control cell proliferation at a distinct developmental time window

It was hypothesised that the amplification of lineage traced cells at P28 is due to increased proliferation of *Fgfr1*/*Fgfr2* deficient cells. Bromodeoxyuridine is a synthetic thymidine analogue that is incorporated into dividing cell DNA and is therefore often used to assess cell proliferation (Wojtowicz and Kee, 2006). Immunohistochemical detection of BrdU requires tissue treatments that destroy tdTomato staining, therefore an alternative method to detect cycling cells was sought. PCNA is a cell cycle marker and it reaches its highest expression during the S phase (Celis and Celis, 1985). To test if proliferation of *Fgfr1/Fgfr2* deficient cells is increased, PCNA staining was performed on hypothalamus sections of long-chase (p28) CT and CKO animals.

While small numbers of PCNA+ cells were seen in the β-tanycyte domain and the parenchyma (Fig 5.9), there were no cells that were labelled for both PCNA and tdTomato at this age. This suggested that if there is an increased proliferation of *Fgfr1*/*Fgfr2* deficient cells, this effect is limited to either a restricted developmental time window or only happens shortly after recombination occurs.

To test this hypothesis, PCNA staining was performed on mice tamoxifen pulsed at P4/P5 and analysed at P10. One CT (not completely intact) and 2 CKO brains (1 intact, 1 not completely intact) were analysed. At this age, there were many α-tanycytes that express PCNA and a small number of PCNA+/tdTomato+ α-tanycytes were detected, only in one the CKO animals (Fig. 5.10 C-C'''; Fig. 5.12 B). No PCNA+/tdTomato+ were found in the parenchyma of both CKO brains analysed (Fig. 5.11 A-A'''; Fig. 5.12 B'). Interestingly, at this age, two cells with clear tanycytic morphology were found outside of the 3V wall (Fig. 5.11 C), suggesting that the cells were migrating into the parenchyma. No PCNA+/tdTom+ cells were detected in the one CT brain that was stained. However, it was not fully intact, and previous work in our lab has reported PCNA+/tdTomato+ α-tanycytes at this age using the same tamoxifen treatment paradigm (Goodman et al., in preparation).

Lineage traced cell numbers were higher in the intact CKO brain and similar density was apparent in the non-intact one (Fig.5.13 A, B) than in any of the long chase brains. Additionally, one intact P10 CT brain had been stained for tdTomato and S100β and its cell counts were similar to P28 CT (Fig. 5.13 A, B). This suggests that by P10 most of the lineage traced cells were generated, therefore any amplifying effects of *Fgfr1*/*Fgfr2* are likely to manifest at earlier stages.

The next step was to perform equivalent experiments but dissect brains at an earlier age. In brains dissected from P7 pups, a large number of PCNA stained cells were seen in the α-tanycyte domain. Small numbers of PCNA+/tdTomato+ tanycytes, most likely in the α-domain, were detected in some of the CKO and CT brains (Fig. 5.10 B-B'''; Fig. 5.12 A), but none were found in the parenchyma. Numbers of CKO lineage traced parenchymal cells were increased at P7 compared to P6 (Fig. 5.13 B).

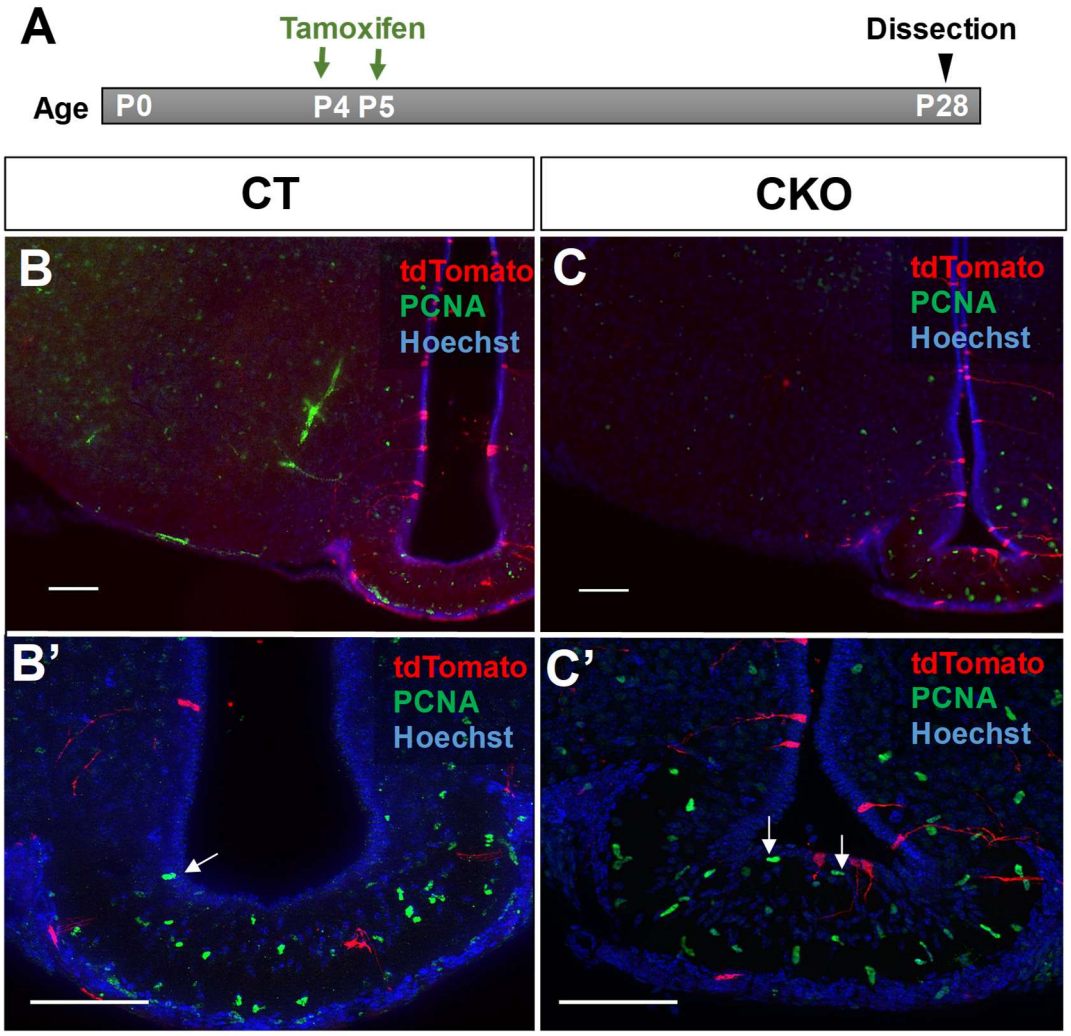

Figure 5.9 – PCNA expression in the 3V ependymal is rare and is absent from long-chase lineage traced cells in the post-weaned hypothalamus (P28). Schematic displays the timing of tamoxifen administration and brain dissection (A). Immunohistochemistry for PCNA detected some cycling parenchymal cells (B, C) and β-tanycytes (B', C') in CT and CKO animals, however, no co-localisation of PCNA and tdTomato was observed in long-chase post-weaned mouse hypothalamus. Scale bar – 100 μm.

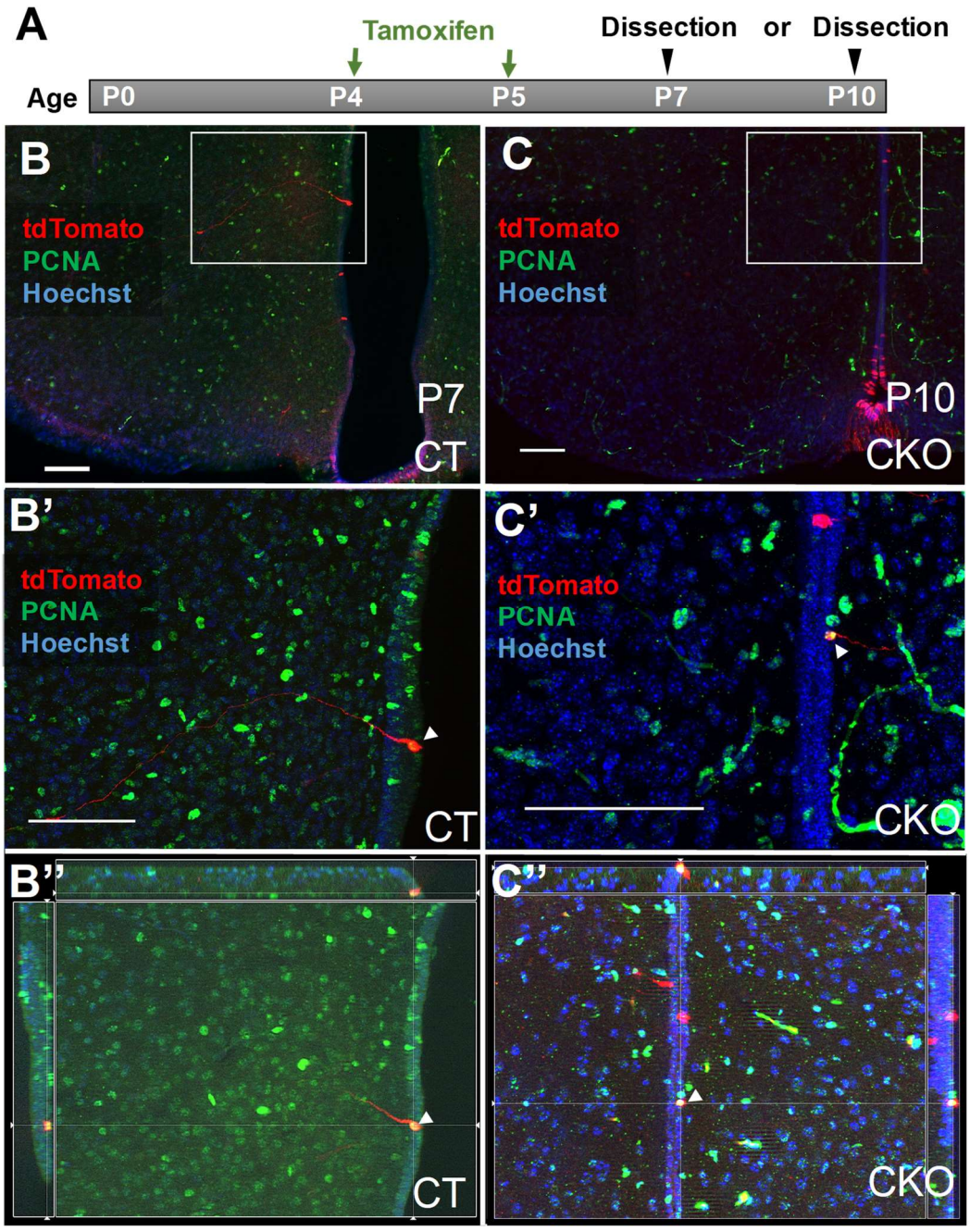

Figure 5.10 – Rare PCNA+ lineage traced tanycytes were found at P7 and P10. Schematic displays the timing of tamoxifen administration and brain dissection (A). Immunohistochemistry for PCNA revealed rare lineage traced cycling tanycytes (B, B', C, C') in CT and CKO animals a few days after tamoxifen induction. Cut view confirms co-localisation of tdTomato and PCNA in these tanycytes (B'', C''). Scale bar – 100 µm.

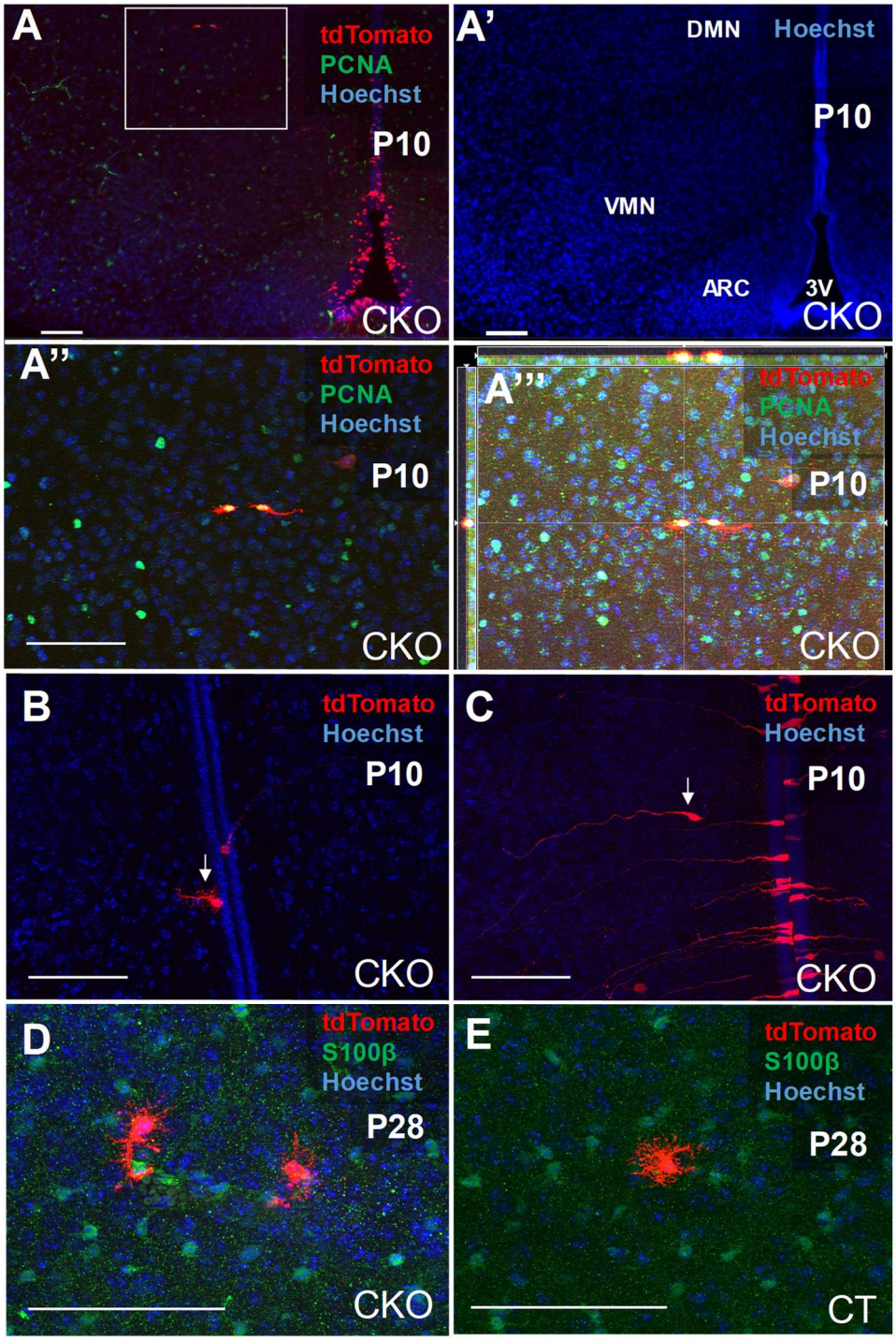

Figure 5.11 – Cycling and non-neuronal lineage traced cells were present in the hypothalamus parenchyma. PCNA+/tdTomato+ cells in the DMN (A-A''') were occasionally found in CKO hypothalamus at P10. A cell with similar morphology was found nearby or in the 3V wall (B) and cells of this morphology were also sometimes found in the parenchyma at other ages (D). Cells with clear tanycytic morphology were rarely (twice) found nearby, but outside of the 3V wall (C) in CKO hypothalamus at P10. Cells of glial morphology with short processes surrounding the cell body (E) were occasionally seen at P28 and P55. Scale bar – 100 μm.

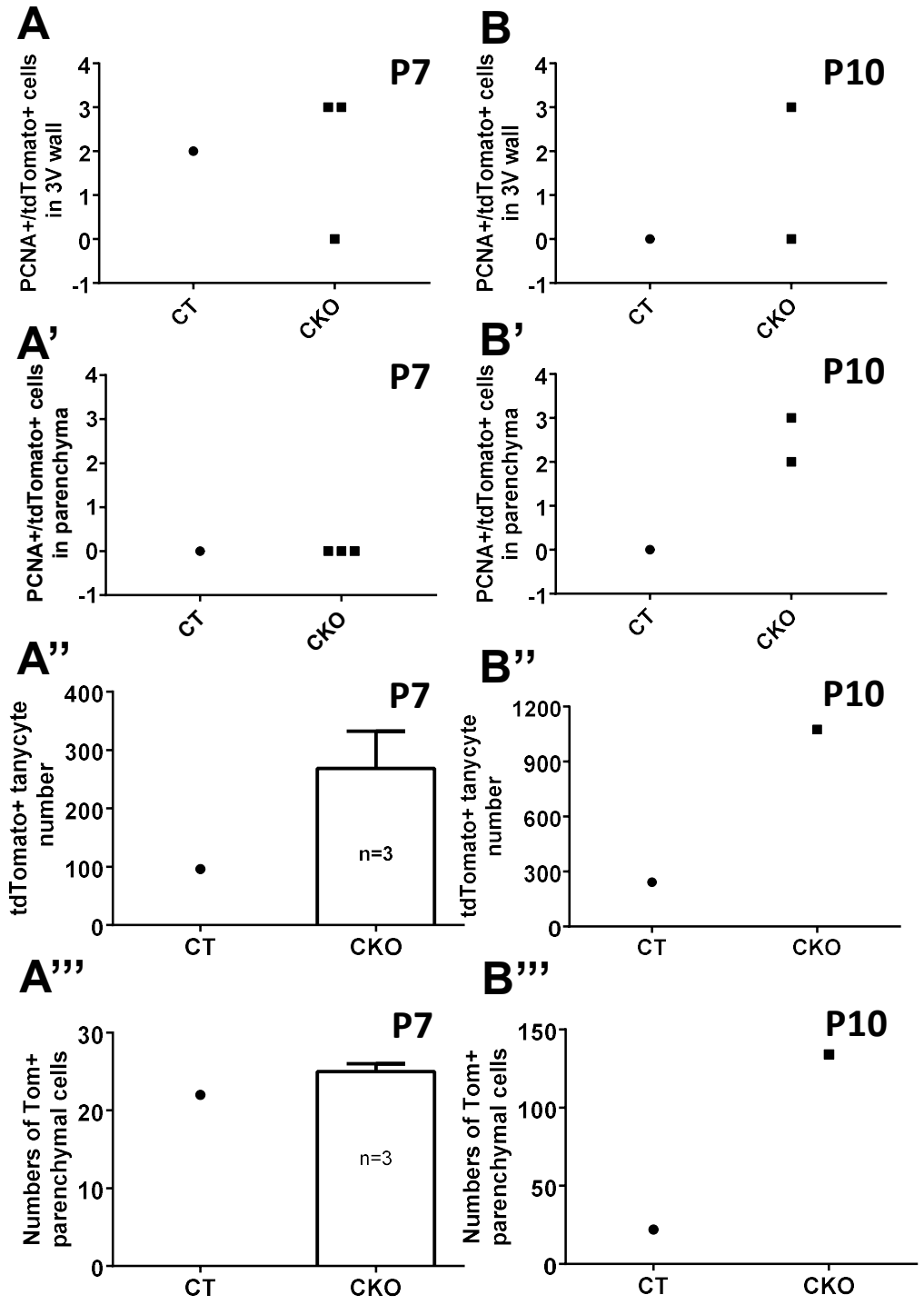

Figure 5.12 – Very few PCNA+/tdTomato+ cells were found in P7 and P10 hypothalamus. At most 3 PCNA+/tdTomato cells were found in the 3V wall per hypothalamus at P7 (A) and P10 (B). Parenchymal PCNA+/tdTomato cells were only seen in P10 CKO hypothalamus (B'). Lineage traced cell numbers in the CKO 3V ependyma and parenchyma had more than doubled by P7 (A'') compared to P6 and were more numerous at P10 (B'') than at P28 (Fig. 5.8). Each dot or square represents a single analysed brain. Note that the numbers of brains analysed were low and many of the sections had some amount of damage, therefore the numbers are not definitive.

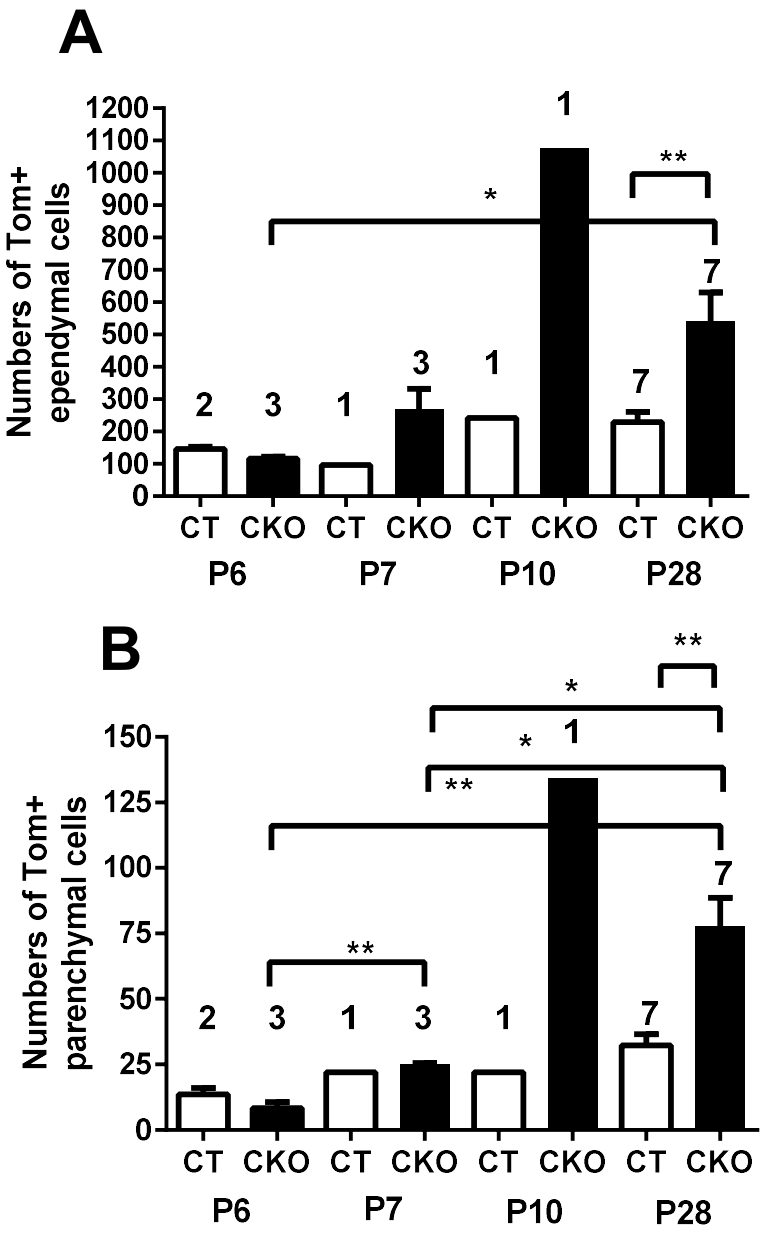

Figure 5.13 – The number of lineage traced cells potentially peaks by P10. Graphs show the number of CKO and CT lineage traced cells in the ependyma (A) and parenchyma (B) at ages P6 to P28. Numbers above bars indicate the number of brains analysed. In the CKO hypothalamus ependymal and parenchymal tdTomato+ cell numbers are significantly increased at P28 compared to P6, but numbers as high or higher are potentially reached by P10. Significant cell number differences between CT and CKO were only observed at P28. However, CT data for ages P6, P7 and P10 is incomplete due to low numbers of observations or damaged tissue, therefore statistical analysis cannot be done or is not definitive, warranting further work. Unpaired t-test was carried between CKO - CT at the same age, or CT – CT and CKO – CKO between different ages. * - $P \leq 0.05$, ** - $P \leq 0.01$; *** - $P \leq 0.001$.

5.3 – Discussion

The functions of endogenous FGFR signalling in postnatal and adult hypothalamic neurogenesis have not been previously explored. This was attempted here by lineage tracing a subset of β-tanycytes that are *Fgfr1*/*Fgfr2* deficient. The main cellular phenotype of impaired FGFR signalling was the amplification of lineage traced cells in the postnatal hypothalamus, both in the 3V ependyma and parenchyma.

5.3.1 – Amplification of *Fgfr1/Fgfr2* deficient cell numbers are potentially caused by changes in cell proliferation

One possible cause of this cell number increase could be due to decreased cell death of FGF receptor-deficient lineage traced cells. This was previously assessed in our lab with the use of Caspase-3 immunohistochemistry and very few Caspase-3 immunopositive cells were found in the hypothalamus at P10 in CT mice (Goodman et al., in preparation). In accordance with this, very few cells were detected by Caspase-3 immunohistochemistry and the TUNEL assay in the hypothalamus of young rats (Guyenet et al., 2013). This suggests that apoptosis is likely not a major factor in causing the cell number amplification that we observed. A caveat of this is that Caspase-3 does not detect all types of cell death (Kroemer et al., 2009). In addition, cell counts suggest that most or all of the lineage traced cells would have been generated by P10. Therefore, it is possible, that there is a developmentally restricted time-window of cell death before P10, and this may be attenuated in FGF receptor-deficient cells.

Another possibility is that FGF signalling may inhibit lineage traced cell proliferation. Here, proliferation was assessed using the S phase marker PCNA. Very few cycling cells were found in the 3V wall in the P28 hypothalamus, and none that co-localised with tdTomato, which suggested that proliferative effects capable of producing the marked amplification in cell numbers that was seen in CKO hypothalamus would mostly be restricted to earlier postnatal ages. Indeed, by P10 lineage traced cells had reached numbers as high as or higher than at P28. Many cycling cells were found in the α-tanycyte domain at P7 and P10, in both CT and CKO animals. PCNA+/tdTomato+ cells were also detected in the 3V wall of some CKO (P7, P10) and CT (P7) animals, but their numbers were very low and variable. A major caveat is the incompleteness of these experiments, as very few brains were examined and, in some cases,, the sections had broken to an extent during the

immunohistochemistry protocol, most likely due to the acid-alcohol pre-treatment making postnatal sections too delicate. What the results do suggest, however, is that the numbers of lineage traced proliferating cells were low in all the brains examined.

There are some scenarios that may still explain how proliferation could cause the amplification of lineage traced cells. First, PCNA staining provides a 'snapshot' of cells in S phase at a particular moment in time and although the numbers of proliferating lineage traced cells detected at these individual time-points were low, if there are slight increases in proliferation in CKO animals throughout the P4-P10 period, they may add up to an observable increase of newly generated cells by the end of this period. Secondly, it may be that the proliferation promoting effects are restricted to the ages that were not analysed, specifically P8 or P9. This is supported by the fact that at P7 and P10, the vast majority of PCNA+ cells and the only ones that colocalised with tdTomato were located in the dorsal 3V wall. At P6, there were very few lineage traced cells outside of the β-tanycyte domain, but by P28 there are many more α-tanycytes, both in relative and absolute terms. In addition, previous analysis of CT brains at P6, P8 and P10, showing that the number and proportion of lineage traced cells in the α-tanycyte domain increases with age (Goodman et al., in preparation). One model is that β-tanycytes migrate to the α-tanycyte domain with time. Perhaps by P8/P9, a high number of lineage traced cells reach the α-tanycyte domain and a short-lived, intense proliferative event takes place that is mostly over by P10. It may be that it is this event that is fine-tuned by FGFR signalling. *Fgfr2,* but not *Fgfr1* was detected in the α-tanycyte domain at P8, but was absent in mice older than P60, suggesting that maybe *Fgfr2* has a role in inhibiting proliferation in that domain in the early postnatal hypothalamus. The fact that at P28 there were almost no PCNA+ cells in the α-tanycyte domain also suggests that this is an event restricted to early postnatal ages. This scenario is highly speculative but would be an interesting hypothesis to test. In addition, it is also possible that this hypothetical proliferative event may not be so specific to P8/P9, and the amplification effect would be seen at different postnatal ages if tamoxifen administration was performed at time points different to P4/P5.

Interestingly, only tdTomato+ β-tanycytes, but not α-tanycytes were significantly amplified at P28. Some lineage traced *GLAST* expressing α-tanycytes have been shown to migrate into the β-tanycyte domain (Robins et al., 2013). Given the previously outlined hypothesis that some β-tanycytes migrate into the α-tanycyte domain, where they proliferate, and the apparent lack of lineage traced proliferating β-tanycytes, it may be possible that in CKO a higher fraction of lineage traced cells

then migrate back into the β-tanycyte domain. Of course, the PCNA analysis reported here was not exhaustive both in terms of the ages tested, the lack of domain markers and the low number of brains analysed at P7 and P10, so it may well be that some lineage traced cells do proliferate in the β-tanycyte domain as well.

FGFR signalling often acts to increase proliferation, as is the case in the subventricular zone and dentate gyrus neurogenic niches (Zhao et al., 2007; Stevens et al., 2012). The opposite has precedent in lung epithelium stem cell niche, where *in vivo* conditional deletion of *Fgfr1* in tracheal basal cells (BCs) causes increased steady-state proliferation, as assessed by Ki67 staining, while FGF2 applied to wild-type BC cell culture decreased colony size (Balasooriya et al., 2016). In *Fgfr1* deficient basal cells, MAPK and AKT phosphorylation levels were increased. Interestingly, there was a decrease in the protein levels of the smaller Sprouty2 isoform, which inhibits MAKP and AKT pathways, and an increase in the larger isoform that is not effective at inhibiting these pathways (Lao et al., 2007). The authors proposed a model where FGFR1 signalling in BC cells causes post-translational changes of Sprouty2 protein, therefore inhibiting MAKP and AKT pathways and weakening other pro-proliferative signals, for example, EGFR signalling. It is possible a similar mechanism may be at play in *Fgfr1*/*Fgfr2* deficient tanycytes, since *Spry2* is also expressed in β-tanycytes, as well as various receptors that activate the MAPK pathway, such as Ntrk2, VEGFR-3, ErbB1 and ErbB2 (Prevot et al., 2003; Lein et al., 2007; Hou et al., 2011).

The same group performed conditional, heterozygous *Fgfr2* deletion in BC cells and saw no significant effects on cell proliferation rates, but instead a promotion of symmetric cell divisions and impairments in self-renewal (Balasooriya et al., 2017). Effects on self-renewal were not assessed in our experiments. Additionally, in the trachea, the FGFR2-IIIb isoform is expressed, along with its cognate ligands, FGF7 and FGF10. In the hypothalamus, only the FGFR2-IIIc isoform is expressed (Hajihosseini et al., 2008), therefore a different set of ligands would bind tanycytic FGF receptors. Regardless of whether *Fgfr2* has a similar function in tanycytes and basal cells, it is possible *Fgfr2* also has distinct and shared functions with *Fgfr1* in tanycytes. Therefore, it would be very valuable to perform conditional knockout experiments of Fgfr1 or Fgfr2 alone, to dissect their unique contributions to tanycyte function.

How may the observation that exogenous stimulation of FGF receptors increases tanycyte proliferation (Robins et al., 2013) be reconciled with the observation

presented here of *Fgfr1*/*Fgfr2* deficiency causing amplification of tanycytes numbers? Firstly, FGF receptors were exogenously stimulated by intracerebroventricular injection of FGF2, but as shown in chapter 4, in P60-P80 mouse hypothalamus *Fgf2, Fgf18, Fgf1* and *Fgf9* are expressed in the 3V wall and likely bind to FGF receptors in tanycytes. Therefore, potentially non-physiological levels of exogenous FGF2 may override more subtle and fine-tuned endogenous signalling. Additionally, it has been demonstrated that in some cells, FGFR signalling is biphasic, and that activation of downstream signalling pathways is highest at an intermediate concentration of ligand and lowest at both high and low ligand concentration (Kanodia et al., 2014). A consistent model may be that in tanycytes, intermediate levels of FGF receptor activation inhibit proliferation, while low and high levels release this inhibition and result in heightened proliferation. Indeed, high levels of FGF signalling potentially inactivate the formation of the trimeric signalling unit (FGF receptor, heparan sulfate proteoglycans and FGF ligand) (Kanodia et al., 2014), thereby both FGFR knockout and exogenous overstimulation might have essentially the same effect of inactivating FGF receptors. The FGF2 ICV experiments were performed in mice 8 weeks old or older, while the conditional knockout was performed during the first 4 weeks after the birth of the animals, therefore the role of FGFR signalling may also differ with age. Finally, as mentioned before, β-tanycytes are heterogeneous and therefore FGF receptors in *Fgf10* expressing tanycytes may have different or even opposing functions in other subpopulations.

As is the case with the FGF signalling system, the IGF signalling system has often been found to promote proliferation (Teng, Jeng et al. 2018). Interestingly, the disruption of insulin-like growth factor 1 receptor (IGF-1R) in nestin expressing tanycytes and their subsequent lineage tracing revealed an amplification of mature neurons and tanycytes (Chaker, George et al. 2016). This amplification bears resemblance to the one identified in the current study of FGF receptor deficient tanycytes and illustrates how growth factor signalling inhibition in tanycytes can cause amplification of cell numbers. The exact nature of this amplification was not explored in the IGF-1R deletion study. However in a related study of IGF-1R deletion in SVZ niche NSPCs, an increase in the numbers of neuroblasts and integration of neurons was seen, along with a decrease in the phosphorylation of Akt in the NSPCs (Chaker, Aïd et al. 2015). It is therefore possible that a change in Akt signalling may also take place and is involved in the amplification of FGFR and IGF-1R deficient tanycytes.

5.3.2 – FGFR signalling in β-tanycytes and their progeny may not be crucial for cell fate determination or migration

The cell morphology of lineage traced cells in CKO and CT animals were similar with no gross differences observed: most of the cells observed in the 3V ventricle had classical tanycytic morphology, each β-tanycyte and α-tanycyte possessing a long process or short process respectively. In the parenchyma, the vast majority of cells possessed neuronal morphology, with large soma and long processes. Previous experiments in our lab using the same pulse-chase with CT animals have confirmed that some of the tdTomato+ cells express NeuN (Goodman et al., in preparation), a marker for postmitotic neurons (Mullen et al., 1992). In addition, P28-P35 lineage traced neurons in CT mice have been shown to respond to fasting and Leptin through phosphorylation of STAT3, indicating that they are functionally integrated (Haan et al., 2013). It is likely that some lineage traced cells possessing neuronal morphology in either CKO or CT hypothalamus are mature and functionally integrated. However, relying on morphology is not a robust approach, as processes may span more than one section and therefore it is not possible to measure them accurately. The use of cell markers such as NeuN for mature neurons and DCX for immature neurons (Vukovic et al., 2013), as well as indications of functional integration in the networks, would be helpful to more definitively ascertain if there are any neural maturation and integration effects in FGFR deficient cells.

A small number of cells in the parenchyma possessed glial morphology. These cells were seen in mice of both genotypes but were very rare and therefore it is difficult to assess if FGFR deficiency caused any changes in their numbers or subtle changes in morphology. Using cell morphology to distinguish cell types, it seems unlikely that FGFR signalling had a significant role in fate determination in these experiments. However, other approaches for determining cell type and maturity can be more informative. Data collected in our lab showed that some P28 lineage traced cells with glial morphology express GFAP, an astrocyte marker, or Olig2, an oligodendrocyte marker (Goodman et al., in preparation). Therefore, the cells that exhibited glial morphology in these experiments were also likely of astroglial or oligodendroglial lineage. Although no S100β co-localisation was observed in my studies, the onset of S100β expression has been reported to be later than that of GFAP, therefore serving as a marker for astrocyte maturity (Raponi et al., 2007).

Interestingly, some cells seen in the parenchyma at P28 and P10 had similar morphology to oligodendrocyte progenitors and neuroblasts of the subgranular and

subventricular zones and at P10, some co-localised with PCNA. Previous reports have shown the presence of DCX+ cells in the hypothalamus parenchyma (Battailer et al., 2014), including the DMN where the neuroblast-like cells were found in these experiments. It would be interesting to see whether these cells also express DCX and if any parallels can be drawn between them and neuroblasts of the other neurogenic niches that eventually give rise to neurons.

It has been recently found that mature FGF2 responsive GFAP- ventral α2/β-tanycytes migrate into the parenchyma (Jourdon et al., 2016). In P10 hypothalamus some cells with clear tanycytic morphology with long processes reminiscent of β-tanycytes were seen far from the 3V wall, in the hypothalamic parenchyma. It is possible that these are mature tanycytes that migrate into the parenchyma and may then potentially transdifferentiate, giving rise to neural or glial cell types.

The migration of lineage traced cells did not seem to be affected by *Fgfr1*/*Fgfr2* deficiency, as the distribution of cells in the different tanycyte compartments and parenchymal cell nuclei was not changed. More detailed investigations, for example using imaging live slice brain cultures, may be able to uncover more subtle changes in migration patterns, if any.

5.3.3 – Technical considerations

While there was a general trend of increased tdTomato+ cell numbers in the 3V ependymal of young adult CKO animals, the cell numbers were very variable. This may be partly due to natural variation in the absorption and metabolism of tamoxifen or recombination efficiency. In addition, intraperitoneal injections are not always accurate and do not always result in tamoxifen being deposited in the peritoneal cavity, as one study found this error may occur around 14% of the time even when IP is performed by experienced investigators (Steward et al., 1968). Any natural variability, as well as errors in technique, would be exacerbated by the low number of IP injections and animals used (4 per group).

It should be noted that not all β-tanycytes express *Fgf10* (Haan et al., 2013) and not all of them may express *Fgfr1* or *Fgfr2*. This means that individual β-tanycytes may express any combination of these genes or none of them. Two points follow from this: tanycytes expressing *Fgf10* may be biologically different, therefore using the $Fgf10^{CreERT2}$ driver we did not investigate FGFR function in all β-tanycyte subtypes and their progeny. Secondly, recombination may happen in a cell that may or may not

express FGF receptors. This, along with other factors such as stochastic recombination efficiency, may also add to the variability seen in the CKO animals.

Cre recombination in $Fgf10^{CreERT2}$ mice requires administration of tamoxifen. For lineage tracing studies, information on its administration method, metabolism and degradation of the active metabolites is crucial for the proper interpretation of the experiments. A recent report looked into the time-course of tamoxifen-induced recombination in $Pdx1^{PB\text{-}CreERTm}$*::*$Rosa26^{lacZ}$ pancreatic islet cells transplanted underneath the renal capsule in adult mice (Reinert et al., 2012). They found that high doses of subcutaneous tamoxifen injections caused some recombination even in cells that were transplanted 4 weeks after the last injections, while low doses caused recombination in cells 1 week after the last injection. Another study approached this issue by monitoring the degradation of active tamoxifen metabolites and recombination in adult mouse brain after IP injections (Valny et al., 2016). They found that at higher doses (two injections of 200 mg/kg tamoxifen) all metabolites are degraded within 8 days and reaches ineffective concentration after 6 days, while at lower doses (two injections of 100 mg/kg tamoxifen) it was fully degraded within 6 days and reached ineffective concentration after 4 days.

There is a dearth of information regarding these parameters in tamoxifen orally administered to neonatal mice. It should be noted that at P6, one day after the last tamoxifen dose, there were many cells that had very low levels of tdTomato. At P7, the numbers of tdTomato+ cells were much higher in CKO animals, and the faint cells were not observed. Since PCNA+/tdTomato+ cell numbers were very low, it seems likely that the increase in the number of cells seen was mainly due to ongoing recombination and increasing tdTomato+ expression. It is possible that by P7 tamoxifen metabolites would have reached ineffective concentrations, but more extensive studies would have to be done to test this. While these are important considerations in many lineage tracing experiments, this may not have much influence on the main finding of these experiments - the large relative amplification of FGFR signalling deficient tdTomato cells.

FGF10 is expressed in neuroepithelial cells during corticogenesis and has a role in regulating their transition into radial glial cells, and consequently impacting neurogenesis (Sahara and O'Leary, 2009). Heterozygous $Fgf10^{CreERT2/+}$ mice have reduced function of FGF10 (El Agha et al., 2012), tend to have lower body weight (unpublished observations and Chapter 6). It is possible that this may have some

subtle influence on hypothalamic neurogenesis and therefore our experiments may not have isolated just the effects of *Fgfr1* and *Fgfr2* deficiency.

Conclusion

The experiments described in this chapter have shown that FGF receptor signalling has a role in regulating postnatal hypothalamic neurogenesis, namely in controlling the number of tanycytes and newborn neurons that they generate. This is likely due to FGF receptors modulating proliferation of tanycyte NSPCs at a restricted window of time during postnatal development. However, the specifics of this regulation still have to be characterised.

Chapter 6

Conditional knockout of Fgfr1 and Fgfr2 in Fgf10+ compartments leads to no or subtle changes in metabolism

6.1 – Introduction

The hypothalamus plays a pivotal role in the CNS regulation of metabolism. Recently, tanycytes have been attracting more interest as an important component of the neuroendocrine system and its control of metabolic processes (Ebling and Lewis, 2018). Early studies suggested a link between FGF signalling, cells lining the 3V wall and metabolic control. For example, FGF1 was found to be present in rat tanycytes (Tooyama et al., 1991) and its release and potent feeding suppression effects are brought upon by increased glucose concentration in the CSF after feeding or glucose infusions (Oomura et al., 1992). Indeed, recent studies have shown that tanycytes are capable of directly sensing glucose and amino acids in the CSF (Benford et al., 2017; Lazutkaite et al., 2017). In addition, injections of FGF1 and FGF2 into the 3V decrease food intake, while injections of anti-FGF1 or anti-FGF2 antibodies have the opposite effect (Sasaki et al., 1991; Sasaki et al., 1994).

More recently, interest in how FGF signalling impacts central control of metabolism has been stimulated by reports that IP and ICV administration of antibodies that block FGFR1-IIIc accumulate in the mediobasal hypothalamus and median eminence, including the 3V floor, and subsequently cause potent hypophagia and weight loss in mice, rats and cynomolgus monkeys (Sun et al., 2007). In Siberian hamsters, administration of this antibody results in reduced food intake and increased energy expenditure and was linked to downregulation of deiodinase 2 (Dio2) in tanycytes (Samms et al., 2015). Similar effects were seen using a different FGFR1-IIIc antibody that binds to central targets including, but not limited to, tanycytes (Lelliott et al., 2014). In this study, a single IP injection of this antibody caused reduced food intake and weight loss for 14 days in diet-induced obese mice and even more dramatic effects when 4 injections were administered over 30 days, returning diet-induced obese animal weight and glucose sensitivity to their lean counterpart levels.

Intriguingly, a single subcutaneous, IP or intravenous injection of endocrinised recombinant FGF1 to diet-induced or genetically obese hyperglycaemic mice lowered blood glucose levels and caused normoglycemia for over 48 hours, while not causing glucose-lowering effects in normoglycemic, non-obese mice (Suh et al., 2014). The mice also experienced a transient decrease in food intake and loss of body weight. In this study, the glucose-lowering effects were abolished in mice that lacked *Fgfr1* in adipose tissue ($aP2^{Cre}$::$Fgfr1^{Flox/Flox}$). By contrast, a single ICV injection of FGF1 in genetically diabetic ob/ob mice caused long-term remission of diabetic symptoms (lowering of *ad-lib* fed blood glucose levels to <200 mg/dl for over 17 weeks) and

transient decrease in weight and food intake (Scarlett et al., 2016). This effect was concurrent with the induction of c-Fos in tanycytes and HSP25 in tanycytes and subependymal astrocytes. The long-term effects suggest that synaptic changes or neurogenesis may be the underlying mechanism (Seeley and Sandoval, 2016).

These studies illustrate the potential promise of FGF signalling modulating therapies in the treatment of metabolic disorders, as well as the need for a more detailed understanding of the specific sites of action. In addition, both the stimulation and blocking of FGF receptors results in decreased food intake and weight and this is something that should be reconciled.

The expression pattern data described in chapter 4 revealed that in the third ventricle wall FGF receptor signalling is restricted to β-tanycytes as they express *Fgfr1* and *Fgfr2.* Their cognate ligands *Fgf1/2/9/18* are also expressed in the 3V ependyma and likely bind tanycytic FGF receptors and are therefore potentially part of endogenous FGF signalling that regulates metabolism.

The $Fgf10^{CreERT2}$::$Rosa26^{tdTomato}$::$Fgfr1^{Flox/Flox}$::$Fgfr2^{Flox/Flox}$ (conditional knockout, referred to as CKO) mice described in chapter 5 present a useful model to study endogenous *Fgfr1* and *Fgfr2* metabolic functions in β-tanycytes. Both receptors should be deleted in anticipation of potential redundancy or cooperation described in other contexts (Furusho et al., 2009). $Fgf10^{CreERT2}$::$Rosa26^{tdTomato}$::$Fgfr1^{Flox/+}$::$Fgfr2^{Flox/+}$ mice (conditional heterozygous knockout, referred to as Het) can also be used as a model for intermediate loss of function to study gene dosage effects. Therefore, these mouse models can be used to elucidate which effects detailed in the recent studies can be attributed to FGF signalling in β-tanycytes as well as their precise nature.

To determine any changes in glucose homeostasis, glucose tolerance tests (GTT) and insulin tolerance tests (ITT) can be employed (Bowe et al., 2014). GTT is performed by injecting glucose into fasted mice and taking regular blood glucose measurements. Any deviations between mice on different diets or of different genotypes may indicate alterations in glucose metabolism. This can then be further assessed by ITT, which is carried out in a similar fashion, but insulin is injected instead of glucose. This test can be used to determine if alterations in glucose metabolism are due to changes in insulin sensitivity.

6.1.1 – Aims

The metabolic effects FGF signalling in tanycytes were explored by deleting *Fgfr1* and *Fgfr2* in *Fgf10* expressing β-tanycytes. This was done by measuring weight, glucose and insulin tolerance of mice fed chow or high-fat diet (HFD).

6.2 – Results

6.2.1 – *Fgfr1* and *Fgfr2* CKO mice fed normal chow exhibit no or subtle changes in body mass and glucose or insulin metabolism compared to wild-type mice

The tamoxifen administration regime described in the previous chapter (two doses by manual suckling or intraperitoneal injection) was optimal for lineage tracing studies. However, to impact whole-body metabolism, it is likely that deletion of *Fgfr1* and *Fgfr2* needs to occur in a larger number of tanycytes. To achieve this, mice received daily intraperitoneal injections for a week starting at P44, followed by 2 weeks of a special diet supplemented with tamoxifen citrate (Fig. 6.1 A). After this period of tamoxifen administration, the mice were first subjected to the glucose tolerance test and, two weeks later the insulin tolerance test to establish baseline glucose metabolism measurements, before being put on a high-fat diet. Comparable studies that measure the effects of FGF signalling modulation specifically in hypothalamic tanycytes have not been performed previously. As such, it is difficult to estimate the effect size of such interventions and calculate the needed statistical power. These experiments were therefore carried out as a pilot study which may then inform the feasibility of future studies and their power calculations (Sullivan and Feinn 2012).

During this five-week period, mice were fed either regular chow diet, or chow diet supplemented with tamoxifen. The starting weight of WT mice was significantly higher than that of Het and KO mice and remained so throughout this period (Fig. 6.1 B). KO and Het weights never differed significantly. However, mice carrying the $Fgf10^{CreERT2}$ allele have been observed to be smaller (unpublished observations). In addition, $Fgf10^{CreERT2/+}$ animals have reduced *Fgf10* expression. Since both KO and Het mice carry this allele, their smaller weight may be due to reduced *Fgf10* expression, deficiency in tanycyte *Fgfr1/Fgfr2* expression, or both. Regardless, due to significant differences in baseline weight, a more appropriate measure may be percentage weight change. All experimental groups gained between 13.11 % ± 1.5 % (KO) and 17.55 % ± 0.92 % (WT) weight during the first 5 weeks and no significant

differences were observed (Fig. 6.1 C). Therefore, this most likely reflected the normal growth rates at this age (Gall and Kyle, 1968).

Glucose tolerance tests were carried out immediately after all tamoxifen administration had finished. Two weeks later, insulin tolerance tests were carried out. No statistically significant differences were found in glucose homeostasis (Fig. 6.2) or insulin sensitivity (Fig. 6.3).

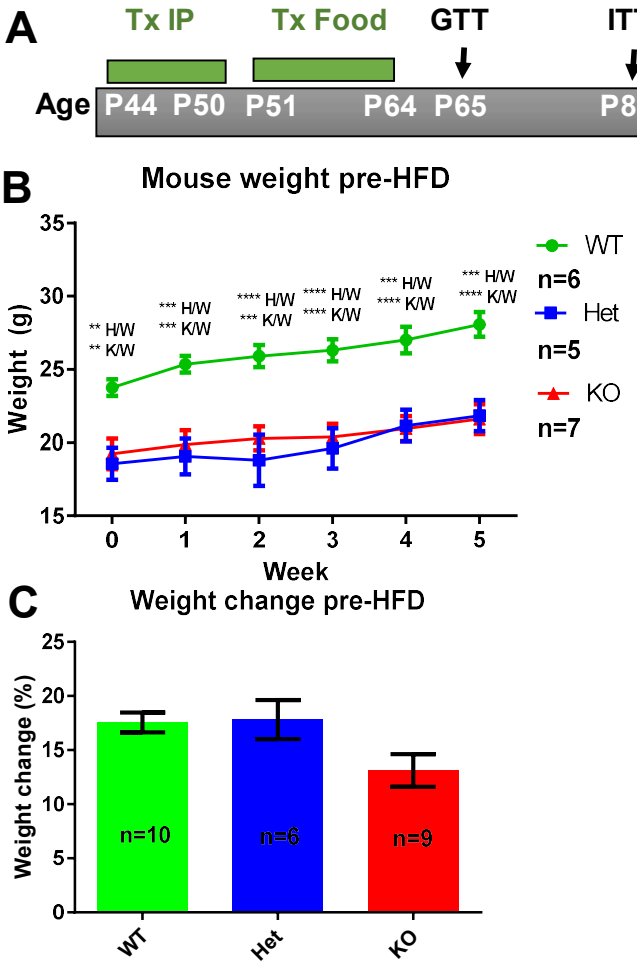

Figure 6.1 – Body weight change on a chow diet is not substantially altered in *Fgfr1* and *Fgfr2* deficient mice. Schematic shows the age of mice and procedures performed before high-fat diet regime (A). Graphs display weight change during the first five weeks before animals were challenged by high-fat diet (B) and their percentage weight gain (C). KO and Het animals were significantly lighter compared to WT from the beginning. No significant differences (one way multiple comparisons ANOVA) were observed in percentage weight change (C). H/W – Het compared to WT using multiple-comparisons repeated measures two-way ANOVA; K/W – KO compared to WT using multiple-comparisons repeated measures two-way ANOVA. **- P ≤ 0.01; ***- P ≤ 0.001; **** - P ≤ 0.0001.

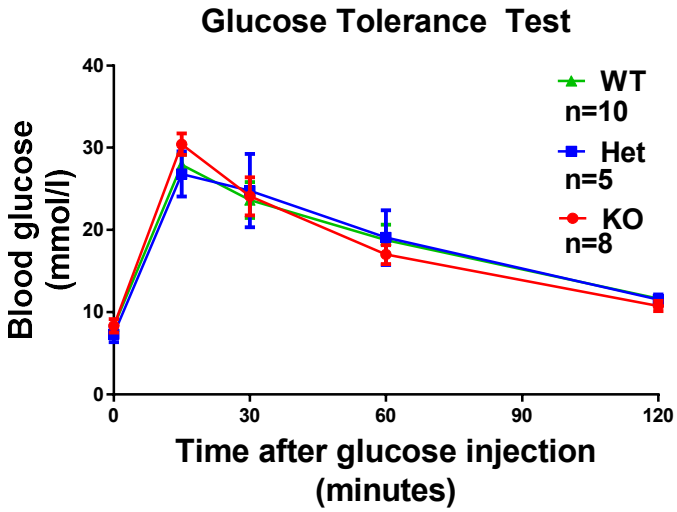

Figure 6.2 – Glucose homeostasis is not affected in *Fgfr1* and *Fgfr2* deficient mice prior to HFD treatment. Graphs show mouse blood glucose levels at defined periods of time after glucose IP injection as an indication of glucose tolerance. Blood glucose levels increase rapidly in the first 15 minutes before slowly returning to near-baseline levels. All animal groups showed similar responses. All significance testing was performed using multiple-comparisons repeated measures two-way ANOVA.

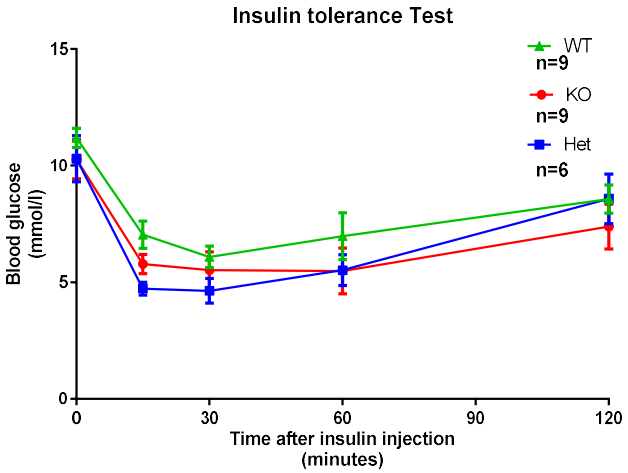

Figure 6.3 – Insulin sensitivity is not affected in *Fgfr1* and *Fgfr2* deficient mice prior to HFD treatment. Graphs show blood glucose levels at defined periods of time after insulin IP injection as an indication of insulin sensitivity. Blood glucose levels decrease sharply 15 and 30 minutes after the insulin injection, before gradually returning to levels close to the baseline. All animal groups showed similar responses. All significance testing was performed using multiple-comparisons repeated measures two-way ANOVA .

6.2.2 – High-fat diet induces changes in weight and glucose/insulin sensitivity

After tamoxifen administration and initial GTT and ITT experiments, mice were challenged with high-fat diet for 16 weeks (Fig. 6.4 A). All groups increased body weight during 16 weeks of HFD treatment (Fig. 6.4 B, C, D).

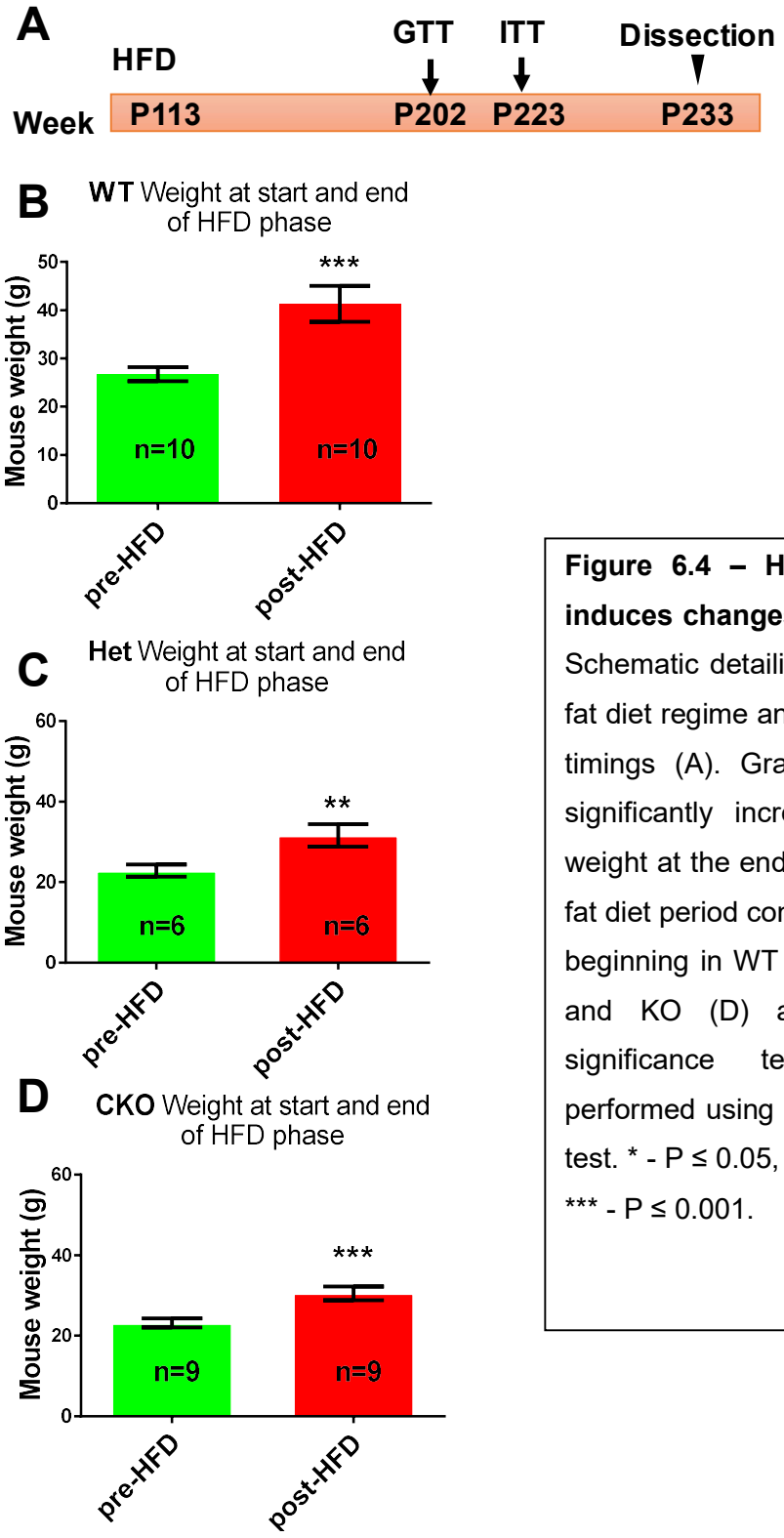

Figure 6.4 – High-fat diet induces changes in weight. Schematic detailing the high-fat diet regime and procedure timings (A). Graphs display significantly increased body weight at the end of the high-fat diet period compared to its beginning in WT (B), Het (C) and KO (D) animals. All significance testing was performed using the paired t-test. * - $P \leq 0.05$, **- $P \leq 0.01$. *** - $P \leq 0.001$.

After 12 weeks of HFD, WT and KO mice had impaired clearing of glucose compared to GTT data gathered before HFD (Fig. 6.5 A, C). Although the initial spike at the 15-minute time point after glucose IP injection was identical, in pre-HFD animals blood glucose levels start decreasing by the 30-minute time point and reach levels similar to baseline by the 2-hour time point. In HFD challenged WT and KO mice, blood glucose still rises by the 30-minute time point before gradually subsiding, but still not reaching baseline levels by the 2-hour time point. A similar effect was seen in Het animals, however, the values were not significantly different compared to pre-HFD measurements.

Baseline ITT blood glucose levels were significantly higher in HFD challenged mice compared to unchallenged mice, in all groups (Fig. 6.6. A, B, C). Therefore, the area under the curve analysis was performed and revealed trends for decreased insulin sensitivity in all groups, although these were not significant (Fig. 6.6 A', B', C').

6.2.3 – No or subtle metabolic changes are observed in *Fgfr1* and *Fgfr2* deficient mice compared to wild-type mice fed a high-fat diet

During the HFD period, mice steadily gained weight (Fig. 6.7 A). Het and KO mouse weights were nearly identical, while WT mice showed a trend for higher body weight. By the end of week 7, KO mice were significantly lighter than WT animals, while for Het mice this difference developed by week 10. However, analysis of percentage weight change revealed no significant differences (Fig. 6.7 B).

In GTT analysis, CKO animals had significantly higher blood glucose levels compared to Het mice 15 minutes after glucose injection (Fig. 6.8 A. **KO**: 31.99 ± 1.02, n=9; **Het**: 24.08 ± 3.07; multiple comparisons repeated measures two-way ANOVA, $P \leq 0.05$, 95% confidence interval on the difference between means = 0.08 to 15.73), but not at other time-points.

No statistically significant differences were observed in the analysis of ITT experiment data (Fig. 6.9 A).

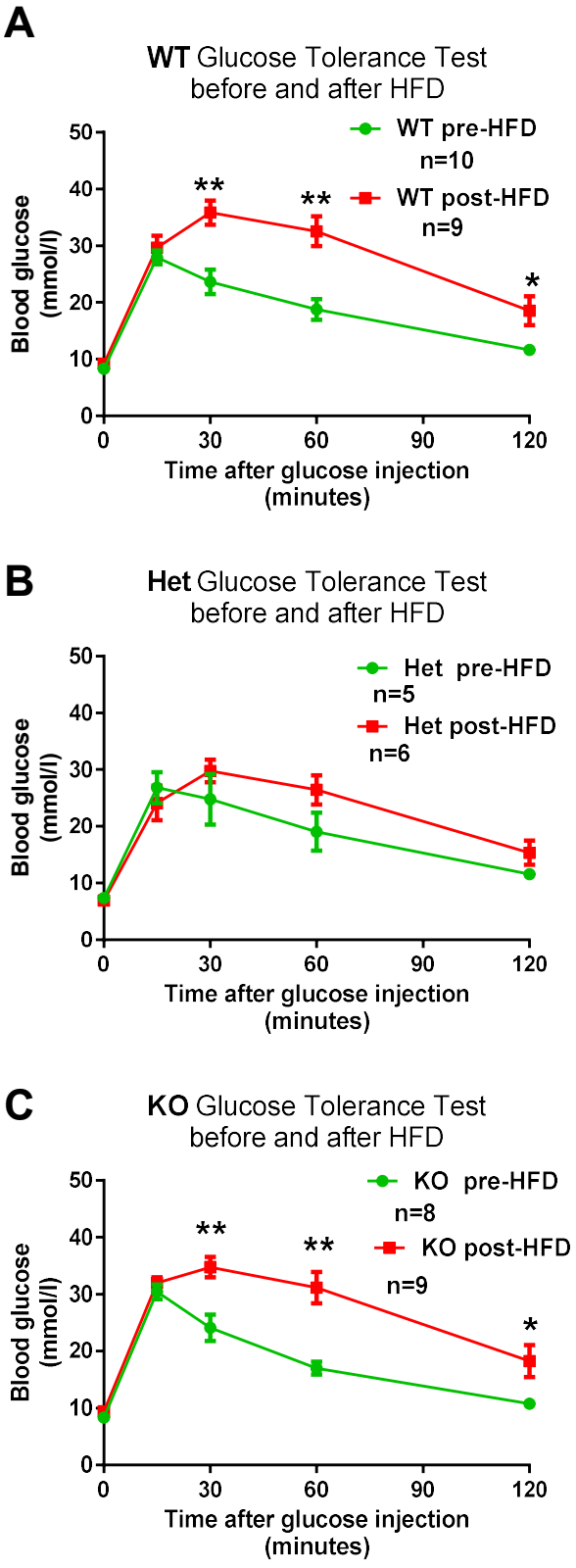

Figure 6.5 – Glucose tolerance is impaired in mice challenged with high fat diet. Graphs compare HFD challenged and unchallenged mouse blood glucose levels at defined periods of time after glucose IP injection as an indication of glucose tolerance (A, C, D). In unchallenged animals, blood glucose levels increase rapidly in the first 15 minutes before slowly returning to near-baseline levels. However, in HFD challenged animals glucose levels increase further at the 30-minute time point, before slowly subsiding, indicating decreased glucose tolerance (A, C). A similar time-course is seen in HFD challenged Het animals, although less pronounced and at no point significantly different from unchallenged Het response (B). All significance testing was performed using paired d t-test. * - P ≤ 0.05, **- P ≤ 0.01.

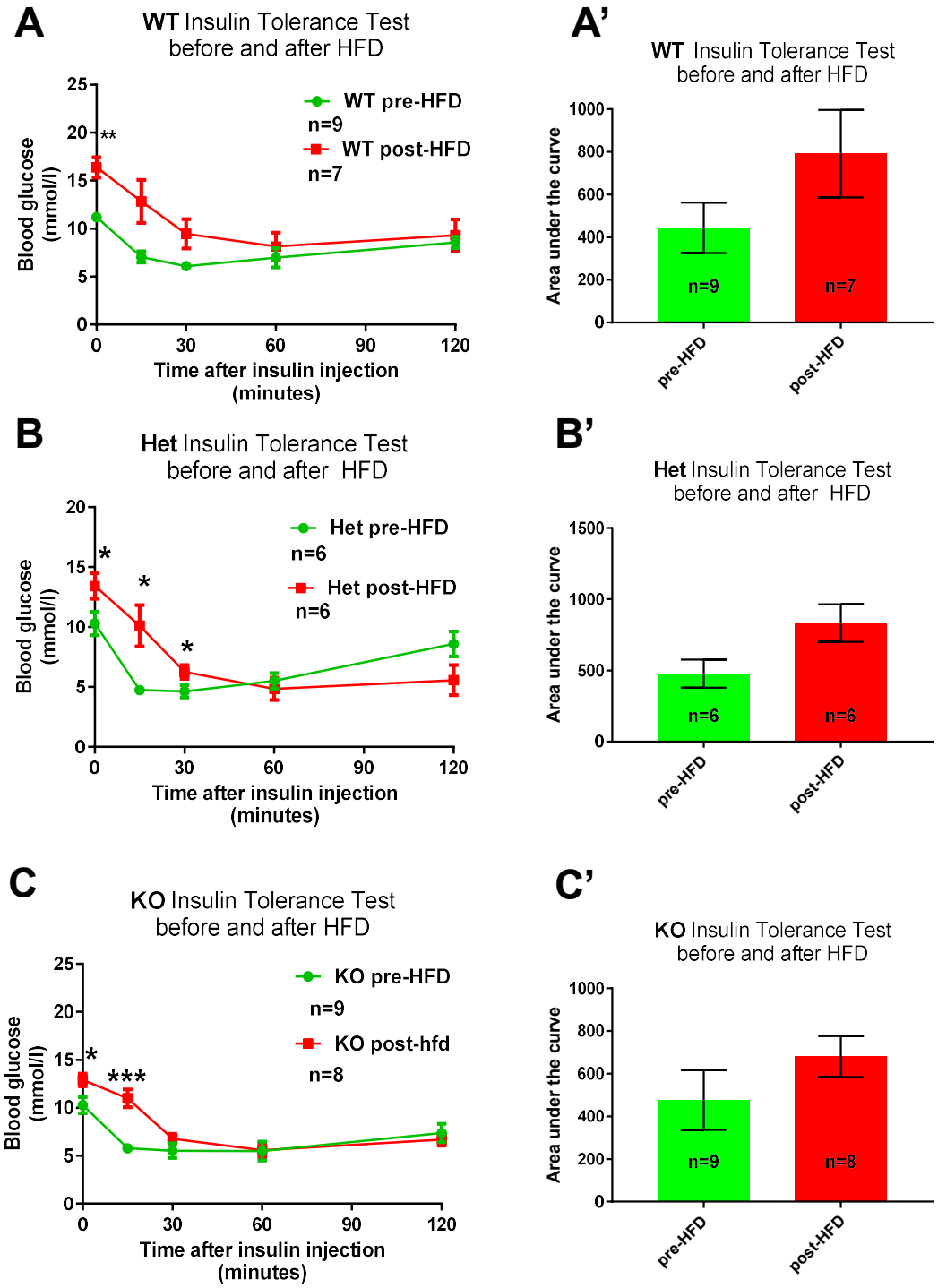

Figure 6.6 – Insulin sensitivity is unaffected in mice challenged with high-fat diet. Graphs compare HFD challenged and unchallenged mouse blood glucose levels at defined periods of time after insulin IP injection as an indication of insulin sensitivity in WT (A), Het (B) and KO (C) animals. In all groups, HFD challenged mice had higher baseline blood glucose levels, therefore the area under the curve measurements were compared (A', B', C'). Insignificant trends for decreased insulin sensitivity were observed in all groups. All significance testing was performed using the paired t-test. * - $P \leq 0.05$, **- $P \leq 0.01$. *** - $P \leq 0.001$.

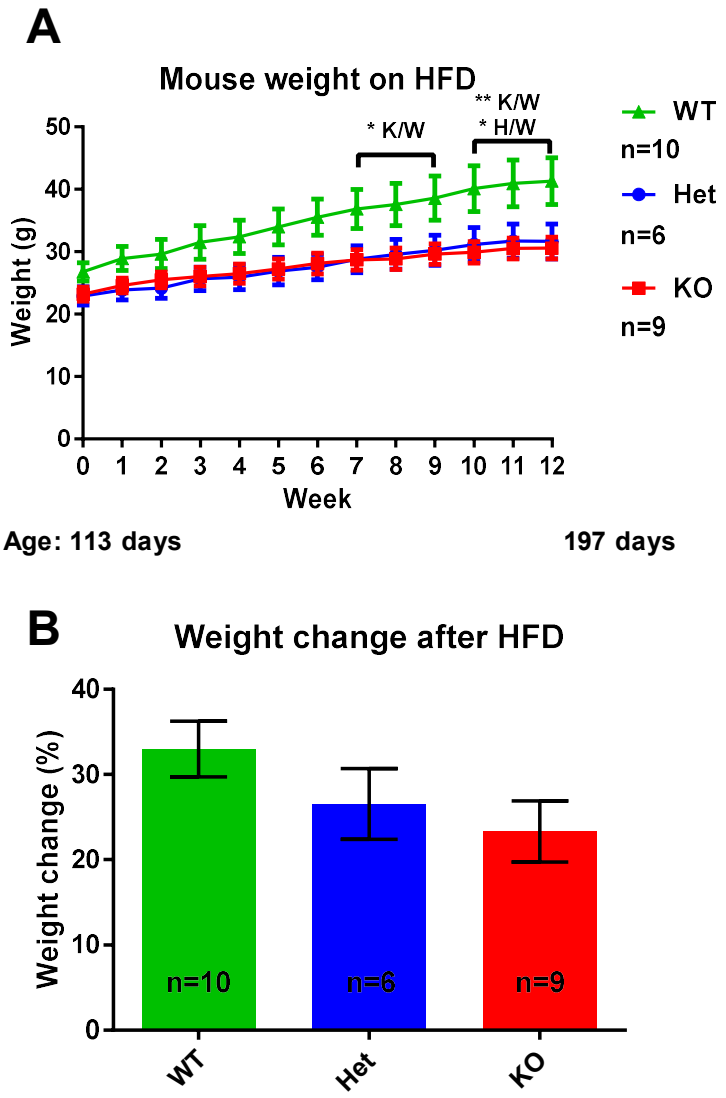

Figure 6.7 – Body weight change post high-fat diet is not substantially altered in *Fgfr1* and *Fgfr2* deficient mice compared to wild-type. Graphs compare WT, Het and KO mouse body weight during 12 weeks of high-fat diet (A). Het and KO weights were nearly identical during this period and rose slowly, while WT weights were significantly larger than KO starting at week 7 and compared to Het from week 10. No significant changes were seen in percentage weight change (B). H/W – Het compared to WT using multiple-comparisons repeated measures two-way ANOVA; K/W – KO compared to WT using multiple-comparisons repeated measures two-way ANOVA. * - P ≤ 0.05; **- P ≤ 0.01.

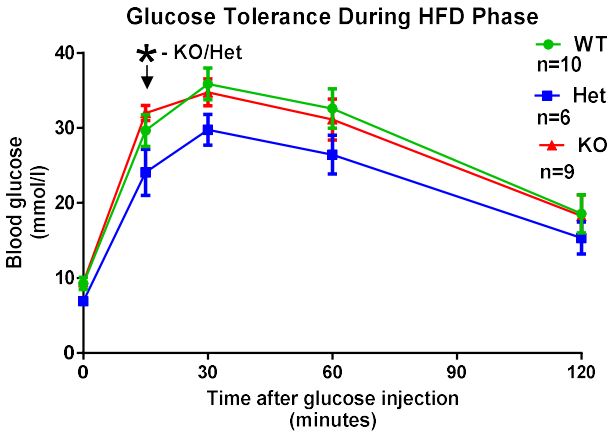

Figure 6.8 – Glucose metabolism may be slightly affected in Het mice fed a high-fat diet. Graphs compare WT, Het and KO mouse blood glucose levels at defined periods of time after glucose IP injection as an indication of glucose tolerance. KO animals were significantly more glucose sensitive compared to Het animals as evidenced by the higher blood glucose levels at the 15-minutes post-glucose injection. All significance testing was performed using multiple-comparisons repeated measures two-way ANOVA. * - P ≤ 0.05.

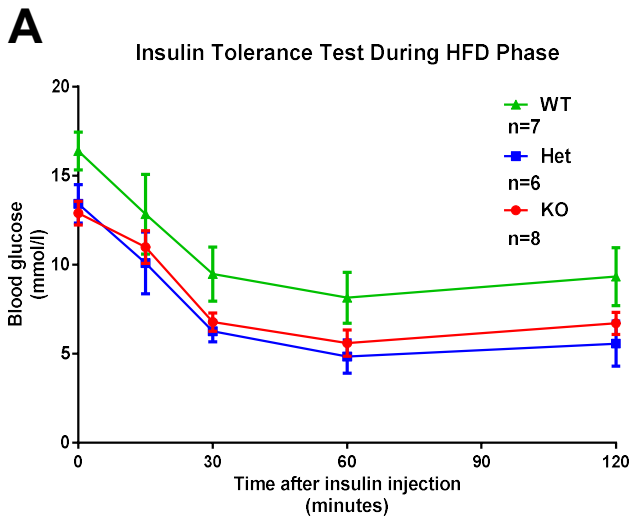

Figure 6.9 – Insulin sensitivity is not affected by *Fgfr1* and *Fgfr2* deficiency in mice fed a high-fat diet. Graphs compare WT, Het and KO mouse blood glucose levels at defined periods of time after insulin IP injection as an indication of insulin sensitivity. No significant differences were found (A). All significance testing was performed using multiple-comparisons repeated measures two-way ANOVA.

6.2.4 – Lineage tracing of *Fgfr1/Fgfr2* deficient β–tanycytes after HFD treatment

Het mice were more glucose tolerant than KO mice after the high-fat diet regime. To determine if this may be related to changes in neurogenesis or other cellular processes, lineage traced cell populations in HFD challenged Het and CKO animals were analysed in brains dissected from these animals at P233. This amounted to very long-term lineage tracing (Fig. 6.10 A; 27 weeks from the start of tamoxifen administration). S100β was used as a marker for the α-tanycyte domain to assess for the relative distribution of lineage traced cells in tanycyte compartments (Goodman and Hajihosseini, 2015).

No gross morphological differences were detected in cells of the 3V wall, or the parenchyma (Fig. 6.10 B, B', B'', C, C', C''). Parenchymal cells had neuronal morphology in both CKO and Het animals (Fig. 6.10 B'', C'').

Quantification revealed large numbers of lineage traced cells in the ependyma (Fig. 6.11 A) and parenchyma (Fig. 6.11 C), but no significant differences were observed. The distribution of tdTomato+ cells in regard to tanycytes domains (Fig. 6.11 B) and parenchymal nuclei (Fig. 6.11 D) also did not differ. Unlike in the experiments described in chapter 5, these comparisons were between Het and KO animals, with no WT group, the lineage tracing was much more long term and the animals were fed high-fat diet. Therefore, direct comparisons with the amplification of lineage-traced FGFR deficient cells seen in the postnatal ages (Fig. 5.8) are not possible due to these factors.

Interestingly, the number of lineage traced cells in the β- and α-tanycytes domains were roughly equal, regardless of genotype, in contrast to P4/P5 – P28 and P44/P45 – P55 lineage tracing experiments described in chapter 5, where lineage traced α-tanycytes comprised only roughly a third of the ependymal total, in both WT and FGFR deficient animals (Fig. 5.3; Fig. 5.8). Here, too, further experiments would be needed to determine if these potential differences in distribution are due to high-fat diet or long-term lineage-tracing.

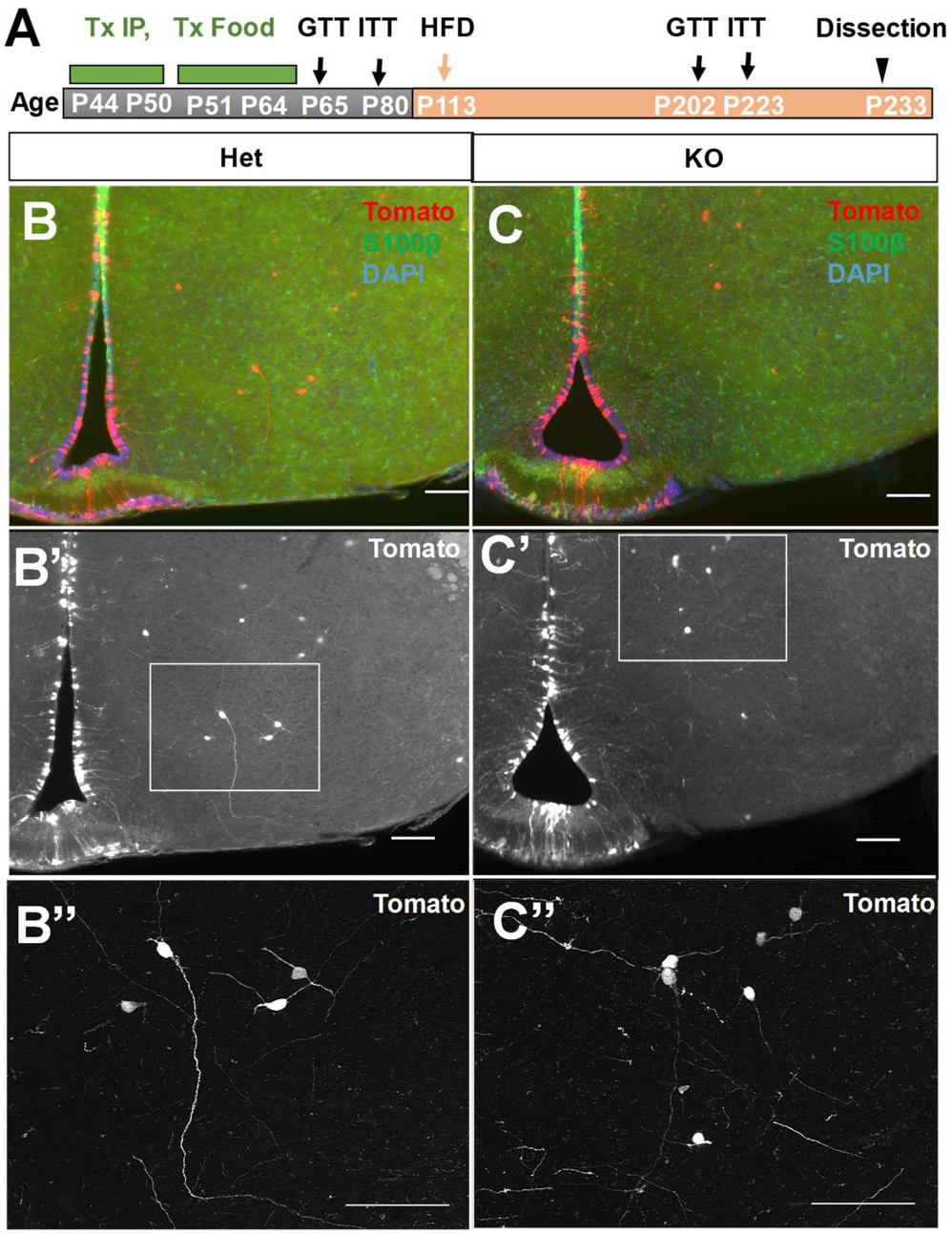

Figure 6.10 - Morphology of lineage traced FGF receptor-deficient cells is unaltered in HFD challenged *Fgfr1* and *Fgfr2* CKO compared to Het mice. Schematic displays the timing of tamoxifen administration and brain dissection (A). Immunohistochemistry revealed no visible differences in the morphology of lineage traced tanycytes (B, B', C, C'), and parenchymal cells (B', B'', C', C'') in Het and CKO P233 hypothalamus. Cells in the parenchyma had neuronal morphology with long processes (B'', C''). Scale bar – 100 µm.

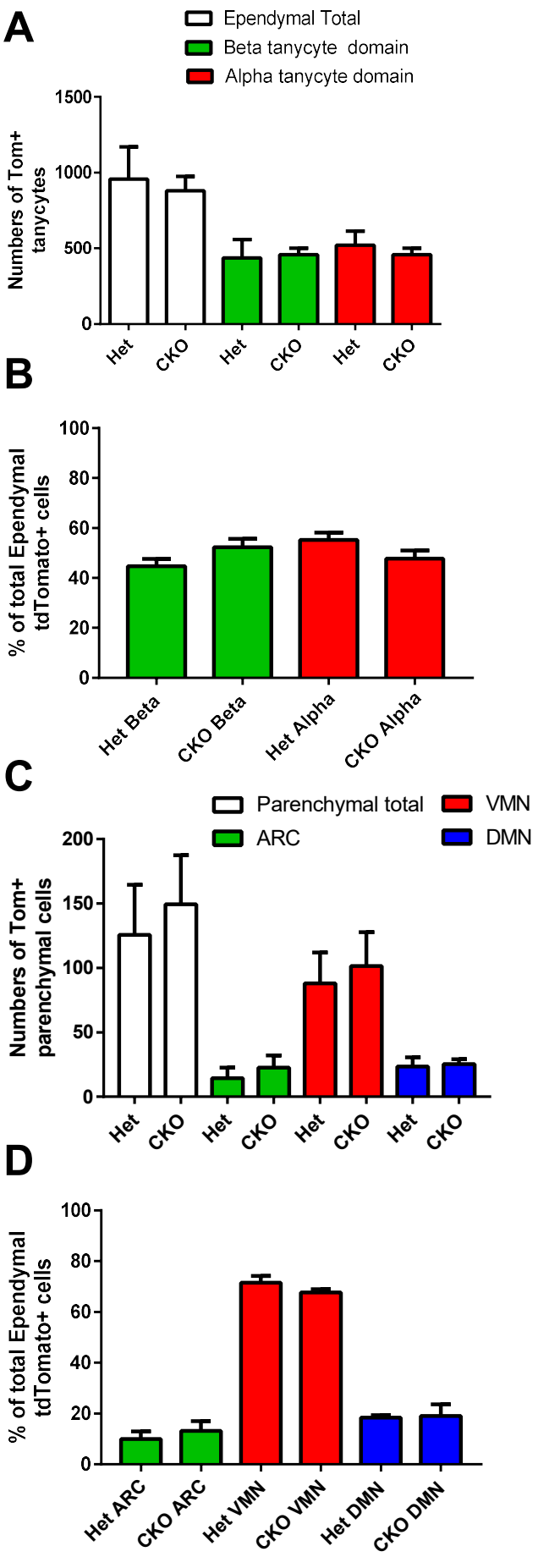

Figure 6.11 – Lineage traced cell numbers and distribution are similar in HFD challenged Het and CKO animal P233 hypothalamus. Graphs display numbers and distribution of lineage traced cells in the 3V wall (A, B) and parenchyma (C, D) of Het (n=3) and CKO (n=3) hypothalamus. No significant differences were detected. Note the approximately equal number of lineage traced cells in β- and α-tanycyte domains (B), which differs from the distribution in shorter-chase chow-fed animals where β-tanycytes are more numerous (Chapter 5).

6.3 – Discussion

FGF signalling is important for central control of food intake and glucose metabolism, as evidenced by exogenous hypothalamic stimulation with FGF1 or studies where FGFR1 function is blocked by neutralizing antibodies. These effects are likely at least partially mediated by FGFR1/FGFR2 expressed in β-tanycytes. In experiments reported here, we attempted to isolate the contribution of endogenous FGF receptor signalling in β-tanycytes in the regulation of these processes.

Using $Fgf10^{CreERT2}$::$Rosa26^{tdTomato}$::$Fgfr1^{Flox/Flox}$::$Fgfr2^{Flox/Flox}$ transgenic animals FGF receptor function is disrupted permanently in cells where *Fgfr1* and *Fgfr2* floxed alleles are excised. Deletion had been previously confirmed by detection of specific PCR products in mice after two tamoxifen doses (Chapter 5). In this study, the animals received 7 consecutive doses and were afterwards fed diet supplemented with tamoxifen for 2 weeks to ensure that a large number of β-tanycytes will undergo efficient recombination.

Both inhibition and exogenous stimulation of FGF signalling in hypothalamus results in rapid-onset hypophagia and consequently reduced body weight (Sun et al., 2007; Lelliott et al., 2014; Samms et al., 2015; Scarlett et al., 2016). These effects are observed in both lean and obese animals and maintained for as long as the interventions are continued and a return to normal feeding patterns and weight is observed shortly after treatments are stopped. In this study, during the first period of the experiment, before mice were challenged with HFD, all mice gained weight as is expected at this age (Gall and Kyle, 1968). However, KO and Het mice were significantly lighter compared to WT animals from the start of the experiments. At the start of the high-fat diet period, weights of the groups were not significantly different. KO and Het mice weight was significantly lower compared to WT animals by the end of the high-fat diet period (weeks 7 and 10 of HFD, respectively).

It has been observed that mice carrying the $Fgf10^{CreERT2}$ allele tend to be smaller in size (unpublished observations and Fig. 6.1 A). Both CKO and Het carry this allele, while WT mice do not. This likely affects the trends and significant differences for lower weight in these animals compared to WT. Due to this, analysis of individual timepoints should probably not be interpreted directly. Percentage weight change is likely a better indicator and it suggests only a modest long-term trend for KO animals towards the reduction of body weight gain, but not the rapidly occurring onset loss roughly 30-40% of body weight in other studies.

Scarlett et al., (2016) reported that obese and hyperglycaemic animals returned to normoglycaemia after a single ICV injection of FGF1. Here, high-fat diet challenged WT and KO animals had impaired glucose homeostasis as indicated by the GTT comparison with pre-HFD animals. Curiously, Het HFD fed animals seemed to have a largely unaltered response to glucose injection compared to HFD unchallenged animals. In addition, they were less sensitive to glucose compared to KO animals. FGF signalling levels determine its functional outcome and are regulated by both intracellular modulators and concentration of ligand (Garcia-Maya et al., 2006; Ekerot et al., 2008). FGF2 activation of FGF receptors is biphasic, following a bell-shaped curve where medium concentrations induce strongest FGFR signalling, low and high concentrations induce very little signalling, while medium-low and medium-high levels result in medium induction (Zhu et al., 2010; Kanodia et al., 2014). It is possible, that a partial deletion of FGF receptors results in lowered FGF signalling levels that are similar to signalling induced by high concentrations of exogenous ICV FGF1 and in both cases such signalling may have similar beneficial effects on insulin and/or glucose sensitivity. Recently an FGF1 variant was engineered that has reduced ability to induce FGFR dimerization due to its reduced heparan sulfate binding (Huang et al., 2017). Interestingly, in this study the modified FGF1 lost its mitogenic function but had retained the glucose metabolism regulating effects, indicating that FGF1-FGFR signalling levels are important for determining its function.

Sexual dimorphisms are common in mouse glucose metabolism (Tiraby et al., 2007; Shi et al., 2008; Macotela et al., 2009). In addition, it has been reported that HFD stimulates median eminence neurogenesis in female mice, but not male mice, and that ablation of this process also causes weight reduction effects only in female mice (Lee et al., 2014). One caveat of our study is that the experiments were performed on both female and male mice. Although the proportion of females and males was similar (WT: 4F, 6M; Het: 3F, 3M; KO: 4F, 5M), the high variability and low numbers preclude a meaningful interpretation of sex-specific data. However, Lelliott et al. (2014) performed FGFR1-IIIc inhibition experiments on male and female mice and observed similar effects on glucose homeostasis and weight loss regardless of sex.

In contrast to the FGFR1-IIIc blocking studies, here, *Fgfr2* function was also disrupted. These receptors may have similar roles in tanycytes, but they may also differ due to their differential binding affinities of the ligands that are expressed in the 3V wall, for example FGF2 which has a higher affinity to FGFR1-IIIc while FGF9 and FGF18 which preferentially bind FGFR2-IIIc (Chapter 4; Zhang et al., 2006a) It would be informative to perform a similar set of experiments using conditional knockout mice

that carry either only the *Fgfr1* or *Fgfr2* flox alleles to explore their distinct contributions. On the other hand, deletion of both receptors is more relevant to studies of exogenous application of FGF1, as both receptors are expressed in tanycytes, can be stimulated by FGF1 and may have compensatory or cooperative effects.

Although in the hypothalamus of CKO mice, *Fgfr1* and *Fgfr2* deletion would occur only in β-tanycytes that express *Fgf10*, the effects may not be isolated to these cells. That is because *Fgf10* is expressed in other parts of the brain (Hajihosseini et al., 2008). Furthermore, the progeny of *Fgf10*+ β-tanycytes in the parenchyma may normally be responsive to FGF signalling. Additionally, since tamoxifen administration was performed via IP injections, recombination would happen in all tissues that contain *Fgf10* expressing cells. In terms of metabolically significant organs, *Fgf10* is expressed in adult rat kidney (Cancilla et al., 2001), adult rat white adipose tissue (Yamasaki et al., 1999), adult mouse skeletal muscle (Christina Stratford thesis, UEA, 2014), adult mouse small intestine (Al Alam et al., 2015), adult mouse liver (Utley et al., 2014), adult mouse pancreas (Hart et al., 2000) and in all these tissues *Fgfr1* and *Fgfr2* expression was also found. If *Fgf10* and *Fgfr1* and/or *Fgfr2* are expressed in the same cells in some of these tissues, the deletion of these genes may possibly have synergistic or opposing effects on metabolism compared to ones arising from tanycytes. The most direct way of restricting deletion to brain tissue would be to inject 4-hydroxy-tamoxifen into the third ventricle. However, it is not clear if in this case, a single injection would cause recombination in a sufficient number of cells, therefore cannulation might be preferred (DeVos and Miller, 2013).

These caveats may help explain the lack of overt metabolic phenotype in CKO mice. However, a different explanation is that metabolic roles of endogenous FGF signalling in tanycytes may be minimal, synergistic with effects on other cell types, or easily compensated by other mechanisms due to the long-term nature of these experiments. In the studies cited previously that linked FGF signalling interventions with metabolic effects, not only tanycytes were affected. For example, in addition to tanycytes, Sun et al. (2007) found FGFR1-IIIc antibody deposition in the median eminence and arcuate nucleus. In addition to these sites, Lelliott et al. (2014) found that FGFR1-IIIc antibodies affected cells in area postrema and subfornical organ. Meanwhile, ICV injection of FGF1 causes induction of heat shock protein-25 in tanycytes and periventricular astrocytes (Scarlett et al., 2016). Indeed, glucose ICV application results in the release of FGF1 from the 3V ependyma into hypothalamus parenchyma (Oomura et al., 1992). Therefore, tanycytes may have either minor or synergistic roles in eliciting metabolic changes, not seen when their contribution is isolated.

In terms of lineage tracing, while no differences were seen in Het and KO animals in cell morphology and number, it is worthwhile noting that the distribution of lineage traced cells in the ependyma of these mice was very different compared to the P44/P45 – P55 lineage traced animals. In these mice, sacrificed at P233, lineage traced β-tanycytes and α-tanycytes were roughly equal in number, while in P55 animals, α-tanycytes made up approximately a third of the total number of lineage traced tanycytes. This may indicate that α-tanycytes generated by β-tanycytes are not transient but remain in the α-domain long-term, at least when *Fgfr1/Fgfr2* are deleted. The caveat to this is that these animals were challenged with HFD, and the lineage traced cells are *Fgfr1*/*Fgfr2* deficient and may not reflect normal processes. Further long-term lineage tracing experiments could therefore be designed to investigate the dynamics of lineage traced tanycyte distribution in the ependyma, their migration, turnover and whether FGF receptor deficiency in β-tanycytes results in the amplification of lineage-traced tanycytes, as it does at postnatal ages, described in chapter 5.

Further gain-of-function studies could be performed using mice that carry a conditionally expressed activated FGFR3 allele (Kang et al., 2014). Bred with mice that carry inducible Nestin or FGF10 CreERT2 drivers, this would allow to determine the effects of increased FGF signalling in tanycytes on metabolism and/or neurogenesis. Loss-of-function studies similar to ones described here could also be performed using a different inducible Cre driver such as Nestin, since *Fgf10* is expressed in only a subpopulation of β-tanycytes that does not completely overlap with expression of Nestin and other markers (Haan et al., 2013) and different subpopulations may have different functions.

Conclusion

In conclusion, only very subtle metabolic effects were seen upon ablation of FGFR signalling in β-tanycytes. Namely, this resulted in a long-term trend in reduction of body weight gain in both chow and HFD fed animals, and, in the case of partial deletion (Het), a resistance to glucose homeostasis impairments seen in high-fat diet challenged mice. The tenuousness of these effects may suggest that other central targets are responsible for the fast-acting and dramatic changes in food intake, body weight and glucose homeostasis in response to exogenous FGF1 or FGFR blocking antibodies. This warrants a further exploration of both the contribution of tanycytes and these other potential targets while addressing the methodological caveats of the present study.

Chapter 7

Fgf10 is required for expression of Agouti-related peptide (Agrp) in embryonic hypothalamus

7.1 – Introduction

Paracrine FGFs form the largest subfamily of FGFs and signal by binding to FGF receptors, causing transphosphorylation of their tyrosine kinase domains and initiation of intracellular signalling cascades (Itoh and Ornitz, 2011). FGFs 1, 2, 3, 8 and 22 are canonically paracrine but have been shown to directly enter the nucleus and have an intracellular mode of action (Kiefer and Dickson, 1995; Beyer et al., 2003; Wesche et al., 2005; Wesche et al., 2006; Suzuki et al., 2012). Recently, FGF10 was also described as being capable of translocating into the nucleus and having intracrine roles (Mikolajczak et al., 2016). As mentioned in chapters 4 and 5, *Fgf10* is expressed in β-tanycytes, yet its cognate receptors FGFR1-IIIb and FGFR2-IIIb are not present in the hypothalamus (Hajihosseini et al., 2008), therefore suggesting that FGF10 may operate in an intracrine fashion in tanycytes. However, intracellular FGF10 signalling is largely unexplored and our knowledge of its functions, intracellular binding partners and molecular targets are largely unknown.

One effective way to study the noncanonical mode of action of FGF10 is by knocking out FGF10 and observing the effects this has in tissues that do not express its cognate receptors. In chapter 5 and 6, lineage tracing using the $Fgf10^{CreERT2}$ mouse line was described. Heterozygous $Fgf10^{CreERT2/+}$ (FGF10 Het) animals have reduced *Fgf10* expression, while homozygous $Fgf10^{CreERT2/CreERT2}$ mice lack *Fgf10* expression and can be considered FGF10 knockouts (FGF10 KO), while (El Agha et al., 2012). FGF10 KO mice do not survive after birth due to defects in organogenesis but can be used to explore the function of FGF10 in embryos.

Previously Dr Niels Haan carried out work in our lab, characterising the expression of *Fgf10* in embryonic mouse hypothalamus at various stages (Niels Haan PhD Thesis, 2012; Fig. 7.1) through the use of the $Fgf10^{LacZ}$ transgenic mouse line (Kelly et al., 2001). This revealed that *Fgf10* expression in the E10-E12.5 hypothalamus is limited to the ependyma. At E14.5-E16.5, some fainter cells are also found lateral to the ependyma. At E18.5, there is strong staining not only in the ependyma but also in the lateral stream and the arcuate nucleus. By P4 this strong staining is again restricted to the ependyma and the arcuate nucleus is only faintly stained. β-galactosidase is a bacterial protein and therefore degrades slowly. This suggests that the faint cells are potentially transiently lineage traced and may not express *Fgf10* themselves.

It has been shown that cells lining the third ventricle give rise to neurons in hypothalamic nuclei (Shimada and Nakamura, 1973). In addition, a population of *Fgf10*+ progenitors is present in developing chick hypothalamus (Fu et al., 2017). It is

possible that the cells labelled laterally to the ependyma are neurons generated from *Fgf10*+ progenitors. However, most neurons in the hypothalamic nuclei are generated between E10-E16, including the arcuate nucleus (Shimada and Nakamura, 1973). Therefore, the intense staining seen only in E18.5 arcuate nucleus presents either an undescribed neurogenic event or short-lived induction of *Fgf10* expression in the arcuate nucleus.

FGF10 KO mice can be used to explore the role of FGF10 in this event. In addition, FGF10 mode of action in the embryonic hypothalamus is likely intracellular, and this presents an excellent opportunity to clarify which genes this signalling may impact. Comparing gene expression profiles of both FGF10 KO, FGF10 Het and WT E18 hypothalamus through RNA sequencing (RNA-Seq) may, therefore, provide invaluable answers to both questions. Indeed, as described further in this chapter, RNA-Seq showed that the orexigenic neuropeptide *Agrp* (agouti-related neuropeptide) (Yang and Tao, 2016) is greatly downregulated in FGF10 KO embryonic hypothalamus in comparison to FGF10 Het hypothalamus, though not in the FGF10 KO/WT comparison (Table 7.1). This exciting result elicited further validation and investigations of its nature.

7.1.1 – Aims

To gain insights into the roles and molecular mechanisms of noncanonical FGF10 signalling in embryonic hypothalamus, RNA sequencing was performed on mRNA extracted from the hypothalamus of FGF10 KO and WT animals. The results of RNA-seq were then analysed and gene-targets validated by in situ hybridization.

Figure 7.1 – **Dynamic expression of *Fgf10* in embryonic hypothalamus.** Representative images of X-gal stained $Fgf10^{LacZ}$ hypothalamus at different embryonic stages. During the early stages (E10-16.5), *Fgf10* expression is restricted to the ventral wall of the third ventricle, with some faint cells positioned laterally. However, at E18.5 in addition to ependymal cells, there is intense staining in the adjacent hypothalamus parenchyma, chiefly in the arcuate nucleus. This staining is still present at P4 but is considerably weaker in the parenchyma. This may reflect a neurogenesis event that takes place sometime between E16.5 – P4, or a short-term induction of *Fgf10* expression in the parenchyma. Figure modified from Niels Haan PhD thesis (UEA, 2012). Arrows point to anatomical structures. ARC – arcuate nucleus; 3V – third ventricle.

Anterior
Posterior
E10
E12.5
E14.5
E16.5
E18.5
P4
3V
ARC

7.2 – Results

7.2.1 – RNA sequencing of embryonic Fgf10 KO hypothalamus reveals an array of genes controlled by *Fgf10*

Dr Mohammad Hajihosseini and Dr Timothy Goodman had previously collected hypothalami from E18.5 embryonic mice (5 WT, 6 $Fgf10^{Cre/+}$, 5 KO) and isolated mRNA. These samples were then given to Dr James Hadfield at the Cancer Research UK Cambridge Institute Genetics Core where the RNA-Seq differential gene expression experiment was performed. Each sample had: a sequencing depth of at least 5 million reads, average alignment rate of 96.87 %, intragenic alignment rate of 94.21 %, and 17765.5 genes detected on average. Differential gene expression analysis was carried out using the DESeq workflow and p-values were adjusted for multiple-testing by FDR (false discovery rate).

This experiment revealed 23 genes that were differentially expressed in the $Fgf10^{Cre/+}$ (Het) / KO and 3 genes in the KO / WT comparisons ($p < 0.05$), while none were detected in the Het / WT comparison (Table 7.1). Two genes were differentially expressed in both comparisons: apelin receptor (*Aplnr*; upregulated) and RIKEN cDNA 4833420G17 gene (*4833420G17Rik*; downregulated). The confirmation of upregulation and downregulation of these genes was therefore attempted by performing ISH. In addition, agouti-related protein (*Agrp*) was downregulated in KO compared to $Fgf10^{Cre/+}$. *Agrp* is a neuropeptide expressed in a population of arcuate nucleus neurons and has an orexigenic role by acting as a biased agonist of melanocortin receptors (Yang and Tao, 2016). While *Agrp* was not significantly downregulated in the KO / WT comparison, it was still considered a gene worth investigating due to its restricted expression in the arcuate nucleus and importance to energy balance.

cRNA probes for *Aplnr, 4833420G17Rik* and *Agrp* were synthesised and used for in situ hybridisation as described in chapters 2 and 3. Of these, only *Agrp* produced specific staining and could, therefore, be further investigated.

Gene (abbreviation)	Gene (full name)	Ensemble Reference	Comparison	Chromosome	Fold change	p-value
Fgf10	fibroblast growth factor 10	ENSMUSG00000021732	KO / WT	13	0,137815917	9,37444E-08
4833420G17Rik	RIKEN cDNA 4833420G17 gene	ENSMUSG00000062822	KO / WT	13	0,247440695	9,94477E-06
Aplnr	apelin receptor	ENSMUSG00000044338	KO / WT	2	1,784326527	2,00752E-05
Agrp	agouti related protein	ENSMUSG00000005705	KO / WT	8	0,264331922	0,152874324
Aplnr	apelin receptor	ENSMUSG00000044338	KO / Het	2	1,853072723	2,66944E-08
Sepp1	selenoprotein P, plasma, 1	ENSMUSG00000064373	KO / Het	15	1,379804548	2,74947E-05
Cd93	CD93 antigen	ENSMUSG00000027435	KO / Het	2	1,449760805	0,000134242
Tgfbr2	transforming growth factor, beta receptor II	ENSMUSG00000032440	KO / Het	9	1,570914302	0,000134242
Sparc	secreted acidic cysteine rich glycoprotein	ENSMUSG00000018593	KO / Het	11	1,310749044	0,001230215
Enpp1	ectonucleotide pyrophosphatase/phosphodiesterase 1	ENSMUSG00000037370	KO / Het	10	1,62453188	0,00240232
Uaca	uveal autoantigen with coiled-coil domains and ankyrin repeats	ENSMUSG00000034485	KO / Het	9	1,399984082	0,004038409
Lcp1	lymphocyte cytosolic protein 1	ENSMUSG00000021998	KO / Het	14	1,634866401	0,00551328
Slc38a5	solute carrier family 38, member 5	ENSMUSG00000031170	KO / Het	X	1,564926341	0,00551328
Anxa6	annexin A6	ENSMUSG00000018340	KO / Het	11	1,358102769	0,008997666
4833420G17Rik	RIKEN cDNA 4833420G17 gene	ENSMUSG00000062822	KO / Het	13	0,368758255	0,008997666
Cdh5	cadherin 5	ENSMUSG00000031871	KO / Het	8	1,54017845	0,01109658
Pltp	phospholipid transfer protein	ENSMUSG00000017754	KO / Het	2	1,493167979	0,012725016
Agrp	agouti related protein	ENSMUSG00000005705	KO / Het	8	0,24339497	0,021005055
Fgf10	fibroblast growth factor 10	ENSMUSG00000021732	KO / Het	13	0,262672676	0,031247503
Abca1	ATP-binding cassette, sub-family A (ABC1), member 1	ENSMUSG00000015243	KO / Het	4	1,247910096	0,033360647
Lpar1	lysophosphatidic acid receptor 1	ENSMUSG00000038668	KO / Het	4	1,395617799	0,038246474
Fam114a1	family with sequence similarity 114, member A1	ENSMUSG00000029185	KO / Het	5	1,845873515	0,039848652
Dynlt1c	dynein light chain Tctex-type 1C	ENSMUSG00000000579	KO / Het	17	0,759696995	0,044898373
Tie1	tyrosine kinase with immunoglobulin-like and EGF-like domains 1	ENSMUSG00000033191	KO / Het	4	1,464757127	0,044898373
Yap1	yes-associated protein 1	ENSMUSG00000053110	KO / Het	9	1,338002571	0,044898373
Lin28b	lin-28 homolog B (C. elegans)	ENSMUSG00000063804	KO / Het	10	0,769649569	0,044898373
Col3a1	collagen, type III, alpha 1	ENSMUSG00000026043	KO / Het	1	1,960151655	0,044898373

Table 7.1 – **Genes with altered expression levels in *Fgf10* KO embryonic hypothalamus.** Table summary of differentially expressed genes detected in RNA-Seq. Expression comparisons were significantly different (adjusted p-value < 0.05) in all listed cases, except the *Agrp* KO/WT comparison. Genes marked in red were detected in both KO/ Het and KO/WT comparisons and ISH was carried out for these genes. Light blue denotes genes that were downregulated, while yellow marks genes that were upregulated.

7.2.2 – *Fgf10* regulates the expression of *Agrp*, but not *Npy* in embryonic mouse arcuate nucleus

In situ hybridization using *Agrp* probes was performed on cryostat sections of WT, KO and Het E18.5 hypothalami (Fig 7.2 A, C, E). In all cases, its expression was restricted to the arcuate nucleus and some cells in subependymal ME. However, the intensity of staining and the apparent number of stained cells (not quantifiable) was visibly decreased in KO hypothalamus, compared to both Het and WT. *Npy* cRNA probes were also used in these experiments as ISH positive control reactions. Intriguingly, no apparent differences were seen in both the staining intensity and the number of cells expressing *Npy* in the hypothalamic of these animals (Fig. 7.2 B, D, F). In the arcuate nucleus, nearly all neurons that express *Npy* also express *Agrp* and they form a population of orexigenic *Npy*/*Agrp* neurons (Hahn et al., 1998). The lack of apparent alterations in the *Npy* ISH suggests that the *Npy*/*Agrp* population is not affected in terms of numbers, but instead, the expression of *Agrp* is strongly downregulated in KO hypothalamus. Next, immunohistochemistry for AGRP was performed and a similar reduction in AGRP protein levels in KO animals was observed (Fig. 7.2 G, H).

As mentioned previously, FGF10 can only bind to FGFR2-IIIb, and to a lesser extent FGFR1-IIIb. To test whether these FGF receptors are expressed in the embryonic hypothalamus, RT-PCR reactions were performed using mRNA extracted from E16 mouse hypothalamus and primers specific to *Fgfr1* and *Fgfr2* IIIb or IIIc splice isoforms. Only IIIc isoforms of *Fgfr1* and *Fgfr2* were detected (Fig. 7.3 A), suggesting that FGF10 may not signal through the canonical autocrine/paracrine mode of action in the embryonic hypothalamus.

For further confirmation that *Fgf10* may not act through its receptors in the embryonic hypothalamus, *Agrp* and *Npy* ISH was performed on wild-type and FGFR2-IIIb KO (De Moerlooze et al., 2000) E18.5 embryonic hypothalamus. Unlike KO animals, *Agrp* and *Npy* expression in FGFR2-IIIb KO animals was unchanged compared to WT (Fig. 7.3 B, C, D, E). This adds further credence to the notion that FGF10 signalling in the embryonic hypothalamus may be noncanonical.

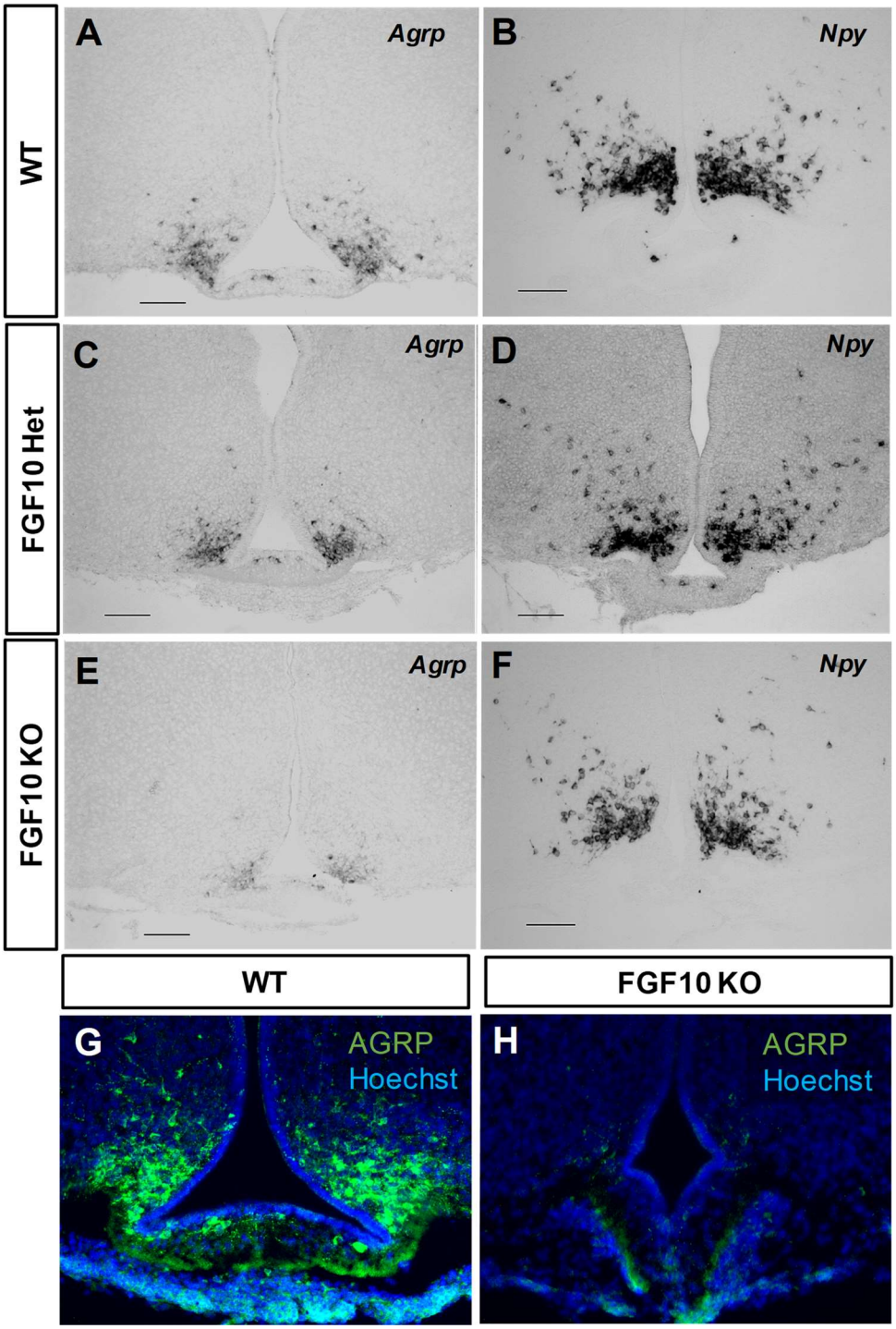

Figure 7.2 – **Expression of *Agrp* is downregulated in *Fgf10* KO arcuate nucleus, while *Npy* expression is unaltered.** Representative pictures of ISH using *Agrp* or *Npy* probes on E18 hypothalamus sections. Note the highly reduced intensity of *Agrp* staining in KO (E) animals compared to both WT (A) and Het (C), while *Npy* signal was comparable in all genotypes (B, D, F). The same reduction in AGRP protein level was observed in KO animals compared to WT by using IHC (G, H). Note that the sections in G and H are from comparable regions, but the section depicted in (H) has been slightly stretched during mounting. Scale bar – 100 µm.

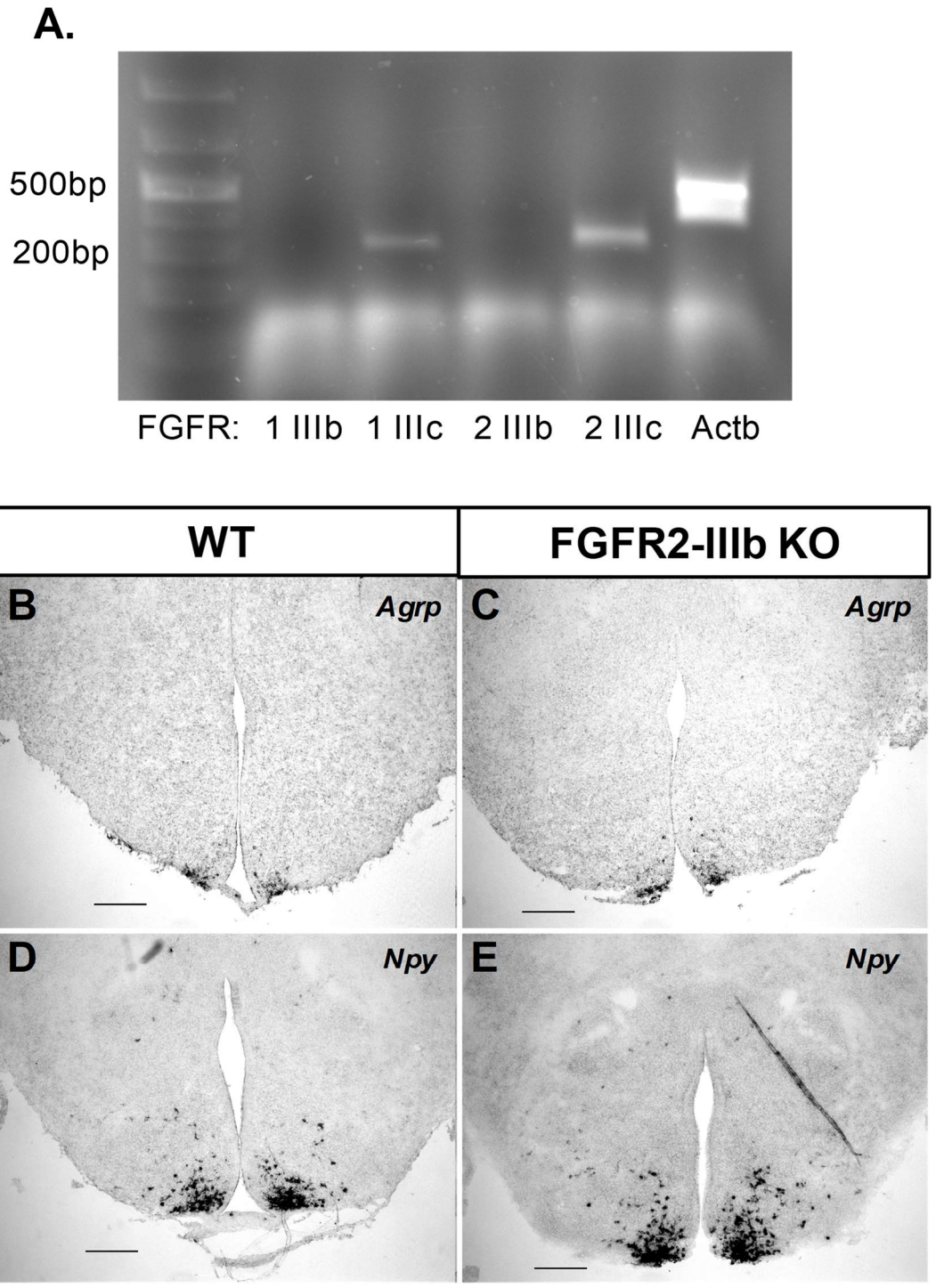

Figure 7.3 – Expression levels of *Agrp* and *Npy* are unchanged in FgfR2–IIIb KO arcuate nucleus. RT-PCR performed on E16 hypothalamus detected only IIIc splice isoforms of *Fgfr1* and *Fgfr2*, but not IIIb (A). Expected band sizes as follows: *Fgfr1*-IIIb – 301 bp; *Fgfr1*-IIIc – 306 bp; *Fgfr2*-IIIb – 318 bp; *Fgfr2*-IIIc – 310 bp. Representative pictures of ISH using *Agrp* (B, C) or *Npy* (D, E) probes on E18 hypothalamus sections. Expression strength and patterns of both *Agrp* and *Npy* were similar in both WT (B, D) and Fgfr2–IIIb KO (C, E) hypothalamus. Scale bar – 100 µm.

7.2.3 – Examination of *Yap1* and Tead4 expression in *Fgf10* deficient hypothalamus by ISH

To shed light on possible molecular mechanisms and components that may link *Fgf10* to the regulation of *Agrp* expression, other genes were considered that were differentially expressed according to RNA-Seq. Yes-associated protein 1 (*Yap1*) is upregulated in KO hypothalamus (Table 7.1) and stood out as it directly interacts with the TEAD family of transcription factors and therefore participates in gene expression regulation. Furthermore, TEA Domain Transcription Factor 4 (*Tead4*) has binding sites on an enhancer for *Agrp* (Fishilevich et al., 2017; GeneHancer ID: GH16J067486). To test the hypothesis that *Yap1* and *Tead4* are involved in the regulation of *Agrp* expression and are affected by Fgf10, ISH for these genes was performed on E18 KO and WT hypothalamus sections.

The ISH reactions using *Yap1* cRNA probe were successful and revealed its expression solely in the 3V ependyma within the hypothalamus (Fig.7.4 A, A', B, B'). However, no discernible difference in intensity or localisation of staining was observed in the KO hypothalamus. Perhaps this is due to the ISH protocol not being sensitive enough to reveal relatively subtle differences in gene expression levels (1.34-fold upregulation of *Yap1,* in contrast to *Agrp* which was downregulated 4.11 times; Table 7.1).

The *Tead4* probe produced only weak, diffuse staining that did not appear to be specific (Fig. 7.4 C, C', D, D').

7.2.4 – Expression of *Foxo1* is altered in *Fgf10* KO arcuate nucleus

Forkhead Box O1 (*Foxo1*) and Brain-Specific Homeobox (*Bsx*) are transcription factors that are well characterised as regulators of *Agrp* transcription (Kitamura et al., 2006; Lee et al., 2013a). *Foxo1* is particularly of interest, as it is one of few factors known to differentially regulate *Npy* and *Agrp* transcription – in some cases it inhibits transcription of *Agrp* while not affecting *Npy* (Kitamura et al., 2006). Therefore, ISH for *Foxo1* and *Bsx* was carried out to probe for any changes of their expression in KO hypothalamus.

Expression of *Foxo1* in WT embryonic hypothalamus was restricted to the 3V ependyma and the medial and lateral parts of the arcuate nucleus (Fig. 7.5 A, A'). However, while *Foxo1* was expressed in the 3V ependyma and lateral part of the arcuate nucleus, its expression in the medial part was largely absent in KO

hypothalamus, (Fig. 7.5.B, B'). Expression of *Agrp* is also mostly restricted to the medial part of the arcuate nucleus (Fig. 7.2. A, A', A''), therefore suggesting that *Foxo1* may play a role in FGF10 mediated *Agrp* expression regulation.

Bsx was found to be expressed strongly in the dorsomedial nucleus and weaker in the arcuate nucleus and no apparent alterations were detected in the *Fgf10* deficient hypothalamus (Fig.7.5 C, C', D, D').

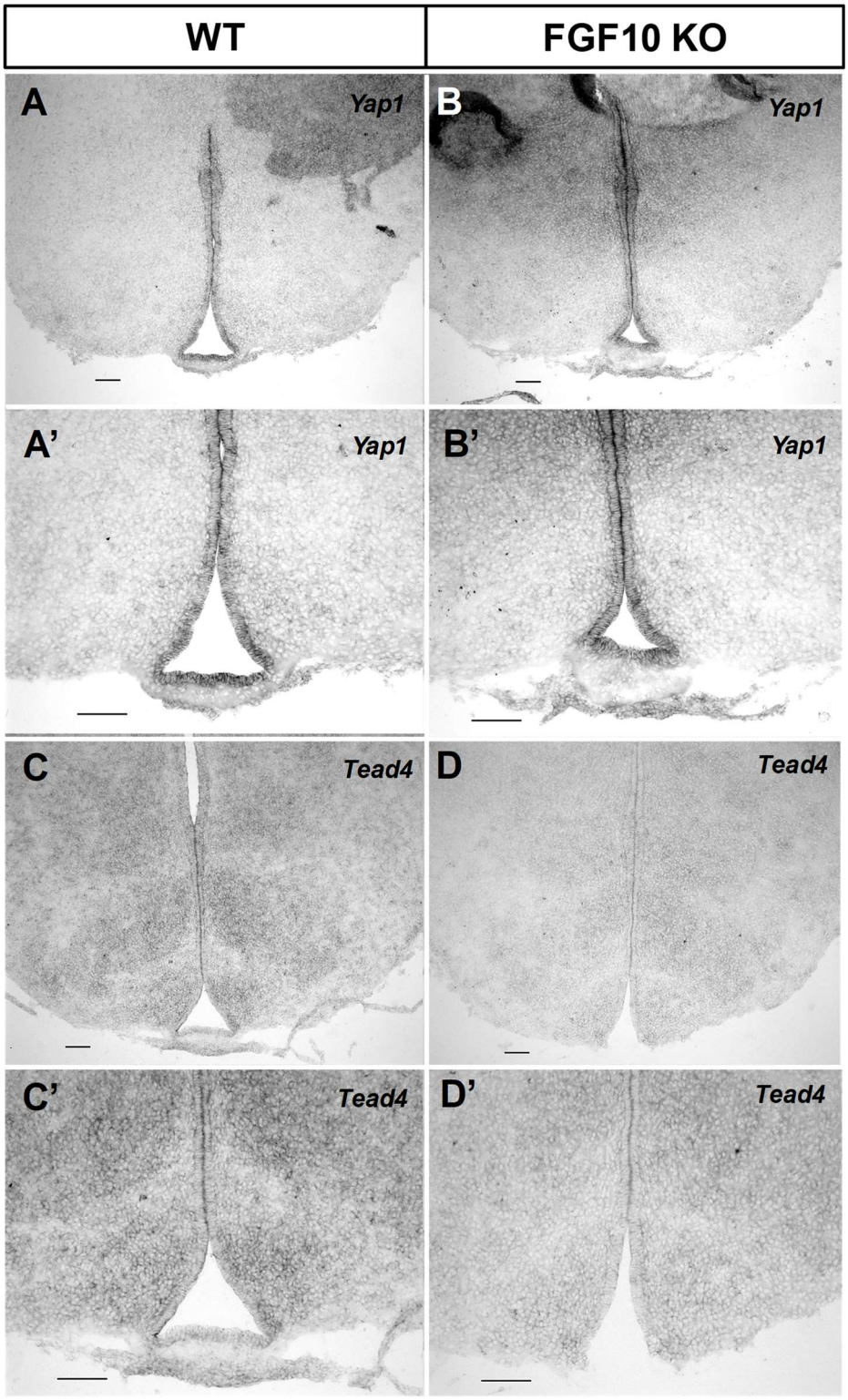

Figure 7.4 – *Yap1* and *Tead4* as potential mediators of suppressed *Agrp* expression in *Fgf10* KO. Representative pictures of ISH using *Yap1* (A, A', B, B') or *Tead4* (C, C', D, D') probes on E18 hypothalamus sections. *Yap1* expression in the embryonic hypothalamus was restricted to the 3V ependymal and was similar in both WT (A, A') and KO (B, B') animals. *Tead4* probe produced only widespread, unspecific staining. Scale bar – 100 μm.

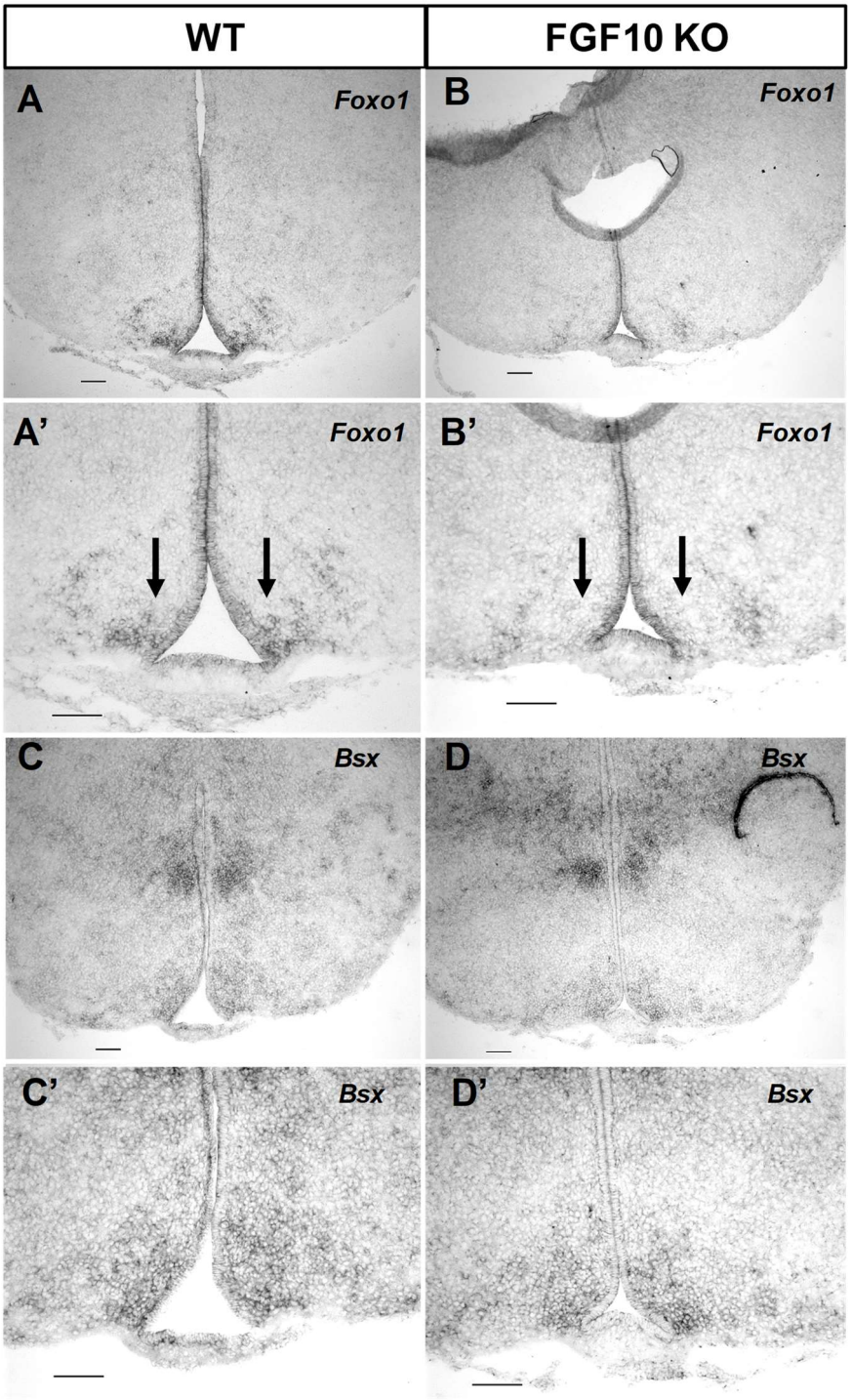

Figure 7.5 – **Altered expression of *Foxo1* but not *Bsx* in the arcuate nucleus of *Fgf10* KO mice.** Representative pictures of ISH using *Foxo1* (A, A', B, B') or *Bsx* (C, C', D, D') probes on E18 hypothalamus sections. *Foxo1* staining was present in the arcuate nucleus and 3V ependymal in WT hypothalamus (A, A'), however, it was absent in the medial part of the arcuate nucleus in KO animals (B, B'). *Bsx* expression was strongest in the dorsomedial nucleus and comparable staining was also observed in the arcuate nucleus of both WT (C, C') and KO (D, D') hypothalamus. Arrows point to medial part of the arcuate nucleus. Scale bar – 100 µm.

7.3 – Discussion

The intracellular functions and signalling mechanisms of FGF10 are poorly understood, as are its functions in E18 mouse hypothalamus. By performing RNA-Seq on embryonic FGF10 KO hypothalamus mRNA our lab has identified genes that are influenced by 'intracrine' FGF10 signalling. Remarkably, among other effects, it was found to be involved in the establishment of AGRP expression in the embryonic arcuate nucleus.

According to classic studies, neurons in the arcuate nucleus are produced between E11 and E16 (Shimada and Nakamura, 1973). The neurons of the anterior arcuate nucleus are generated earlier, between E11-E14, while in the caudal arcuate nucleus this process is extended and persists until E16, and a similar time-frame is seen in rat hypothalamus (Shimada and Nakamura, 1973; Altman and Bayer, 1978). Two well-characterized, important populations of neurons reside in the arcuate nucleus: these are the anorexigenic pro-opiomelanocortin (POMC) and orexigenic AGRP/NPY neurons. These populations integrate central and peripheral signals to exert opposing influences on feeding behaviour – POMC neurons suppress, while AGRP/NPY neurons stimulate appetite (Sohn, 2015). Detailed analysis of their ontogenesis showed that both POMC and NPY neurons are born between E11.5 and E12.5 (Padilla et al., 2010). At E13.5, only neurons in the lateral arcuate are born that do not express POMC or NPY. This study also found that a subset of POMC expressing neurons differentiate into NPY/AGRP or other neurons. The expression of the *Pomc* starts at E10.5-E11.5, *Npy* at E13.5 and *Agrp* at E15.5 (Padilla et al., 2010; Díaz et al., 2014). However, although expression starts in the embryonic hypothalamus, the expression of these neuropeptides continues to increase and develop postnatally (Nilsson et al., 2005; Cottrell et al., 2009).

Considering the development of these populations, it seems unlikely that reduction in *Agrp* staining detected in ISH and IHC is caused by an alteration in neurogenesis in FGF10 KO animals. This is further confirmed by the fact that *Npy* expression is unperturbed by FGF10 deficiency, indicating that the NPY/AGRP population is unaffected in terms of numbers. A more likely explanation is that FGF10 signalling is influencing *Agrp* expression levels. Here, we found only IIIc splice isoforms of *Fgfr1* and *Fgfr2* expressed in the embryonic hypothalamus. As no cognate receptors for FGF10 are expressed, and FgfR2-IIIb KO does not show the same phenotype of reduced *Agrp* expression, the mode of action is likely intracrine. Therefore, a plausible interpretation is that FGF10 expression extends to the arcuate nucleus at E18.5 and

affects the expression of genes, including *Agrp*, through its intracellular mode of action.

Analysis of RNA-Seq results did not reveal any transcription factors that are differentially regulated in FGF10 KO hypothalamus. However, *Yap1* is upregulated in FGF10 KO tissue. YAP1 is part of the Hippo-YAP signalling pathway which is involved in the regulation of cell proliferation, apoptosis, migration, differentiation and therefore important for organ growth and tumorigenesis (Zhao et al., 2010). It is a transcriptional regulator whose activity is mediated by the TEAD family of transcription factors (Stein et al., 2015). TEAD4 has binding sites in an *Agrp* enhancer (GeneHancer ID: GH16J067486), but not in *Npy* promoters or enhancers (Fishilevich et al., 2017). The ISH reaction for *Tead4* was unsuccessful, while the difference in *Yap1* expression was likely not large enough (1.34-fold upregulation) to detect by ISH. However, *Yap1* ISH did reveal that its expression is limited to the third ventricle wall at E18.5, with no expression in the arcuate.

FOXO1 is a transcription factor that promotes *Agrp* expression in the mouse hypothalamus (Kitamura et al., 2006). Crucially, the *Npy* promoter does not contain FOXO1 binding sites and FOXO1 does not seem to affect *Npy* expression (Kitamura et al., 2006), though some studies report that it may influence the expression of both *Agrp* and *Npy* (Kim et al., 2006; Kim et al., 2012). This disagreement may be due to different experimental strategies and contexts employed in the studies. In this study, *Foxo1* expression was found in the 3V wall and arcuate nucleus of the E18.5 hypothalamus. However, *Foxo1* expression in the medial part of the arcuate nucleus was absent in the KO hypothalamus. This perfectly matches the fact that *Agrp* expression at E18.5 is only present in the medial part of the arcuate nucleus and it is there that it is reduced in the KO hypothalamus. Therefore, intracellular FGF10 signalling may be required for *Foxo1* expression in the embryonic medial hypothalamus, which in turn promotes expression of *Agrp*. Since the alteration in the expression pattern is quite subtle, it could be that absolute levels of *Foxo1* mRNA were also changed only slightly and therefore not detected by RNA-Seq.

Recently, YAP1 has been shown to directly bind FOXO1 in cardiomyocytes, forming a functional complex that influences gene transcription (Shao et al., 2014). At E18.5, both *Yap1* and *Foxo1* are expressed in cells of the 3V ependyma, and therefore it is possible that they directly interact in these cells. It may be that coexpression of these genes in *Fgf10*+ progenitors resident in the ependyma at earlier embryonic ages

predisposes the newly generated neurons to express *Agrp* and *Foxo1*, but a deficiency in intracellular FGF10 signalling alters this process.

Interestingly, the expression of *Fgf10* can be upregulated or downregulated by Yap1, possibly by interactions with Wnt or Shh signalling systems, although the precise molecular mechanism is unclear (Reginensi et al., 2013; Lin et al., 2017; Volckaert et al., 2017). There is a possibility, that in FGF10 deficient cells *Yap1* expression is upregulated as a compensatory mechanism, which then has knock-on effects on *Foxo1, Agrp* and maybe other genes.

In a similar vein, Transforming Growth Factor Beta Receptor 2 (*Tgfbr2*) is upregulated in FGF10 KO hypothalamus (Table 7.1). TGFBR2 signalling can induce *Fgf10* expression cranial neural crest cells (Hosokawa et al., 2010). In addition, YAP1 promotes *Tgfrb2* transcription by binding to its promoter along with TEAD transcription factors (Fan et al., 2017). Therefore, a likely scenario is that to compensate for the loss of FGF10 function, *Yap1* is upregulated, which in turn upregulates *Tgfrb2*. Changes in expression of other genes, such as *Foxo1* and *Agrp* may then be knock-on effects (Fig. 7.6).

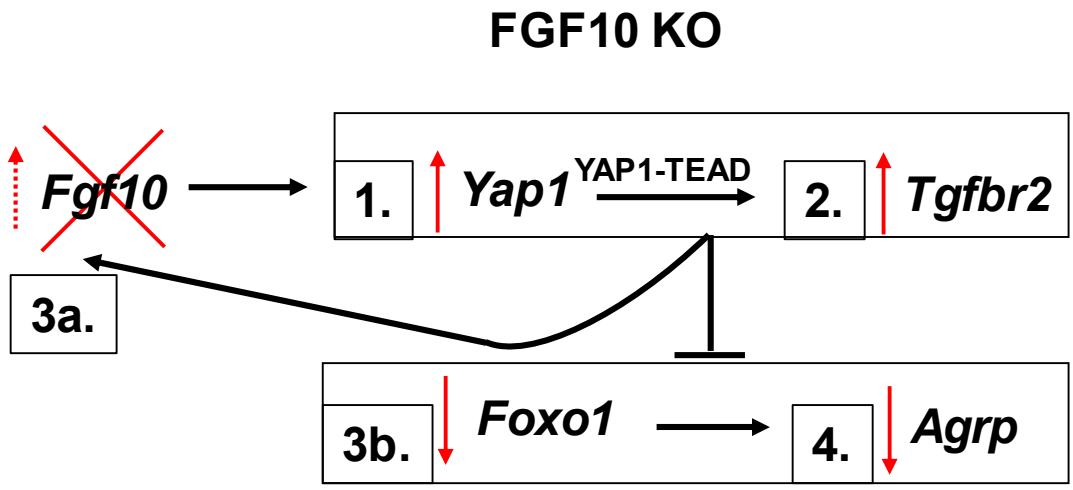

Figure 7.6 – Upregulation of *Yap1* and Tgfbr2 in FGF10 KO hypothalamus may cause downregulation of *Agrp*. A schematic model of possible interactions that may result in *Agrp* downregulation in FGF10 KO hypothalamus. 1 – to compensate for FGF10 loss of function, *Yap1* is upregulated. 2 – YAP1-TEAD complexes stimulate and upregulate *Tgfbr2* expression. 3 – YAP1 and TGFRB2 may stimulate *Fgf10* expression (3a) or inhibit *Foxo1/Agrp* expression in the arcuate nucleus (3b). 4 – due to lowered *Foxo1* expression, *Agrp* expression is downregulated.

To explore these possibilities, it would be helpful to acquire expression pattern information of these genes in WT and KO hypothalamus at different embryonic ages, starting at E10, when the birth of ARC neurons begins. In addition, as the expression of *Agrp* develops from adulthood to late postnatal ages (Nilsson et al., 2005; Cottrell et al., 2009), it would be important to understand whether intracellular FGF10 also affects *Agrp* expression in postnatal and adult animals, or if this regulation is short-lived and incidental. $FGF10^{CreERT2/CreERT2}$ mice cannot be used in this case, as they do not survive after birth (El Agha et al., 2012). However, this can be addressed through the use of $FGF10^{CreERT2/Flox}$ conditional knockout animals (Abler et al., 2009).

The roles of intracrine FGF10 signalling may differ in adult and embryonic hypothalamus. In the adult, comparisons can be made between $FGF10^{CreERT2/Flox}$::$Rosa26^{tdTomato}$ and $FGF10^{CreERT2/+}$::$Rosa26^{tdTomato}$ animals. FGF10 expressing adult cells could be sorted through FACS, followed by single-cell transcriptomics (Nguyen et al., 2018) to detect differential gene expression.

One potential way for nuclear FGF10 to exert its effects as a transcriptional cofactor is by binding to DNA and/or other proteins involved in transcription regulation. Chromatin Immunoprecipitation Sequencing (ChIP-Seq) would be a good method to test if FGF10 can bind to DNA (Furey, 2012). Two-dimensional gel electrophoresis can be used to determine what proteins intracellular FGF10 binds to (Lasserre and Ménard, 2012). These approaches would provide essential information for understanding the molecular basis of intracrine FGF10 signalling and provide hints to its function.

Conclusion

The experiments detailed here are an early effort in understanding the nature of intracellular (non-canonical) FGF10 signalling. RNA sequencing provided tantalizing clues as to the functions of this signalling. In situ hybridization experiments confirmed that FGF10 is required for establishing *Agrp* expression in AGRP/NPY neurons during embryonic development by altering the expression of *Foxo1*. This is likely due to compensatory upregulation of *Yap1* and *Tgfrb2* in response to FGF10 signalling deficiency. Further studies are warranted to determine if this role is maintained in the postnatal and adult hypothalamus. In addition, many other genes were found that seemingly point to other possible functions. Finally, there is a need to elucidate the protein partners and the exact molecular basis for ‘intracellular’ FGF10 signalling.

Chapter 8

General Discussion and Future Perspectives

8.1 - Discussion

Constitutive neurogenesis in adult rodent brain is now widely accepted to occur in the subgranular and subventricular niches and this process has been extensively explored. Part of the enthusiasm of research into adult neurogenesis is due to the promise of therapeutic benefits for stroke, neurodegenerative and psychiatric diseases (Winner and Winkler, 2015; Apple et al., 2017; Lu et al., 2017). The rising prevalence of obesity, type II diabetes and eating disorders is a strong motivator to pursue a better understanding of adult neurogenesis in the hypothalamus due to its potential implications in energy homeostasis (Recabal et al., 2017). These investigations are at an early stage and there is little clarity over the identity of the neural stem/progenitor cells (NSPCs), the physiological and molecular determinants that regulate neurogenesis in adult hypothalamus and the function of newborn neurons and glial cells.

Studies suggest that exogenous growth factors such as BDNF, CNTF, IGF-1, EGF and FGF2 can promote proliferation and neurogenesis in the hypothalamus, similar to effects of exogenous growth factors in the canonical niches (Pencea et al., 2001; Kokoeva et al., 2005; Perez-Martin et al., 2010; Xu et al., 2005; Robins et al., 2013). Counterintuitively, both administration of exogenous IGF-1 and deletion of its endogenous receptor, IGF-1R, enhance neurogenesis (Perez-Martin et al., 2010; Chaker et al., 2016), illustrating the importance of studying endogenous growth factor signalling. While endogenous FGF signalling has been shown to be important in SGZ and SVZ niches, this has not been explored in the hypothalamus niche.

To bridge this gap in knowledge, this project sought to map the expression patterns of FGF signalling system components in the hypothalamus neurogenic niche. Then, the distribution and function of endogenous FGF receptors in the regulation of neurogenesis and metabolism was explored through their conditional deletion in tanycytes.

8.1.1 – The mapping of FGF signalling pathway components suggests its roles in regulating hypothalamic neurogenesis and energy balance

Although the expression of *Fgfr1* and *Fgfr2* in tanycytes has been reported previously (Lein et al., 2007), the tanycyte domain specificity of this expression had not been explored. Here, *Fgfr1* and *Fgfr2* expression was found in ventral tanycyte populations, mutually exclusive from that of GFAP which demarcates the α-tanycyte domain

(Goodman and Hajihosseini, 2015). Meanwhile, expression of *Fgfr4* was not detected in the niche and *Fgfr3* was expressed only in parenchymal S100β glial cells. It can, therefore, be concluded that the expression of FGF receptors in tanycytes is restricted to the β2 and ventral α2/β1-tanycyte domains. This matches the observation of increased ventral α2/β1-tanycyte proliferation in response to intracerebroventricular FGF2 injection (Robins et al., 2013). One possibility for a lack of proliferative effect on β2-tanycytes upon FGF2 administration is that FGF receptors in β2-tanycytes are not expressed on the apical side that contacts the CSF, but instead potentially on their basal processes in the median eminence. However, intracerebroventricular injection of FGF1 causes expression of c-Fos, a marker for cell activation (Bullitt, 1990), in both β2-tanycytes lining the floor of the third ventricle and tanycytes that form the lateral walls of the ventricle (Scarlett et al., 2016). This suggests that β2-tanycytes likely express *Fgfr1* and *Fgfr2* on their apical surface contacting the CSF and can, therefore, respond to FGFs in the CSF, but does not preclude their expression on basal processes. The lack of a proliferative FGF2 effect on β2-tanycytes may then reflect differences in the function of these receptors between these subtypes. This is supported by the much stronger expression of *Fgfr1* and the FGF receptor signalling modulator *Spry2* in β2-tanycytes compared to ventral α2/β1-tanycytes. It can be hypothesised that FGF signalling may play a role in controlling the proliferation of ventral α2/β1-tanycytes, while also being important for the barrier function of β2-tanycytes (Langlet et al., 2013; Balland et al., 2014).

β-tanycytes express many other RTK receptors, such as Ntrk2, VEGFR-3, CNTFRα, ErbB1 and ErbB2 (Prevot et al., 2003; Lein et al., 2007; Hou et al., 2011; Severi et al., 2012). The intracellular signalling pathways of these receptors often overlap with that of FGFR1/FGFR2. It is likely that there are some synergistic effects, as reported elsewhere for FGF and BDNF, IGF-1, VEGF-A, CENTF and EGF (Ciccolini and Svendsen, 1998; Albrecht et al., 2002; Kano et al., 2005; Johnson-Farley et al., 2007; Singh et al., 2017). The expression of *Sprouty1* and *Sprouty2* in β-tanycytes reported here, suggests a tight regulation and fine-tuning of these inputs to achieve specific cellular responses.

The expression of *Fgf2* and *Fgf18* in dorsal α2, ventral α2/β1 tanycytes and their high affinity for IIIc splice isoforms of FGF receptors (Zhang et al., 2006a) suggest that they are potential endogenous autocrine/paracrine ligands for tanycytic FGFR1 and FGFR2. *Fgf1* and *Fgf9* can also bind FGFR1-IIIc and FGFR2-IIIc, but their expression was found only in the GFAP+ α-tanycyte domain. They may still be released into the CSF and reach tanycytic FGF receptors through the currents created by beating cilia

(Faubel et al., 2016). Indeed, FGF1 is released from cells lining the 3V wall into the CSF and mediobasal hypothalamus parenchyma after feeding or ICV injection of glucose (Oomura et al., 1992).

While expression of *Fgf18* mRNA is restricted to GFAP- ventral α2/β1 tanycytes (Robins et al., 2013), even with an acute pulse-chase paradigm (tamoxifen IP at P50-P52, dissection at P53), we find many tdTomato+ cells in the GFAP+ α-tanycyte domain of $FGF18^{CreERT2}$::$Rosa26^{tdTomato}$ animals. Ventral α2/β1 tanycytes have been shown to be a population of FGF responsive NSPCs (Robins et al., 2013), therefore the location of tdTomato cells more dorsal to the expression domain of *Fgf18* may reflect the amplification and migration of these progenitors and their descendants. Animals carrying the $FGF18^{CreERT2}$ allele may, therefore, be a useful tool for studying hypothalamic NSPCs and their lineage progression through lineage tracing or conditional inactivation of genes of interest.

Parenchymal expression of *Fgfr1* is widespread, and especially strong staining was observed in the ventromedial nucleus. No co-localisation of GFAP and *Fgfr1* was observed, indicating that *Fgfr1* is likely expressed by neurons of appetite-regulating centres and can be activated by FGF1 released from tanycytes or parenchymal cells to inhibit feeding (Sasaki et al., 1994). *Fgfr3* expression was found solely in parenchymal S100β+ glial cells and although their function is unknown, FGFR3 signalling in paraventricular astrocytes may be important for regulation or glucose homeostasis, as discussed later.

8.1.2 – *Fgfr1* and *Fgfr2* control the amplification of β–tanycytes and consequently the numbers of new cells in energy balance controlling hypothalamic nuclei

Deletion of *Fgfr1* and *Fgfr2* in FGF10+ β-tanycytes caused the amplification of lineage traced tanycyte and newborn parenchymal neuron numbers in the postnatal hypothalamus. This effect seemed restricted to an early postnatal time window (P6-P10) and the amplification is likely due to increased cell proliferation. One model of this process is that lineage traced *Fgfr1/Fgfr2* deficient β-tanycytes migrate to the α-tanycyte domain where they proliferate further, giving rise to new neurons and other tanycytes. This is based on the observations that at postnatal ages, the α-tanycyte domains contain large numbers of proliferating cells (Goodman et al., in preparation;

Chapter 5), tdTomato+ tanycytes were seen to proliferate only in this domain (Chapter 5), and that lineage traced *Fgfr1/Fgfr2* deficient β-tanycytes and newborn neurons are amplified (Chapter 5).

There are reasons to believe that this scenario is restricted to early postnatal ages. Firstly, lineage traced cell numbers seem to reach their apex at P10, and longer chase at P28 does not produce higher cell counts. Second, the high numbers of proliferating cells in the α-tanycyte domain in basal conditions have not been reported for mice above the age of P10, when β2-tanycytes become the main proliferative cells in the 3V ependyma (Lee et al., 2012). Finally, expression of *Fgfr2* at P8 is found in both β and GFAP+ α tanycytes domains, while its expression is restricted to β2- and ventral α2/β1-tanycytes in adult mice. This may suggest a role for *Fgfr2* in controlling the level of proliferation in the α-tanycyte domain at postnatal ages.

Exogenous ICV injection of FGF2 causes greatly increased proliferation of ventral α2/β1-tanycytes, but not of β2-tanycytes, in adult mice (Robins et al., 2013). Is this consistent with our finding of lineage traced cell amplification upon deletion of FGF receptors in tanycytes? Very high concentrations of FGF2 have been shown to inhibit FGFR signalling (Kanodia et al., 2014), therefore the overdose of exogenous FGF2 may bring about a similar effect as the deletion of FGF receptors.

Alternatively, FGFR1 has been previously shown to act as an inhibitor of lung epithelial stem cell proliferation, through its role in inducing post-translational modification of Spry2, which then inhibits the MAPK/ERK pathway activated by other pro-proliferative growth factors such as EGF (Balasooriya et al., 2016). A similar mechanism might be at play in the hypothalamic niche, as both *Fgfr1/Fgfr2* and *Spry1/Spry2* are expressed in β-tanycytes (Chapter 4) and deletion of these receptors causes amplification of lineage traced cells as discussed above (Fig. 8.2). Notably, the strongest expression of both *Fgfr1* and *Sprouty2* is in β2-tanycytes, rapidly tapering off dorsally with little expression in β1-tanycytes, where *Fgfr2* expression predominates. It may be that stimulation of FGFR1 in β2-tanycytes inhibits proliferation by inducing SPRY2 posttranslational modifications, while in ventral α2/β2 tanycytes FGFR2 signalling can induce proliferation, and this could explain the effects of exogenous FGF2.

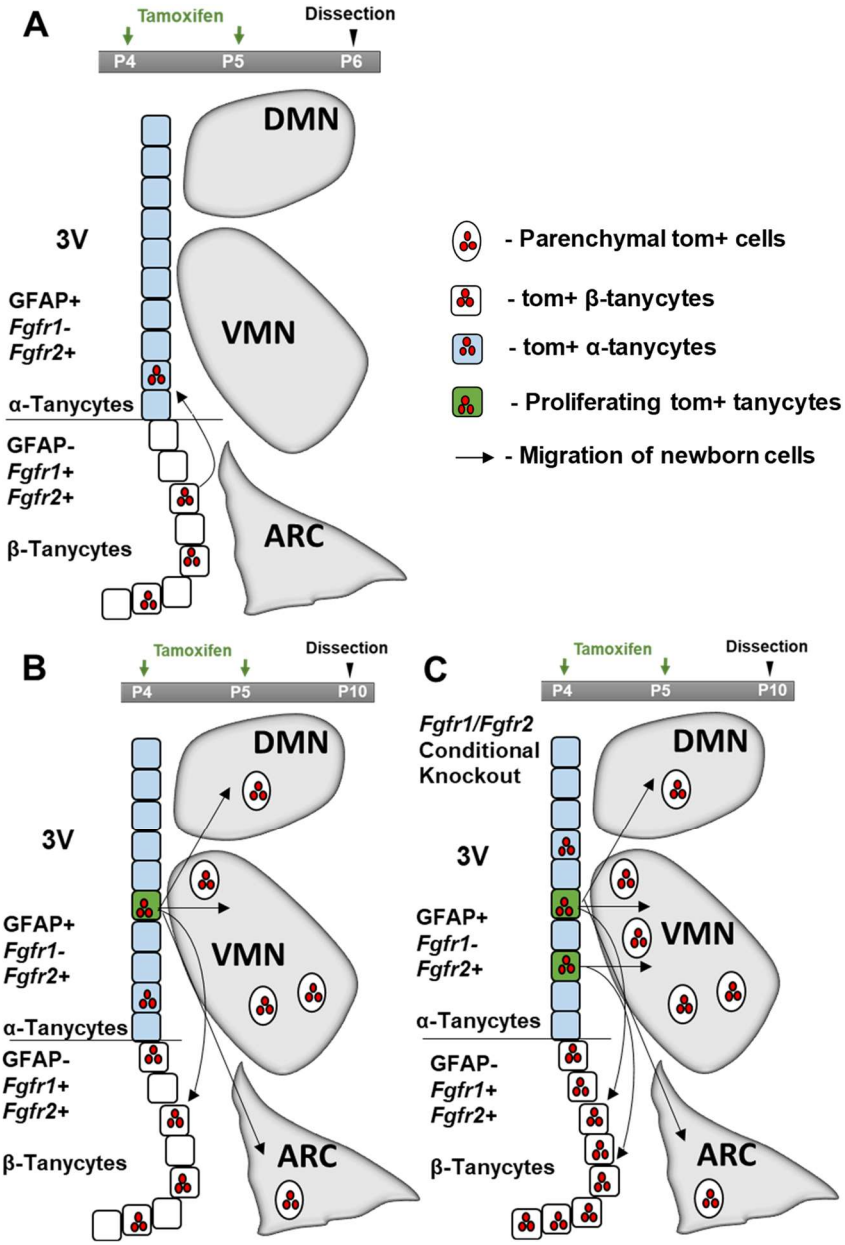

Figure 8.1 – A model of postnatal hypothalamus neurogenesis and its regulation by FGFR signalling. Schematics represent the relative distribution of lineage traced *Fgf10*+ tanycytes and a model of their migration and proliferation at P6 (A) and P10 (B, C). At P6, lineage traced β-tanycytes are migrating into the α-tanycyte domain. Between P6 and P10, lineage traced α-tanycytes proliferate and give rise to newborn neurons and to a lesser extent glial cells in the parenchyma, or to new tanycytes. *Fgfr1/Fgfr2* deficient lineage traced cells numbers are greatly amplified by P10 (C) compared to tanycytes with non-impaired FGF receptor function. This amplification is especially pronounced in the β-tanycyte domain and ventromedial nucleus, likely caused by the increased proliferation of α-tanycytes. *Fgfr2* is normally expressed in α-tanycytes in the postnatal hypothalamus and may act to inhibit proliferation. Adapted from Goodman et al., in preparation.

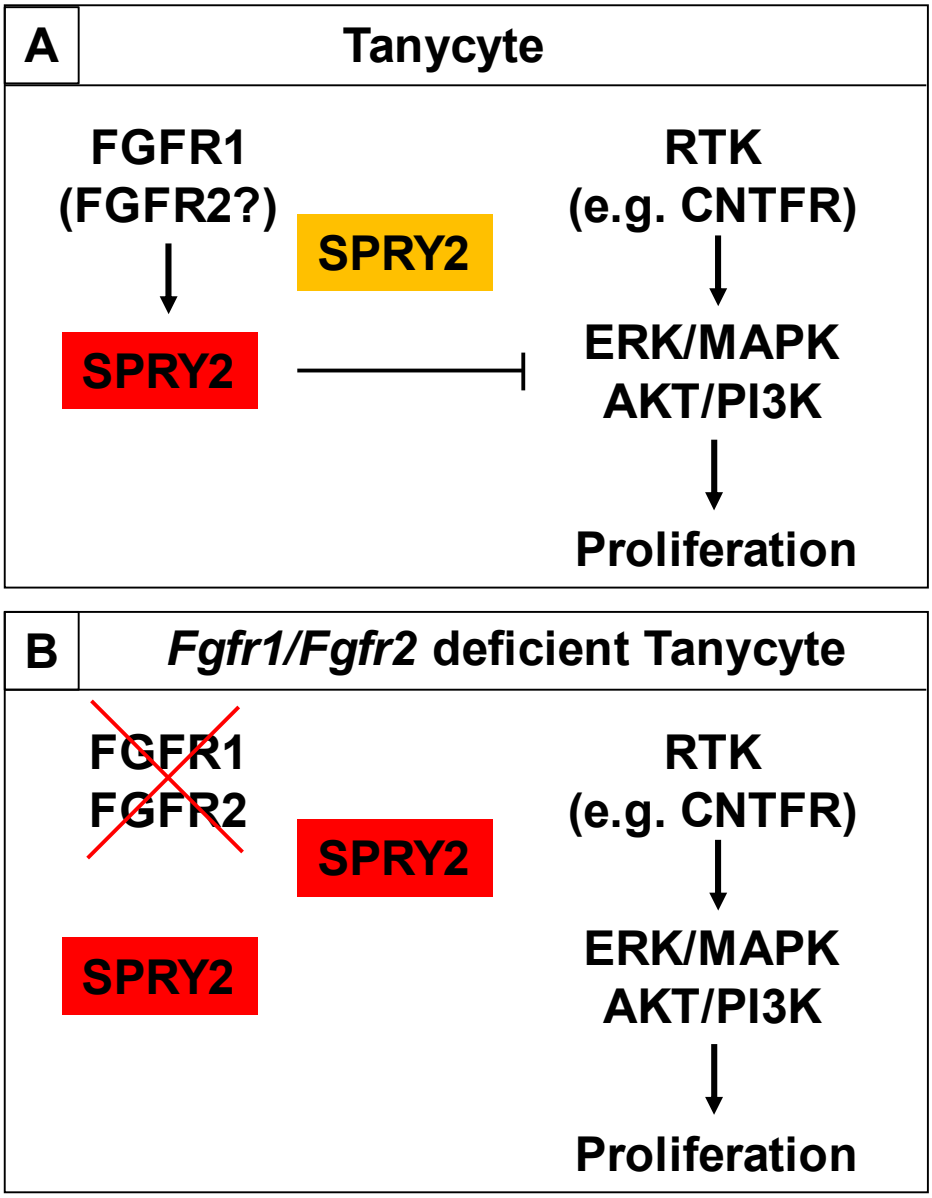

Figure 8.2 – A model of the molecular mechanism by which FGFR signalling may regulate tanycyte proliferation. (A) FGF receptor signalling in tanycytes may result in post-translational modifications of SPRY2, increasing the abundance of the active isoform (in orange) which actively inhibits proliferation stimulating MAPK and AKT pathways initiated by other receptor tyrosine kinase receptors (RTKs). In *Fgfr1/Fgfr2* deficient tanycytes, the active SPRY2 isoform is less abundant, causing a reduction in the inhibition of proliferation stimulating signalling of other RTKs. Adapted from (Balasooriya et al., 2016).

Interestingly, a similar mismatch exists between the effects on tanycytes of exogenous stimulation with IGF-1 and endogenous deletion of IGF-R1, whereby both manipulations stimulate hypothalamic neurogenesis (Perez-Martin et al., 2010; Chaker et al., 2016). There is an increase in the number of lineage traced Nestin+ tanycytes and new-born neurons that are deficient in IGF-R1, akin to the amplification of FGF10+ tanycytes and neurons lacking FGF receptors. Since there is much overlap between FGF10 and Nestin in tanycytes (Haan et al., 2013), it is possible that some cells coexpress FGFR1/FGFR2 and IGF-R1 and that these signalling pathways may be synergistic, as reported elsewhere (Jiang et al., 2001; Johnson-Farley et al., 2007; Chen and Wang, 2014). Indeed, in a study of the effects of IGF-1R deletion in SVZ NSPCs, it was found that this growth factor signalling deficiency resulted in the production of more neuroblasts and that these NSPCs exhibited reduced phosphorylation of Akt (Chaker, Aïd et al. 2015). It is possible, therefore, that in tanycytes, a reduction in FGFR and/or IGF-1R activity results in reduced Akt pathway signalling, which may then affect cell division dynamics, survival and differentiation. In the Chaker et al., (2016) study, these effects were seen in older animals, 9 or 16 months of age. Further studies could therefore be conducted to see whether FGFR signalling disruption also has similar effects in older animals.

Recently, *Prss56* has been described as a marker for NSPCs in the adult subgranular and subventricular zone neurogenic niches (Jourdon et al., 2016). In addition, its expression in the hypothalamus is restricted to GFAP- ventral α2/β1 tanycytes and lineage tracing of these cells using a $Prss56^{Cre}$::$Rosa26^{tdTomato}$ mouse line revealed their neurogenic potential. In addition, they strongly proliferate in response to exogenous FGF2. There is likely some overlap between FGF10 and Prss56 expressing tanycytes. Interestingly, some lineage traced Prss56+ tanycytes were seen to translocate into the parenchyma where they maintained tanycytic morphology and expression of tanycytic markers such as Vimentin and Nestin. This echoes the findings reported in chapter 5, where lineage traced tanycytes-like cells were seen in the parenchyma. The fate and significance of these cells are unknown: do they transdifferentiate into cells of neural/glial lineage? Do they divide in the parenchyma? Indeed, some lineage traced cells in the parenchyma that expressed PCNA and exhibited morphology akin to tanycytes with a shortened process were seen. In this report, tanycyte-like cells in the parenchyma were very rare and only found at P10, but the Jourdon et al., (2015) study reports their presence in adult hypothalamus too and it seems likely that these cells arise from ventral α2/β1 *Prss56/Fgf10* expressing tanycytes.

8.1.3 – FGF receptor signalling in *Fgf10*+ β–tanycytes may not be crucial for regulating metabolic functions

Central blockade of FGFR1 through neutralising antibodies and ICV injection of FGF1 can both induce changes in food intake, body weight and glucose metabolism. Hypothalamic cells, including tanycytes, are likely at least partially involved in mediating these effects (Sun et al., 2007; Lelliott et al., 2014; Samms et al., 2015; Scarlett et al., 2016). Here, tanycytic FGF receptors were conditionally deleted in $Fgf10^{CreERT2/+}$::$Fgfr1^{flox/flox}$::$Fgfr2^{flox/flox}$::$Rosa26^{tdTomato}$ (KO) mice fed chow diet and afterwards turned obese by high-fat diet. Their weight, glucose and insulin sensitivities were analysed and compared to mice with normal FGFR function.

Unlike other reports that describe the rapid onset of hypophagia and weight gain upon administration of FGFR1 blocking antibodies, only very subtle, statistically insignificant trends were seen whereby *Fgfr1/Fgfr2* deficient mice gained less weight during HFD treatment. No effects on glucose homeostasis were observed.

There may be a few reasons for this apparent lack of metabolic phenotype. First, *Fgfr1/Fgfr2* deletion would occur in these mice only in *Fgf10* expressing cells and in the hypothalamus, this is restricted to β-tanycytes (Hajihosseini et al., 2008). This may mean that FGF receptors in other cells of the hypothalamus or in other parts of the brain are responsible for the effects seen in other studies. For example, in the Scarlett et al., (2015) study, FGF1 administration caused expression of heat-shock protein not only in tanycytes but also in periventricular astrocytes. As described in Chapter 4, periventricular S100β+ astrocytes express *Fgfr3*, so it may be that FGFR3 in these cells may be important for the hyperglycaemia ameliorating effects of FGF1. Likewise, in addition to non-tanycytic targets in the mediobasal hypothalamus, FGFR1 antibodies also bind to area postrema and subfornical organ (Lelliott et al., 2014).

There are some technical caveats that should be addressed by future studies. Since tamoxifen was administered systemically, other metabolically important organs such as the liver, kidneys, adipose tissue and muscles may also have been impacted, although we do not know if *Fgfr1/Fgfr2* and *Fgf10* are co-expressed in cells within these tissues. Additionally, experiments were performed on mixed-sex animal groups. As sexual dimorphisms exist in metabolic processes (Tiraby et al., 2007; Shi et al., 2008; Macotela et al., 2009), the lack of only-male or only-female analyses may mask subtler phenotypes. A control group comprised of $Fgf10^{CreERT2/+}$ animals should also be included, as the $Fgf10^{CreERT2}$ allele may have metabolic effects on its own, as evidenced by lower weight of adult $Fgf10^{CreERT2/+}$::$Fgfr1^{flox/+}$::$Fgfr2^{flox/+}$::$Rosa26^{tdTomato}$

(Het) animals compared to mice with normal FGF10 function ($Fgfr1^{flox/flox}$::$Fgfr2^{flox/flox}$::$Rosa26^{tdTomato}$) before tamoxifen injections. Finally, the FGFR1 and FGFR2 may have non-overlapping functions, so conditional disruption of only *Fgfr1* or *Fgfr2* may be informative of their individual contributions.

Interestingly, glucose homeostasis did not seem to be impaired in $Fgf10^{CreERT2/+}$::$Fgfr1^{flox/+}$::$Fgfr2^{flox/+}$::$Rosa26^{tdTomato}$ (Het) animals fed a high-fat diet, and glucose tolerance test results suggested that they were more resistant to glucose compared to KO mice. This may mean that intermediate FGFR signalling levels have metabolically positive effects compared to intact (WT) and minimal (KO) FGFR function. High levels of FGF2 have been shown to disrupt FGFR1 signalling (Kanodia et al., 2014). It is possible that exogenous FGF1 injections reported in Scarlett et al., 2015 may, in fact, result in partial blockade of FGFR signalling, having a similar effect to partial deletion of FGF receptors in Het animals, reported here.

8.1.4 – A noncanonical *Fgf10* function regulates the expression of *Agrp* in developing mouse hypothalamus

The expression of *Fgf10* in β-tanycytes and a lack of its cognate receptors FGFR1-IIIb and FGFR2-IIIb suggest a receptor-independent noncanonical, possibly intracellular mode of action (Hajihosseini et al., 2008; Mikolajczak et al., 2016). To determine the function and molecular targets of FGF10 signalling, RNA sequencing had previously been performed on FGF10 deficient and wild-type embryonic hypothalamus. This revealed an array of genes that are up- or downregulated in FGF10 KO hypothalamus. The significant downregulation of *Agrp* in the arcuate nucleus was confirmed by ISH and IHC. No expression of *Fgfr1-IIIb* and *Fgfr2-IIIb* was detected in the embryonic hypothalamus and no downregulation of *Agrp* occurred in FGFR2-IIIb KO, suggestive of an FGF10 function independent of FGF receptors. Finally, the expression of *Npy* was not affected by FGF10 deficiency, indicating that there are no defects in the generation of NPY/Agrp neuron population and that FGF10 can affect gene *Agrp* expression.

FOXO1, a transcription factor important for *Agrp* expression (Kitamura et al., 2006) was also downregulated in the medial part of the arcuate nucleus. Based on the RNA sequencing data and known interactions between the following genes, a plausible scenario can be proposed: as a compensatory mechanism to FGF10 deficiency, the expression of *Yap1* is upregulated (Reginensi et al., 2013; Lin et al., 2017; Volckaert

et al., 2017), which in conjunction with TEAD transcription factors promotes *Tgfrb2* expression (Fan et al., 2017), which can also influence *Fgf10* expression (Hosokawa et al., 2010). Since FOXO1 and Yap1 are known to directly interact and affect transcription (Shao et al., 2014), it is possible that the compensatory upregulation of *Yap1/Tgfrb2* can negatively influence *Foxo1/Agrp* (Fig. 8.3).

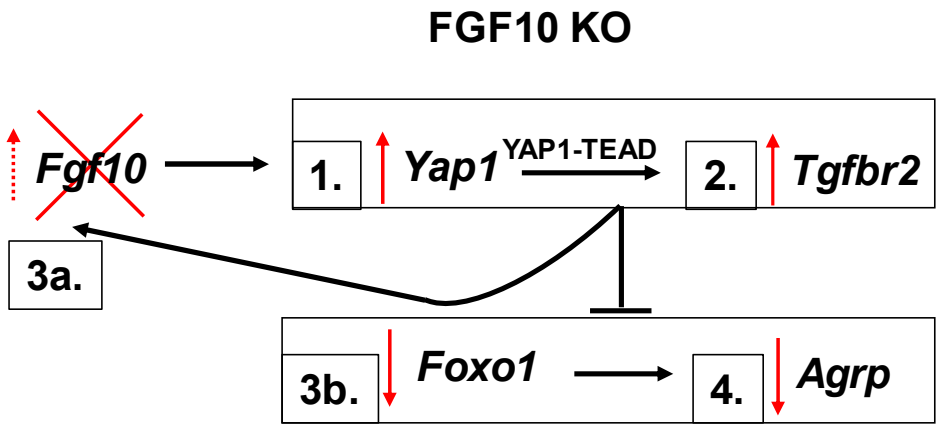

Figure 8.3 – Upregulation of *Yap1* and Tgfbr2 in FGF10 KO hypothalamus may cause downregulation of *Agrp*. A schematic model of possible interactions that may result in *Agrp* downregulation in FGF10 KO hypothalamus. 1 – to compensate for FGF10 loss of function, *Yap1* is upregulated. 2 – YAP1-TEAD complexes stimulate and upregulate *Tgfbr2* expression. 3 – YAP1 and TGFRB2 may stimulate *Fgf10* expression (3a) or inhibit *Foxo1/Agrp* expression in the arcuate nucleus (3b). 4 – due to lowered *Foxo1* expression, *Agrp* expression is downregulated. Reproduced from Chapter 7 (Figure 7.6) for clarity.

The detection of both *Yap1* and *Foxo1* in the 3V ependyma of embryonic hypothalamus by in situ hybridization lends some support to this model. It also suggests that the regulation of *Agrp* expression reported here may occur at the level of progenitor cells, before the birth of the neurons that eventually express AGRP/NPY. As such, this function of FGF10 may be a short-lived developmental effect. However, newborn AGRP/NPY neurons are generated in adulthood too (Pierce and Xu, 2010; Haan et al., 2013). The AGRP/NPY neuron population is essential for stimulating feeding behaviour in adult mice (Luquet et al., 2005; Essner et al., 2017). AGRP itself has a role in energy balance and a study reports that downregulation of AGRP mRNA by RNA interference in adult animals causes increased metabolic rate, resulting in reduced weight without affecting food intake (Makimura et al., 2002). $FGF10^{CreERT2/+}$ mice have reduced FGF10 function (El Agha et al., 2012) and adults tend to be lighter

than wild-type mice (unpublished observations; Chapter 6). This may reflect a role for FGF10 in regulating food intake or metabolic rate by controlling the generation of AGRP/NPY neurons and/or expression of *Agrp* in adult mice.

Apart from regulating the expression of *Agrp*, FGF10 expressed in tanycytes likely has multiple roles as indicated by the differential expression of a diverse set of genes in FGF10 KO hypothalamus. For example, *Aplnr* is highly upregulated in the knockout and has a role in the hypothalamic control of fluid homeostasis (Roberts et al., 2010). *Tgfbr2* is also upregulated in FGF10 deficient hypothalamus and in adult mice, its ligand TGFβ1 regulates the access of GnRH nerve terminals to the anterior pituitary by inducing tanycytes to retract their processes (Prevot et al., 2003). FGF10 may, therefore, participate in multiple physiological processes, but this needs to be investigated and confirmed. A better understanding of the exact molecular mechanisms of noncanonical FGF10 signalling is crucial if any of its potential roles were to be harnessed therapeutically, but they also remain to be determined.

8.2 – Future Directions

There are many further experiments that can be performed to expand upon the work presented here or to address potential caveats.

Short-term lineage tracing suggests that expression in FGF18 ventral α2/β1-tanycytes may mark a population of progenitors. Long-term lineage tracing using the $Fgf18^{CreERT2}$::$Rosa26^{tdTomato}$ mouse line could be used to determine if these cells give rise to cells in the parenchyma of neural and glial fate. In addition, they are likely FGF responsive, so the effects of exogenous FGF stimulation or deletion of *Fgfr1/Fgfr2* in these cells could be explored.

To determine the exact nature of the amplification seen in *Fgfr1/Fgfr2* deficient lineage traced cells, it is necessary to perform additional analyses of cell proliferation. Although the PCNA/dsRed co-localisation experiments at P7 and P10 were incomplete, the preliminary results suggest that amplification likely happens at P8 or P9 and the next experiments should, therefore, focus on these ages. If this is a cumulative effect where a slight continuous increase in proliferation between P6-P10 results in significant amplification by P10, then BrdU labelling may be more beneficial, as the mice can be injected with BrdU every day between P6-P9 and the labelled cells counted at P10.

Although an attempt was made to investigate the function of FGF receptors in adult tanycytes, the lineage traced cell counts were highly variable, potentially due to errors in IP injection technique (Steward et al., 1968). To address this issue, tamoxifen administration to adult animals could be performed through oral gavage, as it may be more reliable for delivery of tamoxifen consistently.

The functions of FGFR1 and FGFR2 can differ in the same stem cell population, as exemplified by airway epithelium basal cells (Balasooriya et al., 2016; Balasooriya et al., 2017). It would, therefore, be useful to perform the lineage tracing and metabolic experiments using mice that carry either $Fgfr1^{Flox/Flox}$ or $Fgfr2^{Flox/Flox}$ alleles, but not both. This would allow for the characterisation of potentially distinct or even opposing functions of these receptors in the control of neurogenesis and metabolism. In the same vein, sex differences can have an impact on both neurogenesis and metabolism, so increasing numbers of animals used sufficient for sex-split analysis may uncover effects otherwise hidden in sex-pooled analyses (Tiraby et al., 2007; Shi et al., 2008; Macotela et al., 2009; Lee et al., 2014).

Tanycytes have important roles in maintaining a barrier between the fenestrated capillaries of the median eminence/ventromedial arcuate nucleus and the CSF (Mullier et al., 2010; Langlet et al., 2013). Any contribution of FGF receptors to this role could be investigated by examining the expression of tight junction proteins in *Fgfr1/Fgfr2* deficient cells.

To test the hypothesis that FGFR1 signalling in β-tanycytes causes posttranslational modification of Spry2, therefore inhibiting proliferation as reported in airway stem cells (Balasooriya et al., 2016), conditional knockout of *Fgfr1* could be performed and the expression of *Spry2* assessed either through qRT-PCR of mRNA isolated from median eminence tissue, or by *Spry2* mRNA in situ hybridization combined with dsRed chromogenic IHC. Since the FGFR1-induced posttranslational modification of Spry2 results in decreased phosphorylation of ERK, the proportion of lineage traced tanycytes that co-localise with pERK would be expected to be higher in *Fgfr1* deficient cells and this could also be quantified.

To delineate central effects of *Fgfr1/Fgfr2* deletion in metabolic experiments, 4-hydroxy-tamoxifen could be administered to the ventricles via a mini-pump (DeVos and Miller, 2013). In addition, BrdU labelling analysis could be performed following an injection of FGF1 into the ventricles of obese mice to ascertain if neurogenesis is affected and may be part of the mechanism causing sustained beneficial effects on glucose metabolism (Scarlett et al., 2016). If neurogenesis is affected, abrogation of

cell division by AraC or focal irradiation would help establish whether there is a causal relationship between the effects of FGF1 on glucose homeostasis and neurogenesis.

To test whether intracellular FGF10 has similar functions in adult mice as in embryonic mice, $FGF10^{CreERT2/flox}$::$Rosa26^{tdTomato}$ animals can be utilised. FACS sorting of cells where recombination takes place is possible, followed by single-cell transcriptomics (Nguyen et al., 2018). Additionally, in situ hybridization or qRT-PCR of *Agrp* in postnatal and adult $Fgf10^{CreERT2/+}$ animals can be performed and compared to wild-type, as the $Fgf10^{CreERT2/+}$ animals have reduced FGF10 function and weight, which might suggest reduced function of orexigenic AGRP. To determine intracellular protein binding partners FGF10, two-dimensional gel electrophoresis can be performed (Lasserre and Ménard, 2012), while the potential for FGF10 to bind DNA directly can be assessed through Chromatin Immunoprecipitation Sequencing (ChIP-Seq) (Furey, 2012). Such experiments should help to elucidate the molecular partners and mechanisms of noncanonical FGF10 signalling.

8.3 – Concluding Remarks

The research undertaken in this project has provided novel information on the expression of FGF signalling system components in the hypothalamus and their enrichment in β-tanycytes. The function of endogenous FGF signalling was then explored in the context of postnatal neurogenesis and metabolic control, revealing roles in controlling the amplification of tanycytes and new-born neurons. In addition, a potential noncanonical function of intracellular FGF10 in regulating expression of *Agrp* was described. Metabolic disorders have become a global epidemic and they continue to rise in prevalence (O'Neill and O'Driscoll, 2015). Further investigations into the neural circuitry involved in energy homeostasis, its establishment, plasticity and molecular regulators are needed to inform future therapeutic approaches for treating and preventing these maladies. Combined, the finding presented here may form a meaningful contribution as they serve to improve our understanding of neurogenesis in postnatal and adult hypothalamic neurogenesis, control of energy homeostasis and the roles that FGF signalling may play in regulating these processes.

List of abbreviations

3V	Third ventricle
AAV	Adeno-associated virus
AER	Apical ectodermal ridge
AGRP	Agouti related peptide
AKT	Protein kinase B
aP2	Fatty acid binding protein 4
Aplnr	Apelin receptor
Ara-C	Cytosine arabinoside
ARC	Arcuate nucleus
AUC	Area under curve
BAC	Bacterial artificial chromosome
BBB	Blood brain barrier
BC	Basal cell
BDNF	Brain-derived neurotrophic factor
BLBP	Brain lipid-binding protein
BMP	Bone morphogenetic protein
BrdU	Bromodeoxyuridine
BSX	Brain-specific homeobox factor
Camk2a	Calcium/calmodulin dependent protein kinase II alpha
CCK-A	Cholecystokinin
ChIP-Seq	Chromatin immunoprecipitation sequencing
CKO	$Fgf10^{CreERT2}$::$Rosa26^{tdTomato}$::$Fgfr1^{Flox/Flox}$::$Fgfr2^{Flox/Flox}$ mice
CNTF	Ciliary neurotrophic factor
CNTFR	Ciliary neurotrophic factor receptor

Cre	Cre recombinase
CRH	Corticotropin Releasing Hormone
CSF	Cerebrospinal fluid
CT	$Fgf10^{CreERT2}$::$Rosa26^{tdTomato}$ mice
DAB	3,3′-Diaminobenzidine
DCX	Doublecortin
DEPC	Diethyl pyrocarbonate
DIG	Digoxigenin
Dio2	Iodothyronine deiodinase 2
Dio3	Iodothyronine deiodinase 3
Dlx1as	Distal-Less homeobox 1, antisense
Dlx2	Distal-Less homeobox 2
DMN	Dorsomedial nucleus
Drop-seq	Droplet-Sequencing
dsRed	Discosoma red fluorescent protein
EDTA	Ethylenediaminetetraacetic acid
EGFP	Enhanced green fluorescent protein
EGFR	Epidermal growth factor receptor
ERK	Extracellular signal-regulated kinase
ETV4	ETS Variant 4
FACS	Fluorescence-activated cell sorter
FGF	Fibroblast growth factor
FGFR	Fibroblast growth factor
FOXO1	Forkhead box O1
GABA	Gamma-Aminobutyric acid
GFAP	Glial fibrillary acidic protein

GFP	Green fluorescent protein
GK	Glucokinase
GLAST	Glutamate aspartate transporter
GLUT2	Glucose transporter 2
GnRH	Gonadotropin-releasing hormone
GTT	Glucose tolerance test
Het	$Fgf10^{CreERT2}$::$Rosa26^{tdTomato}$::$Fgfr1^{Flox/+}$::$Fgfr2^{Flox/+}$ mice OR $Fgf10^{CreERT2/+}$ mice
HFD	High fat diet
hiNGS	Heat inactivated new goats serum
HPA	Hypothalamic–pituitary–adrenal axis
HPG	Hypothalamic–pituitary–gonadal axis
HPT	Hypothalamic–pituitary–thyroid axis
HRP	Horseradish peroxidase
HSP25	Heat shock protein 25
HSPG	Heparan sulfate proteoglycan
ICV	Intracerebroventricular
IGF-1R	Insulin-like growth factor 1 receptor
IGF-2	Insulin-like growth factor 2
IGFBP6	IGFBP6
IL-1β	Interleukin 1 beta
IL-6	Interleukin 6
INFS	Integrative nuclear FgfR1 signaling
IP	Intraperitoneal
ISH	In situ hybridization
ITT	Insulin tolerance test

K-ATP	ATP-sensitive potassium channel
Klb	Klotho Beta
KO	Knockout
LacZ	Beta-galactosidase
LHA	Lateral hypothalamic area
LIF	Leukemia inhibitory factor
MAPK	Mitogen-Activated Protein Kinase
MC4R	Melanocortin 4 Receptor
MCH	Melanin-concentrating hormone
MCH1R	Melanin-concentrating hormone receptor 1
MCT8	Monocarboxylate transporter 8
MEK	Mitogen-activated protein kinase
mGluR4	Metabotropic glutamate receptor 4
Mll1	Mixed-lineage leukemia 1
MKP3	Mitogen-activated protein kinase phosphatase 3
NeuN	Neuronal nuclei
NeuroD	Neurogenic differentiation
NPY	Neuropeptide Y
NSPCs	Neural stem/progenitor cells
Ntrk2	Neurotrophic receptor tyrosine kinase 2
OCT	Optimal cutting temperature compound
OLETF	Otsuka long-evans tokushima fatty
Olig2	Oligodendrocyte transcription factor 2
P	Postnatal day
Pax6	Paired box protein Pax-6
PBS	Phosphate-buffered saline

PCNA	Proliferating cell nuclear antigen
PDGF	Platelet-derived growth factor
PDGFαR	Platelet-derived growth factor-α receptor
Pdx1	Pancreas/duodenum homeobox protein 1
PFA	Paraformaldehyde
PGK	Phosphoglycerate kinase
pH3	Phospho-Histone H3
PI3K	Phosphoinositide 3-kinase
pkB	Protein kinase B
PLCγ	Phospholipase C gamma
POD	Peroxidase
POMC	Pro-opiomelanocortin
PPII	Polyproline II
Prox1	Prospero homeobox protein 1
Prss56	Serine protease 56
PSA-NCAM	Polysialylated-neural cell adhesion molecule
PVN	Paraventricular nucleus
RBP-Jk	Recombination signal binding protein for immunoglobulin kappa j region
RGCs	Radial glial cells
RMS	Rostral migratory stream
RNA-Seq	RNA sequencing
ROBO	Roundabout Guidance Receptor
S100β	S100 Calcium Binding Protein B
SCN	Suprachiasmatic nucleus
SDS	Sodium dodecyl sulfate

Sef	Similar expression to Fgf
SF1	Steroidogenic factor 1
SGZ	Subgranular zone
Shh	Sonic hedgehog
SOX2	Sex determining region Y-box 2
Spry	Sprouty
SSC	Saline-sodium citrate
STAT	Signal transducer and activator of transcription protein
SVZ	Subventricular zone
T3	Triiodothyronine
T4	Thyroxine
Tas1r2	Taste receptor type 1 member 2
Tas1r3	Taste receptor type 1 member 3
TBE	Tris/Borate/EDTA
tdTomato	Tandem dimeric Tomato
Tead4	Tea domain transcription factor 4
Tgfbr2	Transforming growth factor β receptor type-2
TGFβ1	Transforming growth factor β1
TRH	Thyrotropin-releasing hormone
TrkB	Tropomyosin receptor kinase B
TSA	Tyramide signal amplification
TSH	Thyroid-stimulating hormone
TUNEL	Terminal deoxynucleotidyl transferase dUTP nick end labeling
TX	Triton X-100
UTP	Nucleoside triphosphate

VEGF	Vascular endothelial growth factor
vmARC	Ventromedial arcuate nucleus
VMN	Ventromedial nucleus
WMISH	Whole-mount in situ hybridization
X-gal	5-bromo-4-chloro-3-indolyl-β-D-galactopyranoside
Yap1	Yes-associated protein 1
ZO1	Zonula occludens-1
α-MSH	alpha-Melanocyte-stimulating hormone

References

Abler LL, Mansour SL, Sun X (2009) Conditional Gene Inactivation Reveals Roles for Fgf10 and Fgfr2 in Establishing a Normal Pattern of Epithelial Branching in the Mouse Lung. Developmental dynamics : an official publication of the American Association of Anatomists 238:1999-2013.

Adickes ED, Folkerth RD, Sims KL (1997) Use of perfusion fixation for improved neuropathologic examination. Arch Pathol Lab Med 121:1199-1206.

Aguirre AA, Chittajallu R, Belachew S, Gallo V (2004) NG2-expressing cells in the subventricular zone are type C-like cells and contribute to interneuron generation in the postnatal hippocampus. J Cell Biol 165:575-589.

Al Alam D, Danopoulos S, Schall K, Sala FG, Almohazey D, Fernandez GE, Georgia S, Frey MR, Ford HR, Grikscheit T, Bellusci S (2015) Fibroblast growth factor 10 alters the balance between goblet and Paneth cells in the adult mouse small intestine. American Journal of Physiology-Gastrointestinal and Liver Physiology 308:G678-G690.

Albrecht PJ, Dahl JP, Stoltzfus OK, Levenson R, Levison SW (2002) Ciliary neurotrophic factor activates spinal cord astrocytes, stimulating their production and release of fibroblast growth factor-2, to increase motor neuron survival. Exp Neurol 173:46-62.

Allen-Mouse-Brain-Atlas (2011) Technical white paper: in situhybridization data production. In http://mouse.brain-map.org/.

Altman J, Das GD (1965) Autoradiographic and histological evidence of postnatal hippocampal neurogenesis in rats. J Comp Neurol 124:319-335.

Altman J, Bayer SA (1978) Development of the diencephalon in the rat. I. Autoradiographic study of the time of origin and settling patterns of neurons of the hypothalamus. J Comp Neurol 182:945-971.

Apple DM, Fonseca RS, Kokovay E (2017) The role of adult neurogenesis in psychiatric and cognitive disorders. Brain Research 1655:270-276.

Armstrong WE, Stern JE (1998) Phenotypic and state-dependent expression of the electrical and morphological properties of oxytocin and vasopressin neurones. Prog Brain Res 119:101-113.

Ashton RS, Conway A, Pangarkar C, Bergen J, Lim K-I, Shah P, Bissell M, Schaffer DV (2012) Astrocytes regulate adult hippocampal neurogenesis through ephrin-B signaling. Nature Neuroscience 15:1399.

Atasoy D, Betley JN, Su HH, Sternson SM (2012) Deconstruction of a neural circuit for hunger. Nature 488:172-177.

Azim K, Raineteau O, Butt AM (2012) Intraventricular injection of FGF-2 promotes generation of oligodendrocyte-lineage cells in the postnatal and adult forebrain. Glia 60:1977-1990.

Auer H, Mobley JA, Ayers LW, Bowen J, Chuaqui RF, Johnson LA, Livolsi VA, Lubensky IA, McGarvey D, Monovich LC, Moskaluk CA, Rumpel CA, Sexton KC, Washington MK, Wiles KR, Grizzle WE, Ramirez NC (2014) The effects of frozen tissue storage conditions on the integrity of RNA and protein. Biotechnic & histochemistry : official publication of the Biological Stain Commission 89:518-528.

Baertschi S, Zhuang L, Trueb B (2007) Mice with a targeted disruption of the Fgfrl1 gene die at birth due to alterations in the diaphragm. The FEBS Journal 274:6241-6253.

Baker N, Tuan RS (2013) The less-often-traveled surface of stem cells: caveolin-1 and caveolae in stem cells, tissue repair and regeneration. Stem cell research & therapy 4:90.

Balasooriya GI, Johnson JA, Basson MA, Rawlins EL (2016) An FGFR1-SPRY2 Signaling Axis Limits Basal Cell Proliferation in the Steady-State Airway Epithelium. Dev Cell 37:85-97.

Balasooriya GI, Goschorska M, Piddini E, Rawlins EL (2017) FGFR2 is required for airway basal cell self-renewal and terminal differentiation. Development (Cambridge, England) 144:1600-1606.

Balland E, Dam J, Langlet F, Caron E, Steculorum S, Messina A, Rasika S, Falluel-Morel A, Anouar Y, Dehouck B, Trinquet E, Jockers R, Bouret SG, Prevot V (2014) Hypothalamic tanycytes are an ERK-gated conduit for leptin into the brain. Cell metabolism 19:293-301.

Balthazart J, Meaultsart CC, Ball GF, Cornil CA (2013) Distinct neuroendocrine mechanisms control neural activity underlying sex differences in sexual motivation and performance. European Journal of Neuroscience 37:735-742.

Banasr M, Hery M, Printemps R, Daszuta A (2004) Serotonin-induced increases in adult cell proliferation and neurogenesis are mediated through different and common 5-HT receptor subtypes in the dentate gyrus and the subventricular zone. Neuropsychopharmacology 29:450-460.

Barkho BZ, Song H, Aimone JB, Smrt RD, Kuwabara T, Nakashima K, Gage FH, Zhao X (2006) Identification of Astrocyte-expressed Factors That Modulate

Neural Stem/Progenitor Cell Differentiation. Stem Cells and Development 15:407-421.

Baroncini M, Allet C, Leroy D, Beauvillain JC, Francke JP, Prevot V (2007) Morphological Evidence for Direct Interaction Between Gonadotrophin-Releasing Hormone Neurones and Astroglial Cells in the Human Hypothalamus. Journal of Neuroendocrinology 19:691-702.

Barrett P, Ebling FJ, Schuhler S, Wilson D, Ross AW, Warner A, Jethwa P, Boelen A, Visser TJ, Ozanne DM, Archer ZA, Mercer JG, Morgan PJ (2007) Hypothalamic thyroid hormone catabolism acts as a gatekeeper for the seasonal control of body weight and reproduction. Endocrinology 148:3608-3617.

Batailler M, Droguerre M, Baroncini M, Fontaine C, Prevot V, Migaud M (2013) DCX-expressing cells in the vicinity of the hypothalamic neurogenic niche: A comparative study between mouse, sheep, and human tissues. Journal of Comparative Neurology 522:1966-1985.

Batailler M, Mullier A, Sidibe A, Delagrange P, Prevot V, Jockers R, Migaud M (2012) Neuroanatomical distribution of the orphan GPR50 receptor in adult sheep and rodent brains. J Neuroendocrinol 24:798-808.

Bedard A, Gravel C, Parent A (2006) Chemical characterization of newly generated neurons in the striatum of adult primates. Exp Brain Res 170:501-512.

Bedard A, Cossette M, Levesque M, Parent A (2002) Proliferating cells can differentiate into neurons in the striatum of normal adult monkey. Neurosci Lett 328:213-216.

Belluzzi O, Benedusi M, Ackman J, LoTurco JJ (2003) Electrophysiological Differentiation of New Neurons in the Olfactory Bulb. The Journal of Neuroscience 23:10411.

Benford H, Bolborea M, Pollatzek E, Lossow K, Hermans-Borgmeyer I, Liu B, Meyerhof W, Kasparov S, Dale N (2017) A sweet taste receptor-dependent mechanism of glucosensing in hypothalamic tanycytes. Glia 65:773-789.

Bennett L, Yang M, Enikolopov G, Iacovitti L (2009) Circumventricular Organs: A Novel Site of Neural Stem Cells in the Adult Brain. Molecular and cellular neurosciences 41:337-347.

Bergmann O, Liebl J, Bernard S, Alkass K, Yeung MS, Steier P, Kutschera W, Johnson L, Landen M, Druid H, Spalding KL, Frisen J (2012) The age of olfactory bulb neurons in humans. Neuron 74:634-639.

Bernal GM, Peterson DA (2011) Phenotypic and gene expression modification with normal brain aging in GFAP-positive astrocytes and neural stem cells. Aging Cell 10:466-482.

Bernier PJ, Bedard A, Vinet J, Levesque M, Parent A (2002) Newly generated neurons in the amygdala and adjoining cortex of adult primates. Proc Natl Acad Sci USA 99:11464-11469.

Beyer TA, Werner S, Dickson C, Grose R (2003) Fibroblast growth factor 22 and its potential role during skin development and repair. Exp Cell Res 287:228-236.

Bi S, Ladenheim EE, Schwartz GJ, Moran TH (2001) A role for NPY overexpression in the dorsomedial hypothalamus in hyperphagia and obesity of OLETF rats. Am J Physiol Regul Integr Comp Physiol 281:R254-260.

Bingham NC, Anderson KK, Reuter AL, Stallings NR, Parker KL (2008) Selective Loss of Leptin Receptors in the Ventromedial Hypothalamic Nucleus Results in Increased Adiposity and a Metabolic Syndrome. Endocrinology 149:2138-2148.

Bless EP, Reddy T, Acharya KD, Beltz BS, Tetel MJ (2014) Oestradiol and diet modulate energy homeostasis and hypothalamic neurogenesis in the adult female mouse. J Neuroendocrinol 26:805-816.

Bless EP, Yang J, Acharya KD, Nettles SA, Vassoler FM, Byrnes EM, Tetel MJ (2016) Adult Neurogenesis in the Female Mouse Hypothalamus: Estradiol and High-Fat Diet Alter the Generation of Newborn Neurons Expressing Estrogen Receptor α. eNeuro 3:ENEURO.0027-0016.2016.

Bluteau G, Zhuang L, Amann R, Trueb B (2014) Targeted Disruption of the Intracellular Domain of Receptor FgfrL1 in Mice. PLOS ONE 9:e105210.

Bonaguidi MA, McGuire T, Hu M, Kan L, Samanta J, Kessler JA (2005) LIF and BMP signaling generate separate and discrete types of GFAP-expressing cells. Development 132:5503-5514.

Bonaguidi Michael A, Wheeler Michael A, Shapiro Jason S, Stadel Ryan P, Sun Gerald J, Ming G-l, Song H (2011) In Vivo Clonal Analysis Reveals Self-Renewing and Multipotent Adult Neural Stem Cell Characteristics. Cell 145:1142-1155.

Bookout AL, de Groot MH, Owen BM, Lee S, Gautron L, Lawrence HL, Ding X, Elmquist JK, Takahashi JS, Mangelsdorf DJ, Kliewer SA (2013) FGF21 regulates metabolism and circadian behavior by acting on the nervous system. Nat Med 19:1147-1152.

Boulant JA (2000) Role of the preoptic-anterior hypothalamus in thermoregulation and fever. Clin Infect Dis 31 Suppl 5:S157-161.

Bowe JE, Franklin ZJ, Hauge-Evans AC, King AJ, Persaud SJ, Jones PM (2014) Metabolic phenotyping guidelines: assessing glucose homeostasis in rodent models. J Endocrinol 222:G13-25.

Braissant O, Wahli W (1998) A simplified in situ hybridization protocol using non-radioactively labeled probes to detect abundant and rare mRNAs on tissue sections. Biochemica 1:16.

Brewer JR, Mazot P, Soriano P (2016) Genetic insights into the mechanisms of Fgf signaling. Genes & development 30:751-771.

Brezun JM, Daszuta A (1999) Depletion in serotonin decreases neurogenesis in the dentate gyrus and the subventricular zone of adult rats. Neuroscience 89:999-1002.

Brill MS, Ninkovic J, Winpenny E, Hodge RD, Ozen I, Yang R, Lepier A, Gascón S, Erdelyi F, Szabo G, Parras C, Guillemot F, Frotscher M, Berninger B, Hevner RF, Raineteau O, Götz M (2009) Adult generation of glutamatergic olfactory bulb interneurons. Nature neuroscience 12:1524-1533.

Bullitt E (1990) Expression of c-fos-like protein as a marker for neuronal activity following noxious stimulation in the rat. J Comp Neurol 296:517-530.

Cameron HA, McKay RD (2001) Adult neurogenesis produces a large pool of new granule cells in the dentate gyrus. J Comp Neurol 435:406-417.

Campbell JN, Macosko EZ, Fenselau H, Pers TH, Lyubetskaya A, Tenen D, Goldman M, Verstegen AM, Resch JM, McCarroll SA, Rosen ED, Lowell BB, Tsai LT (2017) A molecular census of arcuate hypothalamus and median eminence cell types. Nat Neurosci 20:484-496.

Campbell NR, Fernandes CC, Halff AW, Berg DK (2010) Endogenous signaling through α7-containing nicotinic receptors promotes maturation and integration of adultborn neurons in the hippocampus. The Journal of neuroscience : the official journal of the Society for Neuroscience 30:8734-8744.

Cancilla B, Davies A, Cauchi JA, Risbridger GP, Bertram JF (2001) Fibroblast growth factor receptors and their ligands in the adult rat kidney. Kidney International 60:147-155.

Casey J, Davidson N (1977) Rates of formation and thermal stabilities of RNA:DNA and DNA:DNA duplexes at high concentrations of formamide. Nucleic Acids Research 4:1539-1552.

Catela C, Bilbao-Cortes D, Slonimsky E, Kratsios P, Rosenthal N, Welscher Pt (2009) Multiple congenital malformations of Wolf-Hirschhorn syndrome are recapitulated in Fgfrl1 null mice. Disease Models & Mechanisms.

Celis JE, Celis A (1985) Cell cycle-dependent variations in the distribution of the nuclear protein cyclin proliferating cell nuclear antigen in cultured cells: subdivision of S phase. Proceedings of the National Academy of Sciences of the United States of America 82:3262-3266.

Chaker Z, Aïd S, Berry H, Holzenberger M (2015) Suppression of IGF-I signals in neural stem cells enhances neurogenesis and olfactory function during aging. Aging cell 14:847-856.

Chaker Z, George C, Petrovska M, Caron J-B, Lacube P, Caillé I, Holzenberger M (2016) Hypothalamic neurogenesis persists in the aging brain and is controlled by energy-sensing IGF-I pathway. Neurobiology of Aging 41:64-72.

Chan WS, Sideris A, Sutachan JJ, Montoya GJ, Blanck TJ, Recio-Pinto E (2013) Differential regulation of proliferation and neuronal differentiation in adult rat spinal cord neural stem/progenitors by ERK1/2, Akt, and PLCgamma. Front Mol Neurosci 6:23.

Chao P-T, Yang L, Aja S, Moran Timothy H, Bi S (2011) Knockdown of NPY Expression in the Dorsomedial Hypothalamus Promotes Development of Brown Adipocytes and Prevents Diet-Induced Obesity. Cell Metabolism 13:573-583.

Chazal G, Durbec P, Jankovski A, Rougon G, Cremer H (2000) Consequences of neural cell adhesion molecule deficiency on cell migration in the rostral migratory stream of the mouse. J Neurosci 20:1446-1457.

Chen H, Tung Y-C, Li B, Iqbal K, Grundke-Iqbal I (2007) Trophic factors counteract elevated FGF-2-induced inhibition of adult neurogenesis. Neurobiology of aging 28:1148-1162.

Chen Q-Q, Wang W-M (2014) Expression of FGF-2 and IGF-1 in diabetic rats with fracture. Asian Pacific Journal of Tropical Medicine 7:71-75.

Ciccolini F, Svendsen CN (1998) Fibroblast Growth Factor 2 (FGF-2) Promotes Acquisition of Epidermal Growth Factor (EGF) Responsiveness in Mouse Striatal Precursor Cells: Identification of Neural Precursors Responding to both EGF and FGF-2. The Journal of Neuroscience 18:7869.

Ciofi P (2011) The arcuate nucleus as a circumventricular organ in the mouse. Neurosci Lett 487:187-190.

Codega P, Silva-Vargas V, Paul A, Maldonado-Soto AR, DeLeo AM, Pastrana E, Doetsch F (2014) Prospective identification and purification of quiescent adult neural stem cells from their in vivo niche. Neuron 82:545-559.

Colak D, Mori T, Brill MS, Pfeifer A, Falk S, Deng C, Monteiro R, Mummery C, Sommer L, Gotz M (2008) Adult neurogenesis requires Smad4-mediated bone morphogenic protein signaling in stem cells. J Neurosci 28:434-446.

Collden G, Balland E, Parkash J, Caron E, Langlet F, Prevot V, Bouret SG (2015) Neonatal overnutrition causes early alterations in the central response to peripheral ghrelin. Molecular Metabolism 4:15-24.

Colucci-D'Amato L, Bonavita V, di Porzio U (2006) The end of the central dogma of neurobiology: stem cells and neurogenesis in adult CNS. Neurol Sci 27:266-270.

Contreras M, Riveros ME, Quispe M, Sanchez C, Perdomo G, Torrealba F, Valdes JL (2016) The Histaminergic Tuberomamillary Nucleus Is Involved in Appetite for Sex, Water and Amphetamine. PLoS One 11:e0148484.

Cooper-Kuhn CM, Winkler J, Kuhn HG (2004) Decreased neurogenesis after cholinergic forebrain lesion in the adult rat. Journal of Neuroscience Research 77:155-165.

Costa-e-Sousa RH, Hollenberg AN (2012) Minireview: The Neural Regulation of the Hypothalamic-Pituitary-Thyroid Axis. Endocrinology 153:4128-4135.

Cottrell EC, Cripps RL, Duncan JS, Barrett P, Mercer JG, Herwig A, Ozanne SE (2009) Developmental changes in hypothalamic leptin receptor: relationship with the postnatal leptin surge and energy balance neuropeptides in the postnatal rat. American Journal of Physiology - Regulatory, Integrative and Comparative Physiology 296:R631-R639.

Coutu DL, Galipeau J (2011) Roles of FGF signaling in stem cell self-renewal, senescence and aging. Aging (Albany NY) 3:920-933.

Cowley MA, Smart JL, Rubinstein M, Cerdan MG, Diano S, Horvath TL, Cone RD, Low MJ (2001) Leptin activates anorexigenic POMC neurons through a neural network in the arcuate nucleus. Nature 411:480-484.

Cowley MA et al. (2003) The distribution and mechanism of action of ghrelin in the CNS demonstrates a novel hypothalamic circuit regulating energy homeostasis. Neuron 37:649-661.

Crossley PH, Martin GR (1995) The mouse Fgf8 gene encodes a family of polypeptides and is expressed in regions that direct outgrowth and patterning in the developing embryo. Development (Cambridge, England) 121:439-451.

Dayer AG, Cleaver KM, Abouantoun T, Cameron HA (2005) New GABAergic interneurons in the adult neocortex and striatum are generated from different precursors. J Cell Biol 168:415-427.

Dayer AG, Ford AA, Cleaver KM, Yassaee M, Cameron HA (2003) Short-term and long-term survival of new neurons in the rat dentate gyrus. The Journal of comparative neurology 460:563-572.

De Moerlooze L, Spencer-Dene B, Revest JM, Hajihosseini M, Rosewell I, Dickson C (2000) An important role for the IIIb isoform of fibroblast growth factor receptor 2 (FGFR2) in mesenchymal-epithelial signalling during mouse organogenesis. Development 127:483-492.

De Seranno S, Estrella C, Loyens A, Cornea A, Ojeda SR, Beauvillain J-C, Prevot V (2004) Vascular Endothelial Cells Promote Acute Plasticity in Ependymoglial Cells of the Neuroendocrine Brain. The Journal of Neuroscience 24:10353.

de Seranno S, d'Anglemont de Tassigny X, Estrella C, Loyens A, Kasparov S, Leroy DI, Ojeda SR, Beauvillain J-C, Prevot V (2010) Role of Estradiol in the Dynamic Control of Tanycyte Plasticity Mediated by Vascular Endothelial Cells in the Median Eminence. Endocrinology 151:1760-1772.

Degirolamo C, Sabba C, Moschetta A (2016) Therapeutic potential of the endocrine fibroblast growth factors FGF19, FGF21 and FGF23. Nature reviews Drug discovery 15:51-69.

Dennis CV, Suh LS, Rodriguez ML, Kril JJ, Sutherland GT (2016) Human adult neurogenesis across the ages: An immunohistochemical study. Neuropathol Appl Neurobiol 42:621-638.

DeVos SL, Miller TM (2013) Direct Intraventricular Delivery of Drugs to the Rodent Central Nervous System. Journal of Visualized Experiments : JoVE:50326.

Dhillon H, Zigman JM, Ye C, Lee CE, McGovern RA, Tang V, Kenny CD, Christiansen LM, White RD, Edelstein EA, Coppari R, Balthasar N, Cowley MA, Chua S, Jr., Elmquist JK, Lowell BB (2006) Leptin directly activates SF1 neurons in the VMH, and this action by leptin is required for normal body-weight homeostasis. Neuron 49:191-203.

Dietrich JW, Landgrafe G, Fotiadou EH (2012) TSH and Thyrotropic Agonists: Key Actors in Thyroid Homeostasis. Journal of Thyroid Research 2012:351864.

Doetsch F, García-Verdugo JM, Alvarez-Buylla A (1997) Cellular Composition and Three-Dimensional Organization of the Subventricular Germinal Zone in the Adult Mammalian Brain. The Journal of Neuroscience 17:5046.

Doetsch F, García-Verdugo JM, Alvarez-Buylla A (1999) Regeneration of a germinal layer in the adult mammalian brain. Proceedings of the National Academy of Sciences 96:11619.

Dorey K, Amaya E (2010) FGF signalling: diverse roles during early vertebrate embryogenesis. Development 137:3731.

Dunham-Ems SM, Lee Y-W, Stachowiak EK, Pudavar H, Claus P, Prasad PN, Stachowiak MK (2009) Fibroblast Growth Factor Receptor-1 (FGFR1) Nuclear Dynamics Reveal a Novel Mechanism in Transcription Control. Molecular Biology of the Cell 20:2401-2412.

Díaz C, Morales-Delgado N, Puelles L (2014) Ontogenesis of peptidergic neurons within the genoarchitectonic map of the mouse hypothalamus. Frontiers in Neuroanatomy 8:162.

Ebling FJP, Lewis JE (2018) Tanycytes and hypothalamic control of energy metabolism. Glia 66:1176-1184.

Ebner K, Muigg P, Singewald N (2013) Inhibitory Function of the Dorsomedial Hypothalamic Nucleus on the Hypothalamic–Pituitary–Adrenal Axis Response to an Emotional Stressor but not Immune Challenge. Journal of Neuroendocrinology 25:48-55.

Ekerot M, Stavridis Marios P, Delavaine L, Mitchell Michael P, Staples C, Owens David M, Keenan Iain D, Dickinson Robin J, Storey Kate G, Keyse Stephen M (2008) Negative-feedback regulation of FGF signalling by DUSP6/MKP-3 is driven by ERK1/2 and mediated by Ets factor binding to a conserved site within the DUSP6/MKP-3 gene promoter. Biochemical Journal 412:287-298.

El Agha E, Al Alam D, Carraro G, MacKenzie B, Goth K, De Langhe SP, Voswinckel R, Hajihosseini MK, Rehan VK, Bellusci S (2012) Characterization of a novel fibroblast growth factor 10 (Fgf10) knock-in mouse line to target mesenchymal progenitors during embryonic development. PLoS One 7:e38452.

Emsley JG, Hagg T (2003a) Endogenous and exogenous ciliary neurotrophic factor enhances forebrain neurogenesis in adult mice. Exp Neurol 183:298-310.

Emsley JG, Hagg T (2003b) alpha6beta1 integrin directs migration of neuronal precursors in adult mouse forebrain. Exp Neurol 183:273-285.

Eriksson PS (1998) Neurogenesis in the adult human hippocampus. Nature Med 4:1313-1317.

Ernst A, Alkass K, Bernard S, Salehpour M, Perl S, Tisdale J, Possnert G, Druid H, Frisen J (2014) Neurogenesis in the striatum of the adult human brain. Cell 156:1072-1083.

Essner RA, Smith AG, Jamnik AA, Ryba AR, Trutner ZD, Carter ME (2017) AgRP Neurons Can Increase Food Intake during Conditions of Appetite Suppression and Inhibit Anorexigenic Parabrachial Neurons. J Neurosci 37:8678-8687.

Fan Y, Gao Y, Rao J, Wang K, Zhang F, Zhang C (2017) YAP-1 Promotes Tregs Differentiation in Hepatocellular Carcinoma by Enhancing TGFBR2 Transcription. Cell Physiol Biochem 41:1189-1198.

Fang X, Stachowiak EK, Dunham-Ems SM, Klejbor I, Stachowiak MK (2005) Control of CREB-binding protein signaling by nuclear fibroblast growth factor receptor-1: a novel mechanism of gene regulation. J Biol Chem 280:28451-28462.

Faubel R, Westendorf C, Bodenschatz E, Eichele G (2016) Cilia-based flow network in the brain ventricles. Science 353:176-178.

Feil R, Wagner J, Metzger D, Chambon P (1997) Regulation of Cre recombinase activity by mutated estrogen receptor ligand-binding domains. Biochem Biophys Res Commun 237:752-757.

Fekete C, Marks DL, Sarkar S, Emerson CH, Rand WM, Cone RD, Lechan RM (2004) Effect of Agouti-Related Protein in Regulation of the Hypothalamic-Pituitary-Thyroid Axis in the Melanocortin 4 Receptor Knockout Mouse. Endocrinology 145:4816-4821.

Fekete C, Legradi G, Mihaly E, Huang QH, Tatro JB, Rand WM, Emerson CH, Lechan RM (2000) alpha-Melanocyte-stimulating hormone is contained in nerve terminals innervating thyrotropin-releasing hormone-synthesizing neurons in the hypothalamic paraventricular nucleus and prevents fasting-induced suppression of prothyrotropin-releasing hormone gene expression. J Neurosci 20:1550-1558.

Felfly H, Klein OD (2013) Sprouty genes regulate proliferation and survival of human embryonic stem cells. Sci Rep 3.

Feliciano DM, Bordey A (2013) Newborn cortical neurons: only for neonates? Trends Neurosci 36:51-61.

Feliciano DM, Bordey A, Bonfanti L (2015) Noncanonical Sites of Adult Neurogenesis in the Mammalian Brain. Cold Spring Harbor Perspectives in Biology 7:a018846.

Feng L, Liao WX, Luo Q, Zhang HH, Wang W, Zheng J, Chen DB (2012) Caveolin-1 orchestrates fibroblast growth factor 2 signaling control of angiogenesis in placental artery endothelial cell caveolae. J Cell Physiol 227:2480-2491.

Ferguson IA, Johnson EM, Jr. (1991) Fibroblast growth factor receptor-bearing neurons in the CNS: identification by receptor-mediated retrograde transport. J Comp Neurol 313:693-706.

Fernando RN, Eleuteri B, Abdelhady S, Nussenzweig A, Andang M, Ernfors P (2011) Cell cycle restriction by histone H2AX limits proliferation of adult neural stem cells. Proc Natl Acad Sci U S A 108:5837-5842.

Filippov V, Kronenberg G, Pivneva T, Reuter K, Steiner B, Wang LP, Yamaguchi M, Kettenmann H, Kempermann G (2003) Subpopulation of nestin-expressing progenitor cells in the adult murine hippocampus shows electrophysiological

and morphological characteristics of astrocytes. Mol Cell Neurosci 23:373-382.

Fisher FM, Maratos-Flier E (2016) Understanding the Physiology of FGF21. Annual Review of Physiology 78:223-241.

Fishilevich S, Nudel R, Rappaport N, Hadar R, Plaschkes I, Iny Stein T, Rosen N, Kohn A, Twik M, Safran M, Lancet D, Cohen D (2017) GeneHancer: genome-wide integration of enhancers and target genes in GeneCards. Database: The Journal of Biological Databases and Curation 2017:bax028.

Fon Tacer K, Bookout AL, Ding X, Kurosu H, John GB, Wang L, Goetz R, Mohammadi M, Kuro-o M, Mangelsdorf DJ, Kliewer SA (2010) Research Resource: Comprehensive Expression Atlas of the Fibroblast Growth Factor System in Adult Mouse. Molecular Endocrinology 24:2050-2064.

Franklin KBJ, Paxinos G (2008) The mouse brain in stereotaxic coordinates.

Frayling C, Britton R, Dale N (2011) ATP-mediated glucosensing by hypothalamic tanycytes. The Journal of Physiology 589:2275-2286.

Friedel RH, Wurst W, Wefers B, Kühn R (2011) Generating Conditional Knockout Mice. In: Transgenic Mouse Methods and Protocols (Hofker MH, van Deursen J, eds), pp 205-231. Totowa, NJ: Humana Press.

Fu T, Towers M, Placzek MA (2017) Fgf10(+) progenitors give rise to the chick hypothalamus by rostral and caudal growth and differentiation. Development (Cambridge, England) 144:3278-3288.

Furdui CM, Lew ED, Schlessinger J, Anderson KS (2006) Autophosphorylation of FGFR1 Kinase Is Mediated by a Sequential and Precisely Ordered Reaction. Molecular Cell 21:711-717.

Furey TS (2012) ChIP–seq and beyond: new and improved methodologies to detect and characterize protein–DNA interactions. Nature Reviews Genetics 13:840.

Furusho M, Dupree JL, Bryant M, Bansal R (2009) Disruption of Fibroblast Growth Factor Receptor Signaling In Non-Myelinating Schwann Cells Causes Sensory Axonal Neuropathy and Impairment of Thermal Pain Sensitivity. The Journal of neuroscience : the official journal of the Society for Neuroscience 29:1608-1614.

Gaiano N, Fishell G (2002) The role of notch in promoting glial and neural stem cell fates. Annu Rev Neurosci 25:471-490.

Gall GAE, Kyle WH (1968) Growth of the laboratory mouse. Theoretical and Applied Genetics 38:304-308.

Garcia M, Millan C, Balmaceda-Aguilera C, Castro T, Pastor P, Montecinos H, Reinicke K, Zuniga F, Vera JC, Onate SA, Nualart F (2003) Hypothalamic

ependymal-glial cells express the glucose transporter GLUT2, a protein involved in glucose sensing. J Neurochem 86:709-724.

Garcia-Maya M, Anderson AA, Kendal CE, Kenny AV, Edwards-Ingram LC, Holladay A, Saffell JL (2006) Ligand concentration is a driver of divergent signaling and pleiotropic cellular responses to FGF. J Cell Physiol 206:386-393.

Gasser E, Moutos CP, Downes M, Evans RM (2017) FGF1 - a new weapon to control type 2 diabetes mellitus. Nature reviews Endocrinology 13:599-609.

Ge S, Pradhan DA, Ming G-l, Song H (2007) GABA sets the tempo for activity-dependent adult neurogenesis. Trends in Neurosciences 30:1-8.

Geras EJ, Gershengorn MC (1982) Evidence that TRH stimulates secretion of TSH by two calcium-mediated mechanisms. American Journal of Physiology-Endocrinology and Metabolism 242:E109-E114.

Gerber SD, Steinberg F, Beyeler M, Villiger PM, Trueb B (2009) The murine Fgfrl1 receptor is essential for the development of the metanephric kidney. Developmental Biology 335:106-119.

Giachino C, Barz M, Tchorz JS, Tome M, Gassmann M, Bischofberger J, Bettler B, Taylor V (2014) GABA suppresses neurogenesis in the adult hippocampus through GABA_B receptors. Development 141:83.

Goetz R, Mohammadi M (2013) Exploring mechanisms of FGF signalling through the lens of structural biology. Nat Rev Mol Cell Biol 14:166-180.

Goldfarb M, Schoorlemmer J, Williams A, Diwakar S, Wang Q, Huang X, Giza J, Tchetchik D, Kelley K, Vega A, Matthews G, Rossi P, Ornitz DM, D'Angelo E (2007) FIBROBLAST GROWTH FACTOR HOMOLOGOUS FACTORS CONTROL NEURONAL EXCITABILITY THROUGH MODULATION OF VOLTAGE GATED SODIUM CHANNELS. Neuron 55:449-463.

Goldman SA, Nottebohm F (1983) Neuronal production, migration, and differentiation in a vocal control nucleus of the adult female canary brain. Proc Natl Acad Sci USA 80:2390-2394.

Goldman SA, Chen Z (2011) Perivascular instruction of cell genesis and fate in the adult brain. Nature Neuroscience 14:1382.

Gomez-Climent MA, Castillo-Gomez E, Varea E, Guirado R, Blasco-Ibanez JM, Crespo C, Martinez-Guijarro FJ, Nacher J (2008) A population of prenatally generated cells in the rat paleocortex maintains an immature neuronal phenotype into adulthood. Cereb Cortex 18:2229-2240.

Gong SG (2014) Isoforms of receptors of fibroblast growth factors. J Cell Physiol 229:1887-1895.

Gonzalez AM, Logan A, Ying W, Lappi DA, Berry M, Baird A (1994a) Fibroblast growth factor in the hypothalamic-pituitary axis: differential expression of fibroblast growth factor-2 and a high affinity receptor. Endocrinology 134:2289-2297.

Gonzalez AM, Carman LS, Ong M, Ray J, Gage FH, Shults CW, Baird A (1994b) Storage, metabolism, and processing of 125I-fibroblast growth factor-2 after intracerebral injection. Brain Res 665:285-292.

Goodman T, Hajihosseini MK (2015) Hypothalamic tanycytes-masters and servants of metabolic, neuroendocrine, and neurogenic functions. Frontiers in neuroscience 9:387.

Gouazé A, Brenachot X, Rigault C, Krezymon A, Rauch C, Nédélec E, Lemoine A, Gascuel J, Bauer S, Pénicaud L, Benani A (2013) Cerebral Cell Renewal in Adult Mice Controls the Onset of Obesity. PLOS ONE 8:e72029.

Gould E (2007) How widespread is adult neurogenesis in mammals? Nat Rev Neurosci 8:481-488.

Gould E, Vail N, Wagers M, Gross CG (2001) Adult-generated hippocampal and neocortical neurons in macaques have a transient existence. Proc Natl Acad Sci USA 98:10910-10917.

Gu X, Kay EP (1998) Distribution and putative roles of fibroblast growth factor-2 isoforms in corneal endothelial modulation. Investigative ophthalmology & visual science 39:2252-2258.

Guillemot F, Zimmer C (2011) From cradle to grave: the multiple roles of fibroblast growth factors in neural development. Neuron 71:574-588.

Guyenet SJ, Nguyen HT, Hwang BH, Schwartz MW, Baskin DG, Thaler JP (2013) High-fat diet feeding causes rapid, non-apoptotic cleavage of caspase-3 in astrocytes. Brain Research 1512:97-105.

Haan N, Goodman T, Najdi-Samiei A, Stratford CM, Rice R, El Agha E, Bellusci S, Hajihosseini MK (2013) Fgf10-expressing tanycytes add new neurons to the appetite/energy-balance regulating centers of the postnatal and adult hypothalamus. The Journal of neuroscience : the official journal of the Society for Neuroscience 33:6170-6180.

Hack MA, Saghatelyan A, de Chevigny A, Pfeifer A, Ashery-Padan R, Lledo PM, Gotz M (2005) Neuronal fate determinants of adult olfactory bulb neurogenesis. Nat Neurosci 8:865-872.

Hahn TM, Breininger JF, Baskin DG, Schwartz MW (1998) Coexpression of Agrp and NPY in fasting-activated hypothalamic neurons. Nature Neuroscience 1:271.

Hajihosseini MK (2008) Fibroblast growth factor signaling in cranial suture development and pathogenesis. Frontiers of oral biology 12:160-177.

Hajihosseini MK, Dickson C (1999) A Subset of Fibroblast Growth Factors (Fgfs) Promote Survival, but Fgf-8b Specifically Promotes Astroglial Differentiation of Rat Cortical Precursor Cells. Molecular and Cellular Neuroscience 14:468-485.

Hajihosseini MK, Heath JK (2002) Expression patterns of fibroblast growth factors-18 and -20 in mouse embryos is suggestive of novel roles in calvarial and limb development. Mechanisms of development 113:79-83.

Hajihosseini MK, De Langhe S, Lana-Elola E, Morrison H, Sparshott N, Kelly R, Sharpe J, Rice D, Bellusci S (2008) Localization and fate of Fgf10-expressing cells in the adult mouse brain implicate Fgf10 in control of neurogenesis. Molecular and cellular neurosciences 37:857-868.

Hammelrath L, Škokić S, Khmelinskii A, Hess A, van der Knaap N, Staring M, Lelieveldt BPF, Wiedermann D, Hoehn M (2016) Morphological maturation of the mouse brain: An in vivo MRI and histology investigation. NeuroImage 125:144-152.

Hart AW, Baeza N, Apelqvist A, Edlund H (2000) Attenuation of FGF signalling in mouse beta-cells leads to diabetes. Nature 408:864-868.

Hattori Y, Yamasaki M, Itoh N (1996) The rat FGF-5 mRNA variant generated by alternative splicing encodes a novel truncated form of FGF-5. Biochimica et Biophysica Acta (BBA) - Gene Structure and Expression 1306:31-33.

Hayamizu T, Chan P, Johanson C (2001) FGF-2 immunoreactivity in adult rat ependyma and choroid plexus: Responses to global forebrain ischemia and intraventricular FGF-2. Neurol Res 23:353-358.

Herman JP, McKlveen JM, Ghosal S, Kopp B, Wulsin A, Makinson R, Scheimann J, Myers B (2016) Regulation of the Hypothalamic-Pituitary-Adrenocortical Stress Response. Compr Physiol 6:603-621.

Herwig A, Wilson D, Logie TJ, Boelen A, Morgan PJ, Mercer JG, Barrett P (2009) Photoperiod and acute energy deficits interact on components of the thyroid hormone system in hypothalamic tanycytes of the Siberian hamster. American Journal of Physiology-Regulatory, Integrative and Comparative Physiology 296:R1307-R1315.

Holmberg J, Armulik A, Senti KA, Edoff K, Spalding K, Momma S, Cassidy R, Flanagan JG, Frisen J (2005) Ephrin-A2 reverse signaling negatively regulates neural progenitor proliferation and neurogenesis. Genes Dev 19:462-471.

Hosokawa R, Oka K, Yamaza T, Iwata J, Urata M, Xu X, Bringas P, Jr., Nonaka K, Chai Y (2010) TGF-beta mediated FGF10 signaling in cranial neural crest cells

controls development of myogenic progenitor cells through tissue-tissue interactions during tongue morphogenesis. Dev Biol 341:186-195.

Hou Y, Shin Y-J, Han EJ, Choi J-S, Park J-M, Cha J-H, Choi J-Y, Lee M-Y (2011) Distribution of vascular endothelial growth factor receptor-3/Flt4 mRNA in adult rat central nervous system. Journal of Chemical Neuroanatomy 42:56-64.

Hsuchou H, Pan W, Kastin AJ (2007) The fasting polypeptide FGF21 can enter brain from blood. Peptides 28:2382-2386.

Hsuchou H, Pan W, Kastin AJ (2013) Fibroblast growth factor 19 entry into brain. Fluids and barriers of the CNS 10:32.

Hu H (1999) Chemorepulsion of neuronal migration by Slit2 in the developing mammalian forebrain. Neuron 23:703-711.

Huang Z, Tan Y, Gu J, Liu Y, Song L, Niu J, Zhao L, Srinivasan L, Lin Q, Deng J, Li Y, Conklin DJ, Neubert TA, Cai L, Li X, Mohammadi M (2017) Uncoupling the Mitogenic and Metabolic Functions of FGF1 by Tuning FGF1-FGF Receptor Dimer Stability. Cell reports 20:1717-1728.

Huh S-H, Warchol ME, Ornitz DM (2015) Cochlear progenitor number is controlled through mesenchymal FGF receptor signaling. eLife 4:e05921.

Hébert JM, Lin M, Partanen J, Rossant J, McConnell SK (2003) FGF signaling through FGFR1 is required for olfactory bulb morphogenesis. Development 130:1101.

Inagaki T, Choi M, Moschetta A, Peng L, Cummins CL, McDonald JG, Luo G, Jones SA, Goodwin B, Richardson JA, Gerard RD, Repa JJ, Mangelsdorf DJ, Kliewer SA (2005) Fibroblast growth factor 15 functions as an enterohepatic signal to regulate bile acid homeostasis. Cell Metabolism 2:217-225.

Itoh N, Ornitz DM (2004) Evolution of the Fgf and Fgfr gene families. Trends in Genetics 20:563-569.

Itoh N, Ornitz DM (2008) Functional evolutionary history of the mouse Fgf gene family. Dev Dyn 237:18-27.

Itoh N, Ornitz DM (2011) Fibroblast growth factors: from molecular evolution to roles in development, metabolism and disease. J Biochem 149:121-130.

Itoh N, Ohta H, Konishi M (2015) Endocrine FGFs: Evolution, Physiology, Pathophysiology, and Pharmacotherapy. Frontiers in Endocrinology 6:154.

Jagasia R, Steib K, Englberger E, Herold S, Faus-Kessler T, Saxe M, Gage FH, Song H, Lie DC (2009) GABA-cAMP Response Element-Binding Protein Signaling Regulates Maturation and Survival of Newly Generated Neurons in the Adult Hippocampus. The Journal of Neuroscience 29:7966.

Jessberger S, Römer B, Babu H, Kempermann G (2005) Seizures induce proliferation and dispersion of doublecortin-positive hippocampal progenitor cells. Experimental Neurology 196:342-351.

Jezova D, Michajlovskij N, Kvetnansky R, Makara GB (1993) Paraventricular and supraoptic nuclei of the hypothalamus are not equally important for oxytocin release during stress. Neuroendocrinology 57:776-781.

Jiang F, Frederick TJ, Wood TL (2001) IGF-I Synergizes with FGF-2 to Stimulate Oligodendrocyte Progenitor Entry into the Cell Cycle. Developmental Biology 232:414-423.

Jin K, Xie L, Childs J, Sun Y, Mao XO, Logvinova A, Greenberg Da (2003a) Cerebral neurogenesis is induced by intranasal administration of growth factors. Annals of neurology 53:405-409.

Jin K, Sun Y, Xie L, Batteur S, Mao XO, Smelick C, Logvinova A, Greenberg Da (2003b) Neurogenesis and aging: FGF-2 and HB-EGF restore neurogenesis in hippocampus and subventricular zone of aged mice. Aging cell 2:175-183.

Johnson-Farley NN, Patel K, Kim D, Cowen DS (2007) Interaction of FGF-2 with IGF-1 and BDNF in stimulating Akt, ERK, and neuronal survival in hippocampal cultures. Brain Res 1154:40-49.

Jourdon A, Gresset A, Spassky N, Charnay P, Topilko P, Santos R (2016) Prss56, a novel marker of adult neurogenesis in the mouse brain. Brain Structure and Function 221:4411-4427.

Kaneko N, Marin O, Koike M, Hirota Y, Uchiyama Y, Wu JY, Lu Q, Tessier-Lavigne M, Alvarez-Buylla A, Okano H, Rubenstein JL, Sawamoto K (2010) New neurons clear the path of astrocytic processes for their rapid migration in the adult brain. Neuron 67:213-223.

Kang W, Hébert JM (2015) FGF Signaling Is Necessary for Neurogenesis in Young Mice and Sufficient to Reverse Its Decline in Old Mice. The Journal of Neuroscience 35:10217.

Kang W, Balordi F, Su N, Chen L, Fishell G, Hébert JM (2014) Astrocyte activation is suppressed in both normal and injured brain by FGF signaling. Proceedings of the National Academy of Sciences of the United States of America 111:E2987-E2995.

Kano MR, Morishita Y, Iwata C, Iwasaka S, Watabe T, Ouchi Y, Miyazono K, Miyazawa K (2005) VEGF-A and FGF-2 synergistically promote neoangiogenesis through enhancement of endogenous PDGF-B-PDGFRbeta signaling. J Cell Sci 118:3759-3768.

Kanodia J, Chai D, Vollmer J, Kim J, Raue A, Finn G, Schoeberl B (2014) Deciphering the mechanism behind Fibroblast Growth Factor (FGF) induced biphasic signal-response profiles. Cell Communication and Signaling : CCS 12:34-34.

Kaur C, Ling EA (2017) The circumventricular organs. Histol Histopathol 32:879-892.

Kawano K, Hirashima T, Mori S, Saitoh Y, Kurosumi M, Natori T (1992) Spontaneous long-term hyperglycemic rat with diabetic complications. Otsuka Long-Evans Tokushima Fatty (OLETF) strain. Diabetes 41:1422-1428.

Keenan TM, Grinager JR, Procak AA, Svendsen CN (2012) In vitro localization of human neural stem cell neurogenesis by engineered FGF-2 gradients. Integr Biol (Camb) 4:1522-1531.

Kelly RG, Brown NA, Buckingham ME (2001) The Arterial Pole of the Mouse Heart Forms from Fgf10-Expressing Cells in Pharyngeal Mesoderm. Developmental Cell 1:435-440.

Kempermann G, Song H, Gage FH (2015) Neurogenesis in the Adult Hippocampus. Cold Spring Harb Perspect Biol 7:a018812.

Kempermann G, Chesler EJ, Lu L, Williams RW, Gage FH (2006) Natural variation and genetic covariance in adult hippocampal neurogenesis. Proceedings of the National Academy of Sciences of the United States of America 103:780.

Kiefer P, Dickson C (1995) Nucleolar association of fibroblast growth factor 3 via specific sequence motifs has inhibitory effects on cell growth. Mol Cell Biol 15:4364-4374.

Kim H-J, Kobayashi M, Sasaki T, Kikuchi O, Amano K, Kitazumi T, Lee Y-S, Yokota-Hashimoto H, Susanti VY, Kitamura YI, Nakae J, Kitamura T (2012) Overexpression of FoxO1 in the Hypothalamus and Pancreas Causes Obesity and Glucose Intolerance. Endocrinology 153:659-671.

Kim KW, Zhao L, Donato J, Kohno D, Xu Y, Elias CF, Lee C, Parker KL, Elmquist JK (2011) Steroidogenic factor 1 directs programs regulating diet-induced thermogenesis and leptin action in the ventral medial hypothalamic nucleus. Proceedings of the National Academy of Sciences 108:10673.

Kim MS, Pak YK, Jang PG, Namkoong C, Choi YS, Won JC, Kim KS, Kim SW, Kim HS, Park JY, Kim YB, Lee KU (2006) Role of hypothalamic Foxo1 in the regulation of food intake and energy homeostasis. Nat Neurosci 9:901-906.

Kim WR, Kim Y, Eun B, Park OH, Kim H, Kim K, Park CH, Vinsant S, Oppenheim RW, Sun W (2007) Impaired migration in the rostral migratory stream but spared olfactory function after the elimination of programmed cell death in Bax knock-out mice. J Neurosci 27:14392-14403.

Kir S, Beddow SA, Samuel VT, Miller P, Previs SF, Suino-Powell K, Xu HE, Shulman GI, Kliewer SA, Mangelsdorf DJ (2011) FGF19 as a Postprandial, Insulin-Independent Activator of Hepatic Protein and Glycogen Synthesis. Science (New York, NY) 331:1621-1624.

Kitamura T, Inokuchi K (2014) Role of adult neurogenesis in hippocampal-cortical memory consolidation. Molecular brain 7:13.

Kitamura T, Feng Y, Kitamura YI, Chua SC, Jr., Xu AW, Barsh GS, Rossetti L, Accili D (2006) Forkhead protein FoxO1 mediates Agrp-dependent effects of leptin on food intake. Nat Med 12:534-540.

Klein OD, Lyons DB, Balooch G, Marshall GW, Basson MA, Peterka M, Boran T, Peterkova R, Martin GR (2008) An FGF signaling loop sustains the generation of differentiated progeny from stem cells in mouse incisors. Development (Cambridge, England) 135:377-385.

Klempin F, Kronenberg G, Cheung G, Kettenmann H, Kempermann G (2011) Properties of Doublecortin-(DCX)-Expressing Cells in the Piriform Cortex Compared to the Neurogenic Dentate Gyrus of Adult Mice. PLOS ONE 6:e25760.

Knoth R, Singec I, Ditter M, Pantazis G, Capetian P, Meyer RP, Horvat V, Volk B, Kempermann G (2010) Murine features of neurogenesis in the human hippocampus across the lifespan from 0 to 100 years. PLoS One 5:e8809.

Kokoeva MV, Yin H, Flier JS (2005) Neurogenesis in the hypothalamus of adult mice: potential role in energy balance. Science 310:679-683.

Koopman ACM, Taziaux M, Bakker J (2017) Age-related changes in the morphology of tanycytes in the human female infundibular nucleus/median eminence. Journal of Neuroendocrinology 29.

Kovalenko D, Yang X, Nadeau RJ, Harkins LK, Friesel R (2003) Sef inhibits fibroblast growth factor signaling by inhibiting FGFR1 tyrosine phosphorylation and subsequent ERK activation. The Journal of biological chemistry 278:14087-14091.

Krashes MJ, Lowell BB, Garfield AS (2016) Melanocortin-4 receptor-regulated energy homeostasis. Nat Neurosci 19:206-219.

Kretzschmar K, Watt Fiona M (2012) Lineage Tracing. Cell 148:33-45.

Kriegstein A, Alvarez-Buylla A (2009) The glial nature of embryonic and adult neural stem cells. Annu Rev Neurosci 32:149-184.

Kroemer G et al. (2009) Classification of cell death: recommendations of the Nomenclature Committee on Cell Death 2009. Cell death and differentiation 16:3-11.

Kuhn HG, Winkler J, Kempermann G, Thal LJ, Gage FH (1997) Epidermal growth factor and fibroblast growth factor-2 have different effects on neural progenitors in the adult rat brain. The Journal of neuroscience : the official journal of the Society for Neuroscience 17:5820-5829.

Kunze A, Congreso MR, Hartmann C, Wallraff-Beck A, Hüttmann K, Bedner P, Requardt R, Seifert G, Redecker C, Willecke K, Hofmann A, Pfeifer A, Theis M, Steinhäuser C (2009) Connexin expression by radial glia-like cells is required for neurogenesis in the adult dentate gyrus. Proceedings of the National Academy of Sciences of the United States of America 106:11336-11341.

Lacar B, Parylak SL, Vadodaria KC, Sarkar A, Gage FH (2014) Increasing the resolution of the adult neurogenesis picture. F1000prime reports 6:8.

Lallemand Y, Luria V, Haffner-Krausz R, Lonai P (1998) Maternally expressed PGK-Cre transgene as a tool for early and uniform activation of the Cre site-specific recombinase. Transgenic Research 7:105-112.

Lamballe F, Genestine M, Caruso N, Arce V, Richelme S, Helmbacher F, Maina F (2011) Pool-Specific Regulation of Motor Neuron Survival by Neurotrophic Support. The Journal of Neuroscience 31:11144.

Langlet F, Levin BE, Luquet S, Mazzone M, Messina A, Dunn-Meynell AA, Balland E, Lacombe A, Mazur D, Carmeliet P, Bouret SG, Prevot V, Dehouck B (2013) Tanycytic VEGF-A Boosts Blood-Hypothalamus Barrier Plasticity and Access of Metabolic Signals to the Arcuate Nucleus in Response to Fasting. Cell metabolism 17:607-617.

Lao DH, Yusoff P, Chandramouli S, Philp RJ, Fong CW, Jackson RA, Saw TY, Yu CY, Guy GR (2007) Direct binding of PP2A to Sprouty2 and phosphorylation changes are a prerequisite for ERK inhibition downstream of fibroblast growth factor receptor stimulation. J Biol Chem 282:9117-9126.

Lasserre JP, Ménard A (2012) Two-Dimensional Blue Native/SDS Gel Electrophoresis of Multiprotein Complexes. In: Protein Electrophoresis: Methods and Protocols (Kurien BT, Scofield RH, eds), pp 317-337. Totowa, NJ: Humana Press.

Lavenex P, Lavenex PB, Bennett JL, Amaral DG (2009) Postmortem changes in the neuroanatomical characteristics of the primate brain: hippocampal formation. J Comp Neurol 512:27-51.

Law AKT, Pencea V, Buck CR, Luskin MB (1999) Neurogenesis and Neuronal Migration in the Neonatal Rat Forebrain Anterior Subventricular Zone Do Not Require GFAP-Positive Astrocytes. Developmental Biology 216:622-634.

Lazutkaite G, Soldà A, Lossow K, Meyerhof W, Dale N (2017) Amino acid sensing in hypothalamic tanycytes via umami taste receptors. Molecular Metabolism 6:1480-1492.

Lechan RM, Toni R (2000) Functional Anatomy of the Hypothalamus and Pituitary: MDText.com, Inc., South Dartmouth (MA).

Lechan RM, Fekete C (2006) The TRH neuron: a hypothalamic integrator of energy metabolism. In: Progress in Brain Research (Kalsbeek A, Fliers E, Hofman MA, Swaab DF, van Someren EJW, Buijs RM, eds), pp 209-235: Elsevier.

Lee B, Kim SG, Kim J, Choi KY, Lee S, Lee SK, Lee JW (2013a) Brain-specific homeobox factor as a target selector for glucocorticoid receptor in energy balance. Mol Cell Biol 33:2650-2658.

Lee DA, Yoo S, Pak T, Salvatierra J, Velarde E, Aja S, Blackshaw S (2014) Dietary and sex-specific factors regulate hypothalamic neurogenesis in young adult mice. Frontiers in Neuroscience 8:157.

Lee DA, Bedont JL, Pak T, Wang H, Song J, Miranda-Angulo A, Takiar V, Charubhumi V, Balordi F, Takebayashi H, Aja S, Ford E, Fishell G, Blackshaw S (2012) Tanycytes of the hypothalamic median eminence form a diet-responsive neurogenic niche. Nat Neurosci 15:700-702.

Lee KW, Yim H-S, Shin J, Lee C, Lee J-H, Jeong J-Y (2016) FGF11 induced by hypoxia interacts with HIF-1α and enhances its stability. FEBS Letters 591:348-357.

Lee MM, Reif A, Schmitt AG (2013b) Major depression: a role for hippocampal neurogenesis? Curr Top Behav Neurosci 14:153-179.

Lehtinen MK, Zappaterra MW, Chen X, Yang YJ, Hill AD, Lun M, Maynard T, Gonzalez D, Kim S, Ye P, D'Ercole AJ, Wong ET, LaMantia AS, Walsh CA (2011) The cerebrospinal fluid provides a proliferative niche for neural progenitor cells. Neuron 69:893-905.

Lein ES et al. (2006) Genome-wide atlas of gene expression in the adult mouse brain. Nature 445:168.

Lelliott CJ, Ahnmark A, Admyre T, Ahlstedt I, Irving L, Keyes F, Patterson L, Mumphrey MB, Bjursell M, Gorman T, Bohlooly-Y M, Buchanan A, Harrison P, Vaughan T, Berthoud H-R, Lindén D (2014) Monoclonal Antibody Targeting of Fibroblast Growth Factor Receptor 1c Ameliorates Obesity and Glucose Intolerance via Central Mechanisms. PLOS ONE 9:e112109.

Li A-J, Ozawa K, Tsuboyama H, Imamura T (1999) Distribution of fibroblast growth factor-5 in rat hypothalamus, and its possible role as a regulator of feeding behaviour. Eur J Neurosci 11:1362-1368.

Li J, Tang Y, Cai D (2012) IKKbeta/NF-kappaB disrupts adult hypothalamic neural stem cells to mediate a neurodegenerative mechanism of dietary obesity and pre-diabetes. Nat Cell Biol 14:999-1012.

Lie D-C, Colamarino SA, Song H-J, Désiré L, Mira H, Consiglio A, Lein ES, Jessberger S, Lansford H, Dearie AR, Gage FH (2005) Wnt signalling regulates adult hippocampal neurogenesis. Nature 437:1370.

Lim DA, Alvarez-Buylla A (2016) The Adult Ventricular–Subventricular Zone (V-SVZ) and Olfactory Bulb (OB) Neurogenesis. Cold Spring Harbor Perspectives in Biology 8:a018820.

Lim DA, Tramontin AD, Trevejo JM, Herrera DG, García-Verdugo JM, Alvarez-Buylla A (2000) Noggin Antagonizes BMP Signaling to Create a Niche for Adult Neurogenesis. Neuron 28:713-726.

Lim DA, Huang YC, Swigut T, Mirick AL, Garcia-Verdugo JM, Wysocka J, Ernst P, Alvarez-Buylla A (2009) Chromatin remodelling factor Mll1 is essential for neurogenesis from postnatal neural stem cells. Nature 458:529-533.

Lin C, Yao E, Zhang K, Jiang X, Croll S, Thompson-Peer K, Chuang P-T (2017) YAP is essential for mechanical force production and epithelial cell proliferation during lung branching morphogenesis. eLife 6:e21130.

Liu H, Song N (2016) Molecular Mechanism of Adult Neurogenesis and its Association with Human Brain Diseases. Journal of Central Nervous System Disease 8:5-11.

Liu X, Wang Q, Haydar TF, Bordey A (2005) Nonsynaptic GABA signaling in postnatal subventricular zone controls proliferation of GFAP-expressing progenitors. Nat Neurosci 8:1179-1187.

Lledo P-M, Valley M (2016) Adult Olfactory Bulb Neurogenesis. Cold Spring Harbor Perspectives in Biology 8:a018945.

Lledo P-M, Alonso M, Grubb MS (2006) Adult neurogenesis and functional plasticity in neuronal circuits. Nature Reviews Neuroscience 7:179.

Lois C, Alvarez-Buylla A (1994) Long-distance neuronal migration in the adult mammalian brain. Science 264:1145-1148.

Lois C, Garcia-Verdugo JM, Alvarez-Buylla A (1996) Chain migration of neuronal precursors. Science 271:978-981.

Lu J, Manaenko A, Hu Q (2017) Targeting Adult Neurogenesis for Poststroke Therapy. Stem Cells International 2017:5868632.

Lu P, Ewald AJ, Martin GR, Werb Z (2008) Genetic mosaic analysis reveals FGF receptor 2 function in terminal end buds during mammary gland branching morphogenesis. Developmental biology 321:77-87.

Lu XY, Barsh GS, Akil H, Watson SJ (2003) Interaction between alpha-melanocyte-stimulating hormone and corticotropin-releasing hormone in the regulation of feeding and hypothalamo-pituitary-adrenal responses. J Neurosci 23:7863-7872.

Luquet S, Perez FA, Hnasko TS, Palmiter RD (2005) NPY/AgRP Neurons Are Essential for Feeding in Adult Mice but Can Be Ablated in Neonates. Science 310:683.

Luzzati F, De Marchis S, Fasolo A, Peretto P (2006) Neurogenesis in the caudate nucleus of the adult rabbit. J Neurosci 26:609-621.

Lévy F, Batailler M, Meurisse M, Migaud M (2017) Adult Neurogenesis in Sheep: Characterization and Contribution to Reproduction and Behavior. Frontiers in Neuroscience 11:570.

Ma MS, Brouwer N, Wesseling E, Raj D, van der Want J, Boddeke E, Balasubramaniyan V, Copray S (2015) Multipotent stem cell factor UGS148 is a marker for tanycytes in the adult hypothalamus. Mol Cell Neurosci 65:21-30.

Macotela Y, Boucher J, Tran TT, Kahn CR (2009) Sex and depot differences in adipocyte insulin sensitivity and glucose metabolism. Diabetes 58:803-812.

Maddaluno L, Urwyler C, Werner S (2017) Fibroblast growth factors: key players in regeneration and tissue repair. Development 144:4047-4060.

Madisen L, Zwingman TA, Sunkin SM, Oh SW, Zariwala HA, Gu H, Ng LL, Palmiter RD, Hawrylycz MJ, Jones AR, Lein ES, Zeng H (2009) A robust and high-throughput Cre reporting and characterization system for the whole mouse brain. Nature Neuroscience 13:133.

Magnusson JP, Goritz C, Tatarishvili J, Dias DO, Smith EM, Lindvall O, Kokaia Z, Frisen J (2014) A latent neurogenic program in astrocytes regulated by Notch signaling in the mouse. Science 346:237-241.

Makimura H, Mizuno TM, Mastaitis JW, Agami R, Mobbs CV (2002) Reducing hypothalamic AGRP by RNA interference increases metabolic rate and decreases body weight without influencing food intake. BMC Neurosci 3:18.

Mao J, McGlinn E, Huang P, Tabin CJ, McMahon AP (2009) Fgf-dependent Etv4/5 activity is required for posterior restriction of Sonic Hedgehog and promoting outgrowth of the vertebrate limb. Developmental cell 16:600-606.

Marins M, Xavier AL, Viana NB, Fortes FS, Froes MM, Menezes JR (2009) Gap junctions are involved in cell migration in the early postnatal subventricular zone. Dev Neurobiol 69:715-730.

Marsh DJ et al. (2002) Melanin-concentrating hormone 1 receptor-deficient mice are lean, hyperactive, and hyperphagic and have altered metabolism. Proceedings of the National Academy of Sciences 99:3240.

Marshall CA, Novitch BG, Goldman JE (2005) Olig2 directs astrocyte and oligodendrocyte formation in postnatal subventricular zone cells. J Neurosci 25:7289-7298.

Martin AJ, Grant A, Ashfield AM, Palmer CN, Baker L, Quinlan PR, Purdie CA, Thompson AM, Jordan LB, Berg JN (2011) FGFR2 protein expression in breast cancer: nuclear localisation and correlation with patient genotype. BMC Research Notes 4:72.

Masoumi-Moghaddam S, Amini A, Morris DL (2014) The developing story of Sprouty and cancer. Cancer metastasis reviews 33:695-720.

Matsumoto T, Yamanouchi K (2000) Acceleration of mounting behaviors in female rats by ibotenic acid lesions in the ventromedial hypothalamic nucleus. Neurosci Lett 291:143-146.

Matsuzaki K, Katakura M, Hara T, Li G, Hashimoto M, Shido O (2009) Proliferation of neuronal progenitor cells and neuronal differentiation in the hypothalamus are enhanced in heat-acclimated rats. Pflügers Archiv - European Journal of Physiology 458:661-673.

McDonald JH (2009) Handbook of biological statistics: sparky house publishing Baltimore, MD.

McGann JP (2017) Poor Human Olfaction is a Nineteenth Century Myth. Science (New York, NY) 356:eaam7263.

McHugh ML (2008) Power analysis in research. Biochemia Medica 18:263.

McIntyre DC (2006) CHAPTER 28 - The Kindling Phenomenon. In: Models of Seizures and Epilepsy (Pitkänen A, Schwartzkroin PA, Moshé SL, eds), pp 351-363. Burlington: Academic Press.

McNay DEG, Briançon N, Kokoeva MV, Maratos-Flier E, Flier JS (2012) Remodeling of the arcuate nucleus energy-balance circuit is inhibited in obese mice. The Journal of Clinical Investigation 122:142-152.

McPherson CA, Kraft AD, Harry GJ (2011) Injury-induced neurogenesis: consideration of resident microglia as supportive of neural progenitor cells. Neurotox Res 19:341-352.

Meister B, Hokfelt T, Tsuruo Y, Hemmings H, Ouimet C, Greengard P, Goldstein M (1988) DARPP-32, a dopamine- and cyclic AMP-regulated phosphoprotein in tanycytes of the mediobasal hypothalamus: distribution and relation to

dopamine and luteinizing hormone-releasing hormone neurons and other glial elements. Neuroscience 27:607-622.

Menn B, Garcia-Verdugo JM, Yaschine C, Gonzalez-Perez O, Rowitch D, Alvarez-Buylla A (2006) Origin of oligodendrocytes in the subventricular zone of the adult brain. J Neurosci 26:7907-7918.

Mercier F (2016) Fractones: extracellular matrix niche controlling stem cell fate and growth factor activity in the brain in health and disease. Cell Mol Life Sci 73:4661-4674.

Merkle FT, Tramontin AD, García-Verdugo JM, Alvarez-Buylla A (2004) Radial glia give rise to adult neural stem cells in the subventricular zone. Proceedings of the National Academy of Sciences of the United States of America 101:17528-17532.

Mich JK, Signer RA, Nakada D, Pineda A, Burgess RJ, Vue TY, Johnson JE, Morrison SJ (2014) Prospective identification of functionally distinct stem cells and neurosphere-initiating cells in adult mouse forebrain. Elife 3:e02669.

Mikolajczak M, Goodman T, Hajihosseini MK (2016) Interrogation of a lacrimo-auriculo-dento-digital syndrome protein reveals novel modes of fibroblast growth factor 10 (FGF10) function. Biochem J 473:4593-4607.

Millan C, Martinez F, Cortes-Campos C, Lizama I, Yanez MJ, Llanos P, Reinicke K, Rodriguez F, Peruzzo B, Nualart F, Garcia MA (2010) Glial glucokinase expression in adult and post-natal development of the hypothalamic region. ASN Neuro 2:e00035.

Ming AYK, Yoo E, Vorontsov EN, Altamentova SM, Kilkenny DM, Rocheleau JV (2012) Dynamics and Distribution of Klothoβ (KLB) and Fibroblast Growth Factor Receptor-1 (FGFR1) in Living Cells Reveal the Fibroblast Growth Factor-21 (FGF21)-induced Receptor Complex. The Journal of Biological Chemistry 287:19997-20006.

Miragall F, Albiez P, Bartels H, de Vries U, Dermietzel R (1997) Expression of the gap junction protein connexin43 in the subependymal layer and the rostral migratory stream of the mouse: evidence for an inverse correlation between intensity of connexin43 expression and cell proliferation activity. Cell and Tissue Research 287:243-253.

Miranda-Angulo AL, Byerly MS, Mesa J, Wang H, Blackshaw S (2014) Rax regulates hypothalamic tanycyte differentiation and barrier function in mice. The Journal of comparative neurology 522:876-899.

Mirescu C, Gould E (2006) Stress and adult neurogenesis. Hippocampus 16:233-238.

Mirzadeh Z, Merkle FT, Soriano-Navarro M, Garcia-Verdugo JM, Alvarez-Buylla A (2008) Neural Stem Cells Confer Unique Pinwheel Architecture to the Ventricular Surface in Neurogenic Regions of the Adult Brain. Cell Stem Cell 3:265-278.

Mirzadeh Z, Kusne Y, Duran-Moreno M, Cabrales E, Gil-Perotin S, Ortiz C, Chen B, Garcia-Verdugo JM, Sanai N, Alvarez-Buylla A (2017) Bi- and uniciliated ependymal cells define continuous floor-plate-derived tanycytic territories. Nature Communications 8:13759.

Moran TH, Katz LF, Plata-Salaman CR, Schwartz GJ (1998) Disordered food intake and obesity in rats lacking cholecystokinin A receptors. Am J Physiol 274:R618-625.

Morrens J, Van Den Broeck W, Kempermann G (2011) Glial cells in adult neurogenesis. Glia 60:159-174.

Muda M, Theodosiou A, Rodrigues N, Boschert U, Camps M, Gillieron C, Davies K, Ashworth A, Arkinstall S (1996) The dual specificity phosphatases M3/6 and MKP-3 are highly selective for inactivation of distinct mitogen-activated protein kinases. The Journal of biological chemistry 271:27205-27208.

Mudò G, Bonomo a, Di Liberto V, Frinchi M, Fuxe K, Belluardo N (2009) The FGF-2/FGFRs neurotrophic system promotes neurogenesis in the adult brain. Journal of neural transmission (Vienna, Austria : 1996) 116:995-1005.

Mullen RJ, Buck CR, Smith AM (1992) NeuN, a neuronal specific nuclear protein in vertebrates. Development 116:201.

Mullier A, Bouret SG, Prevot V, Dehouck B (2010) Differential distribution of tight junction proteins suggests a role for tanycytes in blood-hypothalamus barrier regulation in the adult mouse brain. J Comp Neurol 518:943-962.

Mullur R, Liu Y-Y, Brent GA (2014) Thyroid Hormone Regulation of Metabolism. Physiological Reviews 94:355-382.

Muñoz-Elias G, Marcus AJ, Coyne TM, Woodbury D, Black IB (2004) Adult Bone Marrow Stromal Cells in the Embryonic Brain: Engraftment, Migration, Differentiation, and Long-Term Survival. The Journal of Neuroscience 24:4585.

Murakami M, Simons M (2008) Fibroblast growth factor regulation of neovascularization. Current opinion in hematology 15:215-220.

Murase S-i, Horwitz AF (2002) Deleted in Colorectal Carcinoma and Differentially Expressed Integrins Mediate the Directional Migration of Neural Precursors in the Rostral Migratory Stream. The Journal of Neuroscience 22:3568.

Musiek ES, Holtzman DM (2016) Mechanisms linking circadian clocks, sleep, and neurodegeneration. Science 354:1004-1008.

Müller-Fielitz H, Stahr M, Bernau M, Richter M, Abele S, Krajka V, Benzin A, Wenzel J, Kalies K, Mittag J, Heuer H, Offermanns S, Schwaninger M (2017) Tanycytes control the hormonal output of the hypothalamic-pituitary-thyroid axis. Nature Communications 8:484.

Nakao N, Takagi T, Iigo M, Tsukamoto T, Yasuo S, Masuda T, Yanagisawa T, Ebihara S, Yoshimura T (2006) Possible involvement of organic anion transporting polypeptide 1c1 in the photoperiodic response of gonads in birds. Endocrinology 147:1067-1073.

Neben CL, Idoni B, Salva JE, Tuzon CT, Rice JC, Krakow D, Merrill AE (2014) Bent bone dysplasia syndrome reveals nucleolar activity for FGFR2 in ribosomal DNA transcription. Human Molecular Genetics 23:5659-5671.

Nelson AD, Svendsen CN (2006) Low concentrations of extracellular FGF-2 are sufficient but not essential for neurogenesis from human neural progenitor cells. Molecular and cellular neurosciences 33:29-35.

Newitt P, Boros J, Madakashira BP, Robinson ML, Reneker LW, McAvoy JW, Lovicu FJ (2010) Sef is a negative regulator of fiber cell differentiation in the ocular lens. Differentiation; research in biological diversity 80:53-67.

Nguyen A, Khoo WH, Moran I, Croucher PI, Phan TG (2018) Single Cell RNA Sequencing of Rare Immune Cell Populations. Frontiers in Immunology 9:1553.

Nguyen AD, Mitchell NF, Lin S, Macia L, Yulyaningsih E, Baldock PA, Enriquez RF, Zhang L, Shi Y-C, Zolotukhin S, Herzog H, Sainsbury A (2012) Y1 and Y5 Receptors Are Both Required for the Regulation of Food Intake and Energy Homeostasis in Mice. PLOS ONE 7:e40191.

Nilsson I, Johansen JE, Schalling M, Hokfelt T, Fetissov SO (2005) Maturation of the hypothalamic arcuate agouti-related protein system during postnatal development in the mouse. Brain Res Dev Brain Res 155:147-154.

Nishimura T, Nakatake Y, Konishi M, Itoh N (2000) Identification of a novel FGF, FGF-21, preferentially expressed in the liver11The nucleotide sequence data reported in this paper will appear in the DDBJ, EMBL and GenBank nucleotide sequence databases with accession numbers AB021975 and AB025718. Biochimica et Biophysica Acta (BBA) - Gene Structure and Expression 1492:203-206.

Niwa A, Nishibori M, Hamasaki S, Kobori T, Liu K, Wake H, Mori S, Yoshino T, Takahashi H (2015) Voluntary exercise induces neurogenesis in the

hypothalamus and ependymal lining of the third ventricle. Brain structure & function.

Nonogaki K (2000) New insights into sympathetic regulation of glucose and fat metabolism. Diabetologia 43:533-549.

O'Hagan RC, Hassell JA (1998) The PEA3 Ets transcription factor is a downstream target of the HER2/Neu receptor tyrosine kinase. Oncogene 16:301-310.

O'Neill S, O'Driscoll L (2015) Metabolic syndrome: a closer look at the growing epidemic and its associated pathologies. Obes Rev 16:1-12.

Ollmann MM, Wilson BD, Yang YK, Kerns JA, Chen Y, Gantz I, Barsh GS (1997) Antagonism of central melanocortin receptors in vitro and in vivo by agouti-related protein. Science 278:135-138.

Olsen SK, Garbi M, Zampieri N, Eliseenkova AV, Ornitz DM, Goldfarb M, Mohammadi M (2003) Fibroblast growth factor (FGF) homologous factors share structural but not functional homology with FGFs. J Biol Chem 278:34226-34236.

Oomura Y, Sasaki K, Suzuki K, Muto T, Li AJ, Ogita Z, Hanai K, Tooyama I, Kimura H, Yanaihara N (1992) A new brain glucosensor and its physiological significance. The American journal of clinical nutrition 55:278S-282S.

Orellana JA, Saez PJ, Cortes-Campos C, Elizondo RJ, Shoji KF, Contreras-Duarte S, Figueroa V, Velarde V, Jiang JX, Nualart F, Saez JC, Garcia MA (2012) Glucose increases intracellular free Ca(2+) in tanycytes via ATP released through connexin 43 hemichannels. Glia 60:53-68.

Ornitz DM, Itoh N (2001) Fibroblast growth factors. Genome Biology 2:reviews3005.3001-reviews3005.3012.

Ornitz DM, Itoh N (2015) The Fibroblast Growth Factor signaling pathway. Wiley Interdisciplinary Reviews Developmental Biology 4:215-266.

Ottone C, Krusche B, Whitby A, Clements M, Quadrato G, Pitulescu ME, Adams RH, Parrinello S (2014) Direct cell–cell contact with the vascular niche maintains quiescent neural stem cells. Nature Cell Biology 16:1045.

Owen BM, Ding X, Morgan DA, Coate KC, Bookout AL, Rahmouni K, Kliewer SA, Mangelsdorf DJ (2014) FGF21 Acts Centrally to Induce Sympathetic Nerve Activity, Energy Expenditure and Weight Loss. Cell metabolism 20:670-677.

Ozaki K, Kadomoto R, Asato K, Tanimura S, Itoh N, Kohno M (2001) ERK Pathway Positively Regulates the Expression of Sprouty Genes. Biochemical and Biophysical Research Communications 285:1084-1088.

Padilla SL, Carmody JS, Zeltser LM (2010) Pomc-expressing progenitors give rise to antagonistic populations in hypothalamic feeding circuits. Nature medicine 16:403-405.

Paez-Gonzalez P, Asrican B, Rodriguez E, Kuo CT (2014) Identification of distinct ChAT$^+$ neurons and activity-dependent control of postnatal SVZ neurogenesis. Nature neuroscience 17:934-942.

Palop JJ, Roberson ED, Cobos I (2011) Step-by-Step In Situ Hybridization Method for Localizing Gene Expression Changes in the Brain. In: Alzheimer's Disease and Frontotemporal Dementia: Methods and Protocols (Roberson ED, ed), pp 207-230. Totowa, NJ: Humana Press.

Parkash J, Messina A, Langlet F, Cimino I, Loyens A, Mazur D, Gallet S, Balland E, Malone SA, Pralong F, Cagnoni G, Schellino R, De Marchis S, Mazzone M, Pasterkamp RJ, Tamagnone L, Prevot V, Giacobini P (2015) Semaphorin7A regulates neuroglial plasticity in the adult hypothalamic median eminence. Nat Commun 6:6385.

Parmentier R, Kolbaev S, Klyuch BP, Vandael D, Lin JS, Selbach O, Haas HL, Sergeeva OA (2009) Excitation of histaminergic tuberomamillary neurons by thyrotropin-releasing hormone. J Neurosci 29:4471-4483.

Pellegrino G, Trubert C, Terrien J, Pifferi F, Leroy D, Loyens A, Migaud M, Baroncini M, Maurage C-A, Fontaine C, Prévot V, Sharif A (2017) A comparative study of the neural stem cell niche in the adult hypothalamus of human, mouse, rat and gray mouse lemur (Microcebus murinus). Journal of Comparative Neurology 526:1419-1443.

Pencea V, Bingaman KD, Wiegand SJ, Luskin MB (2001) Infusion of brain-derived neurotrophic factor into the lateral ventricle of the adult rat leads to new neurons in the parenchyma of the striatum, septum, thalamus, and hypothalamus. J Neurosci 21:6706-6717.

Perez-Martin M, Cifuentes M, Grondona JM, Lopez-Avalos MD, Gomez-Pinedo U, Garcia-Verdugo JM, Fernandez-Llebrez P (2010) IGF-I stimulates neurogenesis in the hypothalamus of adult rats. Eur J Neurosci 31:1533-1548.

Peruzzo B, Pastor FE, Blazquez JL, Amat P, Rodriguez EM (2004) Polarized endocytosis and transcytosis in the hypothalamic tanycytes of the rat. Cell Tissue Res 317:147-164.

Petreanu L, Alvarez-Buylla A (2002) Maturation and Death of Adult-Born Olfactory Bulb Granule Neurons: Role of Olfaction. The Journal of Neuroscience 22:6106.

Petryszak R et al. (2016) Expression Atlas update—an integrated database of gene and protein expression in humans, animals and plants. Nucleic Acids Research 44:D746-D752.

Piatti VC, Davies-Sala MG, Espósito MS, Mongiat LA, Trinchero MF, Schinder AF (2011) The Timing for Neuronal Maturation in the Adult Hippocampus Is Modulated by Local Network Activity. The Journal of neuroscience : the official journal of the Society for Neuroscience 31:7715-7728.

Pierce AA, Xu AW (2010) De novo neurogenesis in adult hypothalamus as a compensatory mechanism to regulate energy balance. J Neurosci 30:723-730.

Plant TM (2015) The hypothalamo-pituitary-gonadal axis. The Journal of endocrinology 226:T41-T54.

Prevot V, Langlet F, Dehouck B (2013) Flipping the tanycyte switch: how circulating signals gain direct access to the metabolic brain. Aging (Albany NY) 5:332-334.

Prevot V, Dutoit S, Croix D, Tramu G, Beauvillain JC (1998) Semi-quantitative ultrastructural analysis of the localization and neuropeptide content of gonadotropin releasing hormone nerve terminals in the median eminence throughout the estrous cycle of the rat. Neuroscience 84:177-191.

Prevot V, Cornea A, Mungenast A, Smiley G, Ojeda SR (2003) Activation of erbB-1 signaling in tanycytes of the median eminence stimulates transforming growth factor beta1 release via prostaglandin E2 production and induces cell plasticity. J Neurosci 23:10622-10632.

Prevot V, Dehouck B, Sharif A, Ciofi P, Giacobini P, Clasadonte J (2018) The Versatile Tanycyte: A Hypothalamic Integrator of Reproduction and Energy Metabolism. Endocrine Reviews 39:333-368.

Prevot V, Croix D, Bouret S, Dutoit S, Tramu G, Stefano GB, Beauvillain JC (1999) Definitive evidence for the existence of morphological plasticity in the external zone of the median eminence during the rat estrous cycle: implication of neuro-glio-endothelial interactions in gonadotropin-releasing hormone release. Neuroscience 94:809-819.

Pringle NP, Yu WP, Howell M, Colvin JS, Ornitz DM, Richardson WD (2003) Fgfr3 expression by astrocytes and their precursors: evidence that astrocytes and oligodendrocytes originate in distinct neuroepithelial domains. Development (Cambridge, England) 130:93-102.

Qian S, Chen H, Weingarth D, Trumbauer ME, Novi DE, Guan X, Yu H, Shen Z, Feng Y, Frazier E, Chen A, Camacho RE, Shearman LP, Gopal-Truter S, MacNeil DJ, Van der Ploeg LH, Marsh DJ (2002) Neither agouti-related protein nor neuropeptide Y is critically required for the regulation of energy homeostasis in mice. Mol Cell Biol 22:5027-5035.

Quarles LD (2012) Role of FGF23 in Vitamin D and Phosphate Metabolism: Implications in Chronic Kidney Disease. Experimental Cell Research 318:1040-1048.

Rahmouni K, Sigmund CD, Haynes WG, Mark AL (2009) Hypothalamic ERK Mediates the Anorectic and Thermogenic Sympathetic Effects of Leptin. Diabetes 58:536-542.

Ramos AD, Diaz A, Nellore A, Delgado RN, Park KY, Gonzales-Roybal G, Oldham MC, Song JS, Lim DA (2013) Integration of genome-wide approaches identifies lncRNAs of adult neural stem cells and their progeny in vivo. Cell Stem Cell 12:616-628.

Raponi E, Agenes F, Delphin C, Assard N, Baudier J, Legraverend C, Deloulme J-C (2007) S100B expression defines a state in which GFAP-expressing cells lose their neural stem cell potential and acquire a more mature developmental stage. Glia 55:165-177.

Recabal A, Caprile T, García-Robles MdlA (2017) Hypothalamic Neurogenesis as an Adaptive Metabolic Mechanism. Frontiers in Neuroscience 11:190.

Reginensi A, Scott RP, Gregorieff A, Bagherie-Lachidan M, Chung C, Lim D-S, Pawson T, Wrana J, McNeill H (2013) Yap- and Cdc42-Dependent Nephrogenesis and Morphogenesis during Mouse Kidney Development. PLOS Genetics 9:e1003380.

Reinert RB, Kantz J, Misfeldt AA, Poffenberger G, Gannon M, Brissova M, Powers AC (2012) Tamoxifen-Induced Cre-loxP Recombination Is Prolonged in Pancreatic Islets of Adult Mice. PLOS ONE 7:e33529.

Renzel R, Sadek A-R, Chang C-H, Gray WP, Seifert G, Steinhäuser C (2013) Polarized distribution of AMPA, but not GABAA, receptors in radial glia-like cells of the adult dentate gyrus. Glia 61:1146-1154.

Revest JM, DeMoerlooze L, Dickson C (2000) Fibroblast growth factor 9 secretion is mediated by a non-cleaved amino-terminal signal sequence. J Biol Chem 275:8083-8090.

Reynolds B, Weiss S (1992) Generation of Neurons and Astrocytes from Isolated Cells of the Adult Mammalian Central Nervous System. Science 255:1707-1710.

Rieckmann T, Zhuang L, Flück CE, Trueb B (2009) Characterization of the first FGFRL1 mutation identified in a craniosynostosis patient. Biochimica et Biophysica Acta (BBA) - Molecular Basis of Disease 1792:112-121.

Riquelme PA, Drapeau E, Doetsch F (2008) Brain micro-ecologies: neural stem cell niches in the adult mammalian brain. Philos Trans R Soc Lond B Biol Sci 363:123-137.

Rizzoti K, Lovell-Badge R (2017) Pivotal role of median eminence tanycytes for hypothalamic function and neurogenesis. Mol Cell Endocrinol 445:7-13.

Roberts EM, Pope GR, Newson MJ, Landgraf R, Lolait SJ, O'Carroll AM (2010) Stimulus-specific neuroendocrine responses to osmotic challenges in apelin receptor knockout mice. J Neuroendocrinol 22:301-308.

Robins SC, Stewart I, McNay DE, Taylor V, Giachino C, Goetz M, Ninkovic J, Briancon N, Maratos-Flier E, Flier JS, Kokoeva MV, Placzek M (2013) α-Tanycytes of the adult hypothalamic third ventricle include distinct populations of FGF-responsive neural progenitors. Nature communications 4:2049.

Rodriguez Del Aguila M, Gonzalez-Ramirez A (2014) Sample size calculation. Allergol Immunopathol (Madr) 42:485-492.

Rodriguez EM, Blazquez JL, Pastor FE, Pelaez B, Pena P, Peruzzo B, Amat P (2005) Hypothalamic tanycytes: a key component of brain-endocrine interaction. International review of cytology 247:89-164.

Roehl H, Nusslein-Volhard C (2001) Zebrafish pea3 and erm are general targets of FGF8 signaling. Current biology : CB 11:503-507.

Rojczyk-Golebiewska E, Palasz A, Wiaderkiewicz R (2014) Hypothalamic subependymal niche: a novel site of the adult neurogenesis. Cell Mol Neurobiol 34:631-642.

Saghatelyan A, de Chevigny A, Schachner M, Lledo PM (2004) Tenascin-R mediates activity-dependent recruitment of neuroblasts in the adult mouse forebrain. Nat Neurosci 7:347-356.

Sahara S, O'Leary DDM (2009) Fgf10 regulates transition period of cortical stem cell differentiation to radial glia controlling generation of neurons and basal progenitors. Neuron 63:48-62.

Sairanen M, Lucas G, Ernfors P, Castrén M, Castrén E (2005) Brain-Derived Neurotrophic Factor and Antidepressant Drugs Have Different But Coordinated Effects on Neuronal Turnover, Proliferation, and Survival in the Adult Dentate Gyrus. The Journal of Neuroscience 25:1089.

Sakurai T et al. (1998) Orexins and Orexin Receptors: A Family of Hypothalamic Neuropeptides and G Protein-Coupled Receptors that Regulate Feeding Behavior. Cell 92:573-585.

Samms Ricardo J, Lewis Jo E, Lory A, Fowler Maxine J, Cooper S, Warner A, Emmerson P, Adams Andrew C, Luckett Jeni C, Perkins Alan C, Wilson D,

Barrett P, Tsintzas K, Ebling Francis JP (2015) Antibody-Mediated Inhibition of the FGFR1c Isoform Induces a Catabolic Lean State in Siberian Hamsters. Current Biology 25:2997-3003.

Sanai N (2004) Unique astrocyte ribbon in adult human brain contains neural stem cells but lacks chain migration. Nature 427:740-744.

Sanai N, Nguyen T, Ihrie RA, Mirzadeh Z, Tsai H-H, Wong M, Gupta N, Berger MS, Huang E, Garcia-Verdugo J-M, Rowitch DH, Alvarez-Buylla A (2011) Corridors of Migrating Neurons in Human Brain and Their Decline during Infancy. Nature 478:382-386.

Sanchez E, Vargas MA, Singru PS, Pascual I, Romero F, Fekete C, Charli JL, Lechan RM (2009) Tanycyte pyroglutamyl peptidase II contributes to regulation of the hypothalamic-pituitary-thyroid axis through glial-axonal associations in the median eminence. Endocrinology 150:2283-2291.

Sano K, Mayanagi Y, Sekino H, Ogashiwa M, Ishijima B (1970) Results of stimulation and destruction of the posterior hypothalamus in man. J Neurosurg 33:689-707.

Saper CB, Lowell BB (2014) The hypothalamus. Curr Biol 24:R1111-1116.

Sapru HN (2013) Role of the hypothalamic arcuate nucleus in cardiovascular regulation. Autonomic neuroscience : basic & clinical 175:38-50.

Sarruf DA, Thaler JP, Morton GJ, German J, Fischer JD, Ogimoto K, Schwartz MW (2010) Fibroblast Growth Factor 21 Action in the Brain Increases Energy Expenditure and Insulin Sensitivity in Obese Rats. Diabetes 59:1817-1824.

Sasaki K, Oomura Y, Suzuki K, Muto T, Hanai K, Tooyama I, Kimura H, Yanaihara N (1991) Effects of fibroblast growth factors and platelet-derived growth factor on food intake in rats. Brain Research Bulletin 27:327-332.

Sasaki K, Li A-J, Oomura Y, Muto T, Hanai K, Tooyama I, Kimura H, Yanaihara N, Yagi H, Hori T (1994) Effects of fibroblast growth factors and related peptides on food intake by rats. Physiology & Behavior 56:211-218.

Sawamoto K, Wichterle H, Gonzalez-Perez O, Cholfin JA, Yamada M, Spassky N, Murcia NS, Garcia-Verdugo JM, Marin O, Rubenstein JLR, Tessier-Lavigne M, Okano H, Alvarez-Buylla A (2006) New Neurons Follow the Flow of Cerebrospinal Fluid in the Adult Brain. Science 311:629.

Scarlett JM, Rojas JM, Matsen ME, Kaiyala KJ, Stefanovski D, Bergman RN, Nguyen HT, Dorfman MD, Lantier L, Wasserman DH, Mirzadeh Z, Unterman TG, Morton GJ, Schwartz MW (2016) Central injection of fibroblast growth factor 1 induces sustained remission of diabetic hyperglycemia in rodents. Nature medicine 22:800-806.

Schaeffer M, Langlet F, Lafont C, Molino F, Hodson DJ, Roux T, Lamarque L, Verdié P, Bourrier E, Dehouck B, Banères J-L, Martinez J, Méry P-F, Marie J, Trinquet E, Fehrentz J-A, Prévot V, Mollard P (2013) Rapid sensing of circulating ghrelin by hypothalamic appetite-modifying neurons. Proceedings of the National Academy of Sciences of the United States of America 110:1512-1517.

Schanzer A, Wachs FP, Wilhelm D, Acker T, Cooper-Kuhn C, Beck H, Winkler J, Aigner L, Plate KH, Kuhn HG (2004) Direct stimulation of adult neural stem cells in vitro and neurogenesis in vivo by vascular endothelial growth factor. Brain Pathol 14:237-248.

Schlessinger J, Plotnikov AN, Ibrahimi OA, Eliseenkova AV, Yeh BK, Yayon A, Linhardt RJ, Mohammadi M (2000) Crystal structure of a ternary FGF-FGFR-heparin complex reveals a dual role for heparin in FGFR binding and dimerization. Mol Cell 6:743-750.

Schmahl J, Kim Y, Colvin JS, Ornitz DM, Capel B (2004) Fgf9 induces proliferation and nuclear localization of FGFR2 in Sertoli precursors during male sex determination. Development (Cambridge, England) 131:3627-3636.

Schneeberger M, Gomis R, Claret M (2014) Hypothalamic and brainstem neuronal circuits controlling homeostatic energy balance. The Journal of endocrinology 220:T25-46.

Schuit FC, Huypens P, Heimberg H, Pipeleers DG (2001) Glucose sensing in pancreatic beta-cells: a model for the study of other glucose-regulated cells in gut, pancreas, and hypothalamus. Diabetes 50:1-11.

Seeley RJ, Sandoval DA (2016) Targeting the brain as a cure for type 2 diabetes. Nature Medicine 22:709.

Seeley RJ, Payne CJ, Woods SC (1995) Neuropeptide Y fails to increase intraoral intake in rats. Am J Physiol 268:R423-427.

Semple BD, Blomgren K, Gimlin K, Ferriero DM, Noble-Haeusslein LJ (2013) Brain development in rodents and humans: Identifying benchmarks of maturation and vulnerability to injury across species. Progress in neurobiology 0:1-16.

Severi I, Carradori MR, Lorenzi T, Amici A, Cinti S, Giordano A (2012) Constitutive expression of ciliary neurotrophic factor in mouse hypothalamus. Journal of Anatomy 220:622-631.

Shao D, Zhai P, Del Re DP, Sciarretta S, Yabuta N, Nojima H, Lim D-S, Pan D, Sadoshima J (2014) A Functional Interaction between Hippo-YAP Signaling and FoxO1 Mediates the Oxidative Stress Response. Nature communications 5:3315-3315.

Shapiro LA, Ng K, Zhou QY, Ribak CE (2009) Subventricular zone-derived, newly generated neurons populate several olfactory and limbic forebrain regions. Epilepsy Behav 14 Suppl 1:74-80.

Shetty AK, Hattiangady B, Shetty Ga (2005) Stem/progenitor cell proliferation factors FGF-2, IGF-1, and VEGF exhibit early decline during the course of aging in the hippocampus: role of astrocytes. Glia 51:173-186.

Shi H, Strader AD, Sorrell JE, Chambers JB, Woods SC, Seeley RJ (2008) Sexually different actions of leptin in proopiomelanocortin neurons to regulate glucose homeostasis. Am J Physiol Endocrinol Metab 294:E630-639.

Shido O, Matsuzaki K (2015) Involvement of neurogenesis in the hypothalamic area in establishing long-term heat acclimation in rats. Temperature: Multidisciplinary Biomedical Journal 2:362-367.

Shih-Jen C, Chun-Lan K, Yuh-Lih C, Chih-Ju Y, Jia-Wei S, Chan-Shiu C, Chen IL, Tung-Hu T, Hung-Hai Ku and Shih-Hwa C (2007) Antidepressant Administration Modulates Neural Stem Cell Survival and Serotoninergic Differentiation Through Bcl-2. Current Neurovascular Research 4:19-29.

Shimada M, Nakamura T (1973) Time of neuron origin in mouse hypothalamic nuclei. Exp Neurol 41:163-173.

Siebzehnrubl FA, Buslei R, Eyupoglu IY, Seufert S, Hahnen E, Blumcke I (2007) Histone deacetylase inhibitors increase neuronal differentiation in adult forebrain precursor cells. Exp Brain Res 176:672-678.

Sierra A, Encinas JM, Deudero JJ, Chancey JH, Enikolopov G, Overstreet-Wadiche LS, Tsirka SE, Maletic-Savatic M (2010) Microglia shape adult hippocampal neurogenesis through apoptosis-coupled phagocytosis. Cell Stem Cell 7:483-495.

Silber J, Lim DA, Petritsch C, Persson AI, Maunakea AK, Yu M, Vandenberg SR, Ginzinger DG, James CD, Costello JF, Bergers G, Weiss WA, Alvarez-Buylla A, Hodgson JG (2008) miR-124 and miR-137 inhibit proliferation of glioblastoma multiforme cells and induce differentiation of brain tumor stem cells. BMC Med 6:14.

Singh M, Kakkar A, Sharma R, Kharbanda OP, Monga N, Kumar M, Chowdhary S, Airan B, Mohanty S (2017) Synergistic Effect of BDNF and FGF2 in Efficient Generation of Functional Dopaminergic Neurons from human Mesenchymal Stem Cells. Scientific Reports 7:10378.

Sleeman M, Fraser J, McDonald M, Yuan S, White D, Grandison P, Kumble K, Watson JD, Murison JG (2001) Identification of a new fibroblast growth factor receptor, FGFR5. Gene 271:171-182.

Smith CM, Luskin MB (1998) Cell cycle length of olfactory bulb neuronal progenitors in the rostral migratory stream. Developmental Dynamics 213:220-227.

Smith SM, Vale WW (2006) The role of the hypothalamic-pituitary-adrenal axis in neuroendocrine responses to stress. Dialogues in Clinical Neuroscience 8:383-395.

Sohn JW (2015) Network of hypothalamic neurons that control appetite. BMB Rep 48:229-233.

Song H, Stevens CF, Gage FH (2002) Astroglia induce neurogenesis from adult neural stem cells. Nature 417:39.

Soriano P (1999) Generalized lacZ expression with the ROSA26 Cre reporter strain. Nature Genetics 21:70.

Sousa-Ferreira L, de Almeida LP, Cavadas C (2014) Role of hypothalamic neurogenesis in feeding regulation. Trends Endocrinol Metab 25:80-88.

Spalding KL, Bergmann O, Alkass K, Bernard S, Salehpour M, Huttner HB, Boström E, Westerlund I, Vial C, Buchholz BA, Possnert G, Mash DC, Druid H, Frisén J (2013) Dynamics of hippocampal neurogenesis in adult humans. Cell 153:1219-1227.

Stachowiak EK, Roy I, Lee YW, Capacchietti M, Aletta JM, Prasad PN, Stachowiak MK (2009) Targeting novel integrative nuclear FGFR1 signaling by nanoparticle-mediated gene transfer stimulates neurogenesis in the adult brain. Integrative biology : quantitative biosciences from nano to macro 1:394-403.

Stachowiak MK, Birkaya B, Aletta JM, Narla ST, Benson CA, Decker B, Stachowiak EK (2015) Nuclear FGF receptor-1 and CREB binding protein: an integrative signaling module. J Cell Physiol 230:989-1002.

Stein C, Bardet AF, Roma G, Bergling S, Clay I, Ruchti A, Agarinis C, Schmelzle T, Bouwmeester T, Schübeler D, Bauer A (2015) YAP1 Exerts Its Transcriptional Control via TEAD-Mediated Activation of Enhancers. PLOS Genetics 11:e1005465.

Steiner B, Klempin F, Wang L, Kott M, Kettenmann H, Kempermann G (2006) Type-2 cells as link between glial and neuronal lineage in adult hippocampal neurogenesis. Glia 54:805-814.

Steiner J, Bernstein H-G, Bielau H, Berndt A, Brisch R, Mawrin C, Keilhoff G, Bogerts B (2007) Evidence for a wide extra-astrocytic distribution of S100B in human brain. BMC Neuroscience 8:2-2.

Stevens HE, Jiang GY, Schwartz ML, Vaccarino FM (2012) Learning and memory depend on fibroblast growth factor receptor 2 functioning in hippocampus. Biological psychiatry 71:1090-1098.

Steward JP, Ornellas EP, Beernink KD, Northway WH (1968) Errors in the technique of intraperitoneal injection of mice. Applied Microbiology 16:1418-1419.

Streit M, Gehlenborg N (2014) Bar charts and box plots. Nature Methods 11:117.

Stuber GD, Wise RA (2016) Lateral hypothalamic circuits for feeding and reward. Nature Neuroscience 19:198.

Suh JM, Jonker JW, Ahmadian M, Goetz R, Lackey D, Osborn O, Huang Z, Liu W, Yoshihara E, van Dijk TH, Havinga R, Fan W, Yin Y-Q, Yu RT, Liddle C, Atkins AR, Olefsky JM, Mohammadi M, Downes M, Evans RM (2014) Endocrinization of FGF1 produces a neomorphic and potent insulin sensitizer. Nature 513:436.

Sullivan GM, Feinn R (2012) Using Effect Size-or Why the P Value Is Not Enough. Journal of graduate medical education 4:279-282.

Sun HD, Malabunga M, Tonra JR, DiRenzo R, Carrick FE, Zheng H, Berthoud H-R, McGuinness OP, Shen J, Bohlen P, Leibel RL, Kussie P (2007) Monoclonal antibody antagonists of hypothalamic FGFR1 cause potent but reversible hypophagia and weight loss in rodents and monkeys. American Journal of Physiology-Endocrinology and Metabolism 292:E964-E976.

Sun Y, Jin K, Childs JT, Xie L, Mao XO, Greenberg DA (2006) Vascular endothelial growth factor-B (VEGFB) stimulates neurogenesis: Evidence from knockout mice and growth factor administration. Developmental Biology 289:329-335.

Sunmonu NA, Li K, Li JY (2011) Numerous isoforms of Fgf8 reflect its multiple roles in the developing brain. J Cell Physiol 226:1722-1726.

Suyama S, Sunabori T, Kanki H, Sawamoto K, Gachet C, Koizumi S, Okano H (2012) Purinergic Signaling Promotes Proliferation of Adult Mouse Subventricular Zone Cells. The Journal of Neuroscience 32:9238.

Suzuki A, Harada H, Nakamura H (2012) Nuclear translocation of FGF8 and its implication to induce Sprouty2. Dev Growth Differ 54:463-473.

Suzuki S, Li AJ, Akaike T, Imamura T (2001a) Intracerebroventricular infusion of fibroblast growth factor-1 increases Fos immunoreactivity in periventricular astrocytes in rat hypothalamus. Neurosci Lett 300:29-32.

Suzuki S, Li AJ, Ishisaki A, Hou X, Hasegawa M, Fukumura M, Akaike T, Imamura T (2001b) Feeding suppression by fibroblast growth factor-1 is accompanied by selective induction of heat shock protein 27 in hypothalamic astrocytes. The European journal of neuroscience 13:2299-2308.

Tashiro A, Sandler VM, Toni N, Zhao C, Gage FH (2006) NMDA-receptor-mediated, cell-specific integration of new neurons in adult dentate gyrus. Nature 442:929.

Taupin P (2007) BrdU immunohistochemistry for studying adult neurogenesis: paradigms, pitfalls, limitations, and validation. Brain Res Rev 53:198-214.

Tavazoie M, Van der Veken L, Silva-Vargas V, Louissaint M, Colonna L, Zaidi B, Garcia-Verdugo JM, Doetsch F (2008) A Specialized Vascular Niche for Adult Neural Stem Cells. Cell Stem Cell 3:279-288.

Teng C-F, Jeng L-B, Shyu W-C (2018) Role of Insulin-like Growth Factor 1 Receptor Signaling in Stem Cell Stemness and Therapeutic Efficacy. Cell transplantation 27:1313-1319.

Teven CM, Farina EM, Rivas J, Reid RR (2014) Fibroblast growth factor (FGF) signaling in development and skeletal diseases. Genes & Diseases.

Tholouli E, Hoyland JA, Di Vizio D, O'Connell F, MacDermott SA, Twomey D, Levenson R, Yin JAL, Golub TR, Loda M, Byers R (2006) Imaging of multiple mRNA targets using quantum dot based in situ hybridization and spectral deconvolution in clinical biopsies. Biochemical and Biophysical Research Communications 348:628-636.

Thomzig A, Laube G, Prüss H, Veh RW (2005) Pore-forming subunits of K-ATP channels, Kir6.1 and Kir6.2, display prominent differences in regional and cellular distribution in the rat brain. Journal of Comparative Neurology 484:313-330.

Timper K, Brüning JC (2017) Hypothalamic circuits regulating appetite and energy homeostasis: pathways to obesity. Disease Models & Mechanisms 10:679-689.

Tiraby C, Tavernier G, Capel F, Mairal A, Crampes F, Rami J, Pujol C, Boutin JA, Langin D (2007) Resistance to high-fat-diet-induced obesity and sexual dimorphism in the metabolic responses of transgenic mice with moderate uncoupling protein 3 overexpression in glycolytic skeletal muscles. Diabetologia 50:2190-2199.

Tong Q, Ye CP, Jones JE, Elmquist JK, Lowell BB (2008) Synaptic release of GABA by AgRP neurons is required for normal regulation of energy balance. Nat Neurosci 11:998-1000.

Tooyama I, Hara Y, Yasuhara O, Oomura Y, Sasaki K, Muto T, Suzuki K, Hanai K, Kimura H (1991) Production of antisera to acidic fibroblast growth factor and their application to immunohistochemical study in rat brain. Neuroscience 40:769-779.

Tozuka Y, Fukuda S, Namba T, Seki T, Hisatsune T (2005) GABAergic Excitation Promotes Neuronal Differentiation in Adult Hippocampal Progenitor Cells. Neuron 47:803-815.

Utley S, James D, Mavila N, Nguyen MV, Vendryes C, Salisbury SM, Phan J, Wang KS (2014) Fibroblast growth factor signaling regulates the expansion of A6-expressing hepatocytes in association with AKT-dependent β-catenin activation. Journal of Hepatology 60:1002-1009.

Valny M, Honsa P, Kirdajova D, Kamenik Z, Anderova M (2016) Tamoxifen in the Mouse Brain: Implications for Fate-Mapping Studies Using the Tamoxifen-Inducible Cre-loxP System. Frontiers in Cellular Neuroscience 10:243.

Vann SD (2010) Re-evaluating the role of the mammillary bodies in memory. Neuropsychologia 48:2316-2327.

Veenema AH, Neumann ID (2008) Central vasopressin and oxytocin release: regulation of complex social behaviours. Prog Brain Res 170:261-276.

Venero Galanternik M, Kramer Kenneth L, Piotrowski T (2015) Heparan Sulfate Proteoglycans Regulate Fgf Signaling and Cell Polarity during Collective Cell Migration. Cell Reports 10:414-428.

Volckaert T, Yuan T, Chao C-M, Bell H, Sitaula A, Szimmtenings L, El Agha E, Chanda D, Majka S, Bellusci S, Thannickal VJ, Fässler R, De Langhe SP (2017) Fgf10-Hippo Epithelial-Mesenchymal Crosstalk Maintains and Recruits Lung Basal Stem Cells. Developmental Cell 43:48-59.e45.

von Bohlen und Halbach O (2011) Immunohistological markers for proliferative events, gliogenesis, and neurogenesis within the adult hippocampus. Cell Tissue Res 345:1-19.

Vukovic J, Borlikova GG, Ruitenberg MJ, Robinson GJ, Sullivan RKP, Walker TL, Bartlett PF (2013) Immature Doublecortin-Positive Hippocampal Neurons Are Important for Learning But Not for Remembering. The Journal of Neuroscience 33:6603.

Wagner JP, Black IB, DiCicco-Bloom E (1999) Stimulation of neonatal and adult brain neurogenesis by subcutaneous injection of basic fibroblast growth factor. The Journal of neuroscience : the official journal of the Society for Neuroscience 19:6006-6016.

Walton NM, Sutter BM, Laywell ED, Levkoff LH, Kearns SM, Marshall GP, Scheffler B, Steindler DA (2006) Microglia instruct subventricular zone neurogenesis. Glia 54:815-825.

Wang C, Hennessey JA, Kirkton RD, Wang C, Graham V, Puranam RS, Rosenberg PB, Bursac N, Pitt GS (2011) Fibroblast growth factor homologous factor 13

regulates Na(+) channels and conduction velocity in murine heart. Circulation Research 109:775-782.

Warford A, Akbar H, Riberio D (2014) Antigen retrieval, blocking, detection and visualisation systems in immunohistochemistry: A review and practical evaluation of tyramide and rolling circle amplification systems. Methods 70:28-33.

Weiss S, Dunne C, Hewson J, Wohl C, Wheatley M, Peterson AC, Reynolds BA (1996) Multipotent CNS Stem Cells Are Present in the Adult Mammalian Spinal Cord and Ventricular Neuroaxis. The Journal of Neuroscience 16:7599.

Weissman TA, Riquelme PA, Ivic L, Flint AC, Kriegstein AR (2004) Calcium waves propagate through radial glial cells and modulate proliferation in the developing neocortex. Neuron 43:647-661.

Werner S, Unsicker K, von Bohlen und Halbach O (2011) Fibroblast growth factor-2 deficiency causes defects in adult hippocampal neurogenesis, which are not rescued by exogenous fibroblast growth factor-2. Journal of Neuroscience Research 89:1605-1617.

Wesche J, Malecki J, Wiedlocha A, Skjerpen CS, Claus P, Olsnes S (2006) FGF-1 and FGF-2 require the cytosolic chaperone Hsp90 for translocation into the cytosol and the cell nucleus. J Biol Chem 281:11405-11412.

Wesche J, Malecki J, Wiedlocha A, Ehsani M, Marcinkowska E, Nilsen T, Olsnes S (2005) Two nuclear localization signals required for transport from the cytosol to the nucleus of externally added FGF-1 translocated into cells. Biochemistry 44:6071-6080.

Winner B, Winkler J (2015) Adult Neurogenesis in Neurodegenerative Diseases. Cold Spring Harbor Perspectives in Biology 7:a021287.

Winner B, Cooper-Kuhn CM, Aigner R, Winkler J, Kuhn HG (2002) Long-term survival and cell death of newly generated neurons in the adult rat olfactory bulb. The European journal of neuroscience 16:1681-1689.

Wojtowicz JM, Kee N (2006) BrdU assay for neurogenesis in rodents. Nat Protoc 1:1399-1405.

Wu QF, Yang L, Li S, Wang Q, Yuan XB, Gao X, Bao L, Zhang X (2012) Fibroblast growth factor 13 is a microtubule-stabilizing protein regulating neuronal polarization and migration. Cell 149:1549-1564.

Xu B, Goulding EH, Zang K, Cepoi D, Cone RD, Jones KR, Tecott LH, Reichardt LF (2003) Brain-derived neurotrophic factor regulates energy balance downstream of melanocortin-4 receptor. Nature Neuroscience 6:736.

Xu X, Weinstein M, Li C, Naski M, Cohen RI, Ornitz DM, Leder P, Deng C (1998) Fibroblast growth factor receptor 2 (FGFR2)-mediated reciprocal regulation loop between FGF8 and FGF10 is essential for limb induction. Development 125:753.

Xu Y, Tamamaki N, Noda T, Kimura K, Itokazu Y, Matsumoto N, Dezawa M, Ide C (2005) Neurogenesis in the ependymal layer of the adult rat 3rd ventricle. Experimental neurology 192:251-264.

Yaguchi Y, Yu T, Ahmed MU, Berry M, Mason I, Basson MA (2009) Fibroblast growth factor (FGF) gene expression in the developing cerebellum suggests multiple roles for FGF signaling during cerebellar morphogenesis and development. Dev Dyn 238:2058-2072.

Yamaguchi M, Mori K (2005) Critical period for sensory experience-dependent survival of newly generated granule cells in the adult mouse olfactory bulb. Proc Natl Acad Sci U S A 102:9697-9702.

Yamaguchi TP, Harpal K, Henkemeyer M, Rossant J (1994) fgfr-1 is required for embryonic growth and mesodermal patterning during mouse gastrulation. Genes Dev 8:3032-3044.

Yamamoto T, Ochalski A, Hertzberg EL, Nagy JI (1990) On the organization of astrocytic gap junctions in rat brain as suggested by LM and EM immunohistochemistry of connexin43 expression. J Comp Neurol 302:853-883.

Yamasaki M, Emoto H, Konishi M, Mikami T, Ohuchi H, Nakao K, Itoh N (1999) FGF-10 is a growth factor for preadipocytes in white adipose tissue. Biochem Biophys Res Commun 258:109-112.

Yan D, Lin X (2009) Shaping Morphogen Gradients by Proteoglycans. Cold Spring Harbor Perspectives in Biology 1:a002493.

Yang L, Scott KA, Hyun J, Tamashiro KL, Tray N, Moran TH, Bi S (2009) Role of Dorsomedial Hypothalamic Neuropeptide Y in Modulating Food Intake and Energy Balance. The Journal of Neuroscience 29:179.

Yang X, Steinberg F, Zhuang LEI, Bessey R, Trueb B (2016) Receptor FGFRL1 does not promote cell proliferation but induces cell adhesion. International Journal of Molecular Medicine 38:30-38.

Yang Z, Tao YX (2016) Biased signaling initiated by agouti-related peptide through human melanocortin-3 and -4 receptors. Biochim Biophys Acta 1862:1485-1494.

Yashiro M, Matsuoka T (2016) Fibroblast growth factor receptor signaling as therapeutic targets in gastric cancer. World J Gastroenterol 22:2415-2423.

Yaylaoglu MB, Titmus A, Visel A, Alvarez-Bolado G, Thaller C, Eichele G (2005) Comprehensive expression atlas of fibroblast growth factors and their receptors generated by a novel robotic in situ hybridization platform. Developmental dynamics : an official publication of the American Association of Anatomists 234:371-386.

Yayon A, Klagsbrun M, Esko JD, Leder P, Ornitz DM (1991) Cell surface, heparin-like molecules are required for binding of basic fibroblast growth factor to its high affinity receptor. Cell 64:841-848.

Yeo GSH, Connie Hung C-C, Rochford J, Keogh J, Gray J, Sivaramakrishnan S, O'Rahilly S, Farooqi IS (2004) A de novo mutation affecting human TrkB associated with severe obesity and developmental delay. Nature Neuroscience 7:1187.

Yin W, Gore AC (2010) The hypothalamic median eminence and its role in reproductive aging. Ann N Y Acad Sci 1204:113-122.

Yoo S, Blackshaw S (2018) Regulation and function of neurogenesis in the adult mammalian hypothalamus. Progress in Neurobiology.

Yu JM, Kim JH, Song GS, Jung JS (2006) Increase in proliferation and differentiation of neural progenitor cells isolated from postnatal and adult mice brain by Wnt-3a and Wnt-5a. Mol Cell Biochem 288:17-28.

Yu K, Xu J, Liu Z, Sosic D, Shao J, Olson EN, Towler DA, Ornitz DM (2003) Conditional inactivation of FGF receptor 2 reveals an essential role for FGF signaling in the regulation of osteoblast function and bone growth. Development 130:3063.

Yulyaningsih E, Rudenko IA, Valdearcos M, Dahlén E, Vagena E, Chan A, Alvarez-Buylla A, Vaisse C, Koliwad SK, Xu AW (2017) Acute Lesioning and Rapid Repair of Hypothalamic Neurons outside the Blood-Brain Barrier. Cell Reports 19:2257-2271.

Zhang H, Kamiya N, Tsuji T, Takeda H, Scott G, Rajderkar S, Ray MK, Mochida Y, Allen B, Lefebvre V, Hung IH, Ornitz DM, Kunieda T, Mishina Y (2016) Elevated Fibroblast Growth Factor Signaling Is Critical for the Pathogenesis of the Dwarfism in Evc2/Limbin Mutant Mice. PLoS Genetics 12:e1006510.

Zhang X, Bao L, Yang L, Wu Q, Li S (2012) Roles of intracellular fibroblast growth factors in neural development and functions. Science China Life Sciences 55:1038-1044.

Zhang X, Ibrahimi OA, Olsen SK, Umemori H, Mohammadi M, Ornitz DM (2006a) Receptor Specificity of the Fibroblast Growth Factor Family: The Complete Mammalian Fgf Family. The Journal of biological chemistry 281:15694-15700.

Zhang X, Ibrahimi OA, Olsen SK, Umemori H, Mohammadi M, Ornitz DM (2006b) Receptor specificity of the fibroblast growth factor family. The complete mammalian FGF family. The Journal of biological chemistry 281:15694-15700.

Zhao B, Li L, Lei Q, Guan K-L (2010) The Hippo–YAP pathway in organ size control and tumorigenesis: an updated version. Genes & Development 24:862-874.

Zhao M (2003) Evidence for neurogenesis in the adult mammalian substantia nigra. Proc Natl Acad Sci USA 100:7925-7930.

Zhao M, Janson Lang AM (2009) Bromodeoxyuridine infused into the cerebral ventricle of adult mice labels nigral neurons under physiological conditions--a method to detect newborn nerve cells in regions with a low rate of neurogenesis. J Neurosci Methods 184:327-331.

Zhao M, Li D, Shimazu K, Zhou Y-X, Lu B, Deng C-X (2007) Fibroblast growth factor receptor-1 is required for long-term potentiation, memory consolidation, and neurogenesis. Biological psychiatry 62:381-390.

Zhu H, Duchesne L, Rudland PS, Fernig DG (2010) The heparan sulfate co-receptor and the concentration of fibroblast growth factor-2 independently elicit different signalling patterns from the fibroblast growth factor receptor. Cell Commun Signal 8:14.

Zigova T, Pencea V, Wiegand SJ, Luskin MB (1998) Intraventricular administration of BDNF increases the number of newly generated neurons in the adult olfactory bulb. Mol Cell Neurosci 11:234-245.

Znosko WA, Yu S, Thomas K, Molina GA, Li C, Tsang W, Dawid IB, Moon AM, Tsang M (2010) Overlapping functions of Pea3 ETS transcription factors in FGF signaling during zebrafish development. Developmental biology 342:11-25.

Zodpey SP (2004) Sample size and power analysis in medical research. Indian J Dermatol Venereol Leprol 70:123-128.

Appendices

Gene	Primer sequences (5'-3')	Product size (bp)	Reference
Fgf1	ACCGAGAGGTTCAACCTGCC GCCATAGTGAGTCCGAGGACC	387	Hajihosseini and Heath, 2001
*Fgf1**	AGGAGCAAGGAGACAGGATG ATGCAGTACCCCTGGAGTTG	947	Yaylaoglu *et al.,* 2005
Fgf2	GCCAGCGGCATCACCTCGCT TATGGCCTTCTGTCCAGGTCCCGT	435	Hajihosseini and Heath, 2001
*Fgf2**	AGCGGCATCACCTCGCTTCC TATGGCCTTCTGTCCAGGTC	426	Yaylaoglu *et al.,* 2005
Fgf3	GATGGGCCTGATCTGGCTTCTGCT CACCATCTCATGGTCCTTGTGGCC	573	Hajihosseini and Heath, 2001
Fgf4	ACCACAGGGACGCTGCTGCCCA CCTTCATGGTAGGCGACACTCGGT	567	Hajihosseini and Heath, 2001
Fgf5	CATCTTCTGCAGCCACCTGATCCA AAGTTCCGGTTGCTCGGACTGCTT	652	Hajihosseini and Heath, 2001
*Fgf5**	TCTTCTGCAGCCACCTGATC TCTGTACTTCACTGGGCTGG	749 and 645	Yaylaoglu *et al.,* 2005
Fgf6	CACGCTGCAGGCTCTCGTCTTCTT CAGTCATGATTGGGGACACCTTGC	542	Hajihosseini and Heath, 2001
Fgf7	ATCCTGCCGACTCCGCTCTA CCTTTTGATTTAAGGCCACGAACA	487	Hajihosseini and Heath, 2001
Fgf8	CTGAGCTGCCTGCTGTTGCACTTG GGTAGTTGAGGAACTCGAAGCGCA	568	Hajihosseini and Heath, 2001
Fgf9	ATGGCTCCCTTAGGTGAAGTTGG GCCTCCGCCTGAGAATCCCCTTTAAATG	196	Hajihosseini and Heath, 2001
Fgf10	CTCTTTTTGGTGTCTTCGTTCCC CGCTGACCTTGCCGTTCTTCTC	228	Hajihosseini and Heath, 2001
Fgf16	GAACGAGCGCCTGGGCCAGATCG GGACATGGAGGGCAACTTAGAAGG	497	Hajihosseini and Heath, 2001
*Fgf16**	TCTTTGCCTCCTTGGACTGG ATGGAGGGCAACTTAGAAGG	578	Yaylaoglu *et al.,* 2005
Fgf17	CACCCGTCTCCTAATTTTAACC CGAACTGCTTCTGCCTTTCAGC	505	Hajihosseini and Heath, 2001
*Fgf17**	AAGCCAGTAGCCCAAGAGAGC TCGGTGAACACGCAGTCTTTG	675	N/A
Fgf18	CACCACAGTCACCAAGCGATCC CTTTGGTTTCTCGCAGTTTCCTC	340	Hajihosseini and Heath, 2001
Fgf22	GTGGGCGTCGTGGTCATCAAAGCAG GCAGGAAGTGGGCGGACAGGTGG	256 and 233	Hajihosseini and Heath, 2001

Appendix Table 1. RT-PCR primers for paracrine FGFs. * - primers used to make template for cRNA probe.

*Fgf11**	GTCGCTTTAAGGAGTGCGTC CACTGTGGAGAGAAGGCTCC	219	Hajihosseini and Heath, 2001
*Fgf12**	TGTATCGCCAACAGGAATCAGG GGAGAGGGAAGAACGGAAGAG	278	Hajihosseini and Heath, 2001
*Fgf13**	CTATCGCCAGCTCGCTCATCC CACCAGAGACGCTTCTGCTC	626	Hajihosseini and Heath, 2001
*Fgf14**	GGTGGATATCTTCTCTAAAGTG GGATGGTTCTCGGTACATGG	498	Hajihosseini and Heath, 2001
Fgf15	GGAACAAAGGACAGCCTAGA CAGAACTGAGAGCCAGGAGC	275	Hajihosseini and Heath, 2001
Fgf21	GATGACGACCAAGACACTGAAG GCATGGGCAGGAAGCGCACAG	409	Hajihosseini and Heath, 2001
*Fgf21**	TCAAGTCCGGCAGAGGTACC TGGAGCAGGCCTGGCATG	390	Yaylaoglu *et al.,* 2005
Fgf23	CGTGCTCTGCACTGTCTGCAGC CTTCCTCTGCGCTCGGCAGCTC	614	Hajihosseini and Heath, 2001

Appendix Table 2. RT-PCR primers for intracrine and endocrine FGFs.

***** - primers used to make template for cRNA probe.

Gene	Primer sequences (5'-3')	Product size (bp)	Reference
*Npy**	TCACAGAGGCACCCAGAGCAGAG AATGGGGCGGAGTCCAGCCTAGTG	475	Lein et al., 2006
Agrp	AAAGCTTTGTCCTCTGAAGCTG GTTCTGTGGATCTAGCACCTCC	430	Lein et al., 2006
Foxo1	GTACTTGCACACTCAACGTTCC CCTGCCACTGTCTGTACTTAGG	507	N/A
Bsx	CGAGGACATTCTGCTACACAAGC TTCGTCTTGGCTTTTCCTCAGC	460	Lein et al., 2006
Tead4	CCTTCCACAGTAAAATGGCTCTTG TCGATGTTGGTATTGAGGTCTG	493	Lein et al., 2006
Yap1	TAAAGAACCCGAACCGCAGACAG GCTGAGGTGGAGGCAGAAGG	987	Lein et al., 2006
4833420G17 Rik	AACATCCCTGGATGGACACG GGCAGGGCAGCTGAGTAAC	543	Lein et al., 2006
Aplnr	ACTTCATTCAGCACCATGGAAG GGTAGGTATAAGTGGCCCACAG	280	N/A
*Bdnf**	CGACGACATCACTGGCTG CGGCAACAAACCACAACA	824	Lein et al., 2006

Appendix Table 3. **RT-PCR primers for Neuropeptides, transcription factors and other genes.** ***** - primers used to make template for cRNA probe.

Gene	Primer sequences (5'-3')	Product size (bp)	Reference
Fgfr1 *IIIb Reverse* *IIIc Reverse*	GCAGGGCTGCCTGCCAACGAGACAGTG GGTCTGGTGCAGTGAGCCACGCAGACT G GAACGGTCAACCATGCAGAGTGATGG	301 306	Hajihosseini and Dickson, 1999
*Fgfr1**	CACCGACCCATCCTTCAGG GTCGGACTTCAACATCTTCACG	801	Lein et al., 2006
Fgfr2 *IIIb Reverse* *IIIc Reverse*	CCCATCCTCCAAGCTGGACTGCCT CTGTTTGGGCAGGACAGTGAGCCA CAGAACTGTCAACAATGCAGAGTG	318 310	Hajihosseini and Dickson, 1999
Fgfr3 *IIIb Reverse* *IIIc Reverse*	GACAGACACACGGATGTGCTGGA GTGAACACGCAGCAAAAGGCTTT AGCACCACCAGCCACGCAGAG	348	Hajihosseini and Dickson, 1999
Fgfr4	TACAGCTATCTCCTGGATGTGCTG GAAACCGTCGGCGCCGAAGCTGCT	195 and 166	Hajihosseini and Dickson, 1999
*Fgfr4**	AGCACCCTACTGGACACACC TAGTGGCCACGGATGACTTG	762	Yaylaoglu *et al.,* 2005
*Klb**	AACGGCACAGACAGATCCAC GATCAGGTTGTGTCCCACAG	459	N/A
*Sef**	GTGTGCACATGACCCATAGC CTGGGTGAGTTCAGCCTTTC	721	N/A
*Etv4**	CTTCGCCTACGACTCAGATGTC GCAGGACTCTCATCCAAGTGG	589	N/A
*Sprouty1**	AGCCCTGTCTTTGTGCCTACC CGCACAGAGCTATGCCAAAG	694	N/A
*Sprouty2**	GATGGAGGCCAGAGCTCAGAGTGG GAGCTCCGATTTAGGCTGCACTCGG	475	N/A
*Sprouty3**	CCTATTGAACAGCTGCGCTCTACTC CACACTTGCAGCGCCCACACTCCTC	425	N/A
*Sprouty4**	CGATGCTTGTGACTCTGCAGCTCCTC CACTTACACTTTCCACAGGCCTCAC	580	N/A
*MKP3**	GGAAATGGCGATCTGCAAGACGGTG GGAAGGAAGGCTGGCTGTTGGACAG	592	N/A

Appendix Table 4. RT-PCR primers for FGF receptors and signalling modulators. * - primers used to make template for cRNA probe.